University of Bath

UNIVERSITY OF BATH

PHD

A Process Planning Approach for Hybrid Manufacture of Prismatic Polymer Components

Zhu, Zicheng

Award date:
2013

Awarding institution:
University of Bath

Link to publication

A Process Planning Approach for Hybrid Manufacture of Prismatic Polymer Components

Zicheng Zhu

A thesis submitted for the degree of Doctor of Philosophy

University of Bath

Department of Mechanical Engineering

September 2013

Dedicated to my Mum and Dad
for their constant love, support and encouragement

Abstract

The 21st century demand for innovation is leading towards a revolution in the way products are perceived. This will have a major impact on manufacturing technologies as current product innovation is constrained by the available manufacturing processes, which function independently. One of the most significant developments is the emergence of hybrid manufacturing technologies integrating various individual manufacturing processes. Hybrid processes utilise the advantages of the independent processes whilst minimising their weaknesses as well as extending application areas.

Despite the fact that the drawbacks of the individual processes have been significantly reduced, the application of state of the art hybrid technology has always been constrained by the capabilities of their constituent processes either from technical limitations or production costs. In particular, it is virtually impossible to machine complex parts due to limited cutting tool accessibility. By contrast, additive manufacturing (AM) techniques completely solve the tool accessibility issue, but this increased flexibility and automation is achieved by compromising on part accuracy and surface quality. Furthermore, the shape and size of raw materials have to be specific for each hybrid process. More importantly, process planning methods capable of effectively utilising manufacturing resources for hybrid processes are highly limited.

In this research, a hybrid process, entitled iAtractive, combining additive, subtractive and inspection processes is proposed. An experimental methodology has been designed and implemented, by which a generative reactionary process planning algorithm (GRP^{2}A) and feature-based decision-making logic (FDL) is developed. GRP^{2}A enables a complex part to be accurately manufactured as one complete unit in the shortest production time possible. FDL provides a number of manufacturing strategies, allowing existing parts to be reused and transformed into final parts with additional features and functionalities. A series of case studies have been manufactured from zero and existing parts, demonstrating the efficacy of the iAtractive process and the developed GRP^{2}A and FDL, which are based on a manual process.

The major contribution to knowledge is the new vision for a hybrid process, which is not constrained by the capability of the individual processes and raw material in terms of shape and size. It has been demonstrated that the hybrid process together with GRP^{2}A and FDL provides an effective solution to flexibly and accurately manufacture complex part geometries as well as remanufacture existing parts.

Acknowledgements

It has been a long journey to finally arrive here. In fact, I have been dreaming of writing down the acknowledgements during the past two years as this indicates I am approaching the end of my PhD studies. I own my sincere gratitude to many people, without whom I would not have reached here.

First and foremost I wish to express my gratitude to my supervisor Prof. Stephen T. Newman for your guidance throughout the entire PhD. It has been a wonderful experience to work with you. Thank you for not only teaching me how to conduct research, but also showing me a big picture of doing research and how to be an independent researcher. Your endless encouragement has given me a great courage to believe that I can finish my PhD, particularly in my second year, the toughest time that I have ever had in my life. In addition, special thanks for your tolerance when I broke the machines many times in the lab.

The same gratitude also goes to my co-supervisor, Dr Vimal Dhokia. I consider myself extremely fortunate to be your PhD student. You always went through my thesis and papers word by word, again and again, ensuring they are of high quality. To sit and have a discussion with you on a weekly and sometimes daily basis has been a tremendous privilege. You were willing to spend considerable time with me discussing every detail in my work, which I really appreciate.

I would also like to express my gratitude to Dr Aydin Nassehi. I used to be a bit afraid of talking to you since you usually destroyed my confidence. Looking back now, every time you questioned my work was actually to help me improve it. My fellow colleagues, Dr Parag Vichare, Dr Paul Crabtree, Dr Xianzhi Zhang, Mr Abayomi Debode, Mr Reza Asrai, Mr Mehrdad Safaieh, Mr Alborz Shokrani, Mr Joseph Flynn, Mr Behnood Afshari and Mr Wesley Essink, I thank you for your on-going support. In particular, I would like to thank Dr Rhys Jones and Mr Robin Harris for sharing your knowledge and helping me solve many tough technical problems.

Finally, and most importantly, I wish to thank my parents, a funny couple who always have different opinions on most things but have reached a consensus on my education. Thank you for your constant love, support, patience and encouragement, without which none of the work in my PhD would have been possible.

List of Abbreviations

3DP	Three Dimensional Printing
ABS	Acrylonitrile Butadiene Styrene
AM	Additive Manufacturing
ANOVA	Analysis of Variance
CAD	Computer Aided Design
CAI	Computer Aided Inspection
CAM	Computer Aided Manufacturing
CAPP	Computer Aided Process Planning
CIM	Computer Integrated Manufacturing
CMM	Coordinate Measuring Machine
CNC	Computer Numerically Controlled
DoC	Depth of Cut
DoE	Design of Experiments
DMLS	Direct Metal Laser Sintering
EBM	Electron Beam Melting
ECDM	Electrochemical Discharge Machining
ECM	Electrochemical Machining
EDM	Electrical Discharge Machining
FDL	Feature-based Decision-making Logic
FDM	Fused Deposition Modelling
FFF	Fused Filament Fabrication
GCode	CNC Programming Language
GMAW	Gas Metal Arc Welding
GRP^{2}A	Generative Reactionary Process Planning Algorithm
HDPE	High Density PolyEthylene
HPC	High Pressure Cooling
HSTMP	Hybrid Subtractive and Transformative Manufacturing Processes

iASI	Interchangeably Add, Subtract and Inspect (material/part)
iAtractive	A hybrid process consisting of additive, subtractive and inspection processes
IDEF0	Integration Definition for Functional Modelling
ISO	International Standards Organisation
LAMM	Laser Assisted Mechanical Machining
LN_2	Liquid Nitrogen
LOM	Laminated Object Manufacturing
MIG	Metal Inert Gas
MRR	Material Removal Rate
NAS	National Aerospace Standard
NC	Numerically Controlled
Nd: YAG	Neodymium-doped Yttrium Aluminium Garnet
PCL	Polycaprolactone
PLA	Polylactic Acid
Ra	Surface Roughness
RepRap	Replicating Rapid Prototyper
RP	Rapid Prototyping
RPM	Revolutions Per Minute
SDM	Shape Deposition Manufacturing
SLA	Stereolithography
SLM	Selective Laser Melting
SLS	Selective Laser Sintering
STL	Standard Tessellation Language – a file format defining a triangulated surface of a three dimensional object
TAD	Tool Approach Direction
T_g	Glass Transition Temperature
T_m	Melting Temperature
WEDM	Wire Electrical Discharge Machining

Table of Contents

List of Figures

List of Tables

1 <u>Introduction</u>

1.1   Background

Manufacturing technology has gone through a number of evolutionary developments over the past decades (Brecher *et al.*, 2009). However, due to the technological constraints of independent manufacturing processes, it is not always feasible to produce components in terms of material, geometry, tolerance and strength etc. (Kolleck *et al.*, 2011).

Computer Numerically Controlled (CNC) machining, a subtractive process, is typically used for hard material machining, due to high accuracy and the relatively short production times achievable. Nevertheless, since a cutting tool must be carried in a spindle, there may be certain accessibility constraints or clashes preventing the tool from being positioned on the machining surface of a part. In other words, tool accessibility is a key limitation that determines part complexity that CNC machining processes can create. Injection moulding, another common process widely used, is only applicable to mass production. There costs increase exponentially when the number of items to be produced significantly decreases (Dhokia *et al.*, 2011).

In addition, additive manufacturing (AM) techniques, first introduced in late 1980s, provide the capability to automatically produce components with various part designs even with complex internal features (Levy *et al.*, 2003). AM techniques share some of the manufacturing DNA with CNC machining technology (Gibson *et al.*, 2009), such as using similar GCodes to control machine movements in the orthogonal Cartesian coordinates. CNC technology differs largely in that it is a subtractive rather than additive process, requiring a block of material that must be at least as big as the part that is to be made, whereas, in AM processes, parts are built layer-by-layer from zero. This layer-by-layer fabrication approach indicates that the shapes of cross sections of a part can be arbitrarily complex, up to the resolution of the process (Gibson *et al.*, 2009). As a result, AM processes are not constrained in the same way, and undercuts and internal features can be easily produced without specific process planning (Cheah *et al.*, 2005). Generally, the geometric complexity of AM processes far exceeds that of conventional manufacturing processes. However, a number of limitations hinder its further development, such as limited materials available, long production times, diminished surface quality and reduced

dimensional accuracy, compared to CNC machining. Moreover, the AM processes are designed to produce prototypes using filament, powder or liquid, which means parts are manufactured from zero rather than a block. This further restricts its application areas.

In recent years, the on-going industrial trend towards energy efficiency and material consumption requires new technology to be developed. As a result, the concept of hybrid manufacturing begins to emerge (Zhu *et al.*, 2013). A number of hybrid manufacturing processes have been developed, consisting of various manufacturing process in either a parallel or serial manner. However, all of these hybrid processes are still constrained by the constituent processes in terms of process capability and raw material. This is due to the lack of reasonable combinations of individual processes.

Moreover and today, process planning techniques have been widely used in various domains of production. Generally, process planning comprises of the selection and sequencing of processes and operations to transform a chosen raw material into a finished component (Scallan, 2003). It is the act of preparing detailed work instructions to transform designer's idea into a component economically and competitively (Xu *et al.*, 2011). Two basic methods are widely employed in process planning, which are manual and computer-aided process planning (CAPP). With the rapid development of computing technology, CAPP has been widely used in various domain of production (Li *et al.*, 2004). As the pivotal link between design to end product, process planning is essential and cannot be omitted. However, the majority of process planning research focuses on machining technology (Sankar *et al.*, 2008). Furthermore, the capabilities of the current hybrid processes have not been fully exploited and utilised due to the limited process planning approaches.

1.2   Research Aims

This research aims to propose a novel concept of hybrid process, which is not constrained by the individual processes capabilities and raw material in terms of shape and size. In essence it will investigate the process planning technique to enable the proposed hybrid process to accurately manufacture complex part geometries and reuse existing parts. The aims are further described with detailed objectives in sections 2.2 and 2.3, chapter 2.

1.3   Layout of the Thesis

The research in this thesis has been organised into 10 chapters as illustrated in Figure 1.1. The first two chapters are introduction, research aims, objectives and scope. Chapter 3 provides a comprehensive and critical review of the state-of-the-art in hybrid manufacturing technology, which is used to identify the research gaps and opportunities. Chapter 4 proposes a novel concept of a hybrid manufacturing process consisting of a manual process planning algorithm and decision-making logic. The requirements for such a hybrid process are specified followed by the development of an experimental methodology for realising the hybrid process production. Chapter 5 investigates a part manufacturing strategy for the hybrid process, establishing a number of rules, suggestions and criteria to be included and used in the process planning algorithm and the decision-making logic, presented in chapters 6 and 7, respectively. In chapter 6, the process planning algorithm is developed, which is able to generate static and dynamic process plans where operations are sequenced and process parameters are determined for the manufacture of complex part geometries. Chapter 7 illustrates the decision-making logic, which provides a number of manufacturing strategies for further manufacturing given existing parts with various features. The process planning algorithm and decision-making logic are based on a manual process and although automation is desirable, it has not been addressed in the thesis. Chapter 8 utilises the hybrid process developed in chapters 5, 6 and 7 to produce a number of case study parts for evaluating the process capability and demonstrating the process efficacy. In chapter 9, a number of research issues that have been raised based on the areas of investigation are discussed and suggestions for improving this research are provided. Finally the conclusions drawn from the research together with areas for potential future research are documented in chapter 10.

Introduction and Research Scope

Chapter 1: Introduction

Chapter 2: Research aims, objectives and scope

Background and Literature Review

Chapter 3: State-of-the-art in hybrid manufacturing technology

Theoretical and Experimental Research

Chapter 4: The proposed hybrid process and experimental methodology

Chapter 5: Investigation of a part manufacturing strategy for the hybrid process

Chapter 6: A generative reactionary process planning algorithm for the manufacture of complex part geometries

Chapter 7: Development of feature-based decision-making logic for material reuse

Chapter 8: Evaluation of the hybrid manufacturing process

Research Conclusions

Chapter 9: Concluding discussion

Chapter 10: Conclusions and future work

Figure 1.1 – A structured view of the thesis chapters

2   <u>Research aims, objectives and scope</u>

2.1   Introduction

This chapter defines the aims of the research together with the research objectives. The research boundaries are then established to specify the manufacturing processes and resources which are used to develop the author's hybrid process in the context of manufacture of prismatic parts. Finally, the scope of the research is identified to present the areas of investigation from design to the development and validation of the process planning approach for the proposed hybrid process.

2.2   Research Aims

The manufacturing processes currently used are constrained by their capabilities either from technical limitations, such as limited materials and complex part geometries, to excessive production costs (Ren *et al.*, 2010).

AM methods provide the capability with which to produce complex geometries, for example, internal features, which are virtually impossible to create with any other manufacturing process (Cheah *et al.*, 2005). However, a considerable number of limitations restrict its further development, such as limited materials available, lengthy production times, diminished surface quality and dimensional accuracy when compared to CNC machining.

On the other hand, CNC machining technology, a subtractive process, has become one of the predominant methods for manufacturing industrial and consumer products. It is typically used for hard material machining, due to high accuracy and the relatively short production times achievable. Nevertheless, certain features like internal cavities are still difficult to produce due to limited tool accessibility (Karunakaran *et al.*, 2010). It is also constrained by the available raw material in terms of shape and size. Traditionally, inspection has been considered as a non-value adding activity. Though, today it is seen as essential to control, monitor and maintain product and part quality, maintaining that the products are manufactured according to the specifications (Kwon *et al.*, 2005). The finished parts of which the dimensions are out of tolerance are simply scrapped, resulting in material waste, increased costs and times. The above examples indicate each

manufacturing process has its own or unique advantages but also suffers problems that constrain its applications in certain areas.

The main hypothesis of this research is that it is possible to both flexibly and accurately manufacture complex components without being constrained by the process capabilities and raw material. This can be achieved by adopting a hybrid manufacturing process together with a process planning algorithm and decision-making logic.

The aims of this research are to explore the use of the hybrid process through combining additive (i.e. Fused Filament Fabrication, FFF[*]), subtractive (i.e. CNC machining) and inspection processes to:

(a)   Enhance the flexibility of the manufacturing processes.

(b)   Improve part accuracy.

(c)   Re-use and re-manufacture parts.

This hybrid process will enable:

(1)   Complex to manufacture part geometries to be flexibly and accurately manufactured.

(2)   Existing parts or legacy products to be reused and further manufactured, transforming them into final parts.

2.3   Research Objectives

To achieve the aforementioned research aims, a number of objectives have been identified as follows:

● Review the state of the art in hybrid manufacturing technology, additive manufacturing together with process planning for hybrid manufacture, identifying the research gaps and possible combinations of different processes for achieving the research aims.

● Design an experimental methodology for determining knowledge on the hybrid process. The methodology defines the requirements for the proposed hybrid process and the overall structure of the process planning approach.

---

[*] Fused Filament Fabrication (FFF) is sometimes called Fused Deposition Modelling (FDM). However, the latter term is trademarked by Stratasys Inc., and cannot be used publicly without authorisation from Stratasys Inc.

● Develop the process planning approach, mentioned above, including a process planning algorithm and decision-making logic. This approach facilitates the manufacture of complex parts and the reuse of existing parts, using the hybrid process. The major activities involved in achieving this objective are outlined as follows:

◊ Investigate and develop a part manufacturing strategy to produce parts using appropriate process parameters for the hybrid process.

◊ Develop the process planning algorithm for the manufacture of complex part geometries in the least amount of time.

◊ Develop the decision-making logic for the reuse and remanufacture of existing parts.

● Evaluate the performance of the hybrid process and the feasibility of the process planning approach with a number of case study examples where a series of test parts will be manufactured by using the hybrid process and the process plans as generated by the process planning approach.

2.4   Research Context and the Novelty of the Research

The research has been undertaken within the context of manufacturing technologies where different manufacturing processes are integrated and interchangeably used.

The novelty of this research lies in the capability to accurately manufacture complex parts and to remanufacture parts from various raw materials in terms of shape and size.

To avoid confusion, the definitions used in this research are given as follows:

Geometrical complexity: a prismatic part has the features (e.g. internal features) that are unable to be produced by using CNC machining techniques due to cutting tool inaccessibility. In this case, the geometry of the part is considered to be complex to manufacture.

Flexibility: is defined as the ability of a manufacturing process to directly manufacture a complex part as one complete unit. Manufacturing subparts and assembling them together is not considered as flexible in this research.

*Accuracy***:** is referred to dimensional and geometric accuracy. A final part that has a high degree of accuracy to that of an entirely CNC machined part can be seen as accurately manufactured.

Manufacture of a product from its design to manufacturing stage is usually constrained by, either process capability or available raw material. In this research, the novel concept of hybrid manufacturing is proposed, which combines additive, subtractive and inspection processes in a serial manner. Incorporating an additive process releases design constraints caused by tool accessibility in CNC machining. Using CNC machining methods the final part can achieve a high degree of accuracy comparable to that of an entirely CNC machined part. Furthermore, dimensional information of the existing parts can be obtained by using an inspection technique, enabling the existing part to be further manufactured by additive and/or subtractive processes, providing new functionality. Thus the raw material constraint in terms of shape and size can be eliminated.

Table 2.1 outlines certain limitations of individual FFF and CNC processes, and compares them with the proposed unconstrained hybrid process. The symbol '√' denotes that the process is able to manufacture parts with the selected constraint.

Table 2.1 – Capability comparison of the hybrid process, individual
FFF and CNC machining processes

Constraint / Process	Raw material constraint			Design/manufacture constraint	
	Filament	Existing part – block	Existing part – random shape	Geometrical complexity	Accuracy
FFF	√			√	
CNC		√			√
The hybrid process	√	√	√	√	√

2.5 Research Boundaries

A number of research boundaries have been identified within the context to allow the research to focus on the key issues of process planning on process integration and utilisation. These boundaries are illustrated in Figure 2.1, where the rectangular boxes represent the relevant research areas and the circle highlights the research boundaries. The areas within the circle are the major focus of this research, which are defined as follows:
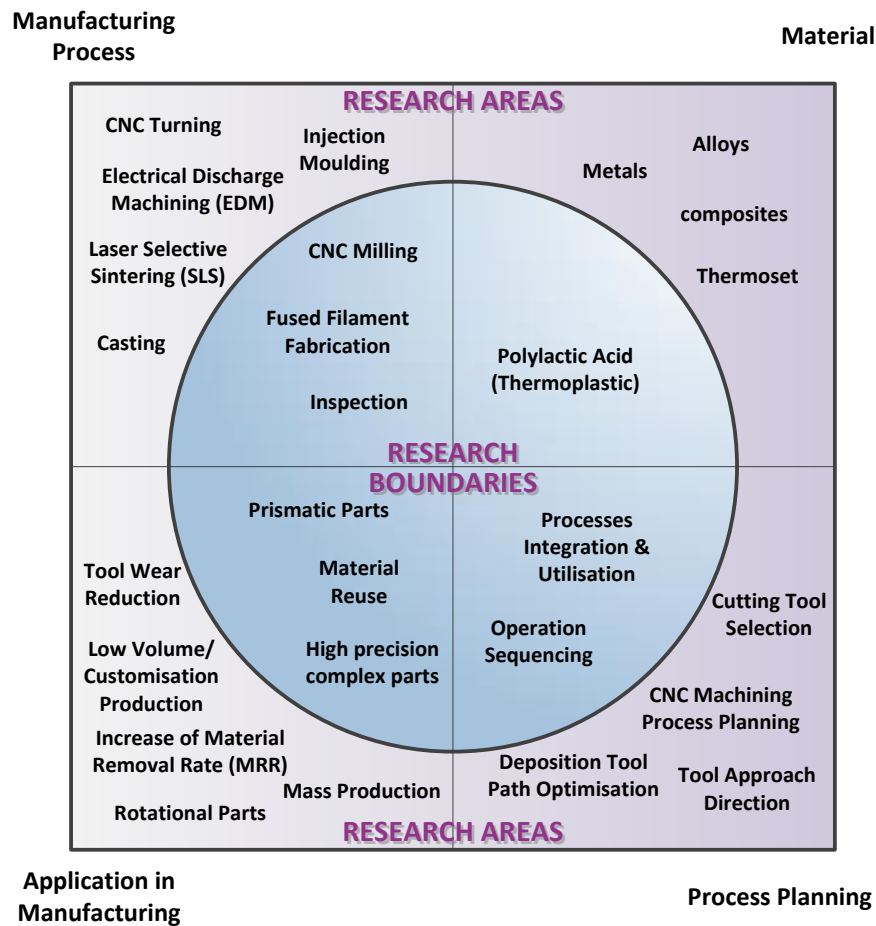
Figure 2.1 – Research boundaries within the context

2.5.1 Manufacturing process

Today, a wide range of manufacturing processes have been used for the production of various types of components. Among these processes, CNC machining technology dominates hard material manufacture. In addition, the accuracy of CNC machined parts is considerably higher when compared with that of parts produced by most of the other manufacturing processes. AM methods are considered to be the state of the art in manufacturing since they provide the capability with which to produce complex geometries, for example, internal features, which are virtually impossible to create with any other single manufacturing process.

Given that both the hardware and software of FFF is open source, flexible modifications to the hardware and software can be made. This allows the modified hardware configuration and the command codes to be well integrated in the hybrid process. Therefore, the FFF and

3-axis CNC milling processes have been chosen, which will provide both flexibility and accuracy. Inspection has also been selected as it is the bridge between CNC milling and FFF, and more importantly, it enables components to be manufactured from existing parts.

2.5.2   Material

Research relating to manufacturing techniques is a very broad area including a wide range of manufacturing processes as well as process planning techniques for manufacture of metal, plastics, composites, etc. Moreover, the manufacturing technologies for each material involve a large number of research themes. The FFF process has traditionally utilised Acrylonitrile Butadiene Styrene (ABS) and Polylactic Acid (PLA) and recently low melting point bespoke alloys have become available (Jones, 2013). Due to the process stability as well as the low coefficient of thermal expansion and glass transition temperature (T_g), the material used in this research was constrained to PLA as the main build material for demonstrating the feasibility and capability of the hybrid process.

2.5.3   Application in manufacturing

Typical CNC machined and FFF manufactured components include prismatic parts, asymmetric rotational parts and sculptured surface products etc. To focus on the research aims, prismatic parts with complexity and accuracy combined with the capability to reuse material have been selected as the main research domains.

2.5.4   Process planning

A plethora of research has been conducted within the process planning domain encompassing a wide range of topics for a number of manufacturing processes such as CNC machining (Xu *et al.*, 2011) and AM processes (Kulkarni *et al.*, 2000). Process planning for processes integration and utilisation has been targeted as the key enabler for the hybrid process to appropriately manufacture parts in terms of the processes capabilities and flexibility.

2.6   Scope of Research: Areas of Investigation

To achieve the research objectives outlined in section 2.3, the research scope is identified as follows:

2.6.1 Review of the state of the art in hybrid manufacturing

A comprehensive state of the art review will be carried out, identifying various hybrid manufacturing processes currently developed together with their applications. This review will be utilised to identify feasible combinations of processes and the research gaps.

2.6.2 Design of an experimental methodology for the hybrid manufacturing process

An experimental methodology will be designed based on the research aims, literature review and the research gaps identified. This methodology specifies the requirements for the hybrid process and defines the overall structure of the process planning approach along with the major stages for developing the approach.

2.6.3 Investigation of the part manufacturing strategy for the hybrid process

Manufacturing of any type of material, by the use of different manufacturing techniques, requires investigation of the part manufacturing strategy including the appropriate process parameters. However, the process parameters for individual additive and subtractive processes are no longer appropriate for the hybrid process due to the process interaction that affects the quality of the part produced. The appropriate process parameters will be explored and then be used in different elements within the process planning approach, forming the basis for the hybrid process.

2.6.4 Development of the process planning algorithm for the manufacture of complex part geometries

Process planning techniques are enablers for effectively utilising specific manufacturing processes. A logical **G**enerative **R**eactionary **P**rocess **P**lanning **A**lgorithm (GRP^{2}A) will be developed for integrating and utilising additive, subtractive and inspection processes, interchangeably and sequentially. It is able to generate the process plan from a given part design and specify process sequences and parameters for shop floor manufacture.

2.6.5 Investigation of the decision-making logic for material reuse

Feature-based **D**ecision-making **L**ogic (FDL) will be specified, designed and implemented with the goal of using existing parts. This logic will provide a number of available manufacturing strategies for further manufacturing the given existing part depending on the type and dimensions of the features on the existing part and final part. By using the

additive and subtractive processes interchangeably, the existing part will be transformed into the final part within the designed tolerances.

2.6.6   Evaluation of the hybrid process and the specific process planning approach

A series of case studies will be used to demonstrate the hybrid process. The process planning approach consisting of GRP^{2}A and FDL will be evaluated by manufacturing a series of test parts that cannot be manufactured solely by any existing individual manufacturing process.

2.7   Research Methodology

An experimental methodology will be developed and introduced in chapter 4. This methodology addresses the requirements for developing the proposed hybrid process, and defines the overall structure of GRP^{2}A and FDL. Three major stages for realising GRP^{2}A and FDL as well as achieving the research aims are also identified in the methodology. These three major stages are comprised of a series of experiments that are designed to develop and validate the concept of the hybrid process. As identified in sections 2.2 and 2.4, the problems in this research are (1) the inability to accurately manufacture parts with complex part geometries; (2) the inability to manufacture parts from any given raw material in terms of shape and size. A number of case studies will be used to evaluate the feasibility of the hybrid process in terms of flexibility and accuracy, and demonstrate the efficacy of GRP^{2}A and FDL.

3   State-of-the-art in hybrid manufacturing technology

3.1   Introduction

This chapter reviews the state-of-the-art in hybrid manufacturing technology. The current manufacturing processes are first classified into technologies. The research conducted over the past two decades regarding efforts to combine additive, subtractive, joining and transformative technologies are presented. The author then classifies the existing hybrid processes in academia and industry. A subsection related to process planning and particularly towards to hybrid manufacturing issue is also provided. The final part of the chapter provides a critique to highlight the advantages and disadvantages of each type of hybrid process, which is used to identify the research gaps. It should be noted that the large majority of the text in this chapter has been published by the author in Zhu *et al*. (2013).

3.2   Existing Methods for Classifying Manufacturing Processes

This section illustrates the classifications of manufacturing processes based on previous researchers' definitions. These are used to provide the basis of the author's categorisation method, forming the foundations of the review, definition and classification of hybrid manufacturing processes in sections 3.4 and 3.6.

3.2.1   Existing manufacturing processes classifications

A number of researchers have previously classified manufacturing processes, from which, two major classifications are widely adopted. The first, by Swift and Booker (2003), classifies processes into casting, cutting, forming and fabrication. The second by Kalpakjian and Schmid (2010) is more comprehensive, as they classify processes into six sub-sections with casting, machining and finishing processes similar to Swift and Booker (2003), but they have four further classes of joining, sheet metal, polymer processing and bulk deformation processes. The major difference lies in the classification of polymer processing methods containing AM processes which today are also applicable to metals.

3.2.2   Classification of manufacturing processes into technologies

Traditional classifications, such as those introduced in the previous sections, have difficulties when identifying newly developed manufacturing technologies. Consequently,

Nassehi *et al*. (2011) proposed a technology based classification method consisting of five categories, namely joining, dividing, subtractive, transformative and additive technologies.

(i)   *Joining technology*: consists of processes by which two or more workpieces are joined to form a new workpiece. Typical examples are welding and assembly.

(ii)   *Dividing technology*: dividing processes are the opposite of joining processes, for example, sawing and disassembly.

(iii)   *Subtractive technology*: subtractive/negative operations are material removal processes, by which material is removed from a single workpiece resulting in a new workpiece, such as machining operations (e.g. milling, water-jet cutting and EDM etc.).

(iv)   *Transformative technology*: a single workpiece is used to create another workpiece and the mass does not change. Forming, heat treatment and also cryogenic cooling are the examples of transformative processes.

(v)   *Additive technology*: material is added to an existing workpiece to build a new workpiece where the mass of the finished workpiece is greater than before. Rapid prototyping processes, die casting and injection moulding are the most widely used additive manufacturing processes.

3.2.2.1 *Additive manufacturing processes*

Today, AM largely refers to rapid prototyping or layered manufacturing (Gibson *et al.*, 2009). It has its origins in photo sculpture and topography that were developed in the 19th century (Cheah *et al.*, 2005). The surge in AM methods came with the development of computers in the manufacturing environment. Particularly, the ever-increasing use of Computer Aided Design (CAD) has made the development of additive manufacturing possible (Chua *et al.*, 2003). It is the use of CAD that begins the additive manufacturing process in all commercial applications. A part is modelled in a CAD program and then converted into a .STL file which converts the geometry of the CAD model into a series of polygons. A computer program that comes along with the AM machine then "slices" the model into a series of cross-sections which are subsequently built physically by the machine. All the AM processes have a common feature, namely parts are produced by adding material instead of removing material (Yan and Gu, 1996).

The number of different AM methods available has increased steadily since the first commercial machine was introduced onto the market by 3D systems in 1988 (Chua *et al.*, 2003). These methods process a variety of materials including polymers, metals, ceramics and paper. The raw materials used also come as solids (as filament, granules and powders), liquids and gases. However, a full review on AM processes as well as other individual manufacturing processes is outside the scope of this research. For the most widely used additive processes, the readers are referred to Table 3.1, which highlights the major properties of these processes. More information can be found in the book by Gibson *et al.* (2009) and the paper by Cheah *et al.* (2005). It is noted that die casting and injection moulding though traditional processes are also considered as additive processes and readers are referred to Amstead *et al.* (1987) for an overview.

Table 3.1 – Overview of commercially available additive manufacturing methods adapted from (Yan and Gu, 1996; Karapatis *et al.*, 1998; Cheah *et al.*, 2005)

Additive process	Material	Material type	Manufacturer/ research centre	Surface roughness (μm)	Tolerance (mm)	Minimum layer thickness (mm)	Build speed
Stereoli-thography (SLA)	Photopolymers	Liquid	3D Systems EOS	12.5	±0.125	0.05	Average
SLS	Thermoplastics Metal Alloys Polycarbonate	Powders	University of Texas DTM EOS KUL 3D Systems	13	±0.25	0.1	Fast
Three Dimensional Printing (3DP)	Metals Elastomers Composites Ceramics	Powders	MIT Soligen Z Corporation	50	±0.127	0.050	Fast
FDM	Polycarbonate Thermoplastics Elastomer Wax	Solid (filament)	Stratasys	12.5	±0.020	0.127	Slow
Laminated Object Manufactur-ing (LOM)	Plastics Metals Paper	Solid (sheet)	Helisys SPARX	25	±0.25	0.050	Fast
Multi jet modelling (MJM)	Thermoplastics Wax	Solid (filament)	3D Systems Solidscape	25	±0.025	0.013	Fast

Two of the most popular AM research interests lie in the areas of part accuracy and additive process production time (i.e. build time). In these two areas, investigations of distortion induced dimension deviations and estimation of build time have drawn significant research attention.

(I)   *Distortion induced dimension deviations*

The following describes state of the art research related to part distortions. Nickel *et al*. (2001) examined the effect of deposition patterns on the resulting stresses and deflections in the shape deposition manufacturing (SDM) process. Both finite element analysis and experiments show that the deposition pattern has a significant effect on the deflection of the manufactured part. The interaction between the process parameters and material properties also influence the deflection. Material properties such as dynamics of polymerisation related to the amount of volume shrinkage in the SLA process was investigated by Wiedemann *et al*. (1995). They further identified that the dynamics of polymerisation can be used to optimise hatching strategies for reducing internal stress, which in turn diminishes curl development of the part surface. Dalgarno (1996) carried out a structural analysis, modelling the curl development of the parts in the SLS process. Double sintering the first two layers was found to be an effective way to reduce the curling level. Sonmez and Hahn (1998) developed a thermo-mechanical model investigating temperature and stress distributions in each layer in the LOM process. A large roller diameter and slow roller speed are recognised as beneficial for laminate bonding, and it is suggested that these two factors could contribute to part warpage. Zhang and Faghri (1999) developed a physical model where melting a mixture of two powders with significant different melting points was explored. It was found that the porosity of the part contributes to the shrinkage, leading to distortions. The shrinkage phenomenon accelerates the melting process while the material is at fixed solid phase. Chin (2001) studied the thermo-mechanical relationship between droplet columns and adjacent droplets in the SDM process. The established model shows that the process-induced pre-heating has noticeable impact on the reduction in thermal gradients and residual stresses, which consequently reduces distortions. Xu *et al*. (2004) studied the distortion deformation of the plate parts and developed a mechanical equivalent model of resin phase change shrinkage in the SLA process. Yang *et al*. (2002a) developed a scale factor in three dimensions to compensate the distortions of the SLS components caused by the material phase changes during the

laser sintering process. The Taguchi method was applied to maintaining dimensional accuracy against the changes in the build positions and part size. The accuracy was improved by up to 24% compared with the counterparts made by other commercial machines.

Wang *et al.* (2007) simplified the factors that affect the part deformation phenomenon and therefore proposed a mathematical model where only temperature, length of cross-section and layer thickness were considered. By theoretically analysing the model, linear and non-linear relations between these factors have been obtained, indicating that the changes of each factor significantly influence the part accuracy. Zhang and Chou (2008) developed a comprehensive finite element model, which is able to simulate the FDM process involving mechanical and thermal processes. Experiments were also conducted and the results were compared with the simulation results, revealing that scan speed is the most significant factor followed by the layer thickness. In slicing Computer Aided Design (CAD) models, the inconsistent layer geometry containment where all the approximated extruded square-edged layers do not correspond to the minimum circumscribed volume results in systematic distortion (Chen and Feng, 2011). Chen and Feng (2011) proposed a layer contour generation approach, creating the minimum circumscribed extruded layered geometries. Along with the developed marching algorithm, which generates the boundary contour for each layer, the systematic distortion in AM parts can be eliminated. Yu *et al.* (2011) explored part distortions, interior quality and mechanical properties of the Laser Solid Forming (LSF) manufactured parts by using four deposition tool path patterns, namely raster, offsetin (offset from the inside to the outside), offsetout (offset from the outside to the inside) and fractal. Both finite element analysis and experiments show that the part distortions are primarily influenced by the transient temperature gradient arising from deposition patterns. The smallest deformation was obtained when using fractal pattern followed by offsetout. Vatani *et al.* (2012) employed the classical lamination theory to model mechanical properties of layers, layer shrinkage and residual stress growth during the SLA process by taking into consideration the heterogeneous property of the SLA parts. The model was then used to predict the curvature of distorted parts, identifying that increasing layer thickness results in decreased degree of distortion. It was also found that the distortion degree is proportional to part height.

(II)   Build time estimation

Research has been conducted on estimating build times for certain additive processes. Han *et al*. (2003) theoretically analysed the deposition parameters and identified that layer thickness, deposition speed and deposition road width are the major parameters that determine the build time for a FDM process. Pham and Wang (2000) discussed the interrelation between build time, roller travel speed, build height, laser scan speed, scan area and part volume in a selective laser sintering process. Subsequently an approximate build time estimation method was introduced, incorporating those key factors. In the paper by Kechagias *et al*. (2004), an algorithm for predicting build times for LOM was presented, in which the part volume and surface area and the flat area were taken into account. The prediction errors were within 7.6% of the actual build times. Instead of using an STL file to represent the part design, Campbell *et al*. (2008) proposed a build time estimator, which is able to predict build times for the Stereolithography process based on a 2D sketch with maximum 23.4% percentage of error. The build time of a part is calculated by using basic volumetric shapes in the drawing. Kumar and Regalla (2012) investigated the influence of the parameters (i.e. layer thickness, raster angle, orientation, contour width and raster width) on the build time and support material volume for a FDM process. The experimental results show that the increase of layer thickness and raster width tends to reduce the build time.

3.2.2.2 Subtractive manufacturing processes

Subtractive manufacturing processes are material removal processes which remove material from the surface of a workpiece by producing chips (Merchant, 2003). A large number of subtractive processes have been developed continuously since the 1700s and Figure 3.1 shows a range of subtractive manufacturing methods. Readers are referred to Kalpakjian and Schmid (2010) for an overview of these processes.
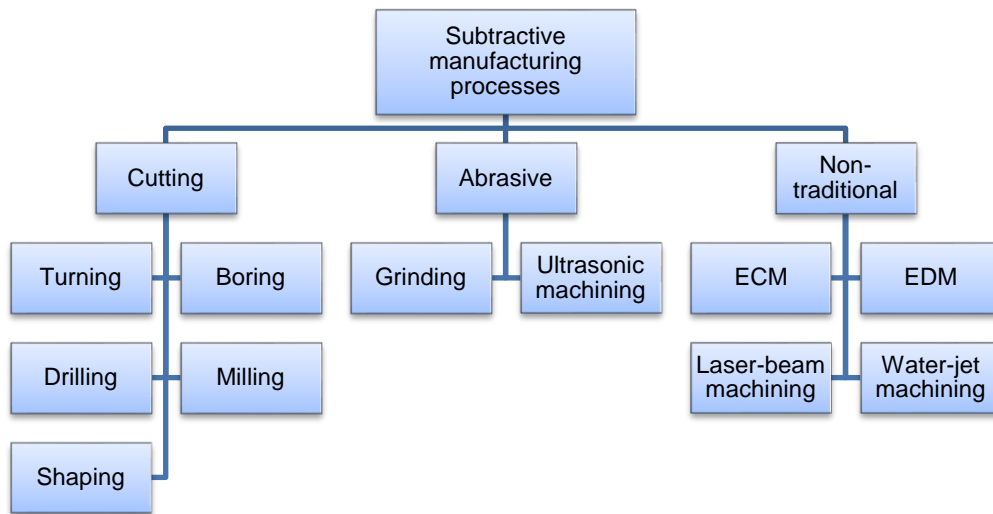
Figure 3.1 – Subtractive manufacturing processes family tree
adapted from Kalpakjian and Schmid (2010)

3.2.2.3 Inspection techniques

Precision inspection has been widely used in the manufacturing domain to ensure certain characteristics of products are in line with the specified requirements and standards (Li and Gu, 2004). For regular geometric features, contact measurements i.e. coordinate-measuring machines (CMM) or non-contact measurements i.e. laser/optical scanner can be applied to examination of part accuracy and tolerances. Certain typical inspection devices are illustrated in Figure 3.2. However, a full review on precision inspection technology is outside the research scope. The inspection technology has been reviewed by Shenghua *et al*. (2000) and Li and Gu (2004), and the readers are also referred to other PhD theses (Bagshaw, 1999; Ali, 2005; Kumar, 2008), which review the state-of-the-art inspection technology.
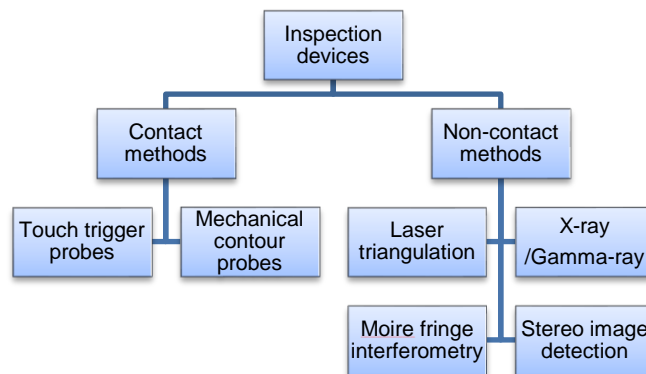
Figure 3.2 – Inspection devices adapted from Li and Gu (2004)

3.3   Definitions of Hybrid Processes in the Literature

This section briefly introduces the definitions of hybrid processes and associated nomenclature used in literature to date, to serve as an introduction to the fundamentals of hybrid processes.

It is recognised that hybrid manufacturing/processes is a vague term. Many researchers refer to the combination of different manufacturing processes as 'hybrid manufacturing' or 'hybrid processes' without a precise definition (Zhu *et al.*, 2013).

Rajurkar *et al*. (1999) described 'hybrid machining' as a combination of two or more machining processes to remove material, which is still deemed to be vague. Kozak and Rajurkar (2000) highlighted that 'the performance characteristics of hybrid machining processes must be considerably different from those that are characteristic for the component processes when performed separately'. Aspinwall *et al*. (2001) stated that the combination of machining operations may be considered either in terms of a hybrid machining method, by which two or more machining processes are applied independently on a single machine, or in terms of an assisted machining approach, by which two or more processes are utilised simultaneously. Similarly, Menzies and Koshy (2008) used 'hybrid machining process' to represent the combination of two or more machining processes with 'distinct mechanisms of material removal'. More recently, Curtis *et al*. (2009) offered a limited definition, stating that only a method, where two or more material removal processes work simultaneously, can be termed 'hybrid'.

An alternative methodology was proposed by Rivette *et al*. (2007), in which a prototype oriented definition was used to describe hybrid manufacturing as, 'the prototype is manufactured by different processes, usually the rapid prototype process and conventional process'. In terms of energy consumption, Klocke *et al*. (2010) and Nau *et al*. (2011) view hybrid processes as an approach where 'different forms of energy or forms of energy caused in different ways respectively are used at the same time at the same zone of impact'. Lauwers *et al*. (2010) stated that 'hybrid' could mean 'a combination of processes having a large influence on the process characteristics', which means hybrid processes combine active principles. Typical examples are laser assisted turning/milling (Dandekar *et al.*, 2010) and laser assisted water-jet cutting (Molian *et al.*, 2008). Moreover, Lauwers *et al*. (2010) and Klocke *et al*. (2011) also define it as 'the combination of effects that are

conventionally caused by separated processes in one single process at the same time'. In addition, Lauwers *et al.* (2010) then extended the definition, stating that 'processes should be created resulting in one or more significant process effects such as large force reductions'. Based on that, cutting through the use of high pressure coolants is also identified as a hybrid process due to a change in the chip formation (Lauwers *et al.*, 2010).

CIRP, namely the International Academy for Production Engineering (CIRP, 2011), suggested three definitions to define hybrid processes, which are:

i)   Integrated application or combination of different physical active principles e.g. laser assisted machining (Dandekar *et al.*, 2010);

ii)   Integrated combination of usually separated performed process steps e.g. stretch forming and incremental sheet metal forming (Araghi *et al.*, 2009);

iii)   Integrated machines, so called hybrid machines, that can perform different processes at one place e.g. mechanical milling and turning (She and Hung, 2008).

In 2010, CIRP refined these definitions and proposed an open definition and a narrow definition (CIRP, 2011):

i)   Open definition: a hybrid manufacturing process combines two or more established manufacturing processes into a new combined set-up whereby the advantages of each discrete process can be exploited synergistically;

ii)   Narrow definition: Hybrid processes comprise a simultaneous acting of different (chemical, physical, controlled) processing principles on the same processing zone.

In addition to this, products that have a hybrid structure or hybrid function (e.g. metal plastic composite components) are seen as hybrid products (Roderburg *et al.*, 2011) or hybrid components (Holtkamp *et al.*, 2010).

3.4   Major Research Areas of Hybrid Manufacturing Processes

The author has classified and defined the research of hybrid manufacturing processes into seven investigation areas. Each of these research areas deals with different combinations of manufacturing operations in five manufacturing categories as presented in section 3.2.2. The first three headings relate to the combinations of processes from the same category,

with the aim of enhancing process capabilities, such as material removal, tool wear and surface quality. The four subsequent headings focus on combining processes from different manufacturing categories in order to extend application areas in terms of materials and part geometry. A list of subsections is given below:

- Hybrid subtractive manufacturing processes (3.4.1)
- Hybrid transformative manufacturing processes (3.4.2)
- Hybrid additive manufacturing processes (3.4.3)
- Hybrid additive & subtractive manufacturing processes (3.4.4)
- Hybrid joining & subtractive manufacturing processes (3.4.5)
- Hybrid additive & transformative manufacturing processes (3.4.6)
- Hybrid subtractive & transformative manufacturing processes (3.4.7)

3.4.1 Hybrid subtractive manufacturing processes

A significant number of papers have reported the development of hybrid processes for integrating different machining methods as described below. These hybrid processes typically aim to achieve higher performance, in terms of MRR, surface integrity and tool wear.

3.4.1.1 Mechanical machining and Electrochemical Machining (ECM)

A few studies have been reported on applying electrochemical and mechanical machining (finishing processes) simultaneously, in which case material is removed mainly by chemical dissolve dissolution. Komanduri *et al*. (1997) reviewed chemical mechanical polishing processes and showed its effectiveness for polishing of semiconductors. Lee and Jeong (2009) conducted experiments for polishing workpieces made of copper, in which the copper ion is dissolved electrochemically in an electrolyte and followed by mechanical polishing on a single machine. However, the electrolyte contamination was unavoidable. Zhu *et al*. (2011) investigated the mechanical-electrochemical machining of small holes by ECM and grinding. Electrochemical machining is also used in the in-process machining of grinding wheels. Lim *et al*. (2002a) and Fathima *et al*. (2007) studied the mechanisms of dressing and grinding operations. The retrofitted grinding machine they developed consists of a metal-bonded grinding wheel and a dressing unit which utilises the effects of electrochemical machining processes for the in-process dressing of the wheel, as depicted in Figure 3.3.
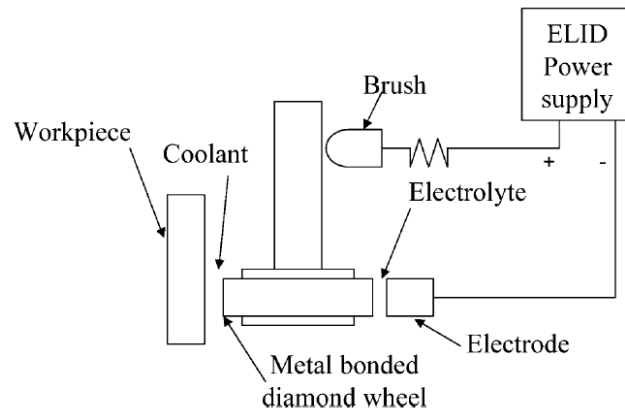
Figure 3.3 – Schematic illustration of the hybrid grinding and
ECM process (Lim *et al.*, 2002a)

3.4.1.2 *Mechanical machining and EDM*

The application of mechanical machining and EDM has enabled the exploration of
machining micro features in hard and brittle materials. Aspinwall *et al*. (2001) combined
EDM and high speed milling (HSM) by mounting a graphite electrode on the spindle of the
HSM centre to machine nickel-based alloys. An attempt has been made by Lim *et al*.
(2002b) to machine components with microstructures by turning and micro-EDM, where
turning was used for fast preparation of the thin tool electrode on-machine as demonstrated
in Figure 3.4. The micro-EDM process was used to machine micro-components by using
the turned shaft.
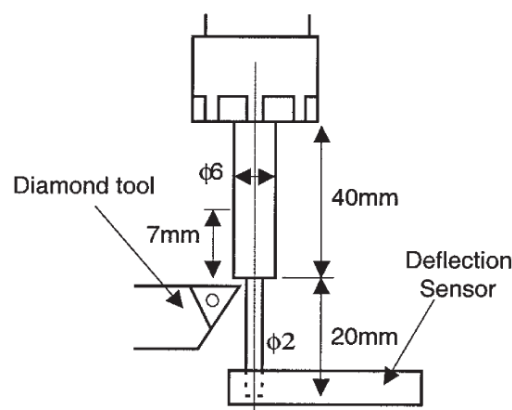
Figure 3.4 – Turning-micro-EDM process (Lim *et al.*, 2002b)

Kozak *et al*. (2003) replaced a graphite and brass grinder with a metal-bonded grinding
wheel in the electro discharge grinding process for rough machining, where the synergistic

interactive effect of the combination of conventional and electro discharge grinding realised a higher material removal rate (Kozak and Oczos, 2001). Similarly, Menzies and Koshy (2008), modified a wire-EDM process in which the original wire was replaced by a fixed wire with a number of electrically non-conductive abrasives, as shown in Figure 3.5 (a). Therefore, the workpiece was machined by spark erosion, which is the inherent mechanism of the wire-EDM process. Moreover, the abrasives abraded the workpiece, as illustrated in Figure 3.5 (b). This process is able to significantly increase MRR by up to an order of magnitude and generate surfaces with minimal recast material, in comparison to an equivalent wire EDM process. However, it can only be used for roughing operations given that the force due to abrasion would negatively influence machining accuracy.
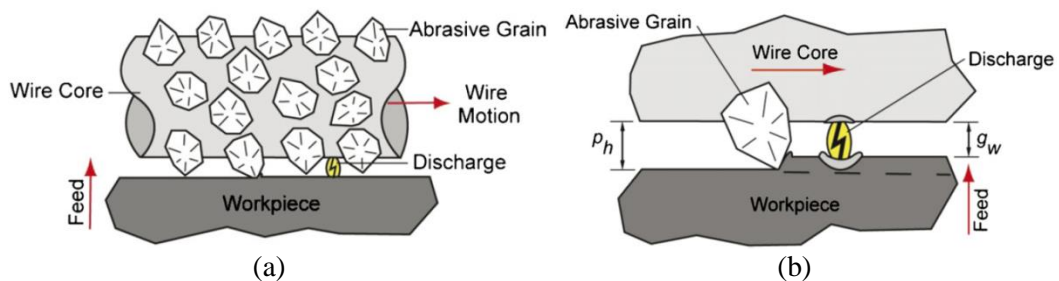
Figure 3.5 – Abrasive wire-EDM process (Menzies and Koshy, 2008)

3.4.1.3 Mechanical machining and laser cutting

As laser cutting provides high precision and zero tool wear, the resulting combination of mechanical machining and laser cutting dramatically reduces tool wear, leading to increased accuracy.

In industry, the most wide-spread application of this technology is the use of mechanical machining centres integrated with laser processing units (DMG, 2011).

In the academic literature, more variations of this technology have been identified and are recognised below. A high speed milling machine equipped with an Neodymium-doped Yttrium Aluminium Garnet (Nd: YAG) laser source has been developed by Quintana *et al* (2009), which is capable of producing micro metallic components. Li *et al*. (2005a) reported a 100% increase in MRR compared to pure laser milling, while simultaneously applying a high speed abrasive jet to the laser melted pool for removing the molten metallic material in-situ, as illustrated in Figure 3.6.
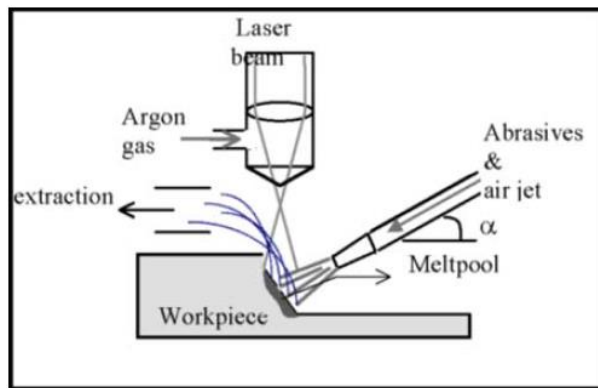
Figure 3.6 – Grit blast assisted laser milling of metallic alloys (Li *et al.*, 2005a)

Instead of using a laser simultaneously, Okasha *et al.* (2010) used a sequential laser and mechanical drill for the micro-drilling of Inconel® 718. Similarly, Biermann and Heilmann (2011) used a laser to pre-drill a pilot hole, followed by single-lip deep hole mechanical drilling on non-planar surfaces. The reduction of burr size and the increased tool life were found, by using either of these two hybrid processes.

3.4.1.4 Laser cutting and EDM

Laser cutting and EDM research concentrates on micro-machining applications for reducing production time and eliminating the recast and heat affected zone caused by laser ablation. Li *et al.* (2006) used a sequential laser and EDM for the micro-drilling of a fuel injection nozzle with a diameter of 137-140μm. Kim *et al.* (2010) applied laser cutting for rough machining of grooves and subsequently, micro-EDM was employed to finish machine the parts, therefore significantly reducing the tool wear of the electrode.

3.4.1.5 Laser cutting and ECM

This is a method that uses laser drilling with an electrochemical dissolution, which has been investigated to improve the quality of drilled holes in terms of recast layer, spatter and heat affected zones (Li and Achara, 2004). A jet electrolyte was aligned coaxially with the laser beam, where the material was removed mainly by the laser with the recast layer and spatter being dramatically reduced by the effect of ECM jet simultaneously (Zhang *et al.*, 2009a).

3.4.1.6 EDM and ECM

The electrochemical discharge machining (ECDM) process, which combines ECM and EDM on a single platform, has been studied since the 1970s (Cook *et al.*, 1973; Tsuchiya *et al.*, 1985; Chikamori, 1991). Electrical discharges between the cathodic electrode and the anodic workpiece occurs, whilst the electrochemical dissolves the workpiece (Chak and Rao, 2007). Bhattacharyya *et al*. (1999) and Schopf *et al*. (2001) successfully utilised an ECDM process in trueing and dressing of metal bonded diamond grinding wheels/tools.

3.4.1.7 Turn-mill, mill-grind

Turn-mill machine tools incorporate both a spindle for milling operations and a spindle for turning operations, and have been on the market for a considerable number of years (She and Hung, 2008). These types of machines have led to other combinations, namely mill-grind, turn-grind and turn-hone machining centres (MAG, 2010; Mazak, 2011).

3.4.1.8 Ultrasonic assisted mechanical machining

Ultrasonic assisted mechanical machining is not a new hybrid process and has been known for over 50 years (Colwell, 1956). It is the simultaneous application of mechanical machining by spindle rotation, and ultrasonic vibration by a high frequency axial ultrasonic oscillation of the cutting tool or workpiece (Markov and Neppiras, 1966).

(I)   Ultrasonic assisted grinding

A large proportion of ultrasonic assisted mechanical machining research lies in ultrasonic assisted grinding, aimed at achieving better surface integrity of ground surfaces. Uhlmann and Hübert (2007) applied the superposition method to combine a grinding operation with a secondary oscillation, by which the oscillation of the grinding tool was excited by piezoelectric oscillators. The tool was vibrating in a vertical direction while it was cutting material horizontally as shown in Figure 3.7.
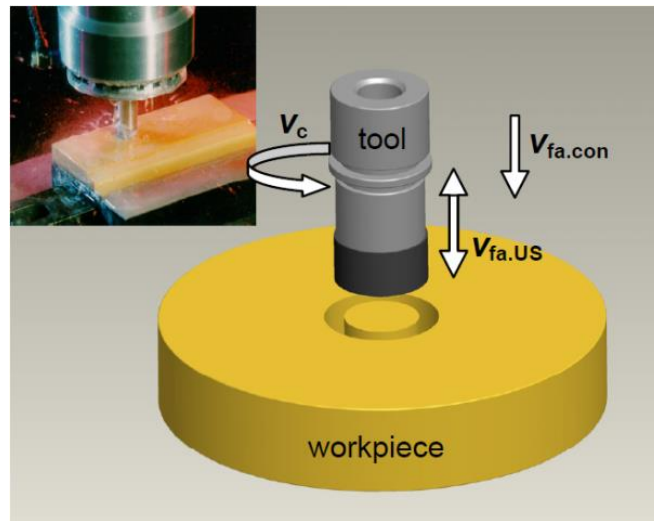
Figure 3.7 – Schematic illustration of ultrasonic assisted grinding
(Uhlmann and Hübert, 2007)

However, in the experiments by Yanyan *et al*. (2009), the ultrasonic vibration actuator was adhered to the workpiece instead of the diamond grinding tool, which led to the oscillations of the workpiece. With vibration assistance, tool wear can be reduced and Lauwers *et al*. (2008) further developed a tool path generation algorithm for machining of ceramic components, obtaining better surface quality. Brecher *et al*. (2010b) suggested a new way to design vibrating components which aims to increase MRR. From the aspect of rotary grinding, Ya *et al*. (2002) built a model for analysing MRR in ultrasonic assisted rotary grinding. Li *et al*. (2005b) designed a series of experiments to drill holes on ceramic matrix composite panels.

(II)   Ultrasonic assisted turning

In the turning of hardened steel, Klocke *et al*. (2009) used a monocrystalline diamond tool with superimposed ultrasonic linear vibration to machine moulds for optical replication. Zhong and Lin (2006) mounted an ultrasonic vibration rig onto a CNC machine tool for the turning of aluminium based metal matrix composite workpieces. Jamshidi and Nategh (2013) developed an analytical model for predicting the normal and friction forces acting on the rack face in ultrasonic-vibration assisted turning. The predicted results have also been verified in the experiments, which reveal that both the tool-chip contact length and the normal stress acting on the tool-chip interface exponentially reduce when increasing cutting speed.

(III)   Ultrasonic assisted drilling

The shortcomings of conventional mechanical drilling gradually emerge in the drilling of deep and micro holes in hard materials, in particular in the aerospace industry. By continuous frequency vibration of cutting tools during drilling operations, the quality of the deep micro-holes can be significantly improved. Azarhoushang and Akbari (2007) developed a drilling tool with high frequency and low amplitude ultrasonic oscillation for the drilling of Inconel® 738-LC, which showed a noticeable improvement in terms of average surface roughness and circularity, but, Liao *et al.* (2007) argued that the vibration amplitude of more than 12 μm is likely to result in negative effects, such as reducing tool life. Heisel *et al.* (2008) and Potthast *et al.* (2008) designed a piezoelectric actuator and a piezoelectric transducer, which was used for deep hole drilling of electrolytic copper. This indicated a decrease in feed force and drilling torque when compared to gun drilling. Although ultrasonic assistance provides superiority, there are a number of drawbacks. For instance, due to the higher tool tip temperature and variations in ultrasonic assisted drilling, Pujana *et al.* (2009) monitored feed force, chip formation and temperature in the drilling of Ti6Al4V, revealing that ultrasonic assistance offered lower feed force and higher process temperatures as compared with conventional drilling. It was also found that higher force reductions and higher temperature increments when increasing vibration amplitude. Due to high temperature that is likely to be detrimental to surface finish, Pujana *et al.* (2009) argued that the heat generation mechanism needed further study. Sadek *et al.* (2013) conducted a series of experiments based on a full factorial design to compare vibration-assisted drilling with conventional drilling in terms of cutting temperature, axial force and surface roughness. It was found that the cutting temperature and axial force were reduced by 50% and 40%, respectively. The feed was shown to be the main parameter controlling the tool temperature. The surface roughness of the vibration-assisted drilled holes does not show significant improvement. However, it was deteriorated by up to 200% while using the highest rotational speed together with the highest axial speed ratio.

3.4.1.9 Ultrasonic assisted EDM

The combination of USM and EDM has the potential to reduce tool wear and electrode deflection in EDM of micro-holes and grooves. In the paper by Jia *et al.* (1997), the mechanical signal was generated and transmitted to the tool-electrode, which was applied to remove material. On the other hand, Jahan *et al.* (2010) attempted to drill micro-holes,

where the tungsten carbide workpiece was being vibrated while the EDM process was carried out. Other studies employing similar configurations have been reported by Yeo and Tan (1999), Zhao *et al*. (2002), Huang *et al*. (2003), Sundaram *et al*. (2008) and Yu *et al*. (2009) for producing high aspect ratio of micro-holes on steel, stainless steel, titanium alloy and nitinol workpieces, respectively.

3.4.1.10 EDM and etching

A novel approach, combining wire electric discharge machining (WEDM) and anodic etching into a single process for slicing/cutting of silicon ingots into wafers has been developed by Wang *et al.* (Wang *et al.*, 2009; Wang *et al.*, 2011). Silicon ingots are sliced by using WEDM and chemical etching simultaneously. However, the surface roughness of 5 μm is considered to be unsatisfactory. Fonda *et al*. (2013) proposed a hybrid fabrication process consisting of EDM and chemical etching for producing 3D hemispherical mould features. An EDM process is first used to rough machine the hemispherical mould followed by wet isotropic etching that is conducted using HNA liquid (HF/nitric/acetic acids) to obtain a smooth and highly axisymmetric mould. Nevertheless, it was found that, applying HNA etching to the EDM machined surface leads to degradation of the geometric accuracy. This may be attributed to over-etching of the EDM finished surfaces. It has also been identified that it is not beneficial from using this hybrid process. This is because the surface machined by the individual micro-milling process has shown higher geometric accuracy than that of the surface manufactured by the hybrid process.

3.4.2 Hybrid transformative manufacturing processes

This section is concerned with the processes combined within the transformative manufacturing operations category such as sheet metal forming (Emmens *et al.*, 2010) and laser heat treatment (Zhang *et al.*, 2009b).

3.4.2.1 Sheet metal forming processes

Each sheet metal forming process has its specific application in terms of the features formed (Micari *et al.*, 2007). The combination of different forming processes enables a part to be produced with various features. Araghi *et al*. (2009) and Galdos *et al*. (2010) first employed the stretch forming process for pre-forming rough shapes. An asymmetric

incremental sheet forming (AISF) process was subsequently carried out to produce the final parts, as shown in Figure 3.8.

(a) machine set up (b) stretch forming (c) AISF
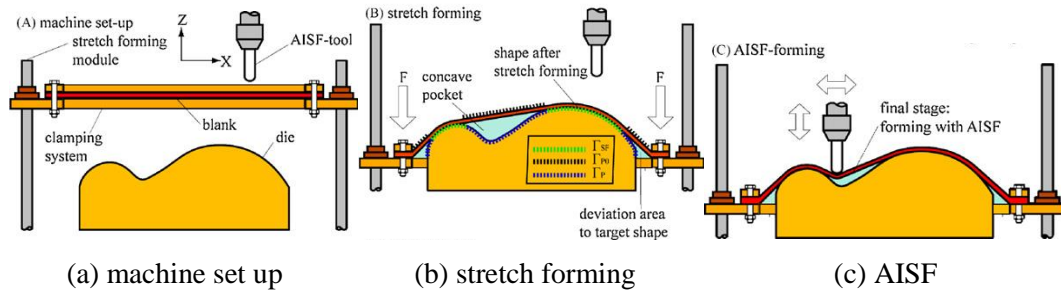
Figure 3.8 – Combination of AISF and stretch forming (Araghi *et al.*, 2009)

3.4.2.2 *Laser heat treatment and sheet metal forming*

The heat energy provided by a laser beam has been found to be effective for changing the microstructure and mechanical properties of the irradiated workpieces, facilitating the following metal forming process. Duflou *et al.* (2007) utilised a laser to heat the underside of the sheet for increasing formability in the single point incremental forming process (Duflou *et al.*, 2008). Alternatively, Biermann *et al.* (2009) used a laser beam to heat the workpiece in front of the forming tool to assist the forming process. In addition, Shen *et al.* (2006) developed a model to predict the bending angle in laser assisted incremental forming. A deep drawing process with laser assistance has been investigated by Schuocker *et al.* (1999) and Kratky *et al.* (2004). Before the drawing operation takes place, laser energy is used to selectively heat the material near the drawing edge, which is able to reduce the drawing force (Schuocker, 2001), reduce forming steps and produce deeper features than that of conventional deep drawing (Geiger *et al.*, 2004).

3.4.3   Hybrid additive manufacturing processes

The majority of additive manufacturing processes (Bingham *et al.*, 2007) can also be considered as layered manufacturing (Levy *et al.*, 2003) and in recent years laser cladding (Onwubolu *et al.*, 2007) and arc welding deposition (Jandric *et al.*, 2004) have received significant attention, especially for hybrid process research.

3.4.3.1 *Melting deposited material*

In general, there are two methods for material deposition i.e. deposit material (usually powders) and then melt them, or directly deposit melted material. In this type of hybrid

additive process, powders are pre-placed on workpiece surfaces waiting to be melted and bonded. Two different additive processes – one as a major heat contributor and another one as an additional heat energy – are applied to build the part, improving the corrosion, wear resistance as well as tensile strength of the workpiece. Ono *et al*. (2002) used a Nd:YAG laser beam as the major contributor to the welding process and an arc welding electrode was located behind the laser radiation point to increase the temperature, whereas, Zhang *et al*. (2006) and Qian *et al*. (2006) used a laser beam to act as an assistant tool rather than the plasma arc, as shown in Figure 3.9. Moreover, there are another two hybrid laser-arc welding processes with similar configurations and functions, which are (i) hybrid CO_2 laser – GMAW (MIG)[†] process (Campana *et al.*, 2007; Casalino, 2007; Bang *et al.*, 2010) and (ii) hybrid Nd: YAG laser – GTAW (TIG)[‡] process (Liu *et al.*, 2004; Song *et al.*, 2006).
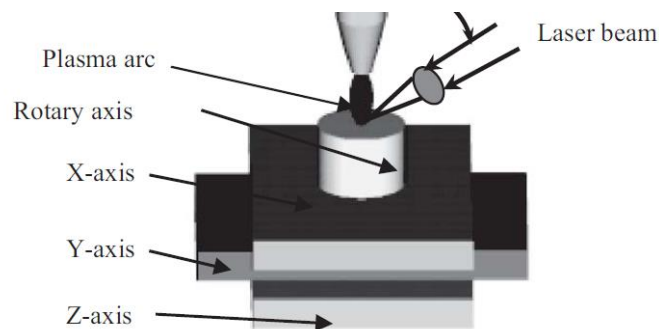
Figure 3.9 – Schematic representation of a hybrid additive process (Zhang *et al.*, 2006)

3.4.3.2 Deposition of melted material

This type of hybrid additive processes is a synergistic process able to build a part consisting of multi-materials by depositing a binder/powder mixture (i.e. one extrusion head), or by means of the depositing different materials alternatively (i.e. multiple extrusion heads).

(I) *Mixed material deposition*

Fessler *et al*. (1997) fabricated an injection moulding tool comprised of functional gradient materials, namely nickel iron alloy, stainless steel and copper, showing that the mixed material provides material properties intermediate to those of the constituent feed powders.

[†] GMAW – Gas Metal Arc Welding, MIG – Metal Inert Gas
[‡] GTAW – Gas Tungsten Arc Welding, TIG – Gas Tungsten Arc

(II)   Multi-material deposition

Allahverdi *et al*. (2000) installed two additive heads on a single machine, where two materials were extruded for the deposition of ceramic microstructures (Gasdaska *et al*., 1998). Jafari *et al*. (2000) and Safari *et al*. (2000) further investigated this process enabling up to four different materials to be deposited in a single deposition step with arbitrary geometry. As shown in Figure 3.10, the deposition unit has one deposition head with four liquefiers and each liquefier is able to deposit one material.
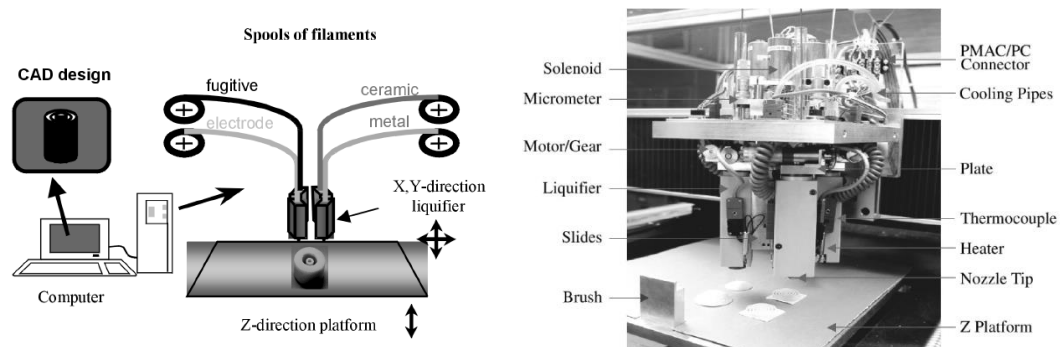
Figure 3.10 – Deposition units for multi-material deposition (Jafari *et al*., 2000)

A freeform fabrication method developed by Malone *et al*. (2004) and Malone and Lipson (2006) uses two separate deposition tools for fabrication of 3D functional assemblies with embedded conductive wiring, power sources and actuators. Other examples of simultaneously using multiple deposition tools are: Hayes *et al*. (1998) investigated a micro-jet printing process for polymer and solder deposition for chip-scale packaging (CSP) in microelectronics manufacturing; Fuller *et al*. (2002) employed multiple ink-jet deposition heads mounted on a computer-controlled 3-axis gantry to continuously squeeze nano-particles to additively build micro electromechanical systems and electrical circuitry.

3.4.4   Hybrid additive and subtractive manufacturing processes

Generally, hybrid additive and subtractive manufacturing processes methods use an additive process to build a near-net shape which will be subsequently machined to its final shape with desired accuracy by a subtractive process.

3.4.4.1 Laser cladding and mechanical machining

Certain research activities were carried out to retrofit traditional milling machines with a laser cladding unit, which aimed to utilise the flexibility of laser cladding operations and

higher surface finishes provided by milling operations, and further reduce set-up time. Jeng and Lin (2001) fabricated metal and alloy injection moulds by conducting laser cladding and milling operations in series. Choi *et al*. (2001) claimed that a reliable mechanical connection between layers was formed. Hur *et al*. (2002) used a five-axis CNC machine performing drilling, milling and grinding to machine laser cladded parts. Nowotny *et al*. (2010) further claimed that this technology has the potential to produce components for gas turbines due to high hardness and accuracy. Liou *et al*. (2001) and Zhang and Liou (2004) incorporated a laser cladding unit with a five-axis milling machine as illustrated in Figure 3.11, where any deposition feature can be built in the horizontal direction by rotating the workstation. Thus, the need for supporting material during the deposition is eliminated, further reducing build time (Ruan *et al.*, 2005). A process planning system has also been developed, which is able to generate non-uniform layer thickness and group operations (Liou *et al.*, 2007). However, the system is not able to identify the most appropriate operation sequence in terms of production time.
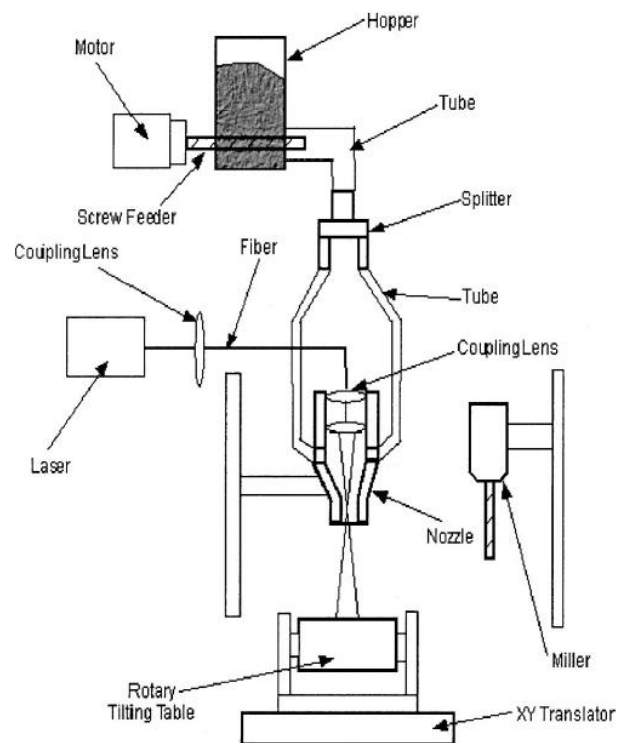
Figure 3.11 – Five-axis milling machine equipped with a laser
cladding unit (Zhang and Liou, 2004)

3.4.4.2 Arc welding and mechanical machining

The principle of this type of hybrid process is similar to laser cladding & mechanical machining, but replaces laser cladding with arc welding. An example by Song and Park (2006) utilised two GMAW guns for deposition of different materials, and CNC milling to fabricate injection mould inserts. Karunakaran *et al*. (2004), and Suryakumar *et al*. (2011) used face milling to individually machine each slice built by MIG and metal active gas (MAG) welding. The retrofitted machine is shown in Figure 3.12.
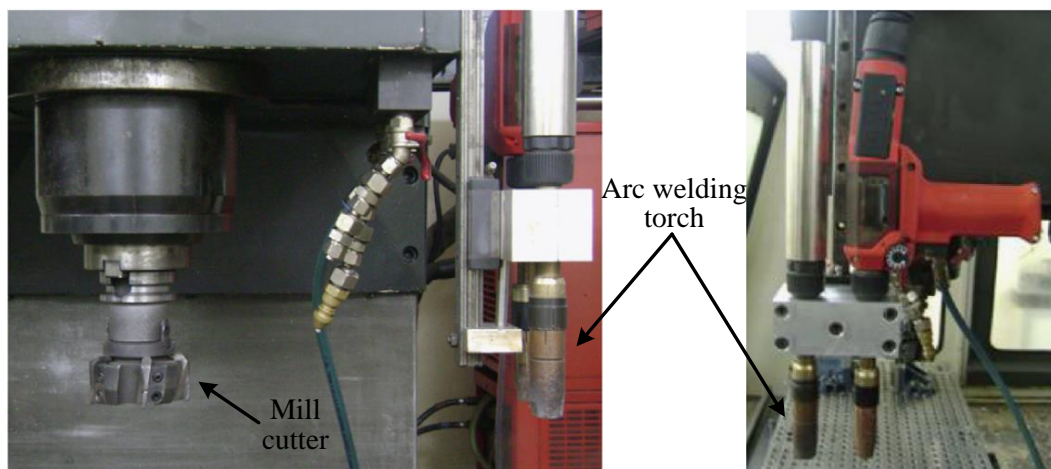
Figure 3.12 – The milling head and the welding torches: (left) front view; (right) side view adapted from Karunakaran *et al*. (2010)

However, there is no robust process planning approach developed. The hybrid process just deposits one layer followed by a face milling operation. Further layers are deposited and machined until the entire part is produced. Therefore, Karunakaran *et al*. (2008) argued that the need to face mill each layer is the major barrier for reducing production time. Furthermore, Karunakaran *et al*. (2009) pointed out that the tools fabricated by this hybrid process might be inferior to their conventional counterparts in composition and tool life. Xiong *et al*. (2009) studied the mechanism of plasma arc deposition and integrated the plasma torch on a milling machine for manufacturing double helix impeller.

3.4.4.3 Shape Deposition Manufacturing and mechanical machining

SDM has been synonymous with Stanford University from the first development phases introduced by Merz *et al*. (1994) through to their continued work (Pinilla and Prinz, 2003; Dollar and Howe, 2006). SDM deposits molten material from a container and the material solidifies almost immediately. Cooper *et al*. (1999) applied SDM by dropping to build the

near-net shape of a part, which were then cured and finally shaped into the final dimensions by milling. The SDM and machining cycle is illustrated in Figure 3.13. Lanzetta and Cutkosky (2008) utilised the combination of SDM and milling to build smooth and sculpted 3D contours of dry adhesives which could be used to aid human and robotic climbing.
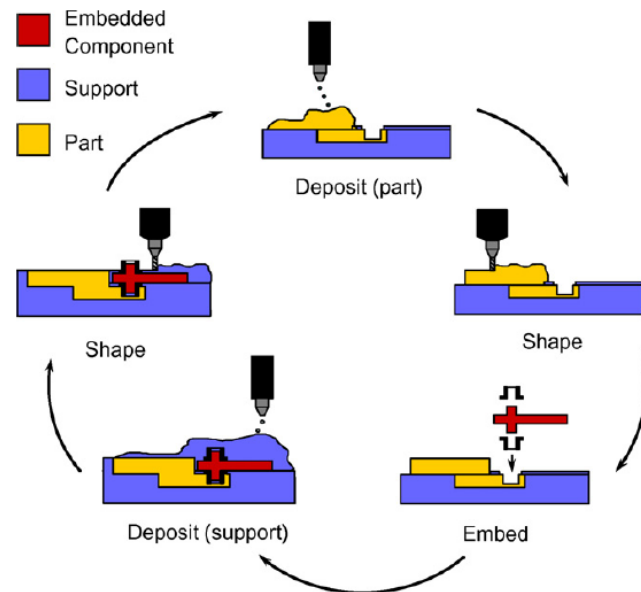
Figure 3.13 – The working procedures of shape deposition manufacturing and machining (Lanzetta and Cutkosky, 2008)

3.4.4.4 *Electroforming and polishing*

Electroforming is a variation of the electroplating process, but with moderate surface quality due to the presence of pinholes and nodules on the coating surfaces. In order to eliminate this drawback, Zhu *et al*. (2006) employed abrasive polishing operations for removing pinholes and nodules by the movement of the spherical ceramic particles filling in the space between the cathode mandrel and the anode.

3.4.4.5 *Injection moulding and milling*

Kelkar *et al*. (2005) developed a re-configurable moulding process where a part surface is approximated using an array of discrete and movable pins so as to generate the part mould cavity. By re-positioning the pins, a new mould cavity can be generated according to the change of product design, as shown in Figure 3.14. Furthermore, Kelkar and Koc (2008)

incorporated re-configurable mould tooling and multi-axis machining. After a part is moulded, multi-axis machining was conducted to improve the surface accuracy of the part.
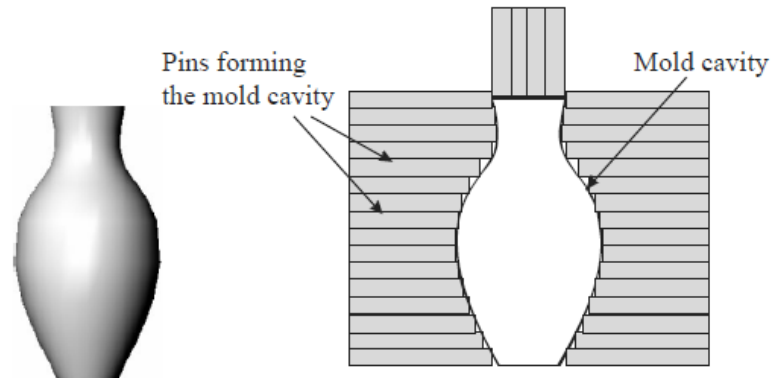
Figure 3.14 – Reconfigurable mould cavity (Kelkar and Koc, 2008)

3.4.5 Hybrid joining and subtractive manufacturing processes

This section reports on the platforms capable of performing joining and milling operations in series. Taylor *et al*. (2001) developed a method which combines CNC milling and solvent welding technology, by which a number of the solvent weldable thermoplastic sheets were welded and machined in sequence. By contrast, Kuo *et al*. (2002) developed a single platform, which combines a micro-EDM mechanism for the micromachining of the metallic parts and Nd:YAG laser welding performing the micro-assembly of parts machined, as shown in Figure 3.15. Further machining operations can be implemented after assembly if needed. However, Kuo *et al*. (2003) revealed that the cumulative errors were likely to increase during the entire hybrid process.
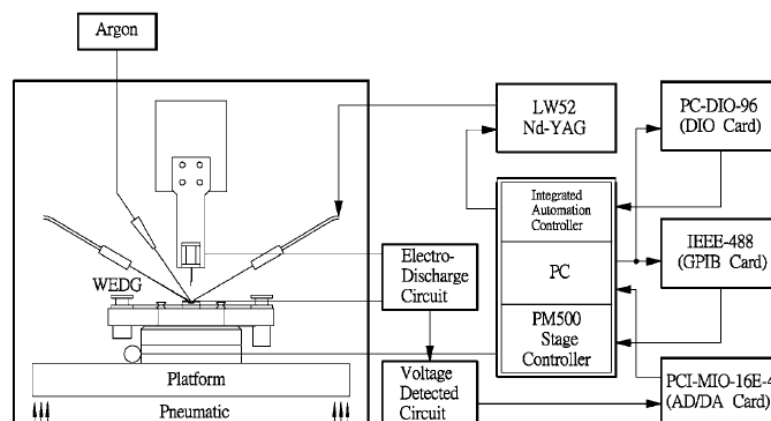
Figure 3.15 – Schematic diagram of the integrated micro-EDM and laser welding workstation (Kuo *et al.*, 2002)

3.4.6   Hybrid additive and transformative manufacturing processes

A small amount of research has focussed on the investigation of effectively applying additive and transformative processes together. Lucchetta and Baesso (2007) tested the feasibility of performing injection moulding and sheet metal forming processes. Sheet metal was inserted between the open halves of a mould, and was bent to form the desired shape while closing the mould cavity. The molten polymer material was subsequently injected into the remaining cavity with adhesion taking place between the metal and the polymer (Bariani *et al.*, 2007; Baesso and Lucchetta, 2007). Yasa *et al.* (2011) used selective laser melting (SLM) to build 2D layers and after building each layer, the same laser source was applied to heat the solidified layer as a laser erosion process, showing significant improvement in surface quality in comparison to individual SLM.

3.4.7   Hybrid subtractive and transformative manufacturing processes

In this category, most of the transformative processes e.g. laser heating are used as an assistant tool to provide better machining conditions for mechanical machining. The subsections below categorise each of the studies into the available process combinations and applications.

3.4.7.1 *Thermally enhanced mechanical machining*

Thermally enhanced mechanical machining applies external heat sources to heat the workpiece locally in front of the cutting tool. With the effect of heating, the workpiece is softened along with a change in the microstructure, facilitating the conventional machining process through the reduction of workpiece hardness, cutting forces and tool wear (Ding and Shin, 2010). The external heat sources that are most frequently used are plasma (Novak *et al.*, 1997) and laser beam (Pfefferkorn *et al.*, 2004; Anderson *et al.*, 2006).

(I)   Laser assisted mechanical machining (LAMM)

Laser assisted mechanical machining has been developed and investigated for over twenty years (Rozzi *et al.*, 2000; Lei *et al.*, 2001). Recently, LAMM has been considered as an alternative process for machining high-strength materials, such as ceramics, metal matrix composites and high-temperature alloys (Rebro *et al.*, 2002; Tian *et al.*, 2008; Bejjani *et al.*, 2011).

Laser assisted turning: Laser assisted turning is considered to be the most favourable laser integration process. This is because the cutting tool keeps stationary during the machining operation. As a result, it is relatively easy to incorporate the laser beam within a conventional turning machine (Sun *et al.*, 2010). A typical configuration of the laser assisted turning process is depicted in Figure 3.16.
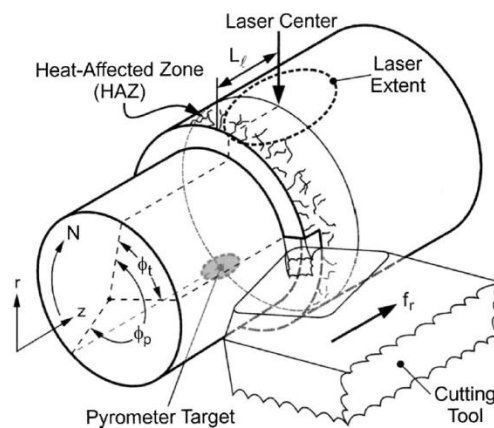
Figure 3.16 – Schematic of laser assisted turning (Pfefferkorn *et al.*, 2004)

Sun *et al.* (2010) provided a comprehensive review, summarising various laser assisted machining processes and identifying their respective materials and surface integrity limitations. For further increases in the capability of LAMM and reductions in tool wear, the researchers have identified two improvement strategies: (1) Dumitrescu *et al.* (2006) attempted to use a high power diode laser instead of a more conventional CO_2 or Nd:YAG laser, suggesting that higher machining efficiency and better metal absorption can be expected. (2) Anderson and Shin (2006) proposed a new configuration in which two laser beams simultaneously irradiate a machined chamfer and an unmachined surface adjacent to the chamfer, respectively. Researchers also realised that a better understanding of heat energy generation during the operations is able to provide optimisation methods for the hybrid process mechanisms. Therefore, research has focused on the modelling of the laser assisted turning processes. Pfefferkorn *et al.* (2005) modelled the heat distribution in laser assisted turning, illustrating that the temperature is mainly affected by laser power and feedrate. Tian and Shin (2006) also built a transient thermal model for predicting heat transfer during laser assisted turning of silicon nitride workpiece. The model has been validated by comparing the predicted results with the actual results obtained from the experiments, demonstrating that the developed model is able to predict heat transfer in

machining of silicon nitride parts. Jung *et al*. (2013) studied the thermal deformation caused by laser heat and friction induced heat in laser assisted turning of silicon nitride. The developed prediction model is able to predict thermal deformation within the average error of 9.59%. Ding and Shin (2013) investigated the effects of material removal temperature, cutting speed and feed on tool wear and surface finish in laser assisted turning of Waspaloy. A thermal model has been developed, which is able to predict the temperature fields with a workpiece undergoing laser heating. A series of experiments have also been conducted and the best machining results, in terms of tool wear, surface roughness (0.6 – 0.8μm) and cutting forces, were obtained under intermediate material removal temperature between 300 – 400 ℃.

Laser assisted milling: Laser assisted milling typically adopts one of two configurations; either the laser beam is located next to a milling tool, or it is integrated on the tool spindle (Sun *et al.*, 2010). Recently, the trend has been towards micro-machining, where Melkote *et al*. (2009) investigated the combined use of micro-milling and laser assistance grooving a hardened A2 tool steel. Brecher *et al*. (2010a) employed a similar configuration for the dry machining of Ti- and Ni-based-alloys. Singh and Melkote (2007) applied an ytterbium fibre laser to assist micro-scale grooving of H-13 mould steel and reported an accuracy improvement in the groove depth.

Laser assisted grinding: Kumar *et al*. (2011) used a laser to scan the surface of the silicon nitride ceramic workpiece, which is subsequently ground to remove the laser affected area. The experimental results indicated that the grinding forces were reduced and the tool life was increased as compared to the individual grinding process.

(II) *Plasma enhanced mechanical machining*

An approach called plasma enhanced machining e.g. turning and milling has been developed in which the plasma jet is primarily used for localised heating and softening of the workpiece to reduce cutting forces and improve surface roughness with respect to traditional machining (Leshock *et al.*, 2001). Wang *et al*. (2003) introduced the application of plasma heating in the turning of Inconel[®] 718 material. De Lacalle *et al*. (2004) used plasma gas and an electrode to generate a plasma beam in the front of a milling cutter to machine Ti6Al4V, as illustrated in Figure 3.17. A certain level of degradation level was

observed in the microstructure of the material, indicating that machining of this alloy does not benefit from using this hybrid process.
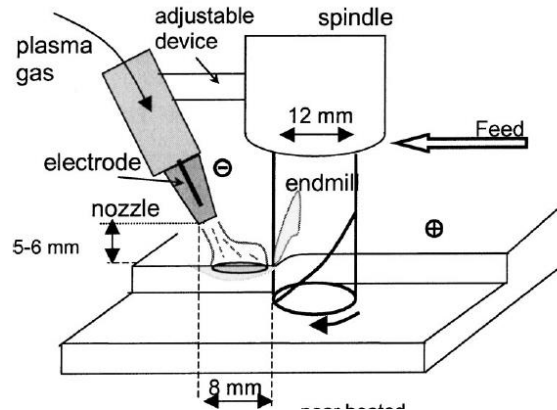
Figure 3.17 – Plasma assisted milling system (de Lacalle *et al.*, 2004)

3.4.7.2 *Laser assisted water-jet cutting*

A laser beam, again, acts as an assistant tool to pre-heat the workpiece followed by a water jet functioning as a material removal process. Molian *et al*. (2008) and Kalyanasundaram *et al*. (2008) conducted experiments whereby a CO_2 laser was used to heat a small zone on a ceramic workpiece to create a temperature gradient. Trailing in the laser beam's path, a pure water-jet was used to produce localised thermal shock fractures. Barnes *et al*. (2007) explained that the increase of cutting efficiency was due to the kinetic energy of the water jet that removes the material and washes debris away. Based on the previous research, Kalyanasundaram *et al*. (2010) established a model that was used for the determination of transient temperature and stress distribution, indicating that thermal shock stresses are primarily responsible for crack propagation and material separation.

3.4.7.3 *Laser assisted ECM*

Unlike laser drilling with chemical dissolution by Zhang *et al*. (2009a), laser assisted ECM employs a laser beam for the purposes of heating the workpiece, which helps and accelerates the electrochemical reaction. In the experiment by Pajak *et al*. (2006) and De Silva *et al*. (2011), a laser beam was coaxially aligned with an electrolyte jet, creating a non-contact tool-electrode to intensify the dissolution in the localised zone (Kozak and Oczos, 2001). Consequently, the material removal rate increased and the localisation enhanced dimensional accuracy through a reduction in stray machining action (De Silva *et*

al., 2004). This process is shown in Figure 3.18. Nevertheless, this hybrid process is not effective in machining of materials with poor electrical and thermal conductivity.
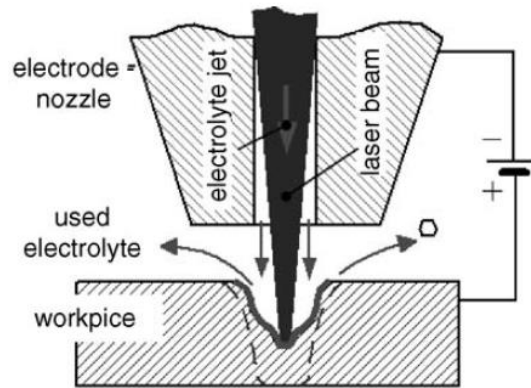
Figure 3.18 – Laser assisted ECM process (Pajak *et al.*, 2006)

3.4.7.4 Laser assisted shearing

Laser assisted shearing has been developed by Brecher and Emonts (2010), where a laser beam was applied to the underside of the shearing zone on a sheet metal plate before the cutting stamp punched the top side of the metal plate. A significant reduction in cutting forces and edge warping were achieved and punch-sheared edges with continuous clear-cut surfaces were observed.

3.4.7.5 Cryogenic machining

Cryogenic machining methods apply a cryogen, primarily liquid nitrogen (LN$_2$) rather than oil coolant, to cool either a cutting tool or a workpiece to a very low temperature e.g. -197 ℃ (Yildiz and Nalbant, 2008). The majority of cryogenic machining research can be split into two areas i.e. cooling of cutting tools and cooling of workpieces.

(I)   Cryogenic machining of hard metal materials

Traditionally, machining of hard materials, especially ceramics and superalloys, is considered to be difficult due to high tool wear rate; partially resulting from the extreme high temperatures in the shear zone (Krain *et al.*, 2007; Zhang *et al.*, 2010). Most of the papers focus on the development of a spray jet system which sprays LN$_2$ directly to the cutting zone to decrease the tool temperature, which in turn reduces the temperature dependent tool wear and increases the tool life in successive cuts (Wang *et al.*, 1996).

Turning: Hong and Ding (2001) introduced an economical cryogenic cooling system, as shown in Figure 3.19, where the LN_2 is directly jetted at the tip of the cutting tool. By the cooling effect of LN_2, crater and flank wear are reduced along with a reduction in temperature at the tip of the cutter (Hong *et al.*, 2001).
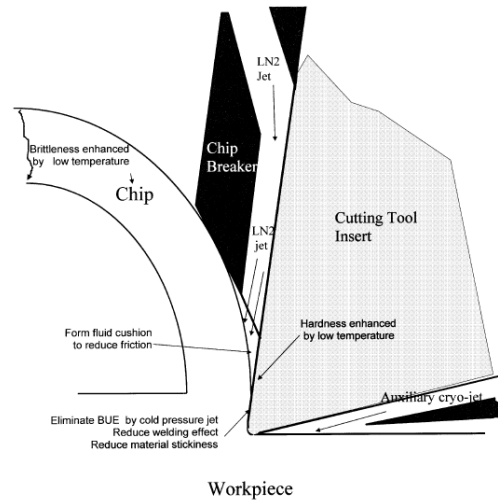
Figure 3.19 – A schematic of the cryogenic machining approach (Hong *et al.*, 2001)

Through experimentation, Wang and Rajurkar (2000) validated that the surface finish of titanium and Inconel® alloy parts machined with cryogenic cooling were far superior to those observed in conventional machining. In addition, Venugopal *et al.* (2003) developed two LN_2 jets in one system for cooling the rake surface and principal flank, tool nose and auxiliary flank, respectively. While machining hard materials, the microstructure alter (often called white layer formation) as a result of local high temperatures in the very small material deformation zone. Such an affected layer is generally considered to be detrimental to the life of the machined component. Umbrello (2013) evaluated the effect of LN_2 coolant on the machined surface alternations in machining of hardened AISI 52100 bearing steel. The experimental results indicate that utilising cryogenic coolant is able to effectively reduce white layer thickness because cutting temperatures are significantly reduced leading to inhibition on martensitic phase changes.

Milling: Goujon *et al.* (2001) conducted a series of experiments on cryogenic milling of Al alloy / AlN powders at -196 ℃ produced by LN_2, suggesting that certain chemical reactions e.g. oxidation and nitridation need to be studied. As shown in Figure 3.20, Rahman *et al.* (2003) employed two nozzles constantly supplying chilled air of -30 ℃ to the workpiece

and the cutting tool on a CNC milling machine, separately. The tool wear and surface roughness was found to be lower in the chilled air milling in comparison to the conventional milling process.
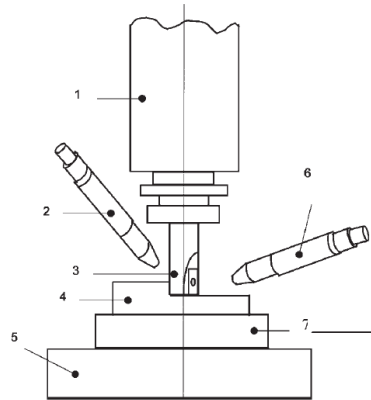
Figure 3.20 – The retrofitted milling machine with two nozzles (No. 2 and 6) supplying chilled air (Rahman *et al.*, 2003)

Grinding: There are only a few research papers reporting on cryogenic grinding (Dhokia, 2009). This may be because, originally, coolant was seldom used in conventional grinding. In the research presented by Ben Fredj *et al.* (2006), it was demonstrated that cryogenic cooling was able to improve surface integrity. Nguyen *et al.* (2007) installed a nozzle on the wheel guard providing steady LN_2 jet to the grinding point. The experimental results show that the surface hardness has been improved due to a generated martensitic layer resulting from a phase transformation during grinding.

(II) Cryogenic machining of soft materials

Shih *et al.* (2004) used solid carbon dioxide as a cryogen to cool an elastomer workpiece during machining operations. The elastomer was cooled to approximately -78.6 ℃ at which point it transformed to a brittle phase. Dhokia *et al.* (2011) developed a novel cryogenic CNC machining method, which sprays LN_2 onto the workpiece (i.e. soft elastomer) to rapidly reduce the material to its glass transition temperature. This increases the stiffness of the low-density workpiece, allowing it to be machined by conventional CNC machining methods.

3.4.7.6 *Thermally and cryogenically machining*

(I)   *Laser assisted and cryogenic machining*

Dandekar *et al*. (2010) utilised a CO_2 laser to alter the material properties of the workpiece, whilst simultaneously cooling CNC turning tools with LN_2 to improve the machinability of titanium alloys. It was reported that 200% increase in tool life was achieved. In the meantime, no discernible difference between the microstructures of the parts machined by the hybrid process and the conventional turning process was observed.

(II)   *Plasma enhanced and cryogenic machining*

Based on plasma enhanced machining, Wang *et al*. (2003) designed a cooling chamber which supplied LN_2 for cooling the cutter during the plasma enhanced turning of Inconel® 718, as shown in Figure 3.21. The surface roughness of 2.35μm was obtained. The tool life was prolonged due to the reduction in temperature-dependent tool wear.
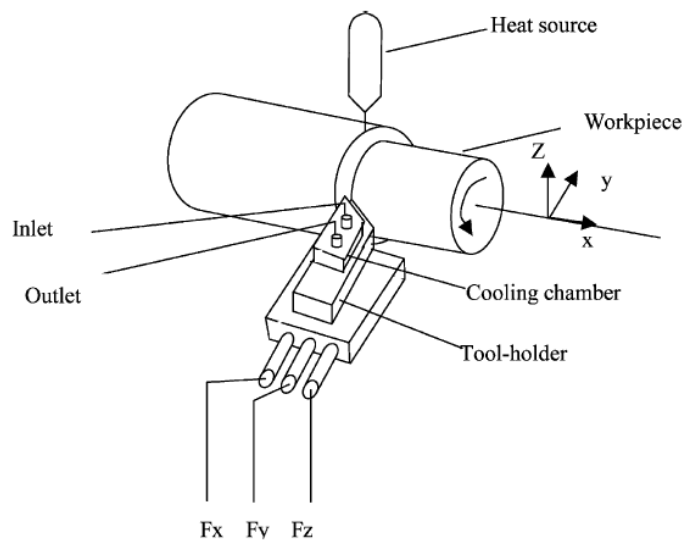
Figure 3.21 – The plasma and cryogenically enhanced machining (Wang *et al.*, 2003)

3.4.7.7 *High pressure cooling assisted mechanical machining*

High pressure cooling (HPC) has been recently found to be an effective way to improve machining conditions in terms of cutting force, chip formation and tool life. Coolant was delivered under pressures of 11 MPa during the drilling and turning of Ti6Al4V and Inconel® 718 by de Lacalle *et al*. (2000). Sanz *et al*. (2007) and Kramar *et al*. (2010)

compared the experimental results of turning titanium alloys with and without HPC, claiming that HPC could provide longer tool life, lower cutting forces and increased chip breakability. In addition, Nandy *et al*. (2009) argued that using water-soluble oil coolant, instead of neat oil coolant, is beneficial in terms of improving cutting tool life. Conversely, Ezugwu *et al*. (2005) studied the effects of using different cooling pressure and suggested that higher cooling pressure does not always lead to higher tool life. Sorby and Tonnessen (2006) revealed that high pressure rake face cooling is likely to result in adverse effects for other parts of the workpiece surface.

3.4.7.8 Grinding and hardening

Brinksmeier and Brockhoff (1996) proposed a concept of the grind-hardening process, where the grinding wheel acts as moving heat source, by which the temperature of the workpiece surface was raised above that of austenitisation. Along with self-quenching via heat dissipation, occurring naturally or through the use of coolant, martensitic phase transformation takes place (Salonitis and Chryssolouris, 2007). Salonitis *et al*. (2008) also claimed that grind-hardened cylindrical parts have high hardness.

3.4.7.9 Milling and forming

In deformation machining, as identified by Smith *et al*. (2007), thin features are machined to the desired accuracy by milling. Forming operations are then carried out to create deformations of the thin sections by bending or stretching the features to finally form the designed shapes, as illustrated in Figure 3.22. This hybrid process provides a less expensive way to create sheet metal parts without dies.
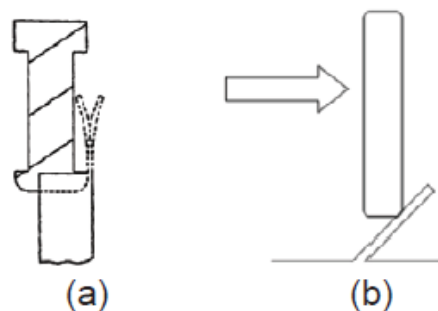
Figure 3.22 – (a) Milling (b) and deforming a thin wall (Smith *et al.*, 2007)

3.4.7.10 Turning and rolling

Hybrid machines which are able to perform turning and cold rolling operations have been reported (Axinte and Gindy, 2004; MAG, 2010). A cold rolling unit is integrated on a turning machine, enabling the gears to be turned and rolled in series, indicating the potential to reduce production cost and time.

3.5   Review of Process Planning for Hybrid Manufacture

This section briefly introduces CAPP history and two major process planning methods, and then reviews the state-of-the-art process planning methods for hybrid processes.

3.5.1   Evolution of CAPP

The desire to increase quality and reduce lead time and cost, or to improve productivity, has led to a widespread interest in CAPP (Halevi and Weill, 1995). CAPP's inception dates back to the mid-1970s (Newman *et al.*, 2012). Since the concept of using computers to help engineers to plan manufacturing operations first introduced by Niebel (1965), vast amount of CAPP research has been conducted during the past decades (Xu *et al.*, 2011). Amongst CAPP research, one of the major pioneers was Wysk (1977) who outlined an automated process planning and selection program entitled APPAS. Weill *et al*. (1982) and Alting and Zhang (1989) reviewed numerous developments of CAPP systems in the 1970s and 1980s, respectively. The computer integrated manufacturing (CIM) systems push of the 1990s saw commercial CAPP systems being integrated within CAD/CAM and tooling systems (Maropoulos, 1995) for micro-process (machine level) planning together with macro process planning linking process planning and production planning and control (ElMaraghy, 1993). Along with these commercial CAPP system developments, Artificial Intelligent and Knowledge Based techniques (Kiritsis, 1995) combined with CAPP research in design and manufacturing features (Case and Gao, 1993) was investigated in academia. In the review by Marri *et al*. (1998), it was identified that the number of CAPP systems was significantly reduced since the 1980s. Today there is an emerging need to integrate process planning and other factory software systems to enable real time planning and decision-making based on the current and predicted status of the factory shopfloor.

3.5.2   Variant and generative process planning approaches

Two major approaches, namely variant and generative, are used in the structure of process planning systems (Chang and Wysk, 1984). They are outlined as follows:

A variant process planning system uses the similarity among components to retrieve existing process plans (Scallan, 2003). A process plan that can be used by a family of components is called a standard plan. A standard plan normally contains at least a sequence of manufacturing operations. When a standard plan is retrieved, a certain degree of modification is usually made so as to adjust the plan and make it appropriate for a new part.

By contrast, in the generative process planning approach, the manufacturing knowledge, equipment capabilities and geometric vision of the part are stored in the computer programs. Process plans are generated by means of technology algorithms, decision logics, formulae and geometry base data to perform uniquely the many processing decisions for converting a part from raw material to the finished state (Halevi and Weill, 1995). A unique process plan for manufacturing a specific part is automatically generated without referring to any previous part plan.

3.5.3   Process planning for hybrid manufacture

Very limited research on process planning for hybrid processes has been reported. These reports though identifying process planning approaches have been developed for specific hybrid processes.

Jeng and Lin (2001) developed control software for the hybrid process of milling and laser cladding. Once one cladding operation was completed, the workpiece was moved to the position beneath the milling head for finish machining. The machined workpiece was moved back to the laser zone for adding the next layer. This process planning approach was used in other hybrid processes consisting of milling and laser melting or arc welding (Choi *et al.*, 2001; Akula and Karunakaran, 2006; Xiong *et al.*, 2009). Hu and Lee (2005) developed a concave edge-based part decomposition method for the hybrid process of milling and sheet welding. A part is decomposed into layers by considering the tool accessibility, the total number of layers, and the allowable sheet thickness. Based on a given build-up direction, the undercut edges, which cause a part to be inaccessible by a

cutting tool, are divided into two parts for eliminating these undercut edges. Ruan *et al.* (2005) proposed a process planning method which was able to generate non-uniform layers and tool paths and sequence operations. Thick layers are used when high part accuracy is not required. Operation sequencing is conducted by taking cutting tool accessibility (i.e. tool length) into account, which means each machining operation can be carried out if the tool spindle does not collide with the deposited part. Liou *et al.* (2007) further extended Ruan *et al.*(2005)'s work, developing an automated process planning system. This system planning uses STL models as input and generates a description that specifies contents and sequences of operations for the hybrid process of 5-axis milling and laser melting. The results consist of the decomposed subpart information and the build/machining sequence. However, this system is unable to deal with complex part geometries as the tool approach direction (TAD) and deposition nozzle accessibility. Karunakaran *et al.* (2010) investigated a process planning approach which uses an edge approximation slicing strategy to calculate each slice thickness to be deposited with the required metal as successive layers from the lowest to the topmost layer. It also generates Numerically Controlled (NC) codes for machining the deposited metallic layers to attain the required contour profile shape.

Moreover, some efforts have been made on process optimisation. Mognol *et al.* (2006) conducted a topologic and dimensional analysis, suggesting suitable features that can be beneficial from being produced by laser cladding or high speed milling. Another method used to estimate manufacturing complexity has been presented by Kerbrat *et al* (2010), which utilises an Octree concept to represent a three-dimensional object by the division of space into small cubic cells or small parallelepipeds. The features are manufactured separately and finally assembled.

3.6   Discussion and Critique

The previous sections provide a comprehensive review on hybrid manufacturing research. The author has classified a range of hybrid processes referred in this chapter, into seven major areas. In addition the author has developed his own classification, which is used in the following subsections to define the term 'hybrid processes', and to structure a critique of research gathered, and identify a number of research gaps.

3.6.1 Definition of hybrid processes

The author's classification of hybrid processes is shown in Figure 3.24. This consists of four hybrid and three sub-hybrid types. From the author's viewpoint, the term 'hybrid manufacturing processes', or 'hybrid processes' for short, is defined as an approach that combines two or more manufacturing operations, each of which is from different manufacturing technology, as introduced in section 3.2.2. The constituent processes influence and interact with each other. This can be achieved from the processes being carried out simultaneously or in a serial manner on a single platform.

To clarify this definition, the following statements are made:

(i)   As hybrid manufacturing is mainly concerned with the combinations of different manufacturing technologies, if all of the constituent processes are from the same manufacturing technology, this type of combination is defined as a sub-hybrid process.

(ii)   Constituent processes should influence or interact with each other. For example, in laser assisted turning (Sun *et al.*, 2010), the laser beam softens the material, which generates the influence that makes the turning easier and faster. Additionally, in laser cladding and milling (Zhang and Liou, 2004), the milling machine removes material from the near-net shape produced by laser cladding; on the other hand, the new layers are deposited on the smooth surface produced by the milling operations, which reduces the stair effects in the laser cladding process. The dimensions of the milled part also affect the subsequent stages of the laser cladding process. This exemplifies the laser cladding's influence on the milling operations.

(iii)   Constituent processes should directly act on the workpiece being manufactured.

Based on the above description, magnetic field assisted finishing (Riveros *et al.*, 2009; Yamaguchi *et al.*, 2010) is not considered as a hybrid process. This method uses the alternating magnetic field to drive the magnetic fluid which contains abrasive slurry, to flush mirror chips in the micro-pore x-ray mirror fabrication process (Yamaguchi *et al.*, 2011). However, the magnetic field actually drives the fluid but the field does not directly work on the workpiece. Similarly, using robot(s) to hold milling cutter(s) in the machining operations (Chen and Song, 2001; Yang *et al.*, 2002b) is not considered as a hybrid process.

In addition, water-jet guided laser cutting (Li *et al.*, 2003; Kray *et al.*, 2007), where the water-jet guides the laser beam before the beam reaches the workpiece surface, is not categorised as a hybrid process, as the jet itself does not change the microstructure of the workpiece or remove the material.

3.6.2   Hybrid subtractive manufacturing processes

Hybrid subtractive manufacturing processes normally involve thermal, chemical, electrochemical and mechanical interactions (Molian *et al.*, 2008). As shown in Figure 3.23, the vast majority of research activities have focused on the combinations of subtractive processes, which have gradually been used to reduce tool wear and production time, and increase machining efficacy through tight tolerances and high levels of surface finish. The implementation of ultrasonic assisted mechanical machining or EDM showed higher machining efficiency than that of the individual mechanical machining, ultrasonic machining and EDM. Similarly, the integration of laser cutting and EDM (Li *et al.*, 2006) facilitates drilling of micro-holes with lower tool wear and better surface quality. These advantages are gained by carrying out the processes simultaneously (e.g. laser cutting and ECM (Zhang *et al.*, 2009a) or in series (e.g. sequential laser drilling and mechanical drilling (Biermann and Heilmann, 2011). It is noted that hybrid subtractive processes are not only applied in the conventional machining scenarios, but also in other application areas e.g. micromachining (Lim *et al.*, 2002b) and in the production of semiconductors in the photovoltaics industry (Wang *et al.*, 2008).

Although encouraging results have been shown, certain issues still need to be resolved. In ultrasonic assisted machining processes, high frequency and amplitude vibration mechanisms are likely to deteriorate the surface quality and the dimensional accuracy of the machined parts (Jahan *et al.*, 2010). In conjunction with this, the machining energy only decreased 10%. In addition, with its high precision, laser processing has the potential to be incorporated in wider application areas. Thus, more research effort will continue to be made in ultrasonic and laser related processes.
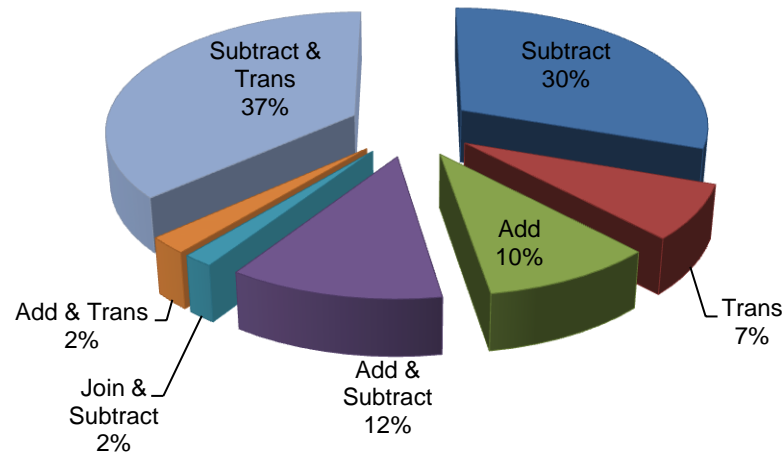
Figure 3.23 – Distribution of the collected hybrid research papers

3.6.3 Hybrid <u>transformative</u>, <u>additive and transformative</u>, <u>subtractive and joining</u> manufacturing processes

There is limited research work reported on each of these three categories. In hybrid transformative processes, two types of sheet metal forming processes were used in series, which improved the accuracy and decreased the forming steps. The use of laser heat treatment with forming tools is a popular machine configuration as the laser beam is able to soften material, increasing formability at higher temperatures as well as reducing springback effects (Duflou *et al.*, 2007). There is an emerging research trend that integrates a laser unit inside a forming tool, which has the potential to effectively utilise the laser beam in the forming processes where the working spaces are enclosed e.g. deep drawing.

The development of hybrid additive and transformative process is still at an early stage. Yasa and Kruth (2008) identified that, in the laser melting and erosion, longer processing times led to lower productivity, which restricts its further development. Lucchetta and Baesso (2007) used a mould to perform the sheet metal forming and injection moulding of sheet metal-polymer composites, providing a new method to produce multi-materials components. However, the feasibility of using the injection mould as a forming tool needs to be further validated.
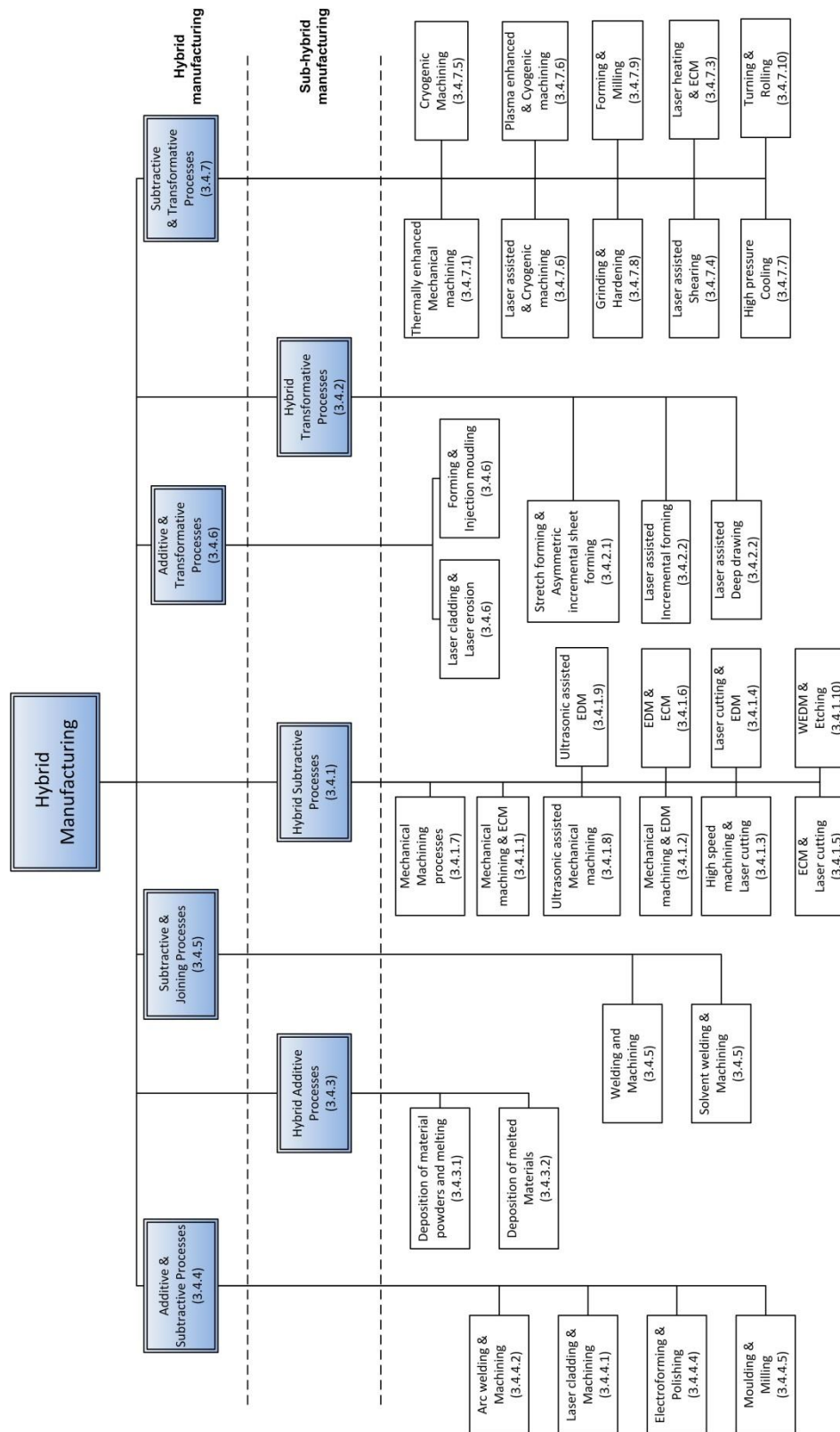
Figure 3.24 – Classification of the major hybrid processes research areas (corresponding section numbers are in brackets)

With regards to hybrid subtractive and joining processes, the machining operations enhance the capability of the welding processes by providing a high level of surface finish. However, cumulative errors are likely to increase over the whole operation (Kuo *et al.*, 2003).

3.6.4 Hybrid additive manufacturing processes

Researchers, who aim to fabricate functional parts comprised of multi-materials, apply a hybrid additive approach, which is able to deposit various materials alternately via the mounted additive heads. Another building approach uses different material powders mixed using a user-defined ratio. As a result, the manufactured parts have new properties intermediate to their constituent materials. In addition, researchers also employed an additional heat source to provide higher energies in the laser cladding and arc welding processes, which accelerated the deposition speed, reduced production time, and more importantly, increased welding stability (Ono *et al.*, 2002). It was also noted that the change of additional energy input remarkably influenced the precision of the layer deposition (Qian *et al.*, 2010). Hence, the investigation of appropriate energy input will receive research attention to some extent. Moreover, it is necessary to point out that hybrid additive processes, based on additive manufacturing techniques, also have inherited their drawbacks, which are slower production times in mass production, moderate surface finish and relatively high cost compared to CNC machined parts. Thus, these issues hinder a broader application of this technology. The improvement in surface roughness and the reduction of production cost will continue to be a major area of further development.

3.6.5 Hybrid additive and subtractive manufacturing processes

The research relating to hybrid processes combining an additive process and a subtractive process concentrates on the increase in manufacturing flexibility with no detrimental effect on surface finish (Choi *et al.*, 2001). Two deposition methods are mainly utilised i.e. laser cladding and arc welding to build near-net shapes directly from CAD models. Meanwhile, a machining process is implemented to ensure dimensional accuracy and eliminate the stair effects after certain layers have been deposited. Finally, the near-net shapes are finish machined to their desired surface finish.

However, this hybrid technology is currently only suitable for small batch production of customised products rather than for mass production. The review has revealed that the

main application is in the production of injection moulds and dies. Other applicable products are limited and it should be noted that the fabricated tools may be inferior to their counterparts produced by conventional machining in terms of tensile strength and tool life (Akula and Karunakaran, 2006). In addition, the restrictive range of materials that can be used for additive processes partly contributes to the limited application areas of hybrid additive and subtractive processes. It is expected that future research will focus on exploring broader application areas, which may include a migration towards the use of metallic and other hard materials alongside the development in rapid prototyping technology.

3.6.6   Hybrid subtractive and transformative manufacturing processes (HSTMP)

Thermally enhanced machining and other laser assisted machining processes, such as the water-jet, have generated significant research interest. In these processes, only one of the participating processes directly removes the material. The other one assists in the material removal operations by changing the machining conditions, which is beneficial for cutting processes (Molian *et al.*, 2008). The author has identified that the research in this category largely focuses on the machining of hard-to-machine materials e.g. ceramics, composites and superalloys. The experiments by Pfefferkorn *et al.* (2004) and Dandekar *et al.* (2010) reported that the cutting tool life can be prolonged by up to 3 times and the material removal rate can be effectively increased.

However, the tremendous advantages notwithstanding, HSTMP does not increase the flexibility of the original machining process. In other words, if a part cannot be machined by conventional CNC machining processes due to tool inaccessibility, likewise, HSTMP will not be able to manufacture it. Further efforts should be made for developing thermally enhanced machining with the capability of machining ductile materials (Sun *et al.*, 2010). Some researchers have been working on the effects of a laser beam input angle and heated area, and have initially identified that these two factors influence the machining efficiency. There is a possibility that future research will focus on these issues. Moreover, for a better understanding of HSTMP mechanisms, modelling of heat transfer is another potential major research topic.

Recently, cryogenic machining has drawn attention as it enables both hard and soft materials to be machined under desirable machining conditions such as lower forces and

temperature. Through cooling the cutting tool using LN_2, tool degradation can be significantly reduced and thus cryogenic machining can increase tool life (Shokrani *et al.*, 2012). The improved surface finish, increased length of cut and reduced cutting force have also been reported.

In summary, cryogenic machining is under investigation and the majority of research focuses on turning of hard material. However, less attention is paid to milling and grinding operations which are also significant in today's CNC manufacturing industry. There is also a lack of knowledge in the machining of soft materials with the exception of Dhokia *et al*. (2010). These issues require further research. With respect to high pressure cooling, research is likely to concentrate on coolant system cost and set-up times (Shokrani *et al.*, 2013).

3.6.7   The importance of hybrid manufacturing research

As discussed above, the research of hybrid manufacturing has gained significant attention both in academia and industry. The importance of hybrid manufacturing processes may be briefly summarised using two key points: (1) conventional manufacturing processes have inherent advantages and disadvantages; (2) some new products cannot be manufactured by using individual conventional manufacturing processes. In other words, it is more feasible to manufacture such products by utilising hybrid processes due to heightened process capability, production time and costs. Some typical and representative examples are outlined below.

• Conventional deep micro-hole mechanical drilling of Inconel® 718 is a time consuming process. A noticeable improvement in terms of circularity was observed and 50% increase of MRR was reported whilst using combined mechanical drilling, laser and ultrasonic vibration technologies (Okasha *et al.*, 2010; Liao *et al.*, 2007).

• On the other hand, recast layer and spatter cannot be completely eliminated if an individual laser drilling process is used. The combination of laser drilling and ECM provides a solution to dramatically reduce recast layer (Zhang *et al.*, 2009a).

• In order to increase tool life, reduce cutting forces as well as obtain better surface finish in mechanical milling, turning and grinding of hard materials (e.g. ceramics, H-13 mould steel, Ti and Ni-based-alloys and Inconel® 718), the concepts of ultrasonic assisted

machining and thermally enhanced mechanical machining have been proposed (Brecher *et al.*, 2010b; Sun *et al.*, 2010).

• EDM process has been widely used in the machining of tungsten carbide and stainless steels, but electrode deflection restricts its further development. Ultrasonic assisted EDM is capable of machining those hard materials with reduced electrode deflection effect (Jahan *et al.*, 2010).

• Long production time is always the major concern in forming processes. Laser assisted sheet metal forming has shown the advantages in improving material formability and more importantly, reducing forming steps (Duflou *et al.*, 2007), which results in reduced production time.

• Making mould inserts is not an economical process for low volume production, but now the costs can be significantly reduced by combining laser cladding and CNC machining (Jeng and Lin, 2001). The manufacture of components for gas turbines is another potential application area for this hybrid process (Nowotny *et al.*, 2010). Furthermore, biomimetic robotics with embedded sensors and circuits can also be produced (Dollar *et al.*, 2006), which was previously considered to be impossible without further assembly operations.

• Recently, a low cost process namely, cryogenic CNC machining, for the production of personalised shoe insoles has been developed (Dhokia *et al.*, 2008), replacing injection moulding processes in the production cycle. This hybrid process has the potential to be widely used in low volume and personalised soft material product manufacture.

3.6.8   Research gaps

Based on the above discussion, a number of research gaps have been identified as follows:

- Lack of a clear definition of hybrid manufacturing processes.
- Limited materials that are available to be used in the hybrid processes. Each hybrid process is constrained in a small range of the specific materials.
- The majority of the hybrid process research has been carried out on enhancing the capability of the individual processes such as reduced surface roughness and improved machinability. However, these approaches do not address the issue that constrains the

application of the manufacturing processes in manufacture of complex part geometries due to the lack of process flexibility.

- Although a vast amount of research has been conducted on developing the hybrid processes which combine additive and subtractive processes, limited process planning approach has been reported. Thus, the developed hybrid processes are only able to deal with very specific applications and their validity fails while applying these hybrid processes to manufacturing other parts with various structures, particularly complex geometries. Additionally, process plans have not been well organised in terms of process capability, flexibility, production times and costs etc. In the meantime, for the hybrid processes where the constituent individual processes are being carried out simultaneously (such as laser assisted machining) rather than interchangeably, there has been no need for process planning since the secondary process is only used to assist the primary process that is actually applied to creating the majority of the part geometries and features.

- The potential of the hybrid additive and subtractive process is underutilised in the current manufacturing environment. To the author's knowledge, the current manufacturing processes are always constrained by the available raw materials in terms of shape and size. The application of such hybrid processes on material reuse has not been thoroughly explored, also due to the lack of process planning techniques.

- There is a need to establish the relationships between constituent processes and their respective control systems. This will largely determine the development of hybrid processes in the future.

4   The hybrid process and experimental methodology

4.1   Introduction

This chapter provides the author's view of the hybrid process and the experimental methodology. It is divided into 3 major sections, consisting of the proposed hybrid process, the requirements and the methodology for realising this hybrid process for manufacture of complex parts and reusing material. This methodology is comprised of three stages, which are utilised to specify the research activities described in chapters 5, 6 and 7.

4.2   The Hybrid Process – iAtractive

This section describes the author's view of the hybrid process together with its specific definition in this research.

4.2.1   The iAtractive process – combination of additive, subtractive and inspection processes

One of the research gaps is that there is no current method that is able to accurately manufacture products with high geometrical complexity (as defined in section 2.4) whilst not being constrained by process capability and raw material in terms of shape and size. High flexibility provided by FFF allows complex structures to be created, which makes it an ideal candidate to be utilised as one of the constituent processes in the iAtractive process. Today, CNC machining is used for the finishing of additive manufactured parts (Gibson *et al.*, 2009). Thus, CNC machining has been used in this research to improve the accuracy and surface roughness of FFF manufactured parts. As a result, the capability constraints of the individual processes (i.e. low level of flexibility of CNC machining and low level of accuracy of the FFF manufactured parts) can be significantly reduced.

In addition, incorporating inspection techniques, the dimensions of raw material, in-process and finished products can be measured and obtained. This enables decisions to be made on how to use FFF and CNC machining to further manufacture the given raw material (i.e. existing part) by adding and/or removing material and transforming it into the final part. Through the interchangeable combination of FFF, CNC machining and inspection processes, the raw material constraint is thus eliminated. The hybrid process in

this research is thereby entitled the iAtractive process. To avoid confusion in the proceeding sections and chapters, additive and subtractive processes refer to FFF and CNC machining, respectively.

4.2.2   The definition of the hybrid process in this research

The term 'hybrid process' has been defined and explained in section 3.6.1. This definition is given for the hybrid process research in academia and industries. To clarify the definition of the hybrid process in this research, it is defined as an approach that combines an additive (i.e. FFF) with a subtractive process (i.e. CNC machining) and the inspection technique (i.e. CMM). This can be achieved from the different individual processes being carried out in a serial manner on a single platform. The purpose of the iAtractive process is to increase the flexibility and enhance the capability of the individual processes, and effectively utilise available manufacturing resources in terms of manufacturing process and raw material.

This definition of the iAtractive process and the material used (i.e. PLA) in this research is illustrated and highlighted in Figure 4.1 below. The rectangular block represents that iAtractive combines the FFF, CNC machining and inspection processes, including all the material that is currently and potentially available to be used in the future, from soft to hard materials as indicated by the red arrow. In order to avoid confusion, hardness is defined as the resistance to permanent indentation (Kalpakjian and Schmid, 2010) and refers to Vickers hardness in this research. At present, a range of materials can be used for the iAtractive process, such as PLA, ABS and low melting point alloys. Considering the current development progress on the FFF technique (Jones, 2013), soft material is an ideal candidate for demonstrating the iAtractive process. PLA has been used in this research and the reasons will be explained in section 5.2.3.
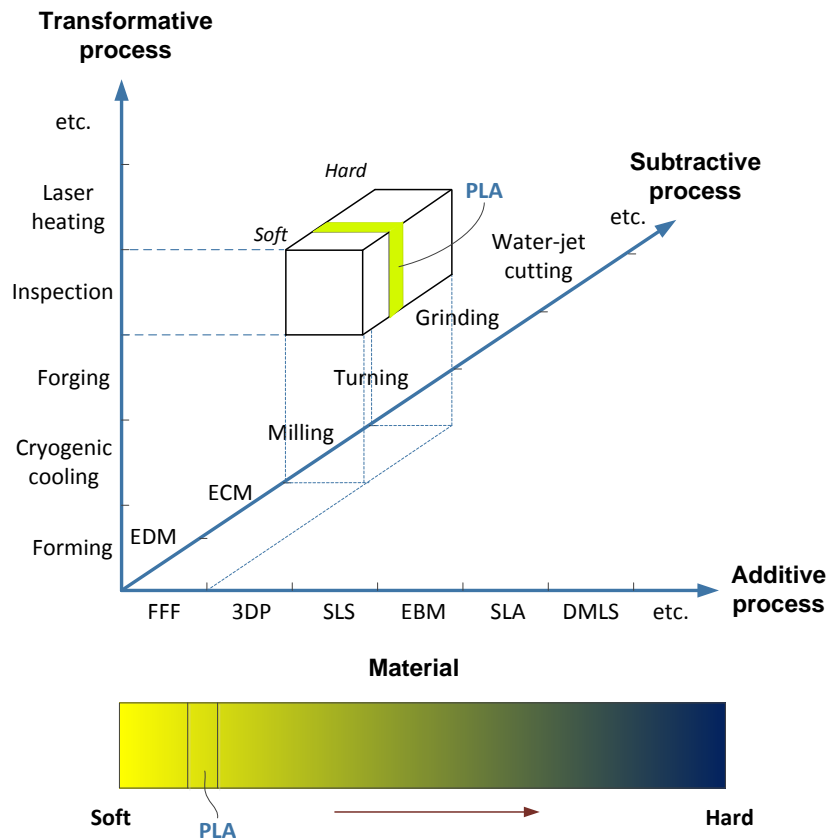
Figure 4.1 – The hybrid process defined in this research

4.2.3 The vision of the iAtractive process production

The top-level functional view of the iAtractive process is depicted in Figure 4.2. Various types of raw materials, in terms of shape and size, together with part designs are input into the iAtractive process. The relevant knowledge used in the iAtractive process for manufacturing the part is multi-process control, material manufacture, process planning and inspection knowledge. As the three processes are eventually integrated on a single platform/machine, multi-process control techniques are needed to control the machine. Inspection knowledge is essential since inspection is used in measurement of raw material, half-finished parts during production and final parts. Material manufacture knowledge is used for determining how to produce the part by utilising the FFF and CNC machining processes interchangeably. This information will be taken into account in the process planning stage, generating feasible process plans. The raw material is then manufactured according to the most appropriate process plan by which the finished part is obtained.
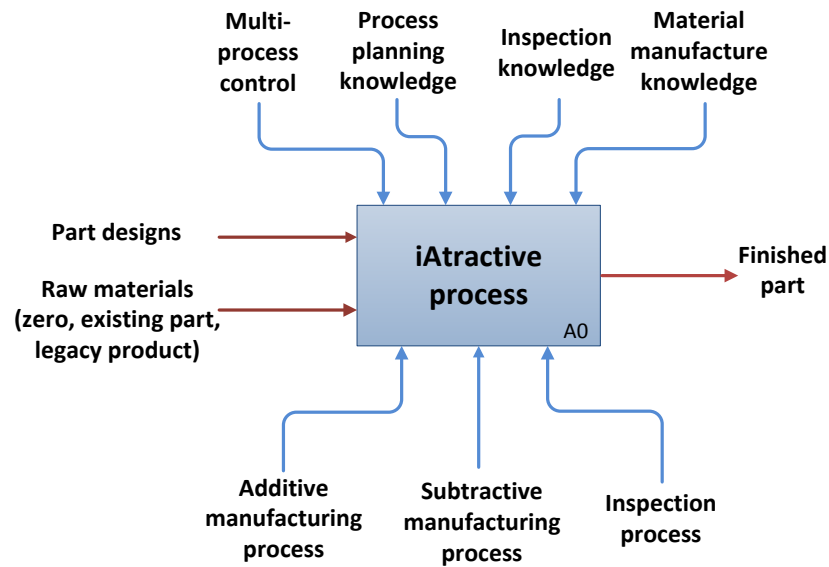
Figure 4.2 – IDEF0 overview of the iAtractive process

The author has utilised the current knowledge on additive manufacture, CNC machining and inspection within the manufacturing engineering domain to depict the primary vision of the iAtractive process, as shown in Figure 4.3. This indicates that the iAtractive process is not constrained by raw material in terms of shape, geometry or features. Raw material can be (1) zero (filament for deposition from zero); or (2) an existing/legacy product; or (3) a billet. By using the additive, subtractive and inspection processes interchangeably, the given raw materials can be further produced to the finished part with complex geometries.
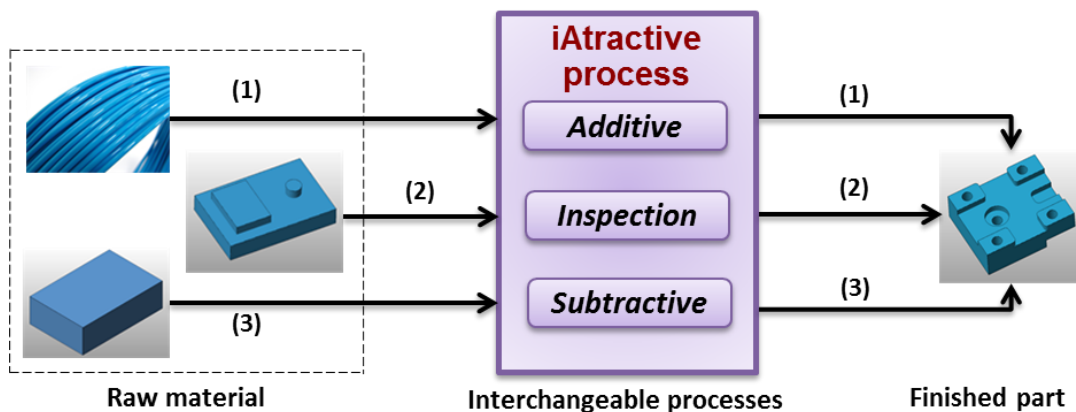
Figure 4.3 – The vision of the iAtractive process production

4.2.4 The overall work flow of the iAtractive process production

The overall work flow of the iAtractive process is shown in Figure 4.4 and outlined as follows:

(i) Raw material is first inspected using a CMM. The importance of this step is to obtain the actual geometrical attributes of the raw material, which becomes the basis of the process plan for determining subsequent operations. It is noted that the raw material is considered as zero if filament or other material that is specifically used in additive processes (e.g. powder and liquid) is given.

(ii) The part design (CAD model) is input into the decision-making engine. Decisions are then made on whether to manufacture the product from zero or reuse the existing part geometry to further manufacture it to the final shape. Figure 4.4 shows certain typical constraints that could determine the decision-making process.

(iii) For the first scenario, additive, subtractive and inspection processes are utilised interchangeably in a serial manner according to both (a) the process plan generated beforehand based on the part design; and (b) the process plan updated during production, based on the inspection feedback. By doing so, the final part is produced.

(iv) For the second scenario, according to the dimensions of the existing part, a new CAD model is generated. The new model shows the shape of the rest of the material required to produce the designed part. Then, the existing part is further manufactured to the final shape and part tolerances by the use of interchangeable additive, subtractive and inspection processes.

(v) At the end of both scenarios, the part is further inspected identifying which dimension is out of tolerance. If this is the case then further decisions can be made on whether to add more manufacturing operations until the dimensions are in tolerance.

Raw
material

Initial inspection

Actual shape of raw material

{production time: }

{material consumption: }

{application requirements: }

Decision-making

{part design: }

[manufacturing from zero]

[remanufacturing existing part]

{existing part geometries: }

Interchangeable add, subtract and inspection processes

{part design: }

Re-generate CAD/CAM model

Parts in progress

{additive process capability: }

New CAD/CAM model

{inspection strategy: }

Interchangeable add, subtract and inspection processes

{subtractive process capability: }

Parts in progress

Final inspection

[out of tolerance]

Decision-making – add operations

[qualified]

Final part

Figure 4.4 – The overall work flow of the iAtractive process

4.3 Requirements for the iAtractive Process

The requirements for developing the iAtractive process have been based on the critique of the literature review, research gaps (section 3.6), research aims and objectives (sections 2.2 and 2.3), and the vision of the iAtractive process production (section 4.2). These requirements are shown in Figure 4.5 and outlined in the following subsections.
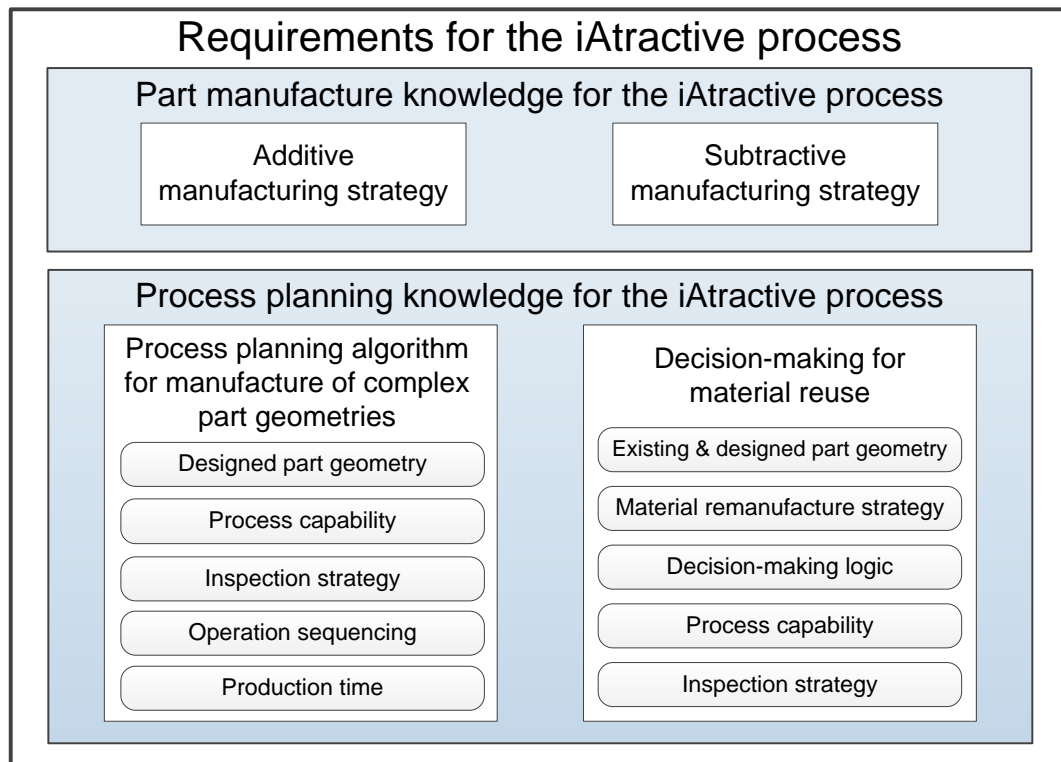
Figure 4.5 – Requirements for the development of the iAtractive process

4.3.1 Major considerations for developing the iAtractive process

The major considerations for developing the iAtractive process can be demonstrated by using an example scenario as shown in Figure 4.6, where the material is first deposited (starting from zero), followed by an inspection and a machining operation. More material is subsequently added and removed, and finally the finished part is inspected. It should be noted that in more complex studies inspection is required multiple times after an additive or machining operation, and different combinations of operations can be obtained according to the given part design.
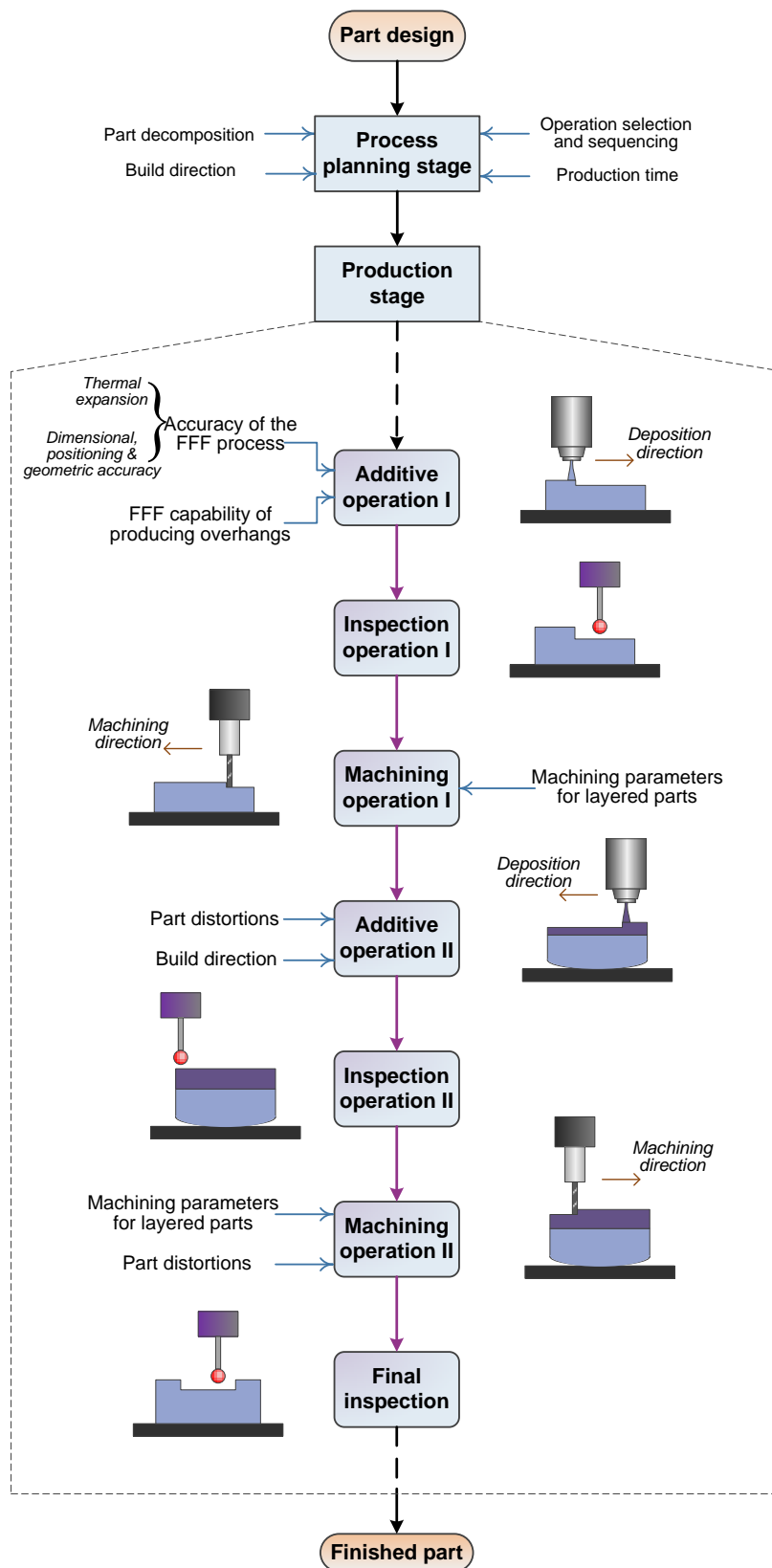
Figure 4.6 – An example scenario for part production using the iAtractive process

In order to manufacture the final part, the following issues have to be considered:

(i)   The first question is how this process plan is generated. To answer this question, the blue part being produced in additive operation I can be seen as a subpart. For producing such a subpart, the entire part has to be first decomposed into numbers of subparts followed by the determination of their build directions.

(ii)   Having decomposed the part, the next questions would be: which subpart is the first subpart to produce (the blue subpart in additive operation I in Figure 4.6); which subparts are the following subparts to produce; and in what orientations and build directions (the purple subpart in addition operation II).

(iii)   Since the blue subpart is produced in a layer by layer manner and each layer is bonded to each other, the process parameters for machining the layered part (machining operation I and II) may be different from the parameters used in traditional machining scenarios (i.e. from blocks).

(iv)   Given that the deposited features will be finish machined, they have to be bigger than their nominal sizes. Due to thermal contraction as well as unknown dimensional and positioning errors of the additive process and the machine, an accuracy index is required to compensate the errors.

(v)   Due to the temperature difference during the deposition of one subpart onto another subpart previously manufactured, the thermal induced stress develops, leading to the part distortions (i.e. the purple subpart is added onto the blue subpart in addition operation II). Therefore, a solution is required to understand part distortion behaviour for achieving high part accuracy.

(vi)   In certain circumstances where a number of process plans are potentially feasible, the most appropriate process plan in terms of production time has to be identified. Thus, an estimation of production time is needed.

(vii)   Furthermore, if the final part is produced from an existing part, the available manufacturing strategies for transforming the existing part into the final part need to be investigated, taking into account the capabilities of the FFF and CNC machining processes.

4.3.2   Part manufacture knowledge for the iAtractive process

The knowledge base is a core part of the iAtractive process, and not only contains material fabrication and machining resources including the information of available machines, tools

and deposition heads etc., but also contains the material manufacture knowledge that will be used in the process planning stage for generating process plans. Although machining technology has been well researched (Kalpakjian and Schmid, 2010), the machining knowledge for combining processes remains relatively unknown. As a newly developed additive process, the FFF capability and its application on the iAtractive process needs to be investigated, which in turn will also be used in the process planning stage, in particular operation sequencing. Due to the iAtractive process that utilises FFF and CNC machining interchangeably, the material delamination behaviour in machining layered parts and the material deformation behaviour in depositing new material onto existing parts become the major concerns.

4.3.3   Process planning knowledge for the iAtractive process

As identified in section 2.5.4, the development of process planning knowledge is the major focus in this research. This is because, for transforming a product from its design to manufacture stage, process planning acts as an enabler, particularly for the iAtractive process production. It specifies appropriate operations and determines operation sequences based on a given part design, identifies and selects appropriate process parameters for the specific additive and subtractive operations, and determines tool paths for each sequenced operation at different production stages. It enables the iAtractive process to flexibly and accurately manufacture complex components as well as reuse existing parts.

Being able to decide, based on the CAD representation of a part, how best to manufacture that part utilising the available resources, is a critical aspect of the process planning approach. The process plan should address the designed part geometries and the capability of FFF and CNC machining. The part can be manufactured in the shortest time possible by implementing the generated process plans. Process planning in this research also involves the development of decision-making logic, which will be able to provide feasible process plans based on various raw materials in terms of shape and size. Moreover, the process planning approach should be capable of dealing with feedback obtained from inspection, adjusting and regenerating new process plans accordingly. In order to realise these functions, a set of rules for utilising the inspection technique will be established.

4.4   The Hybrid Manufacturing Experimental Methodology

To the author's knowledge, there is also very little research conducted on process planning for hybrid processes (see section 3.6.8). Each process planning approach proposed is dedicated to the specific hybrid process (Hu and Lee, 2005; Liou *et al.*, 2007; Kerbrat *et al.*, 2011). Thus, these approaches are not feasible to be adapted for the iAtractive process. As a result, the experimental methodology has been designed based on the requirements described in section 4.3, identifying the research activities for developing GRP^{2}A, FDL and the related part manufacturing strategy. It should be noted that this research is limited to the development of the iAtractive process together with the process planning technique.

The methodology is demonstrated in Figure 4.7 and can be split into three major stages, which are:

- Stage 1: Investigation of the part manufacturing strategy for the iAtractive process.
- Stage 2: Development of GRP^{2}A for the manufacture of complex parts.
- Stage 3: Investigation of FDL for material reuse.

4.4.1   Stage 1: Investigation of the part manufacturing strategy for the iAtractive process

This stage explores part manufacture knowledge for the iAtractive process, which largely involves the investigation of appropriate process parameters, the FFF capability, material delamination and deformation behaviours. This knowledge will be used in the process planning stage since the generation of process plans highly depends on the individual processes capabilities. Stage 1 is comprised of four major phases which are outlined below and illustrated in Figure 4.7.
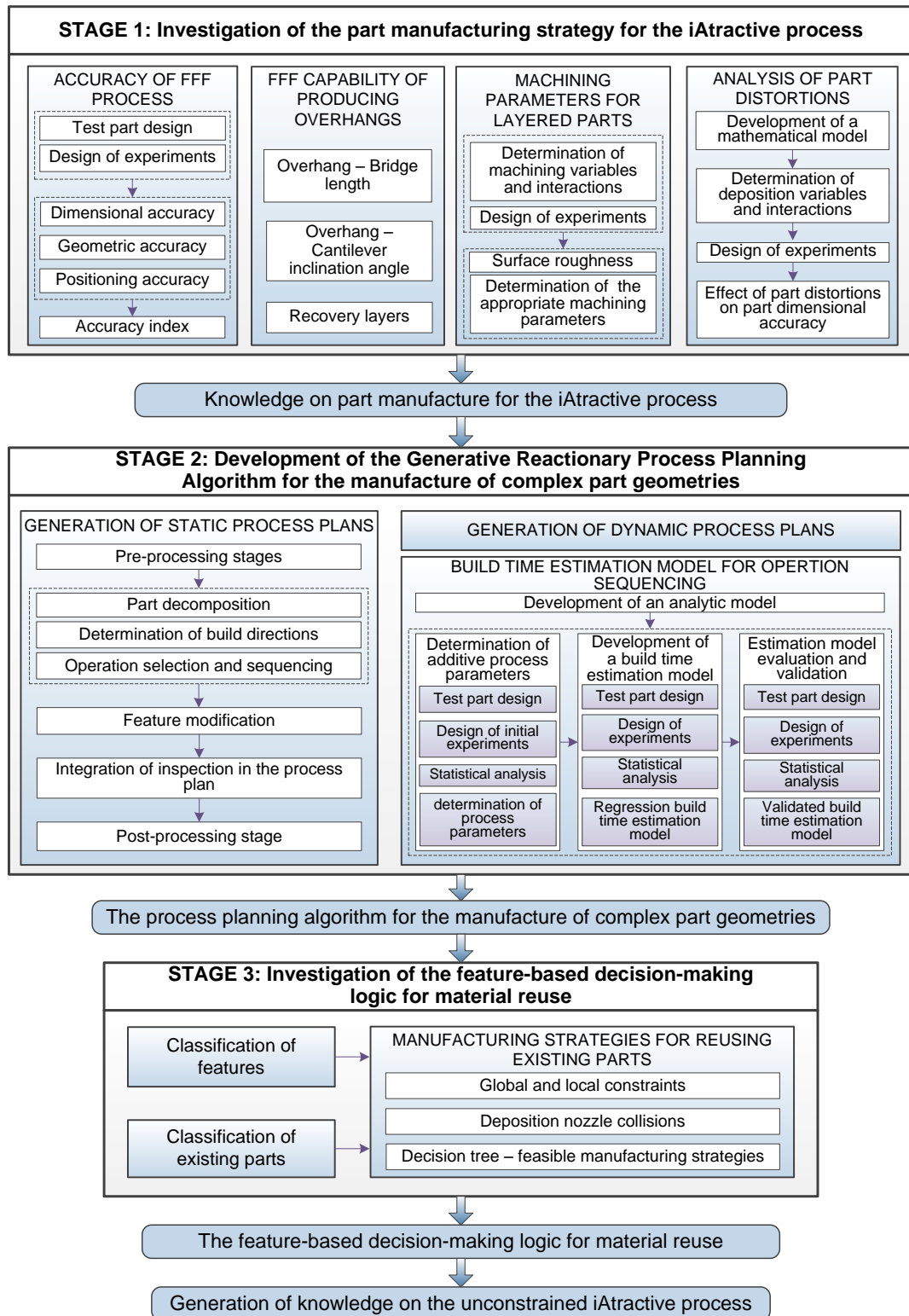
Figure 4.7 – The experimental methodology for the development of
the iAtractive process production

i)   Accuracy of FFF manufactured parts

This phase aims to investigate the dimensional and geometrical accuracy of FFF manufactured components. Accuracy errors of FFF parts can be divided into errors of the FFF machine and thermal contractions. Thermal contractions can alter the geometrical attributes of a feature, resulting in actual dimensions that are smaller than the nominal dimensions. The FFF machine errors contribute to the majority of accuracy errors of the FFF fabricated parts, which will be investigated in section 5.4. When a machining operation (i.e. machining operation I) is needed to finish machine the features fabricated in additive operation I (as shown in Figure 4.6), accuracy errors of the FFF process needs to be considered and compensated in the process planning stage. In addition, for manufacturing a feature, it has to be decided whether to use one additive operation or both additive and subtractive operations or other combinations of operations at the stage of operation selection and sequencing. This is not only dependent on the application requirements but also the accuracy and quality of the feature that FFF can produce, which will be described in section 5.4.2.

ii)   The FFF process capability of producing overhanging features

This phase is to identify the FFF capability in building overhangs in terms of overhang lengths and inclination angle. This will be used to determine build directions for creating features, which will be presented in section 6.5. Moreover, this identified capability also determines the constraints that are used in manufacturing strategy selection in FDL, which will be described in section 7.4.

iii)   Process parameters for machining of layered parts

In this phase, the machinability of FFF layered plastic parts made of PLA and the material delamination behaviour will be investigated, identifying appropriate machining parameters, namely spindle speeds, feed rates and depths of cut, related to friction induced temperature. The appropriate combinations of the parameters will be identified for CNC machining process (e.g. machining operation I and II in Figure 4.6) in various machining scenarios for obtaining high surface quality whilst reducing machining times.

iv)   Part distortions analysis

In the iAtractive process, while new material is deposited onto the top of the previously built part or machined part (e.g. additive operation II in Figure 4.6), the temperature difference between the new material (i.e. the material being extruded with 205 ℃) and the built/machined part (at the room temperature) results in the shrinkage of the newly deposited layers, which is the primary factor that leads to warp deformation. A typical example is shown in additive operation II and machining operation II in Figure 4.6. The deformation behaviour will be explored, taking into account the following factors: deposition tool path styles, part geometry, deposition speed, section length and thickness of stacking layers and part height.

4.4.2   Stage 2: Development of GRP^{2}A for the manufacture of complex part geometries

This stage is concerned with the development of GRP^{2}A for manufacturing complex parts. This process planning algorithm is able to generate a static process plan based on a given part design and further update the plan based on the feedback of inspection results. Therefore, stage 2 can be divided into two major phases, namely, generation of static and dynamic process plans.

i)   Generation of static process plans

The major considerations of generating static process plans are:

•   To be able to determine whether the feature can be solely produced by CNC machining by taking cutting tool accessibility into consideration.

•   To be able to decompose complex part features for reducing manufacturing difficulties and specify appropriate additive and/or subtractive operations for each feature based on the process flexibility and capability identified in stage 1. The author wishes to note that the capability of decomposing complex part geometries is very important in the process planning algorithm, but this is a major area in its own right and is beyond the scope of this research and requires additional significant investigation.

- To be able to determine operation precedence by applying process constraints knowledge (e.g. geometric constraints and technological constraints).

- To be able to estimate total production times and thereupon sequence operations, achieving the shortest amount of production time.

- To be able to utilise the inspection technique for generating dynamic process plans and ascertaining that the dimensions are in tolerances.

ii)   Generation of dynamic process plans

The dynamic process plans will be generated during production based on the knowledge of the static plan generation, according to the feedback obtained from inspection. A dynamic process plan is able to deal with the inspection feedback and adjust the corresponding static process plan accordingly by adding or removing operations and updating the process parameters in the relevant operations. The overall goal of generating dynamic process plans is to ensure the accuracy of the final part.

4.4.3   Stage 3: Investigation of FDL for material reuse

In this stage, FDL will be developed, showing feasible manufacturing strategies for manufacturing a part based on a given existing part. The feasibility of this decision-making logic will be demonstrated through a number of examples. The major activities involved in this stage are:

i)   Investigation of FDL

Various prismatic parts in terms of features will be classified and then used in the development of the decision-making logic. The dimensions of existing features and final part are considered as constraints in the decision-making logic since feasible combinations of operations that can be used to further manufacture the existing parts are highly dependent on them. The material manufacture knowledge gained in the previous stages will also be applied to the decision-making logic. This logic enables available raw material (i.e. existing parts/legacy products) to be reused or reincarnated into additional products.

ii)   Identifying potential deposition nozzle collisions

Depositing material onto an existing part needs to consider certain factors that are not normally taken into consideration for the individual FFF process. The existing features together with the dimensions significantly affect the deposition tool path due to potential collisions between the deposition nozzle and the existing features. The FFF capability identified in stage 1 will be used for avoiding potential deposition nozzle collisions.

4.5   Summary

This chapter first proposed the iAtractive process and its specific definition in this research followed by the author's vision and the overall work flow of the iAtractive process production. The requirements were then presented, specifying the major functions and considerations that are involved in the development of the iAtractive process. An experimental methodology has been developed, of which the functional view is depicted as an IDEF0 diagram in Figure 4.8. This figure shows the operational structure of the methodology with three major stages, which form the basis of the author's research and are described in detail in chapters 5, 6 and 7.
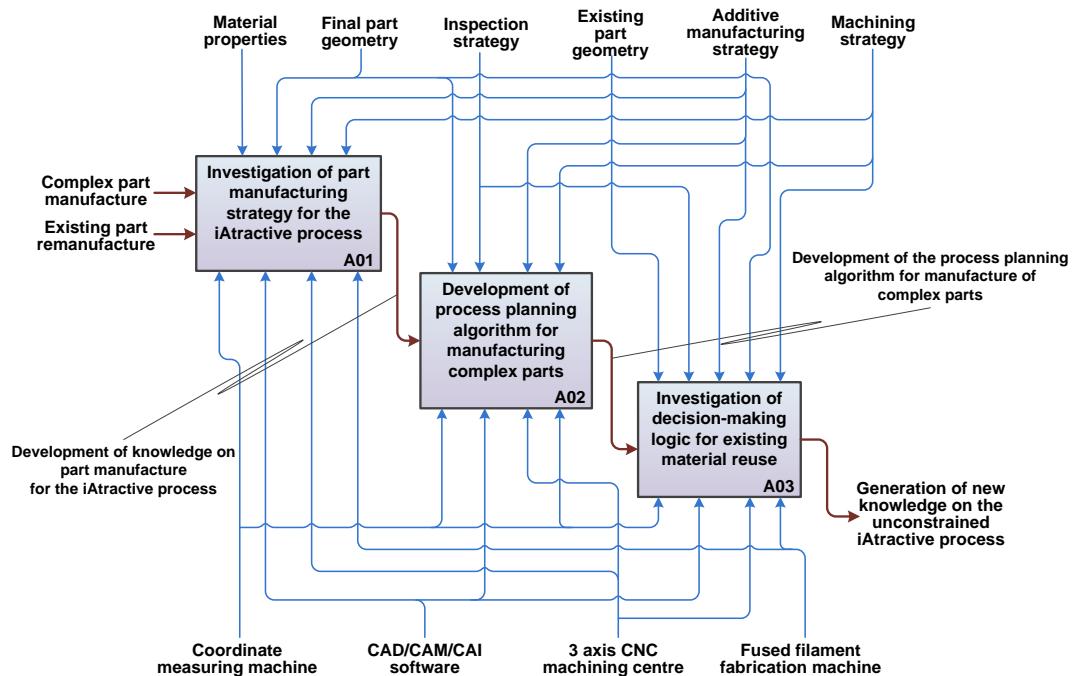
Figure 4.8 – Functional overview of the experimental methodology

5 Investigation of a part manufacturing strategy for the hybrid process

5.1 Introduction

In this chapter, the dimensional and geometric accuracy of FFF manufactured parts is first evaluated, developing an accuracy index of the FFF process to be incorporated in GRP^2A. The capability of the FFF process on producing overhanging features is explored, which is used as the criteria in different elements in GRP^2A and FDL. The appropriate combinations of feeds, speeds and depths of cut (DoC) are experimentally investigated for achieving high surface quality in CNC machining of layered parts. Part distortion behaviour in the material deposition process is also studied. The work presented in this chapter composes the first stage of the hybrid manufacturing experimental methodology, which also becomes the basis for GRP^2A and FDL presented in chapters 6 and 7, respectively.

5.2 Fused Filament Fabrication Process

The FFF process utilised in this research is briefly introduced, including its basic working principle, hardware and software as well as the available materials and material selection.

5.2.1 Overview of the process working principle

One of the current most popular additive manufacturing techniques is Fused Filament Fabrication (Terry, 2010), whereby material in filament form is fed into a liquefier chamber where it is heated to a semi-liquid state and deposited through a nozzle onto a build platform where it quickly solidifies (Jones *et al.*, 2011). In a continuous process, the newly deposited material fuses with adjacent material that has already been deposited. The deposition nozzle continuously extrudes material and simultaneously moves around on the horizontal plane according to specific paths generated based on the part geometry. Once a layer has been completely printed, the deposition nozzle moves upwards a certain distance (i.e. layer thickness) in the vertical direction and then immediately starts printing a new layer onto the top of the previous layer. This process continues until a physical representation of the CAD model is fully produced. The schematic of the FFF process is depicted in Figure 5.1 and a FFF machine is shown in Figure 5.2 where a heated bed is used as the platform holding the part. Moreover, the bed is designed to ensure the part is

kept above the T_g of its constituent material, reducing the part warping effect resulting from thermal contraction occurred after material extrusion (Nickel *et al.*, 2001).
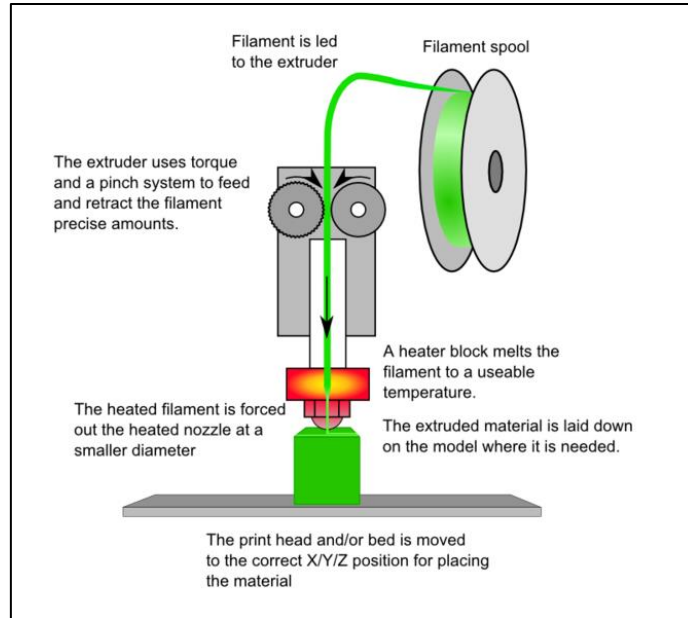
Figure 5.1 – Working mechanism of the FFF process (RepRap, 2012a)
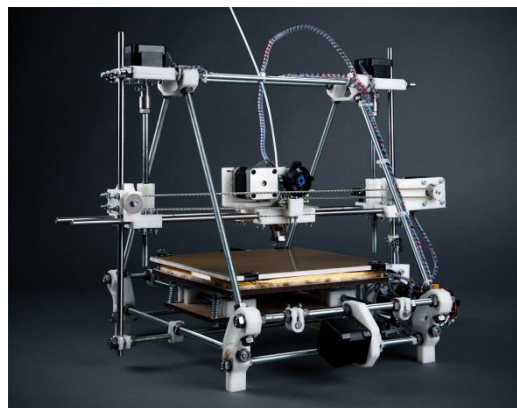
Figure 5.2 – A FFF machine (RepRap, 2012b)

In terms of deposition tool path patterns, a deposition head is traversed relative to the platform to first create one or more outer shells (defined by the user) before filling this shell with an infill hatch. This process is then repeated for subsequent layers. In this research, the direction of each layer of infill is perpendicular to the previous layer, resulting in a structure with anisotropic material properties. Further in an effort to reduce build times and cost, the interior of the component may be manufactured with a different level of porosity compared to exposed layers, which also leads to a component with

varying mesoscale anisotropic mechanical properties (Lee *et al.*, 2007). The outer shells and the infill hatch of a layer of a rectangular block are shown in Figure 5.3.
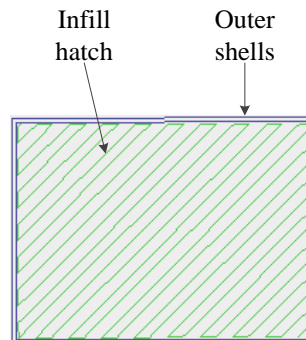
Figure 5.3 – Outer shells and infill hatch

5.2.2 Hardware and Software

This non-commercial machine largely consists of stepper motors, threaded rods, a deposition head, a heated bed and electronics. Three stepper motors are used in conjunction with threaded rods to realise movements in the X, Y and Z directions. The deposition head, which is also called extrusion head or extruder, equipped with a stepper motor, drives filament into liquefier chamber and extrudes it out of the nozzle. The systems electronics receives commands from the computer software and controls the four stepper motors, and temperatures of the heated bed and the extrusion nozzle.

The computer software takes STL files of the objects that the FFF machine is about to print, to horizontally slice them into a series of layers before computing the required infill patterns; and to save the results as G-Code Numerically Controlled (NC) files that the machine expects (Jones *et al.*, 2011). All of the parameters can be individually set in the software for specific part designs.

5.2.3 Available materials and material selection

A number of materials can be used in the FFF process and the majority of these materials falls under the polymer class. Despite the fact that duroplastics have been reported to be available for FFF (RepRap, 2012b), by the time that the author started this research, there were four thermoplastics and one metal that have been successfully used for certain applications. These materials are outlined as follows and the reasons for choosing PLA as the main build material is also explained.

(i)   Polycaprolactone (PCL)

As the first material tested in the RepRap project (Jones *et al.*, 2011), PCL has a very low melting point (i.e. approximately 60 ℃). However, its low friction makes it difficult to be driven into the liquid chamber. More importantly, it is sticky and stringy while it is being deposited, resulting in poor quality of finished parts.

(ii)   ABS

ABS has been widely used in commercial FDM machines (Stratasys, 2012), not only because of its low price but also high quality of built parts (e.g. high rigidity, less viscous during prototyping). It is noted that ABS can have linear thermal expansion coefficient of 37.8 μstrain ℃ depending on the degree of polymerisation. This indicates that its contraction effect during solidification results in the bottom of the part curling away from the base upon which it was built, particularly for large prototypes. The high T_g (approximately 110 ℃) can also contribute to severe warping. Stratasys machine (Stratasys, 2012) accommodates an oven consistently providing heat flow with the temperature above the ABS's T_g, by which the contraction effect can be significantly reduced. Given that the FFF machine is only equipped with a heated bed in order to reduce cost, prototypes made from ABS still suffer significant contraction.

(iii)   High Density PolyEthylene (HDPE)

HDPE, when compared to FDM-friendlier plastics has a very high shrinkage factor upon solidification, which directly leads to severe part distortion. Thus, it is not feasible for the iAtractive process.

(iv)   Bespoke Alloy

This bespoke alloy is comprised of Tin, Bismuth and Indium with mass proportion of 57.98%, 39.9% and 2.1%, respectively (Jones, 2013). Its melting point is approximately 130 – 150 ℃, which means this alloy can be directly used with the current deposition head design with minimal system changes. However, the quality of parts made of this alloy is still under initial test and as a result, it was not chosen to be used in this research.

(v)   PLA

PLA has been used in the Replicating Rapid Prototyper (RepRap) project at the University of Bath since 2008 (Jones *et al.*, 2011) and its T_g is only 55 °C – 60 °C and the linear thermal expansion coefficient is 126 μstrain °C (NatureWorks, 2012). Due to these properties, the contraction effect during cooling can be significantly reduced when using a heated bed as the build platform. In addition, PLA adheres to itself strongly when new layers are being deposited on top of existing ones. This property makes it be an ideal material for the iAtractive process for material reuse application where new material is deposited on existing parts. Moreover, PLA parts are less susceptible to delamination under stress in the vertical build direction than that of ABS parts. Therefore, PLA is suited to the iAtractive process production in which FFF manufactured parts are machined and undesired layer delamination is highly unexpected.

5.3   Definitions of Prismatic Features in this Research

Although 2½D machining features have been defined and presented in ISO 14649:10 (ISO 14649:10, 2002), the features referred to in this research are re-defined due to the combined nature of CNC machining and FFF processes that are utilised in the iAtractive process. Owing to the fundamental differences between FFF and CNC machining, features are produced in completely different manners, which could lead to ambiguity while allocating and sequencing operations. For example, a pocket can be obtained by removing material from a block using CNC machining. However, for the FFF process, material cannot be removed from a block but the pocket can be created by adding material. The following subsections briefly introduce the definitions of the features and specify the terms used to describe the manufacturing of these features.

5.3.1   Positive feature

For the FFF process, each feature can be considered to be positive, since the final product is manufactured from zero. However, only certain features can be seen as positive for CNC machining. In order to avoid definition conflict, this research adopts the definitions of boss, pocket, slot, step, hole and planar face in ISO 14649:10 (ISO 14649:10, 2002). As a result, a boss can be classified as a positive feature because it is a protrusion relative to the planar face. In the iAtractive manufacturing aspect, a boss can be machined from a block by CNC machining or can be added/deposited/built upon a horizontal plane by the FFF process.

5.3.2 Negative feature

Pocket, slot, step and hole are categorised as negative features in this research. A pocket feature can be produced by removing the material (as shown in Figure 5.4(a)) or by adding the material onto a specified area (as shown in Figure 5.4(b)).

(a) removing material   (b) adding material
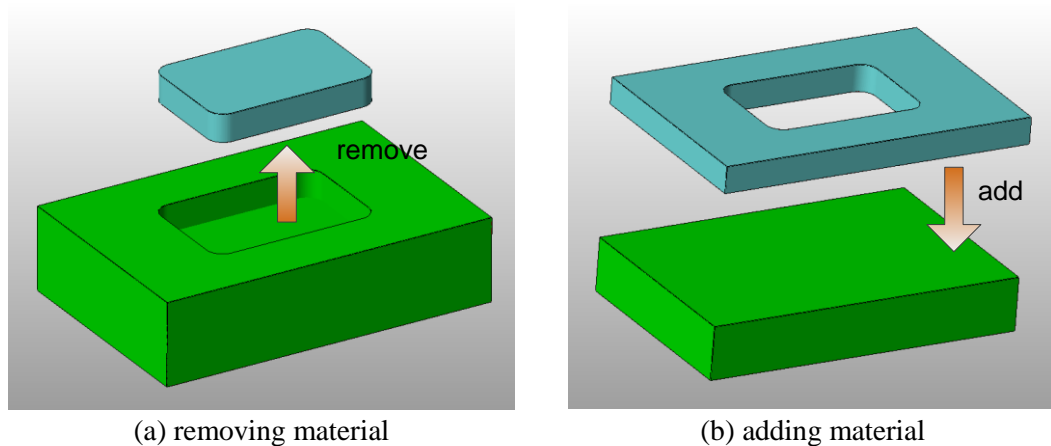
Figure 5.4 – Two ways of manufacturing a pocket (a) by CNC machining; (b) by FFF

5.3.3 Interacting features

The ability to deal with interacting features has been an informal benchmark for industrial acceptability of a feature recognition system (Verma and Rajotia, 2010). For machining processes, the feature(s) in Figure 5.5(a) can be recognised as a pocket (Figure 5.5(b)) or two slots (Figure 5.5(c)), depending on the recognition methods used. For the purpose of facilitating process planning, a feature is only classified as either a positive or negative feature in this research. The features in Figure 5.5(a) are positive features and thus are considered as four bosses. These four bosses can be manufactured by either building four individual bosses on a block or machining a pocket/two slots off.

(a)   (b)   (c)
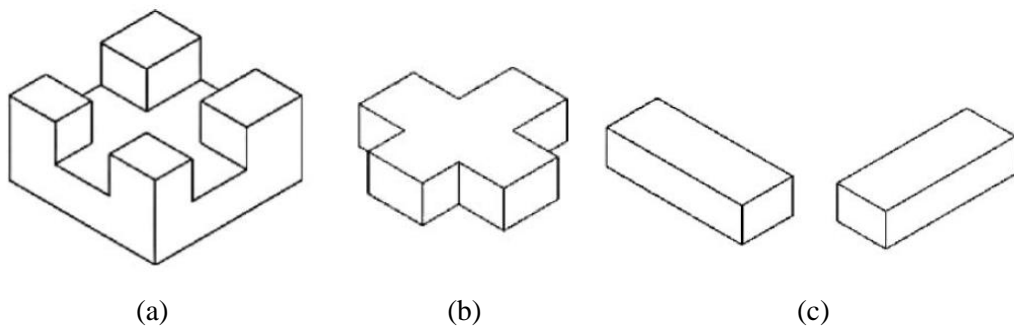
Figure 5.5 – An example of interacting features adapted from (Verma and Rajotia, 2010)

5.3.4 Overhanging feature

An overhanging feature example is shown in Figure 5.6. There is no clear definition for overhanging features in ISO14649:10 (ISO 14649:10, 2002). Given the working principle of the FFF process, overhang refers to cantilever and bridge in this thesis, which is defined in Figure 5.7 and the nomenclature is introduced below.
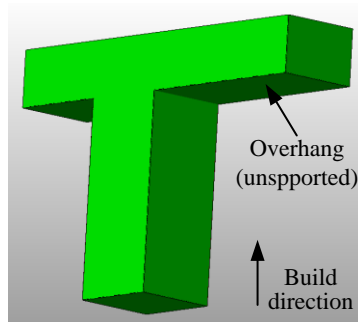
Figure 5.6 – An overhanging feature example
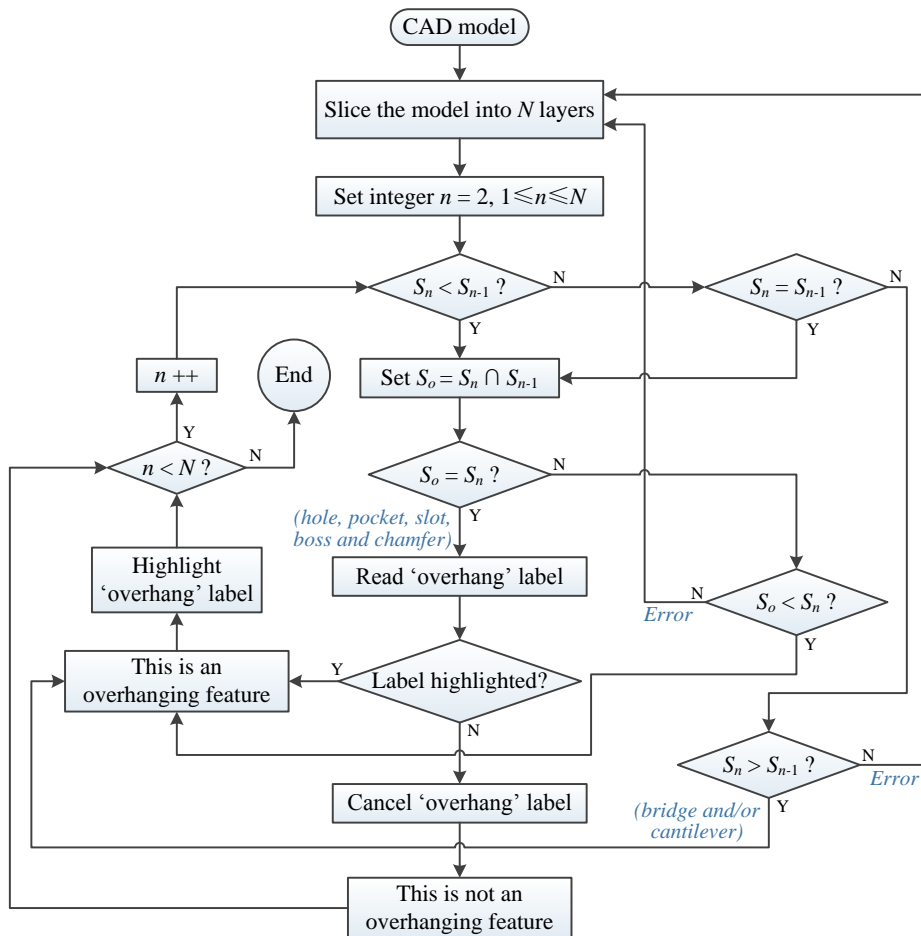
Figure 5.7 – Defining an overhanging feature

In Figure 5.7, a part is first sliced into a number of layers (i.e. N layers). The projected area in the horizontal plane (i.e. the XY plane) is denoted as S. The projected area of the nth layer is therefore denoted as S_n. The area and the location of S_n can be obtained by using the feature recognition approach proposed by Zhang $et\ al.$ (2004). In addition, S_o represents the overlapping projected area between the nth and $(n+1)^{th}$ layer, i.e. $S_o = S_n \cap S_{n-1}$. If $S_n > S_{n-1}$, S_n is recognised as an overhanging layer due to part of S_n that is deposited without the support provided by the layer underneath. The structure could also be an overhang when $S_n \leq S_{n-1}$, in which case S_o is smaller than S_n (i.e. $S_o < S_n$). While $S_o = S_n$, the feature can be a pocket, hole, slot, boss or chamfer, which are obviously not overhanging features.

5.4 Evaluation of Dimensional and Geometric Accuracy of FFF Manufactured Parts

This section evaluates and analyses the variability in the dimensional and geometric accuracy of the FFF manufactured parts. The results are used to develop a part accuracy index for the process planning algorithm.

5.4.1 Design of experiments (DoE) for dimensional and geometric accuracy evaluation

In this subsection, the error sources of the FFF process is briefly introduced, three test parts and a series of experiments are designed.

5.4.1.1 Error sources of the FFF process

A number of factors that contribute to the output accuracy of FFF manufactured parts can be categorised as follows:

(i)   CAD/CAM induced errors:

STL file format used in the FFF process as well as other additive processes causes dimensional, geometrical and surface errors, since the three dimensional surfaces of the part are represented using approximation of triangular facets (Zhou $et\ al.$, 2000). This type of error cannot be completely eliminated and the majority of the errors stays in sculptured surfaces since they are represented as planar triangular patches. Given that this research is only limited to prismatic part manufacture, the CAD/CAM induced errors are ignored.

(ii)   FFF machine errors:

Errors originating from the FFF machine can be further classified into a series of sources such as transmission errors (e.g. stepper motor, gears and pulleys) and extrusion mechanism errors (e.g. nozzle diameter and liquefier chamber blockage). In this research, this type of error is considered as an individual factor to be investigated for developing the part accuracy index.

(iii)   Process parameter errors:

Process parameters such as layer thickness, raster angles, hatching width and air gap individually and interactively affect part accuracy. The dimensional accuracy of a range of additive processes has been investigated (Zhou *et al.*, 2000; Dimitrov *et al.*, 2006; Sood *et al.*, 2009; Campanelli *et al.*, 2007). Therefore, this research only adopts the parameters widely used in the RepRap project, which has been approved to be appropriate in the initial tests (RepRap, 2012b). In other words, the errors caused by the process parameters can be seen as constant in the experiments presented in section 5.4.2.

(iv)   Material shrinkage errors:

As introduced in section 5.2.3, the FFF processed part accuracy is a direct result of the material properties. The effect of thermal expansion/contraction will be compensated in the analysis of the measurement results.

Based on the above, the part accuracy index of the FFF process to be developed can be attributed to the FFF machine and material shrinkage errors. Therefore, test parts are designed and introduced in the next subsection.

5.4.1.2 Test part designs

Unlike the CNC machining techniques which have generic test parts for machine tool evaluation such as the NAS 979 test part (National Aerospace Standard 979, 1969), the test parts for additive process were designed for the specific processes. These test part designs highly depend on the objectives of the experiments that the designer focuses on. This research is targeted at prismatic part manufacture, which is realised by using the hybrid process rather than other individual rapid prototyping processes. As a result, the test parts for 3DP (Stopp *et al.*, 2008) and SLA (Zhou *et al.*, 2000) are not applicable to this research.

Sood *et al.*'s test part (Sood *et al.*, 2009) for the FDM process is a cube specially designed for exploring the process parameter errors rather than dimensional and geometric accuracy. The author has thus decided to design three test parts (named test part A, B and C), which are shown in Figure 5.8, Figure 5.9 and Figure 5.10, respectively. Through manufacturing and measuring these test parts, the part accuracy of the FFF process can be evaluated.

Due to the FFF machine transmission errors, the part dimensional deviation is likely to accumulate while the distance that the deposition nozzle moves increases. Thus, test part A and B were designed to include varying lengths in the X, Y and Z directions. With these two test part designs, the dimensional accuracy for positive and negative features, and the positioning accuracy of the FFF machine can be investigated. Furthermore, the designs allow the author to identify whether the FFF machine errors affect the part dimensional accuracy in terms of distance that the deposition nozzle travels. Test part A is composed of ten stairs with constant thickness of 4mm. The size of the bottom stair is 100mm in length and 100 mm in width. Both the length and width of each stair were designed in a descending order with 10mm difference to that of the stair underneath. Each stair shares the two vertical planes, which aims to simplify the measurement procedures.
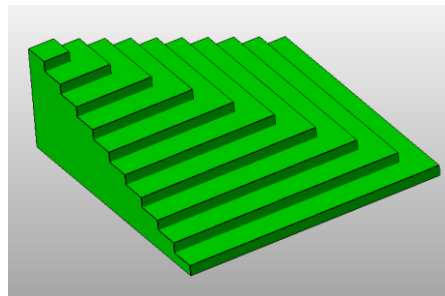
Figure 5.8 – Test part A for the evaluation of dimensional accuracy for positive features
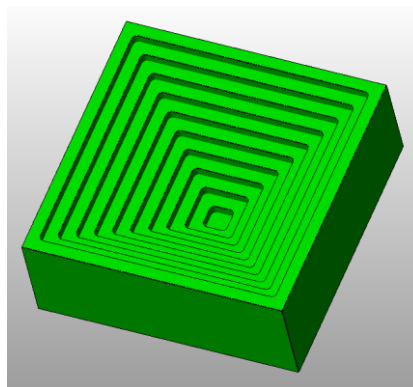
Figure 5.9 – Test part B for the evaluation of dimensional accuracy for negative features

Test part B consists of ten nested square pockets, each centred about the last, with width decreasing in 10mm increments and depth increasing in 4mm increments. The size of the biggest pocket (on the top) is $100 \times 100 \times 4mm^3$. Both the length and width of each pocket are 10mm shorter than that of the pocket located above.
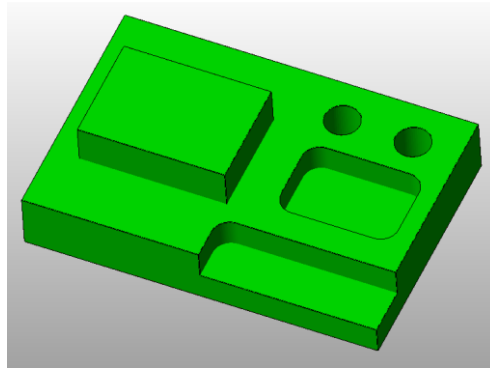
Figure 5.10 – Test part C for the evaluation of geometric accuracy of the FFF process

Test part C consists of typical 2½D features, namely planar faces, a boss, a pocket, a step and two holes. These features are measured for evaluating the geometric accuracy of the FFF manufactured parts.

5.4.1.3 Experimental design

The aim of the experiments was to evaluate the accuracy of the FFF manufactured parts rather than the importance of the FFF process parameters on the finished parts accuracy. Therefore, neither fractional factorial design nor Taguchi design strategy (Ross, 1996) met the experimental requirements. Five samples are the minimum quantity recommended in order to expect reliable results (BS ISO 5725-1:1994, 1994). Thus, five examples for each test part A and B were manufactured. As mentioned before, the FFF machine transmission errors are likely to accumulate while the machine is designated to print large prototypes. Therefore, the length, width and thickness/depth of each stair were measured using a CMM. This was to explore the dimensional accuracy of positive and negative features whilst identifying whether the dimensional accuracy varies accordingly when changing the distance that the machine moves. The positioning accuracy in the X and Y axes was also investigated by measuring the positions of the pockets in test parts B. It is noted that the positioning accuracy in the FFF process directly relates to the dimensional accuracy because the accuracy of the parts that the machine can produce is dependent on the machines movement accuracy. It should also be pointed out that this experimental design

was developed to obtain the accuracy information to be used in the 'feature modification' module, which is included in GRP^{2}A (see section 6.6).

Further to the geometric accuracy, seven test parts C were produced with the same process parameters on the same location of the build platform. Concentricity and roundness of the holes, perpendicularity and angularity of the bosses, pockets and steps were measured and calculated. The flatness of the horizontal surfaces was also identified.

Based on the dimensional, geometric and positioning accuracy, the part accuracy index has been developed and will be presented in section 5.4.4.

5.4.2   Experimental results and discussion

A series of test parts were solely fabricated by the FFF process and then measured on a CMM in a temperature controlled environment. Given that the linear contraction cannot be completely eliminated once the parts are taken off the heated bed, the measurement results were post-processed by removing the deviations caused by the contraction effect so that the FFF machine and process parameter errors can be evaluated. The linear thermal expansion coefficient of the specific PLA used in this study is 126 µstrain ℃. The deviations caused by the contraction can be calculated by using Equation 5.1 below:

Equation 5.1 $$dl = (T_g - T_i) \cdot \alpha \cdot L_0$$

Where, dl is the change in length (unit: mm), T_g is the glass transition temperature (℃), T_i is the inspection room temperature, α is the coefficient of linear thermal expansion and L_0 is the initial length. Note that, in this study, the length in X, Y and Z represents the length, width and depth/height, respectively.

5.4.2.1 Dimensional and positioning accuracy

Five samples for each test part A and B were fabricated. The length, width and depth/height were measured three times for each sample and the mean was calculated as the representative value for each of these dimensions. The error and percentage error in dimensions were calculated using Equation 5.2 and Equation 5.3, respectively, which aims to identify whether the error accumulates while the machine moves a certain specified distance.

Equation 5.2
$$\Delta X = X - X_{CAD}$$

Equation 5.3
$$\%\Delta X = \frac{X - X_{CAD}}{X_{CAD}} \times 100$$

where X is the measured value of length or width or depth/height, X_{CAD} denotes the corresponding value in the CAD model (i.e. nominal dimension), ΔX and $\%\Delta X$ stand for the error and percentage error in the X axis. ΔY, ΔZ, $\%\Delta Y$ and $\%\Delta Z$ were calculated in the same way for width and depth/height.

The percentage dimensional error in length and width for positive and negative features are plotted in Figure 5.11 and Figure 5.12, respectively. It was found that the percentage dimensional error tends to decrease while the distance that deposition nozzle travels increases. This percentage error shows similar trend in both the X and Y axes. The percentage error becomes consistent when printing a part where the length/width is more than 40mm. This indicates that the dimensional error does not accumulate while increasing the machine movement distance. On the other hand, the FFF process is less accurate as parts become smaller (less than $20 \times 20\text{mm}^2$ in the XY plane). The motor synchronisation issues (e.g. jerk, back lash and hysteresis), the low accuracy pulleys and the driving belts may contribute to the decreased part accuracy. It was also observed that the percentage dimensional error of a typical FFF part is more than 20% while producing features with less than 5mm. This is because, in this case, the majority of the error source is not the FFF machine error but the thermally induced error. For printing small features, the cycle time for each layer can be as short as a few seconds. This essentially means the new molten material is continuously laid down onto the deposited material before the deposited material completely cools down below T_g. In other words, the uncooled material can deform when a force acts upon it. Each continuous deposition cycle takes place in a very short period of time (less than 10s). As a result, the weight of the newly deposited material accumulates quickly and the gravity towards the previously deposited material results in part deformation. This also explains the diminished dimensional accuracy in printing small parts and cone geometries. The percentage dimensional error in the Z axis shows similar varying trends and it is thus not shown in Figure 5.11 and Figure 5.12 but is included in section 5.4.4.
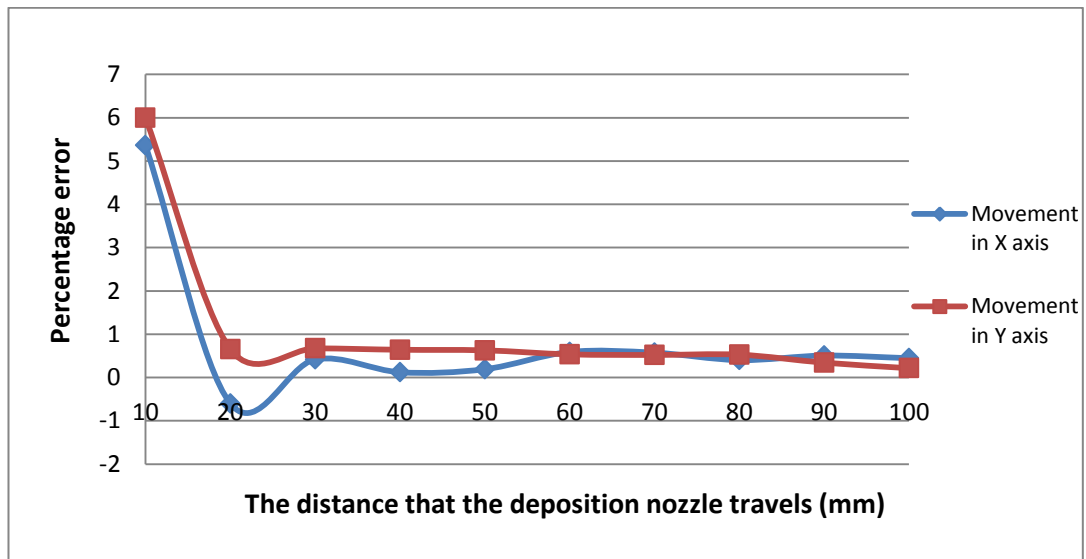
Figure 5.11 – The percentage dimensional error for positive features
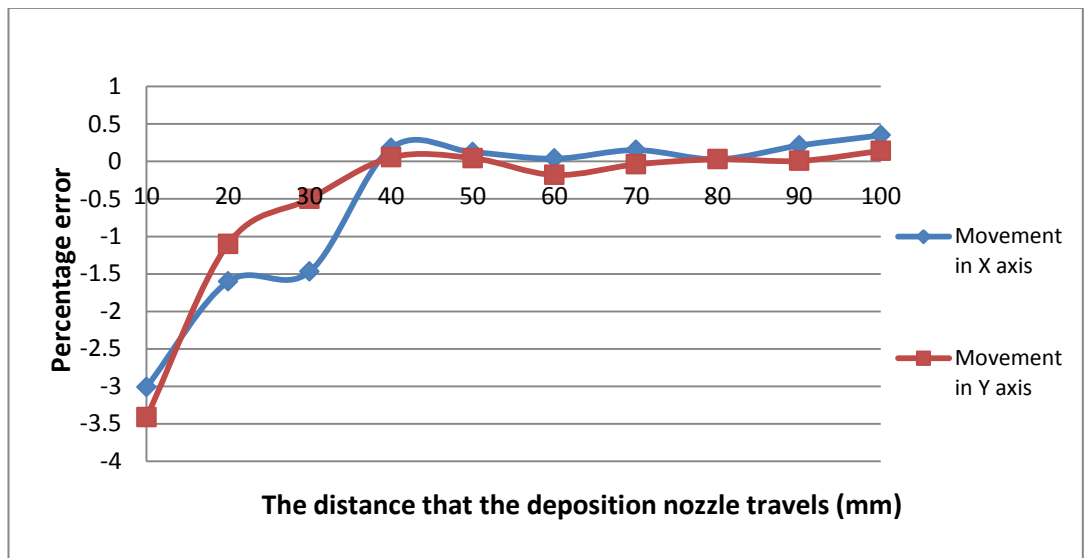
Figure 5.12 – The percentage dimensional error for negative features

For the five test parts B, the distance between each XZ vertical plane (on each pocket) and the origin XZ plane where the machine started printing was measured. The distance between each YZ plane and original YZ plane was also measured, as shown in Figure 5.13, which is the top view of test part B.
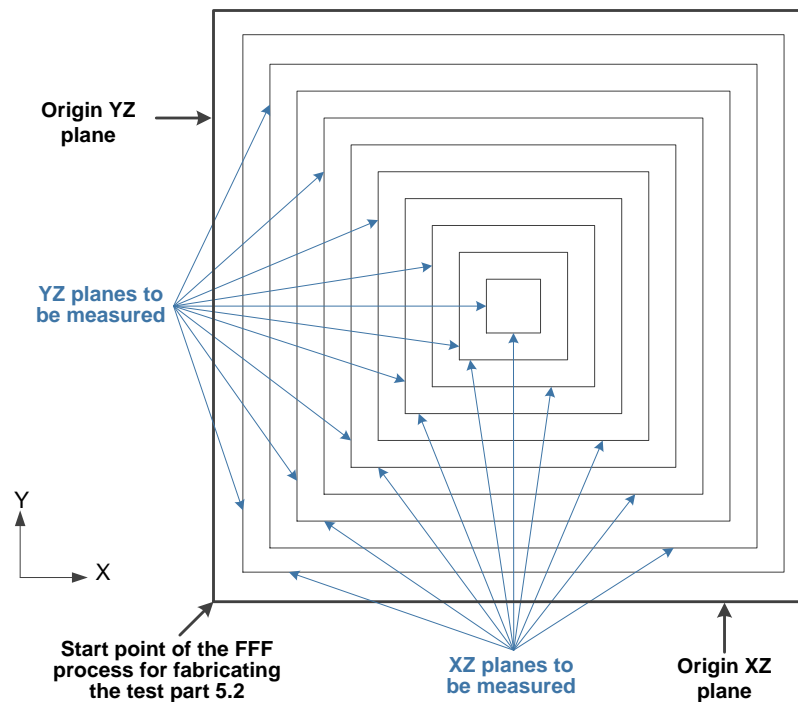
Figure 5.13 – The measured vertical planes in a test part B

The measurement results were post-processed using Equation 5.2 and Equation 5.3. The varying trend of the positioning error with differing distance that the machine moved was examined. The percentage positioning error in the X and Y directions (horizontal plane) are plotted in Figure 5.14, which illustrates that the percentage positioning error in both the X and Y directions decrease with increasing machine travel distance. In each case, the percentage error is positive (>0), indicating that the machine moved beyond the point that it was initially sent to. However, it should be noted that, for the FFF process, the positioning error also contributes to the dimensional error since the actual feature dimensions are dependent on how accurately the position of the deposition nozzle may be controlled. The aim of using this method identified in this section is to develop an accuracy index to be used in GRP^{2}A. It is worth mentioning that while a new feature is added onto a produced feature, the actual height of the previous feature has to be measured. This height will determine the layer thickness to be used in depositing the new feature, of which the coordinate of the start point (in the Z axis) is the actual absolute height of the existing feature measured in the inspection. The details will be provided in section 6.7.2. As a result, there is no need to identify the positioning error in the Z axis. Moreover, the most important factors that affect the part accuracy – in particular, the accuracy of the features that are added on the existing part – are the errors in the XY plane.
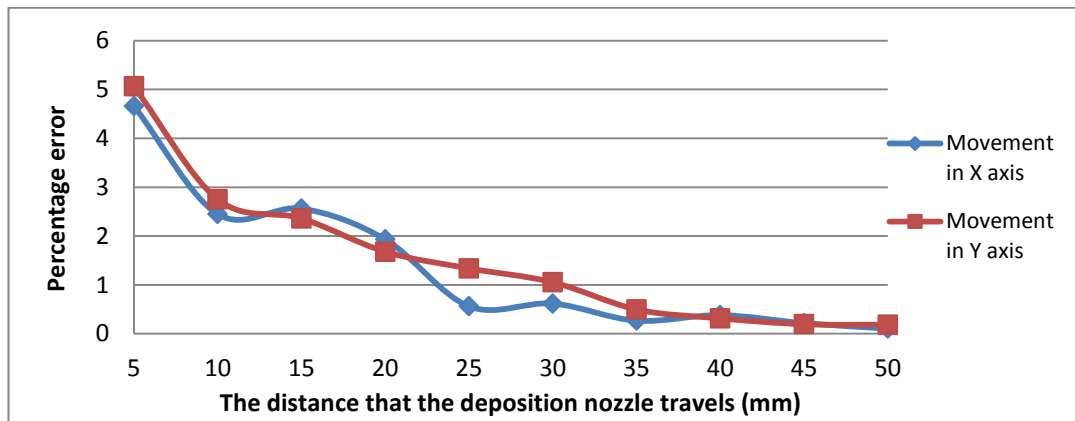
Figure 5.14 – The percentage positioning error in the X and Y directions

5.4.2.2 Geometric accuracy

The geometric accuracy of FFF manufactured parts has been explored and reported under the proceeding subheadings below:

(i)   Concentricity

As parts are built layer by layer, the entire process for fabricating a part can be viewed as a number of consecutive operations. As a result, it is possible that the diameter of a hole varies at different depths. Two holes were designed in test part C, which are named Hole 1 and Hole 2 on the left and right hand side, respectively, in Figure 5.10. The diameters of the holes at different depths were measured in order to investigate the variation of the diameters as well as the concentricity of the holes. Three circles for each hole were selected, representing the diameters of the holes at three different depths.
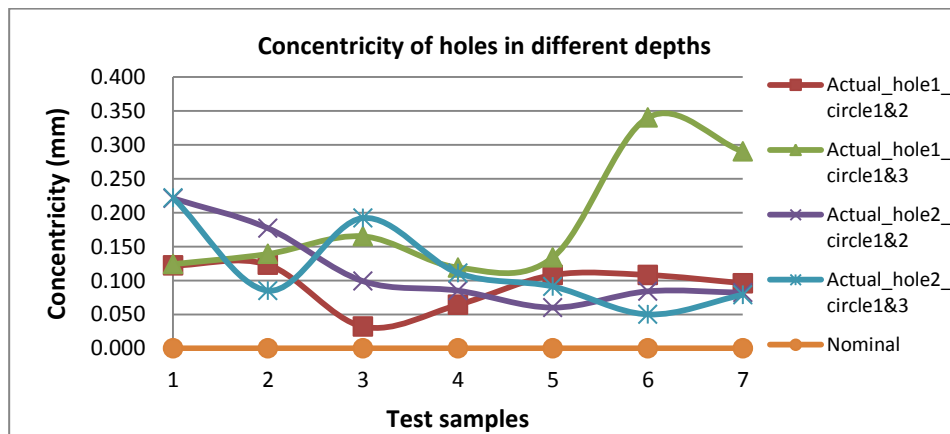
Figure 5.15 – Concentricity of the holes measured at three different depths

Figure 5.15 shows the concentricity of Hole 1 and 2 at three different depths. It can be observed that the maximum discrepancy was 0.340 mm between circle 1 and 3 in Hole 1. There is no trend that has been found related to the concentricity and depth. The majority of the variation in concentricity is caused by the diameter discrepancy in different depths, which is depicted in Figure 5.16 below.
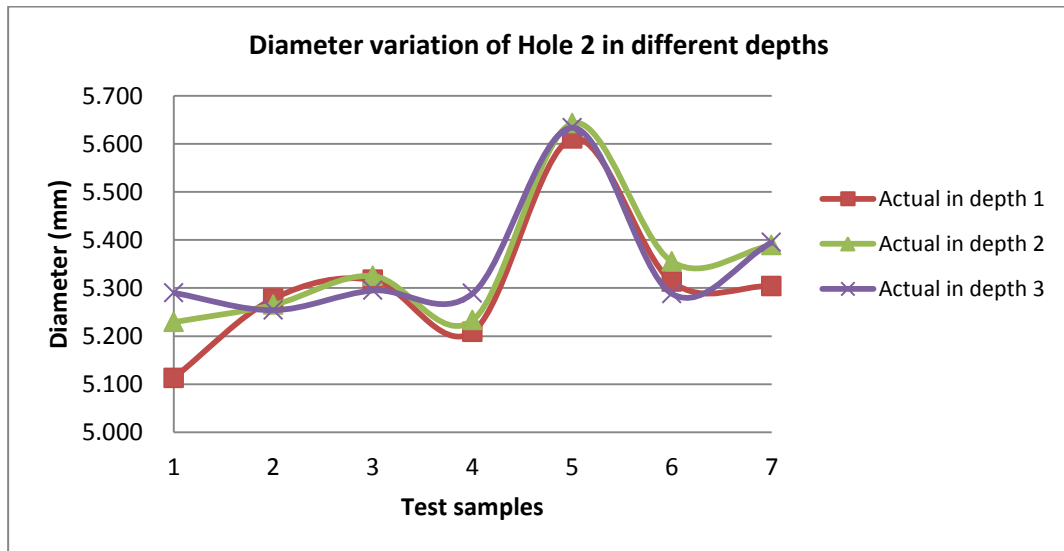
Figure 5.16 – Diameters of Hole 2 at three different depths

Figure 5.16 shows that the diameters vary in different depths where the maximum discrepancy is 0.177 mm and the minimum is 0.024 mm. This implies that the consecutive deposition operations are highly unrepeatable and unstable in terms of geometric accuracy. In turn, there is no need to identify the roundness of the holes due to the high inaccuracy of the holes that the FFF process produced. This result also suggests that a finishing operation is required in the iAtractive process for achieving high accuracy of holes.

(ii)   Angularity

The angle between two adjacent vertical planes on the boss, pocket, and step on each test part C was measured. Figure 5.17 plots the nominal and actual angles. It is identified that the angles for the pockets and the steps in particular, are out of tolerance (tolerance: ±0.8 °). It is also noted that for all of the test parts C, the angles for the bosses, which are positive features, are in tolerance, whereas the angles for the negative features are out of tolerance.
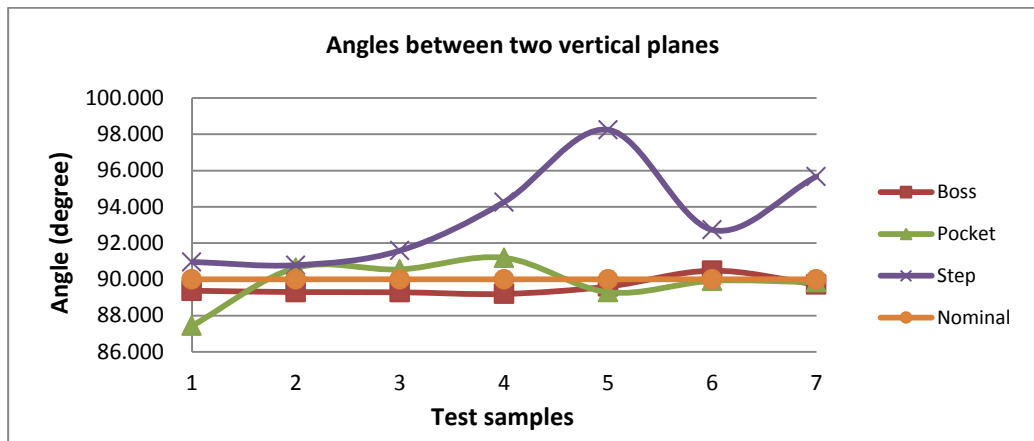
Figure 5.17 – Angles between two adjacent vertical planes

(iii)   Flatness

In order to identify the flatness of the horizontal surface, two random areas on the same plane on each test part were selected and the angle between them was measured. The angle between two random areas on the horizontal plane located on the boss for each test part C is shown in Figure 5.18, where the discrepancy is within +/-0.608 °, which can be considered as satisfactory for the FFF process in this research. This essentially indicates that a face milling operation for each layer is not necessarily required if material is to be deposited continuously onto the surface with the same build direction. This significantly reduces production times compared to that of the process plans proposed by Karunakaran *et al*. (2010), in which each layer has to be face milled before beginning the deposition for the next layer. More importantly, this result indicates that neighbouring subparts can be merged in the process planning stage, which will be presented in section 6.5.3.
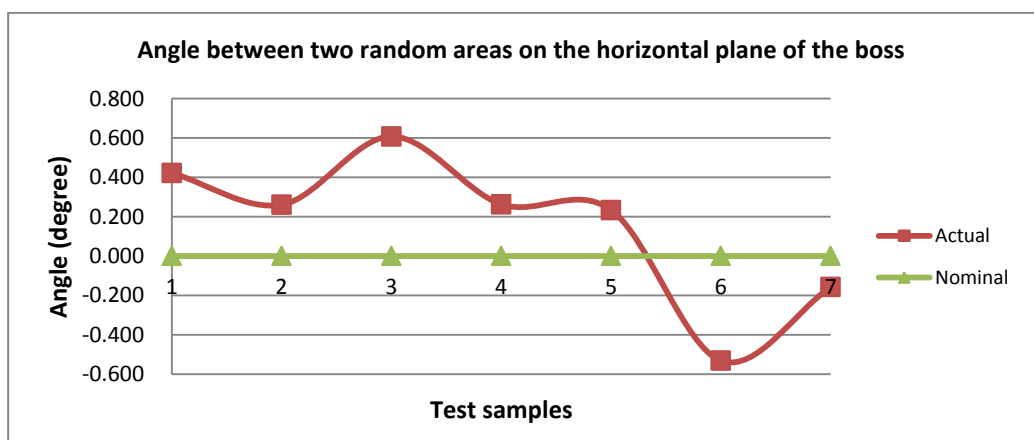
Figure 5.18 – Angle between two random areas on the horizontal plane of the boss

(iv)   Perpendicularity

Due to the flatness of the horizontal planes that is considered to be satisfactory for the iAtractive process, perpendicularity can be simply identified by measuring the angles between the two adjacent vertical and horizontal planes. The graph presented in Figure 5.19 shows the angles between the horizontal and vertical planes for the boss, pocket and step on each test part C. Significant fluctuation was observed in the angles for the negative features (i.e. the pockets and the steps in particular). By contrast, the FFF process is able to produce positive features, achieving better perpendicularity than that of negative features.
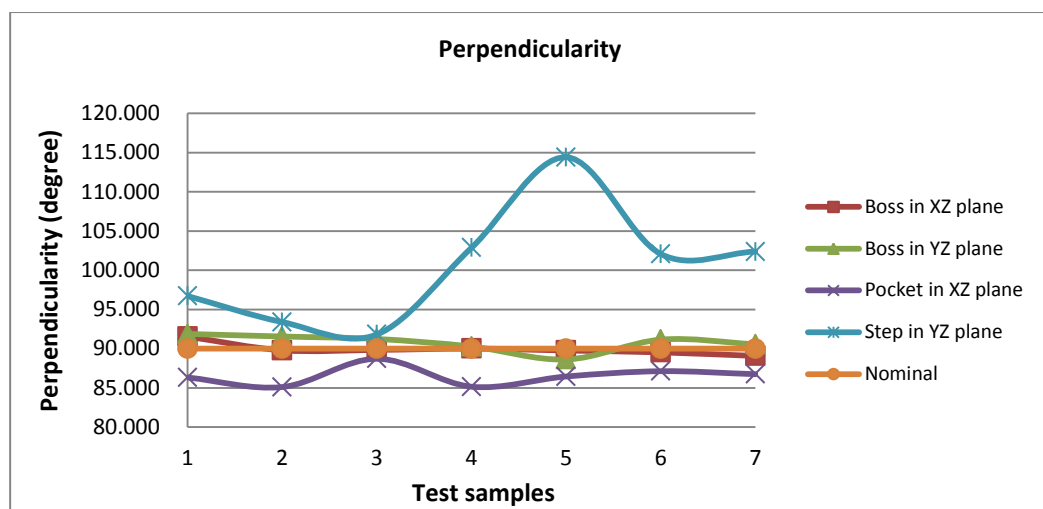
Figure 5.19 – Perpendicularity for boss, pocket and step

5.4.3   Findings and suggestions for the iAtractive process planning

Based on the results and discussion above, the following findings are obtained:

- In the evaluation of dimensional accuracy, it was found that the percentage dimensional error in both the X and Y axes tends to decrease as parts become larger. The thermally induced dimensional error primarily results in the diminished accuracy, implying that small subparts ($10 \times 10 \times 8mm^3$) is detrimental and should be avoided in part decomposition (section 6.4). This is because the highly inaccurate deposited small subparts may lead to print failure or undesired part quality (e.g. dimensional accuracy and layer bonding strength) in depositing new subparts.

- In terms of geometric accuracy, the flatness of the surfaces on the horizontal plane has been identified as satisfactory, which indicates that face milling for each layer (Karunakaran *et al.*, 2010) is not required for manufacturing fully dense parts (100% density, no porous structure). This finding is also used in 'subpart merging' (section 6.5.3) and 'operation sequencing' (section 6.5.5) in GRP^2A.

- The deposition operation for each layer is not highly repeatable, which is reflected in the concentricity of the holes, implying that a finishing operation must be scheduled after the additive operation for producing final features (introduced in section 6.5.5). The FFF process is able to accurately produce positive features rather than negative features in terms of angularity and perpendicularity.

5.4.4   Development of an accuracy index of the FFF process

Figure 5.20 gives an example (top view) of an actual fabricated feature (blue lines) as compared to the designed feature (red dashed lines), when a boss is added onto a rectangular block (black lines). Hence, the relevant features (the boss in this example) have to be modified accordingly to compensate for the dimensional and positioning errors, ensuring that the real positive features fabricated are slightly bigger than their nominal dimensions, and the real negative features are, on the other hand, slightly smaller than the nominals. This allows the machining process to finish machine the part, achieving the required surface quality and accuracy. As a result, a component named 'feature modification' has been designed in GRP^2A, which will be presented in section 6.6. An accuracy index is thereby developed, as shown in Table 5.1. A range of 10 dimensions in the X, Y and Z axes are given. These by no means represent a comprehensive list of part dimensions that the FFF process is able to produce, but provide a suitable range based on the working volume of the specific FFF machine used in this research and the most common part size for the FFF process (Gibson *et al.*, 2009). These values only hold true for certain additive process parameters such as deposition speed and infill hatch. The coordinates (positions) of each feature in 'feature modification' component can then be obtained using Equation 5.4 and referring to Table 5.1.
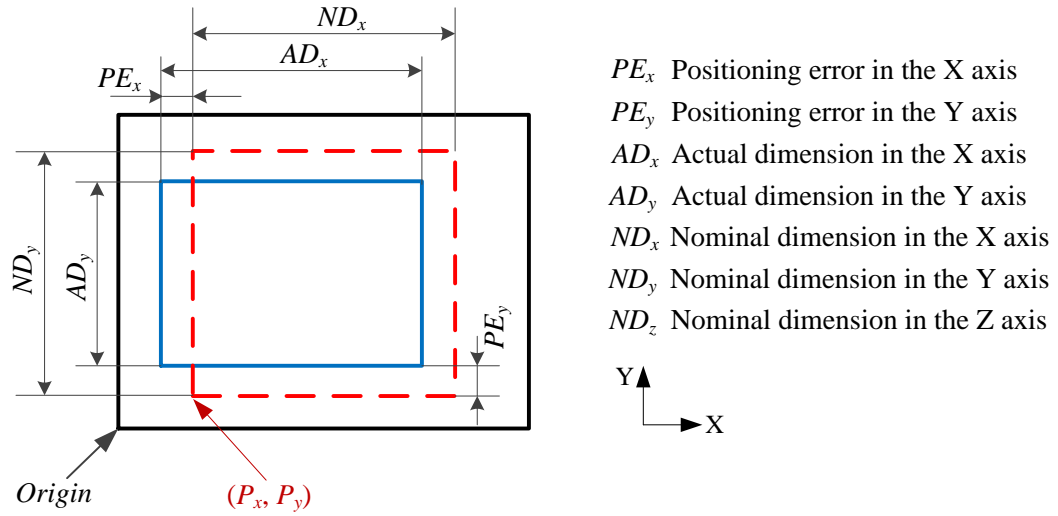
Figure 5.20 – Dimensional and positioning deviations in depositing a boss onto a block

Equation 5.4
$$\begin{cases} C_{x1} = P_x(1 - PE_x\%) \mp 0.5 \cdot dl, C_{x2} = C_{x1} + ND_x(1 + DE_x\%) \pm 0.5 \cdot dl \\ C_{y1} = P_Y(1 - PE_y\%) \mp 0.5 \cdot dl, C_{y2} = C_{y1} + ND_y(1 + DE_y\%) \pm 0.5 \cdot dl \\ C_{z1} = C_{z'2}, C_{z2} = C_{z1} + ND_z(1 + DE_z\%) + 0.5 \cdot dl \end{cases}$$

Where, (P_x, P_y) is the coordinate of the start point of a line. It is the nominal value and is also the start point that the nozzle of the additive head should position for printing. C_{x1} and C_{x2} denote the coordinates of the start point and the end point of the corresponding line in the modified CAD model, respectively, which are the coordinates to be used in the production. $PE\%$ is the percentage positioning error and $DE\%$ is the percentage dimensional error, which are referred to Table 5.1. In this table, P represents positive feature, N represents negative feature and dl is the linear dimension change in length due to thermal contraction. Given that a new feature is added onto another feature previously manufactured, the Z value of the start point of a line on the new feature (C_{z1}) depends on the actual absolute coordinate of the end point of the line (denoted by $C_{z'2}$) on the previous feature. For the combinations of operators such as $\pm$, use the upper operator for positive features, and the lower operator for negative features. This is because printed positive feature should be bigger than its nominal size, whereas printed negative feature should be smaller than the nominal size. All units are in mm.

Table 5.1 – The accuracy index for the additive process integrated in the iAtractive process

	Dimensions of the features that the FFF process produces in the XY plane (mm)									
	10	20	30	40	50	60	70	80	90	100
Dimensional error (DE_x) in X axis (%)_*P*	5.364	-0.599	0.417	0.121	0.192	0.590	0.574	0.402	0.507	0.446
Dimensional error (DE_y) in Y axis (%)_*P*	6.001	0.657	0.674	0.641	0.627	0.534	0.521	0.527	0.343	0.215
Dimensional error (DE_x) in X axis (%)_*N*	-3.011	-1.604	-1.470	0.180	0.125	0.038	0.152	0.029	0.212	0.349
Dimensional error (DE_y) in Y axis (%)_*N*	-3.413	-1.102	-0.499	0.054	0.044	-0.180	-0.039	0.029	0.008	0.141

	Dimensions of the features that the FFF process produces in the XY plane (mm)									
	5	10	15	20	25	30	35	40	45	50
Positioning error (PE_x) in X axis (%)	4.661	2.450	2.561	1.930	0.560	0.618	0.267	0.381	0.216	0.105
Positioning error (PE_y) in Y axis (%)	5.063	2.751	2.360	1.679	1.337	1.054	0.497	0.314	0.194	0.185

	Dimensions of the features that the FFF process produces in the Z axis (mm)									
	4	8	12	16	20	24	28	32	36	40
Dimensional error (DE_z) in Z axis (%)	1.596	1.721	0.981	0.946	0.440	0.395	0.495	0.810	0.627	-0.122

It should also be noted that the method proposed by Jeng and Lin (2001), where the part is simply scaled up 2-3%, has been proved to be incorrect. This is because scaling up negative features (e.g. pocket) leads to less material being deposited, which makes the negative features bigger than the nominal sizes. In this case, they cannot be further machined.

5.5   Investigation of FFF Capability of Producing Overhanging Features

In the initial tests, it was found that FFF is able to produce certain overhanging features without support. However, this capability still remains under developed. Thus, the present section identifies this capability, which more importantly, establishes the criteria enabling

GRP^{2}A and FDL to determine operations and parameters to manufacture/remanufacture parts/existing parts.

The author categorises overhanging features as bridge and cantilever, as depicted in Figure 5.21. The aims of this subsection are to explore the maximum distance between two adjacent bridge piers as well as the minimum inclination angle of cantilever that the FFF process can produce satisfactorily.

(a)   (b)
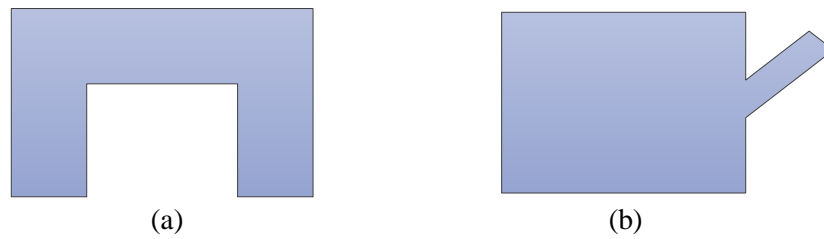
Figure 5.21 – Two types of overhanging feature (a) bridge (b) cantilever

To achieve the aims, the tests were carried out in a simple manner, where – (1) the distance between two bridge piers was increased by 1mm each time; (2) the inclination angle was decreased by 5 ° each time – until print failure was observed.

5.5.1 Printing bridges and recovery layers

The deposition nozzle traverses two adjacent piers whilst keeping depositing material continuously upon the air in printing a bridge, which results in a number of layers that are not flat (from layer i to $i+3$), as demonstrated in Figure 5.22.
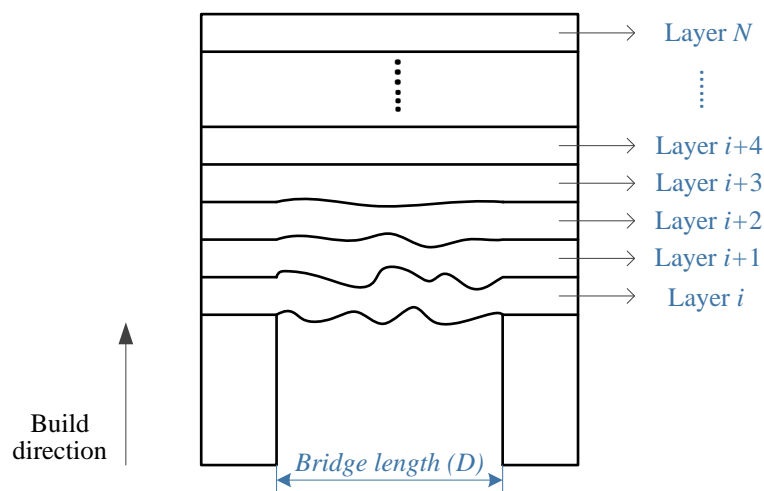
Figure 5.22 – Recovery layers

Layer i is the first layer built upon the air; layer $i+1$ is the second layer built on the top of layer i. Due to no support that exists underneath, the entire layer i cannot be fully formed, leaving some random gaps between the two piers. This leads to part of layer $i+1$ that cannot be fully formed and similarly for the layers deposited afterwards (e.g. layer $i+2$ and $i+3$). After printing a number of layers, the gaps have been gradually filled and the further layers that are deposited (e.g. layer $i+4$ in this example) become flat. Layers i, $i+1$, $i+2$ and $i+3$ are thereby called recovery layers. Due to the existence of random gaps, the structure of recovery layers is porous. The print quality of layers i, $i+1$, $i+2$ and $i+3$ is thus considered to be abnormal and the print quality of layers $i+4$ and onwards is considered to be normal.

The tests started from printing bridge lengths of 5mm. The FFF machine continuously printed the next bridge with 1mm increment in length if the previous print was successful. The print failed when the machine attempted to produce the bridge with the length of 24mm. For the stability and repeatability concerns, three identical sets of tests were conducted and the largest number of recovery layers for each bridge length was recorded. Table 5.2 presents the number of recovery layers required in relation to the bridge length. It should be noted that the results obtained from the tests were based on the certain FFF process parameters such as material extrusion rate, travel speed of the deposition nozzle and the extrusion temperature etc. The change of any of the process parameters may produce different results. In these tests, the process parameters used are the most commonly used values and readers are referred to RepRap (2012b). These parameters were kept consistent in other experiments throughout this research.

Table 5.2 – Bridge lengths and recovery layers

Bridge length (D) (mm)	Number of recovery layers (R)
5, 6, 7	2
8, 9, 10, 11, 12	4
13, 14, 15, 16	5
17, 18, 19, 20, 21, 22, 23	7
> 23	Failed

As shown in Figure 5.22, owing to the porosity and low accuracy of recovery layers, they have to be removed, which brings another issue, namely, the bridge thickness may be less than its designed thickness. Thereupon, it is necessary to modify the CAD model by either

altering the height of the bridge according to Table 5.2 in the 'feature modification' element (section 6.6) or adding support material.

5.5.2 Printing cantilevers

Similar to the tests carried out in section 5.5.1, the first trial for identifying the FFF capability in terms of printing cantilevers was to produce a cantilever with an inclination angle of 80°. A series of trials were conducted, setting up the inclination angle decreasing in 5° decrements for each consecutive trial until the cantilever could not be effectively generated. Again, three sets of trials were carried out, resulting in the minimum inclination angle applicable to the FFF process being 60°. Sells (2009) identified that the FFF process is able to produce cantilevers of minimum 45° angle, but it was observed in the trials that the entire printing process was unstable and print failure took place occasionally. This is because a large area of layers was printed in air as illustrated in Figure 5.23. In addition, producing 45°cantilevers requires reducing the nozzle travel speed and the nozzle temperature, which leads to a quality change in producing non-overhanging features. Based on the above reason, 60° is considered to be the minimum inclination angle for the FFF process.
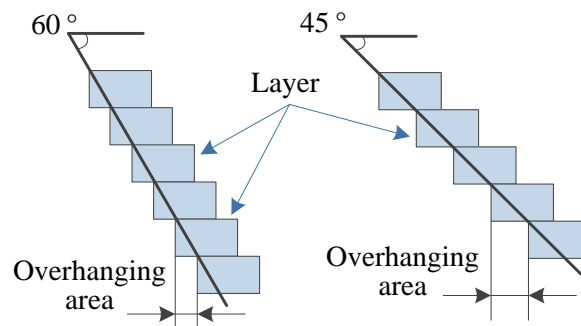
Figure 5.23 – Manufacturing overhanging features with different inclination angles

5.6   Investigation of Machinability of Plastic Layered Parts

This section investigates the machinability of FFF layered parts, made of PLA, and the delamination behaviour, identifying the appropriate machining parameters, namely spindle speed, feed rate and depth of cut, related to friction induced temperature.

5.6.1   Significance of machining process parameters for the iAtractive process

Extensive research has been conducted concentrating on the machining of hard materials, paying less attention on soft material machining. However, machining additively manufactured plastic parts presents a number of challenges as identified by Zhu *et al*. (2012). The parts are built layer by layer along the build direction in different alignment of the polymer chain. As a result, the resultant material only has approximately 1/3 the ductility relative to the natural material (Bellini and Guceri, 2003), which in turn increases brittleness. This increased brittleness implies that it makes material – that is not expected to be removed – easier to chip away during machining. In other words, while machining the nth layer, the $(n-1)^{th}$ layer (the layer located under the nth layer) tends to be taken off together with the nth layer. A CNC machining process is employed to ensure high accuracy and low surface roughness, whereas adopting inappropriate process parameters is, instead, likely to damage the surface quality. In addition, different combinations of the process parameters are required in order to deal with different applications (e.g. roughing/finishing subparts/final parts/existing parts). Moreover, the low melting temperature indicates that it makes the surface being machined easier to melt, leading to surface degradation and increases in surface roughness. Therefore, there is a need to investigate the machinability of layered parts and identify the appropriate process parameters in terms of surface roughness for the iAtractive process.

5.6.2   Design of experiments for machining of layered parts

The success of machining experimentation relies on the selection of appropriate machining variables and their interactions. Three parameters were selected, namely feedrate, spindle speed and depth of cut. This is due to the fact that they are the most accessible factors, which directly affect the geometric accuracy and quality of a machined part (Dhokia *et al.*, 2011). Moreover, these three parameters have been used in the experiments for machining plastics i.e. polypropylene and the results show significant effect on surface roughness (Dhokia *et al.*, 2008).

As the aim of the experiments was to identify the appropriate parameters for machining of layered parts for the iAtractive process, a standard approach for this purpose is to use the full factorial design. Given that there are only three factors to be investigated, the full factorial method is acceptable if each of the factors consists of no more than four levels.

Both the literature on machining of hard materials (Kumar and Choudhury, 2008) and DoE strategies (Holman, 2001) suggest that three levels (i.e. high, medium and low) are widely used and by doing so, the significance of each individual factors and their interactions can be identified. Based on the above reasons, the full factorial design was used. The next step was to determine the levels of the factors to be examined.

There is already a vast array of research on appropriate machining parameters in the metal cutting domain (ToloueiRad and Bidhendi, 1997). However, as already documented, there is virtually no data on machining of plastic layered parts. In this case, spindle speed (revs/min) has to be determined from the following standard cutting equation (Kalpakjian and Schmid, 2010), where *v* is the cutting speed (m/min) and *d* is the diameter of the cutting tool (mm):

Equation 5.5
$$rpm = \frac{1000 \cdot v}{\pi d}$$

Feedrate can then be obtained as follows:

Equation 5.6
$$FR = rpm \times T \times CL$$

where, *FR* is the feed rate (mm/min), *T* is the number of teeth and *CL* is the chip load (mm/tooth).

In order to calculate spindle speed and feedrate, cutting tool and cutting speed should be decided first. A 6mm 2 flute cutter with approximate chip load of between 0.002 and 0.021mm/tooth was taken from the Onsrud cutting tool data catalogue (Onsrud, 2011) and it was used in all the cutting experiments. Obviously there is a large range of tooling options available for CNC machining of different materials. Due to FFF manufactured parts being relatively small as well as prismatic parts that have been identified as final parts in section 2.5, a 6mm diameter solid carbide slot mill cutter was selected. Regarding the chip load selection, it was difficult to produce more accurate chip load characteristic since this can only be achieved by carrying out experiments using dynamometers, which is considered to be outside the research scope. Thus, three different chip loads have been chosen i.e. 0.002, 0.012 and 0.021mm/tooth.

After defining the cutter, the spindle speed and feedrate can be determined. However, the calculation results show that theoretical feedrate is not applicable to real machining scenarios. One example is given below.

Spindle speed: $rpm = \dfrac{1000 \cdot v}{\pi d} = \dfrac{1000 \times 1000}{3.14159 \times 6} = 5305.2$ (revs/min)

Feedrate: $FR = rpm \times T \times CL = 5305.2 \times 2 \times 0.002 = 21.2$ (mm/min)

This slow feedrate indicates long engagement time at the point of cut, which allows the heat to build up leading to undesired material deformation and poor quality machined surfaces. Therefore, empirical data was used based on the DoE strategy. The feedrate was within the reasonable range for machining of soft materials (Dhokia *et al.*, 2008). Depth of cut was chosen according to the layer thickness, which was 0.25mm/per layer. The limiting factor was the vertical machining centres 8000rpm maximum spindle speed. Hence, 1000, 4000 and 8000rpm were selected, representing low, medium and high levels, respectively. The full factorial design method was applied, giving a total of 36 experiments, which are listed in Table 5.3. Slot milling experiments were conducted since the focus of this research is laid on prismatic parts. In order to further explore the effect of friction-induced temperature, these slot-milling experiments were carried out in dry cutting conditions. Having identified the appropriate machining parameters in the dry cutting conditions, another set of wet cutting experiments was carried out, using the appropriate machining parameters identified above, to compare the surface roughness obtained in dry and wet cutting conditions.

5.6.3   Experimental results and discussion

Fully dense PLA blocks were manufactured by using the FFF process in a 45 °raster style tool path strategy. Slot milling experiments in dry cutting conditions were conducted and Figure 5.24 shows six slots of the total 36 slots. The surface roughness was measured on a laser profilometer as shown in Figure 5.25, which is a non-contact measuring instrument. The laser scans the surface of the slot while the surface is being moved relative to the laser. By analysing/post-processing the light interference signals sent back to the profilometer detector, the surface roughness is obtained. The delamination behaviour and the melted surfaces were observed and are analysed below.

Table 5.3 – Design of experiments generated output for the machining of layered parts

Experiment number	Feed (mm/min)	Speed (rpm)	Depth of cut (mm)	Experiment number	Feed (mm/min)	Speed (rpm)	Depth of cut (mm)
1	1500	1000	0.25	19	2500	4000	1
2	2000	1000	0.25	20	3000	4000	1
3	2500	1000	0.25	21	1500	8000	1
4	3000	1000	0.25	22	2000	8000	1
5	1500	4000	0.25	23	2500	8000	1
6	2000	4000	0.25	24	3000	8000	1
7	2500	4000	0.25	25	1500	1000	2
8	3000	4000	0.25	26	2000	1000	2
9	1500	8000	0.25	27	2500	1000	2
10	2000	8000	0.25	28	3000	1000	2
11	2500	8000	0.25	29	1500	4000	2
12	3000	8000	0.25	30	2000	4000	2
13	1500	1000	1	31	2500	4000	2
14	2000	1000	1	32	3000	4000	2
15	2500	1000	1	33	1500	8000	2
16	3000	1000	1	34	2000	8000	2
17	1500	4000	1	35	2500	8000	2
18	2000	4000	1	36	3000	8000	2

Figure 5.24 – Six slots of the total 36 slots in the dry slot milling experiments

Figure 5.25 – The laser profilometer

Variations in the process parameters i.e. speed, feed and DoC affect the surface characteristic of the machined slots. From Figure 5.26, it can be identified that the surface roughness is lowest at the maximum spindle speed, maximum feed and minimum DoC. Although there is no varying pattern observed with regard to the relationship of variation of DoC and surface roughness, the surface roughness is consistent for each depth of cut.
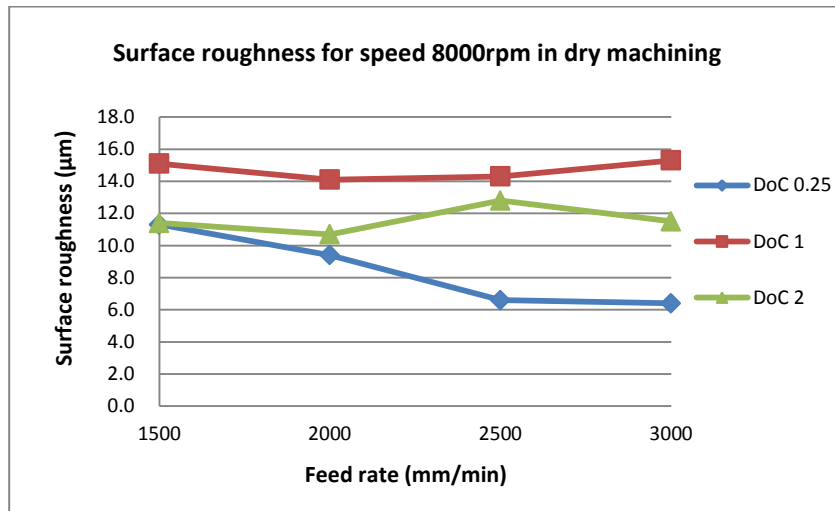
Figure 5.26 – Variation of surface roughness with feed and DoC
at the maximum spindle speed

Figure 5.27 also supports the fact that the surface roughness is the lowest at a DoC of 0.25mm rather than 1mm or 2mm. Figure 5.26 and Figure 5.27 also illustrate that neither low spindle speed (e.g. 1000rpm) nor is high spindle speed (e.g. 8000rpm) beneficial in terms of surface roughness. On the other hand, using spindle speeds in an intermediate range between the maximum and minimum such as 4000rpm is most likely to achieve better surface quality. This is partially due to using high speed and feed that are likely to generate a greater degree of friction and friction induced heat, leading to part deformation and subsequently an increased surface roughness. In particular, the heat generated has significant effect on the machining of PLA, of which the melting point is relatively low at 195 ℃. From this perspective, a lower DoC is recommended as less material is removed during machining, which facilitates heat release and in turn reduces the temperature of the cutting edge and cutting zone.
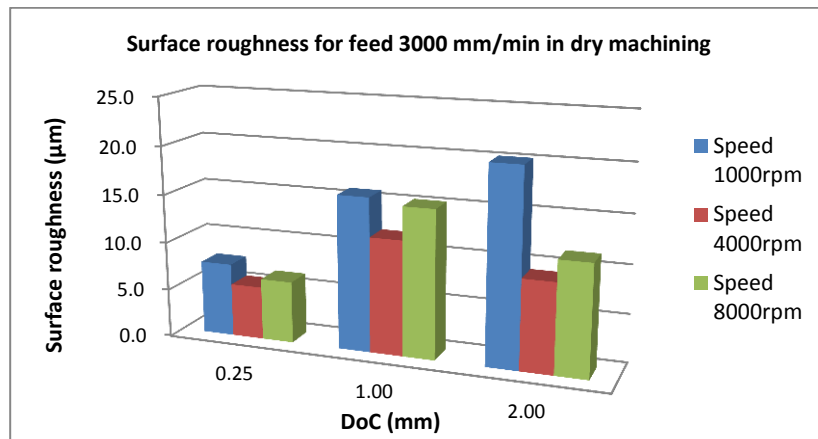
Figure 5.27 – Variation of surface roughness with speed and DoC at the maximum feed

Feedrate is one of the dominant factors that determine machining times since it directly specifies the moving speed of the cutting tool relative to the worktable. For reducing production times in the iAtractive process, appropriate feedrate needs to be identified. Thus, the analysis of variance (ANOVA) technique was used and the results are shown in Table 5.4.

Table 5.4 – ANOVA table for surface roughness analysis

Source	DOF	Sum of squares (*SS*)	Adj Mean square (*MS*)	F	P
Feed (*A*)	3	2.78	0.93	0.18	0.91
Speed (*B*)	2	22.72	11.36	2.22	0.15
DoC (*C*)	2	184.09	92.05	17.99	<0.001
AB	6	79.93	13.32	2.60	0.08
AC	6	41.49	6.92	1.35	0.31
BC	4	45.30	11.33	2.21	0.13
Error	12	61.41	5.12		
Total	35	437.73			

Table 5.4 indicates that depth of cut is the most important factor that determines surface roughness. The change of feedrate has the smallest impact on surface quality as compared to speed and DoC, implying that increasing feedrate is a feasible way of significantly reducing machining time without compromising on surface quality. This finding is very useful for process planning since a given part is decomposed into a number of subparts, on which more material will be added. A high feedrate can be used in the machining of subpart surfaces which are not the exposed surfaces on the final part. Although the surface roughness is relatively higher than that of using low feedrates, it is still considered as adequate for acting as a build platform for the succeeding deposition operations (i.e. Ra <

16 μm). However, it should also be pointed out that the effect caused by the combination of feed and speed is the second significant factor that leads to the variation in surface roughness. The values of R^2 (i.e. 86.0%) and $(R^2)_{adj}$ (i.e. 59.1%) indicate that the surface roughness of the machined layered part does not follow a clear trend. Therefore it is worth identifying the appropriate combinations of feed, speed and DoC. The effects of the individual factors are thus plotted, as shown in Figure 5.28. The three points shown in each plot of the three control factors represent the corresponding measured surface roughness values while such a factor was set at different levels (i.e. from low to high), respectively. The plots illustrate that while applying low DoCs, the surface roughness is significantly lower than that of high DoCs. The medium level of speed is suggested. Unlike the assumption proposed in the DoE, high feeds do not directly contribute to the decreased surface roughness, whereas, using low feeds tend to obtain better surface quality.
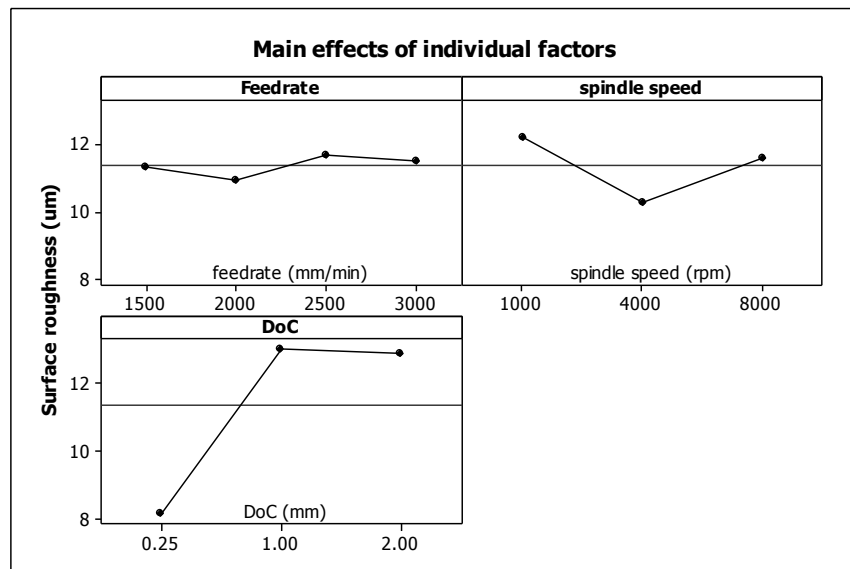
Figure 5.28 – The main effects plots for surface roughness

The effects of factor interactions are plotted in Figure 5.29, where each block represents the effect of the interaction of two factors. 8, 12 and 16 μm are the measured surface roughness; 1000, 4000 and 8000rpm are spindle speed; 1500, 2000, 2500 and 3000mm/min are feedrate. The best combination of each two factors in terms of surface finish can be identified by referring to the corresponding block. For example, in block L3_C1, it is advisable to use 0.25mm DoC and 3000mm/min feed because it can produce the lowest surface roughness. Similarly, using a DoC of 0.25mm and a spindle speed of 4000rpm is recommended as indicated in block L3_C2. For certain scenarios where

machining time is the primary consideration, parts can be beneficial from being produced by using 3000mm/min and 4000rpm (as demonstrated in block L2_C1). A speed of 1000rpm should be avoided because the surface finish will be significantly diminished while increasing either feed or DoC (as shown in block L2_C1 and L2_C3). By considering all the effects of each two factor interaction as well as the consistency of surface finish that can be obtained by using the process parameters, the following process parameters in Table 5.5 are suggested for different applications.
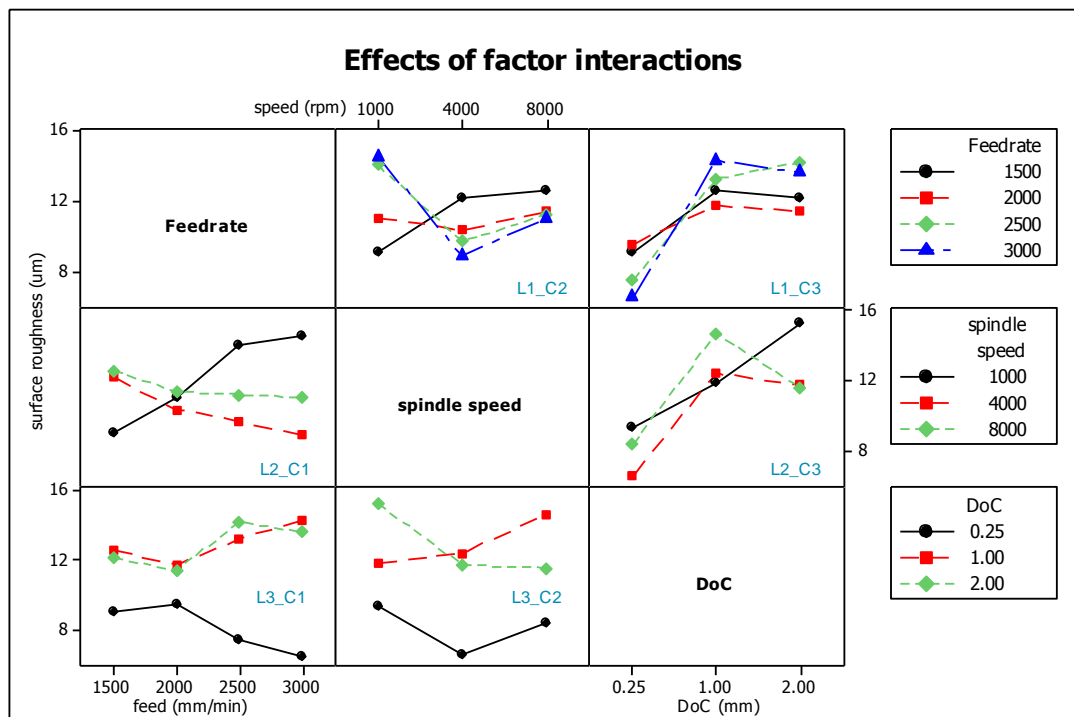
Figure 5.29 – Effects of factor interactions in machining of plastic layered parts

Table 5.5 – Recommended machining parameters for dry cutting

Feed (mm/min)	Spindle (rpm)	DoC (mm)	Achievable Ra (μm)	Application area
2000	4000	0.25	<8	Finishing operation for final parts (see section 6.7.2)
3000	4000	1	8 – 12	Finishing operation for subparts
3000	8000	2	10 – 12	(see sections 6.5.5 and 6.7.2)
3000	4000	2	10 – 12	Roughing operation for subparts, the given existing parts (see section 7.4.4) and support material removal (see sections 6.6 and 6.7.2)

Given that the friction at the point of cut increases as DoC increases, the increased DoC has the potential to increase the amount of heat generated as a result of friction, which possibly leads to the increase in surface roughness. Therefore, a set of slot milling experiments were conducted on both dry and wet cutting conditions by using the appropriate machining parameters identified above. Figure 5.30 shows the detailed surface characteristics while using a speed of 4000rpm, feed of 1500mm/min and DoC of 0.25mm with coolant. Figure 5.31 compares the surface roughness of the machined slots with and without coolant during the machining operation with speed 4000rpm, feed 1000 – 3000mm/min and DoC 0.25mm. The significantly improved surface quality demonstrates that heat is a major factor affecting the machined surface quality.
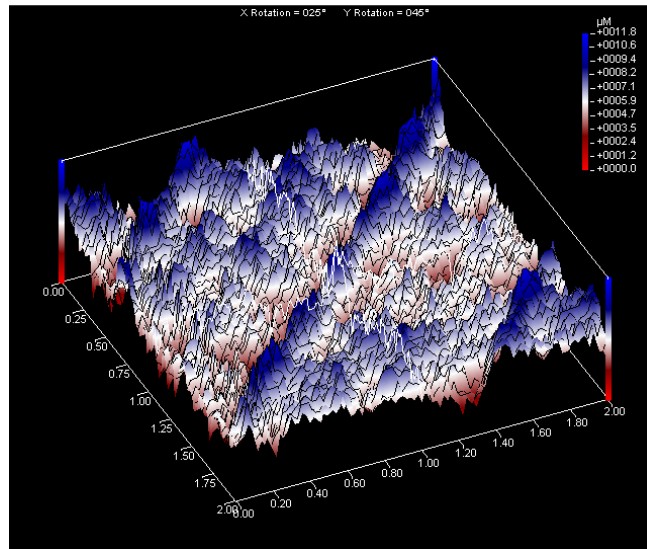
Figure 5.30 – Surface characteristic in speed 4000rpm, feed 1500mm/min and DoC 0.25mm with coolant
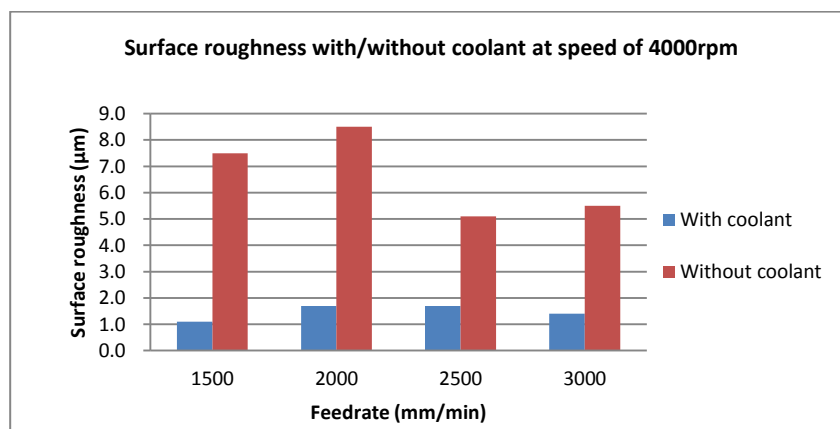
Figure 5.31 – Comparison of surface roughness with/without coolant during machining

The reason for this is that PLA is an amorphous plastic, which essentially implies that even at temperatures below their melting point they can substantially soften at temperatures above their T_g. This is basically the temperature at which they can no longer withstand relatively small amount of stress. Whilst the melting temperature of PLA is technically 195 ℃, the key temperature is actually the T_g which is approximately 50 – 60 ℃. With the absence of coolant, the temperature of the material surface being machined is much higher than 60 ℃, leading to the degradation of the surface quality. This is also the reason why the bed temperature is 60 ℃ and why it stops the contraction and warping effects. Hence, this property of PLA makes the thermal control whilst milling even more important. Above 50 – 60 ℃ the part will become soft and just deform rather than allow material to be removed.

5.6.4   Findings and suggestions for the iAtractive process planning

This section has explored the machinability of additively manufactured parts and identified the appropriate machining parameters and their combinations. The surface roughness measurement results indicate that selecting low DoCs (e.g. 0.25mm) is more likely to obtain less surface roughness. A spindle speed of 4000 – 5000 rpm is recommended and a high feed is feasible for reducing machining times whilst not significantly diminishing surface quality. Different parameter combinations are provided in Table 5.5 for machining parts in various stages of the iAtractive process. In addition, friction induced heat is the major factor that affects surface roughness and thus, using coolant in the finishing operation is required. The above findings and suggestions become the basis for the iAtractive process and GRP^{2}A described in chapter 6.

5.7   Analysis of Part Distortions

This section starts with the theoretical analysis of residual stress induced warping. Based on the theoretical analysis, the experiments were designed and carried out. The distortions of the test parts were measured on a CMM and were then statistically analysed, identifying the relationship between the distortion behaviour and the iAtractive process parameters.

5.7.1   The effects of part distortions on the iAtractive process

One of the major advantages of the iAtractive process is the capability to flexibly and accurately manufacture complex parts. To realise this capability, the sequenced additive, subtractive and inspection operations are required to be carried out interchangeably.

Another prominent advantage is that the iAtractive process is able to remanufacture and reincarnate existing part into another part. In both cases, material is added onto the part that has previously been built or machined. Due to temperature gradients involved in the FFF deposition process, thermal stresses develop (Nickel *et al.*, 2001). These stresses arise from the contraction associated with the deposition of each layer, resulting in distortions or even failure of the deposition process. The previously deposited, machined part, existing part or legacy product (for convenience, all of them are seen as existing parts) is considered as being in a room temperature state (20 °C). This is because warming it up to the T_g is highly time consuming, which significantly increases the production time. More importantly, even though the existing part has been placed and heated on the heated bed of the FFF machine, it is highly unlikely that the heat can be equally distributed in the entire existing part, achieving a constant temperature due to thermal conduction as well as the part geometry. Moreover, once the existing part has been heated, the temperature difference between its bottom and top leads to part distortion behaviour being even more complicated to quantify. As a new additive operation starts, bonding between the newly deposited layer and the previous layer takes place by local re-melting of previously solidified material and diffusion (Sun *et al.*, 2004). The heating and rapid cooling cycles of the material lead to non-uniform thermal gradients that cause continuous stresses accumulation, resulting in further distortions between the existing part and the part built upon it. The distortion behaviour can be found in Figure 5.32 as an example, where the new material (blue part) was built on the existing material (white part). The heat was dissipated during deposition of the blue part. As a result, the rapid temperature reduction after the blue material was extruded caused the material to quickly solidify and contract, which consequently pulled up the existing part.
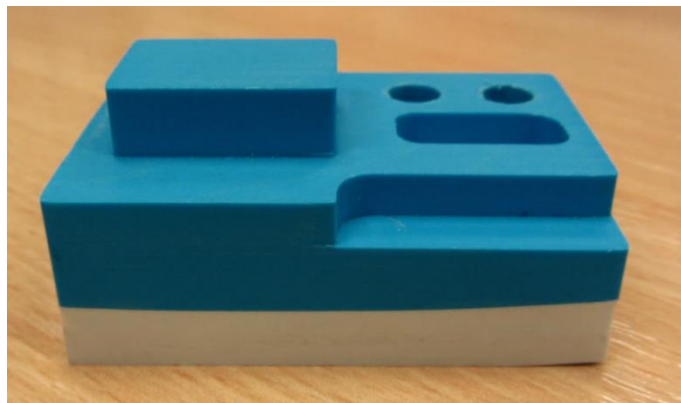
Figure 5.32 – Warping deformation while manufacturing a part from an existing part

In general, parts that are solely manufactured by FFF are placed in a temperature controlled chamber or on a heated bed. By doing so, warping can be significantly reduced. However, the warping effects become evident and unavoidable owing to the working principle of the iAtractive process, which requires material to be continuously added onto the existing part. Moreover, the warped bottom surface of the part leads to difficulty in clamping the workpiece if it is to be subjected to further machining operations. Thus, tolerance loss due to residual stress induced warping is a major concern.

The height of the feature is usually smaller than its nominal dimension since the bottom of the part has been warped, which has to be eventually removed. This also results in more operations leading to increased production time. Simply depositing extra layers while remanufacturing the existing part seems to solve this problem, but this increases unnecessary production time. Printing a single square layer (100% density) with an area of $100 \times 100 \text{mm}^2$ requires approximately 5 minutes. This means printing extra redundant material of 2mm thickness which will be warped and machined afterwards, requires extra 40 minutes build time (0.25mm layer thickness applied). There is a need to reduce this significant waste of time and the distortion behaviour related to the additive process parameters is thus investigated.

5.7.2   The method for investigating part distortion behaviour

Due to each additive process involving a large number of process parameters, the change of any parameter may lead to the quality changes of the final part. It is impractical to explore the effects caused by every FFF process parameter. From the brief literature survey reported section 3.2.2.1, it can be identified that there is no consensus on which process parameters are of the most significance in terms of part distortions. The process parameters that govern the warp deformation behaviour could be completely different depending on each individual additive process. To the author's knowledge, there is no research on part distortions of FFF processed parts.

In order to explore the distortion behaviour in the iAtractive process, the parameters to be investigated in the experiments have to be determined. A simplified mathematical model was first developed, identifying the primary influential process parameters. These parameters were analysed and four parameters were selected. The test parts were designed based on the four parameters. The Taguchi DoE strategy was adopted for designing a

series of experiments. The ANOVA technique was used to analyse the results, identifying the most significant parameters that lead to part distortion. This method is represented in the following IDEF0 representation in Figure 5.33.
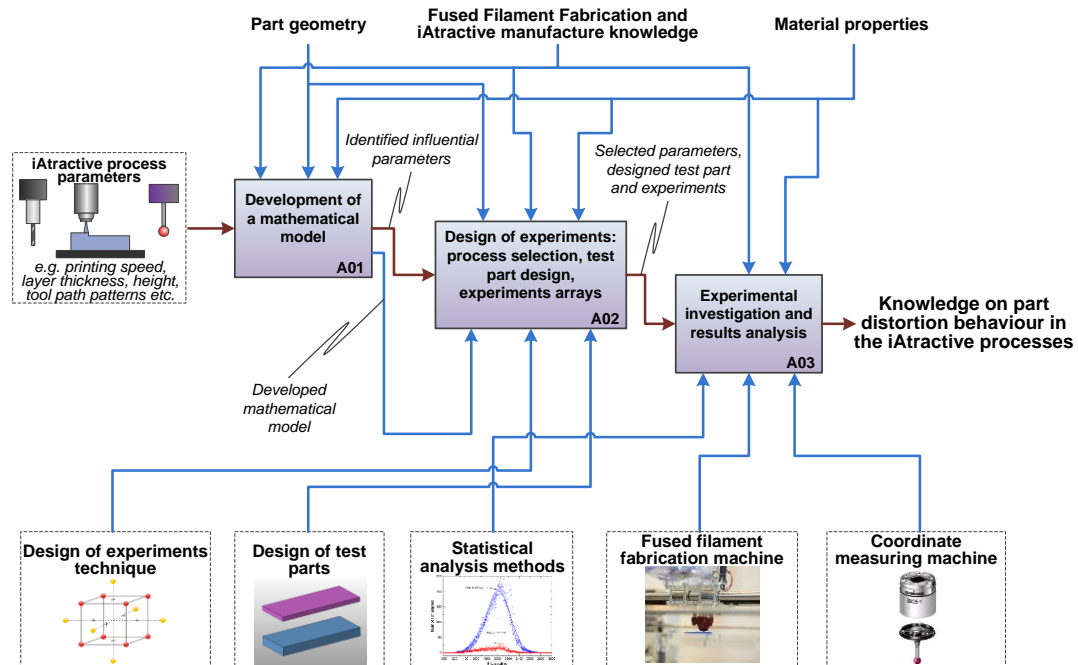
Figure 5.33 – The method for investigating part distortions

5.7.3 A mathematical model of distortion deflection for a subpart built onto another subpart

This mathematical model aims to identify the major factors that affect part distortion behaviour. These factors were involved in the design of experiments stage.

5.7.3.1 Assumptions

The following assumptions are made, which simplifies the FFF process and allows the mathematical model to focus on the major factors that are influential to distortion.

• Deposition speed is constant. The constant and steady deposition speed means the stress inside each deposited fibre of the layer plane can be considered as uniform. If the speed changes frequently, the heat dissipation rate per unit time changes accordingly, leading to cooling rate changes. This essentially indicates the varying levels of stress distributed in different areas of a layer, which significantly increases

the complexity in developing such a model. In addition, this research focuses on how to utilise additive, subtractive and inspection process to manufacture products and thus, for each individual additive operation, the deposition speed is considered to be constant.

- The deposited part does not have voids. The existence of voids between stacking fibres implies the structure changes in micro areas, which means that stresses do not change uniformly and continuously.

- Inner stresses in each layer do not accumulate when the temperature decreases from the melting temperature (T_m) to T_g. As mentioned in section 5.6, PLA is an amorphous plastic. At temperatures above its T_g, it can no longer withstand much stress in which case, significant deformation may occur. In other words, in spite of the fact that the part is subjected to contraction due to the temperature difference between T_m to T_g, no inner stress accumulates. The inner stress is largely induced by the cooling process between T_g to room temperature (T_r), which results in part distortions.

- The existing part or the part directly built on the heated bed is considered to be unwarped. As the FFF process is only able to deposit material on a flat surface, an already warped existing part has to be machined first before more material is deposited. To simplify the process, all surfaces on the existing part are considered to be flat. As mentioned in section 5.2.1, using a heated bed significantly reduces the warping effect.

- Each layer is produced and completed instantaneously in the model. Research has reported that it takes approximately 0.55s to reach the material T_g (94 ℃) once the material (ABS) is extruded from the nozzle ($T_m = 270$ ℃) and only 1.2s is needed from T_g to the FDM machine chamber temperature (70 ℃) (Rodriguez *et al.*, 2000). Although no research data have been published for PLA whose both T_m (195 ℃) and T_g (55 ℃) are much lower than that of ABS, it is obvious that the cooling time for PLA can be regarded as infinitely small compared to the build time for fabricating a middle-sized prototype cube (e.g. $50 \times 50 \times 50$ mm^3). In this case, for simplifying the model, the part is considered as being stacked by a number of layers and each layer is finished instantaneously.

5.7.3.2 *A simplified mathematical model*

Given that the process plan is generated based on part design and existing part geometries including various features, their dimensions and tolerances are the most accessible

geometrical information inputs for GRP^{2}A to make decisions. The model, thus, focuses on the dimensions of the part that affect the degree of part distortions rather than the material properties that essentially cause distortions. Figure 5.34 depicts a scenario before distortions take place, where a layer (thickness of t) with length of L_s is deposited onto an existing part with L_s in length and h_e in height.
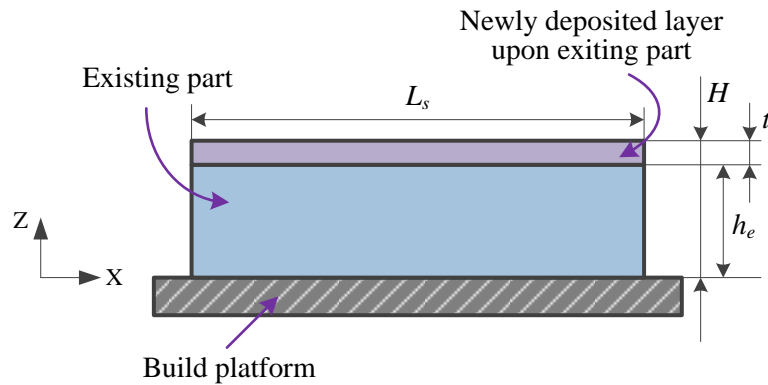
Figure 5.34 – Deposition of a new layer onto an existing part

While distortions occur during the material cooling and deformation finally and completely forms (as shown in Figure 5.35), the main body of the entire part achieves equilibrium. This means the net force between thermal induced stress (σ), the bending stress (τ) and a constant stress (σ_c) has to be zero (Wang *et al.*, 2007), which is depicted in Equation 5.7.

Equation 5.7
$$\int_{0}^{h_e+t} (-E\alpha(T_g - T_r) + \kappa E(z - \gamma)) \cdot dz = 0$$

where, E is Young's modulus of elasticity, α is coefficient of thermal expansion and γ is the distance between the point on the top surface in the neutral axis and the point on the surface where the nozzle moves, κ is the curvature.
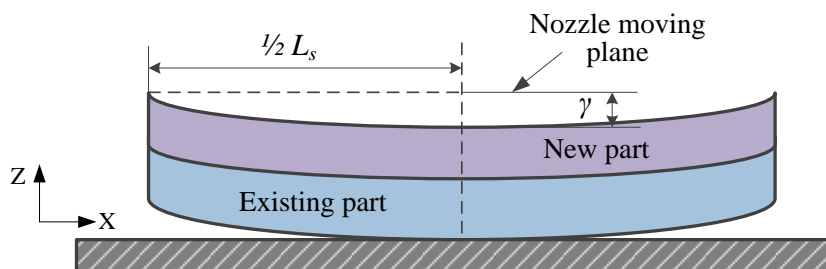
Figure 5.35 – Part distortions occur while adding material to an existing part

In addition, the net moments generated by these forces (σ, τ and σ_c) are equal to zero (Wang *et al.*, 2007), see Equation 5.8.

Equation 5.8
$$\int_{0}^{h_e+t} (-E\alpha(T_g - T_r) + \kappa E(z - \gamma)) \cdot z \cdot dz = 0$$

Solving trigonometric function relationships and simply slicing the part into layers, the distortion displacement (*s*) for depositing *n* new layers can be obtained, using Equation 5.9.

Equation 5.9
$$s = \frac{(N+n)^3 t}{6\alpha N(T_g - T_r)} \times \left[1 - \cos\left[\frac{3\alpha NL_s}{(N+n)^3 t}(T_g - T_r)\right] \right]$$

where, *N* is the number of layers for the existing part, and *n* is the number of layers deposited onto the existing part.

From Equation 5.9, it can be identified that in the scenario specified in the above assumptions, the degree of distortion depends on the height of the existing part, the number of layers to be deposited and the section length of the existing part and the newly deposited part. This finding is used to design the experiments in the proceeding subsection.

5.7.4   Design of experiments: Taguchi DoE strategy for part distortions analysis

5.7.4.1 Determination of process parameters

Prior to conducting the part distortion experiments, the process parameters had to be determined first. As identified in the brief review of the related work presented in section 3.2.2.1, deposition speed (i.e. nozzle travelling speed during material deposition), layer thickness, part porosity, deposition patterns (i.e. patterns of deposition tool path) and road width are the influential factors. In addition, the unique features of the iAtractive process also have to be considered. These factors are discussed as follows:

- *Deposition speed/nozzle travelling speed*: the main effect resulting from the changes of travelling speed is the frequency changes of the material heating and cooling cycle, which essentially alters the degrees of thermal gradients, affecting the thermal-induced stresses accordingly. However, the nozzle travelling speed is considered to be constant during the entire iAtractive process and the reason has already been given in section 5.7.3.1. The effect caused by deposition speed will be discussed in section 5.7.5.

- *Layer thickness (t)*: it directly determines the number of layers to be deposited for printing the part. In other words, fewer layers indicate a lesser number of material heating and cooling cycles and vice versa. On the other hand, applying thick layers diminishes the part quality (Karunakaran *et al.*, 2010). Moreover, for better material bonding, the determination of layer thickness highly depends on the height of the existing part, which will be introduced in section 6.7.2. The influence on part distortions as a result of using different layer thickness is investigated in section 5.7.5.

- *Part porosity/density and extrusion infill width*: increased part density requires more material to fill in certain areas in each layer, increasing the length of the tool path. As a result, more heat is introduced. By contrast, increasing extrusion infill width can effectively reduce the number of loops required for printing a layer, which consequently reduces the tool path length as well as heating and cooling cycles. However, wider infill width will also increase more heat input within a certain period of time, resulting in more obvious distortions during material cooling. Additionally, voids between rasters of two adjacent layers also affect heat dissipation and thus may decrease residual stresses. Hence, for maximising distortion behaviour, 100% density is used. However, it is worth exploring the effect of porosity and infill width in future work.

- *Deposition pattern*: Figure 5.36 demonstrates various deposition patterns available in the fabrication of a layer for a rectangular block. A number of research activities have been carried out, identifying the effects caused by the deposition patterns. The raster pattern with lines oriented $90°$ from the long axis of the rectangular block produces the lowest deflections (Nickel *et al.*, 2001). Klingbeil *et al*. (1998) identified that when depositing in a raster path, material should not be deposited parallel to the longest part dimension. This is because the curvature is the greatest parallel to the deposition direction and depositing parallel to the longest part dimension would result in greater warping deflections and loss of tolerance. The raster pattern with lines $45°$ and concentric pattern generate low and uniform deflection but the part produced by using the former pattern shows better mechanical properties in terms of stiffness and bonding strength between adjacent layers (Bellini and Guceri, 2003). The deflection and mechanical properties of the part by using the Hilbert curve and Octagram spiral are still under development. An initial study has been conducted, showing the Hilbert curve and Concentric patterns generate smaller substrate deflections, compared with

raster $0\,°$ (Yu *et al.*, 2011). Given that the purpose of this study was to investigate the distortion behaviour when adding new material to the existing parts in the iAtractive process, the raster $45\,°$ pattern was chosen for the experimentation, which is also the most widely used pattern in FDM processes (Bellini and Guceri, 2003).

<table>
<tr><td>(a) Raster $0\,°$</td><td>(b) Raster $45\,°$</td></tr>
<tr><td>(c) Raster $90\,°$</td><td>(d) Concentric</td></tr>
<tr><td>(e) Hilbert curve</td><td>(f) Octagram spiral</td></tr>
</table>
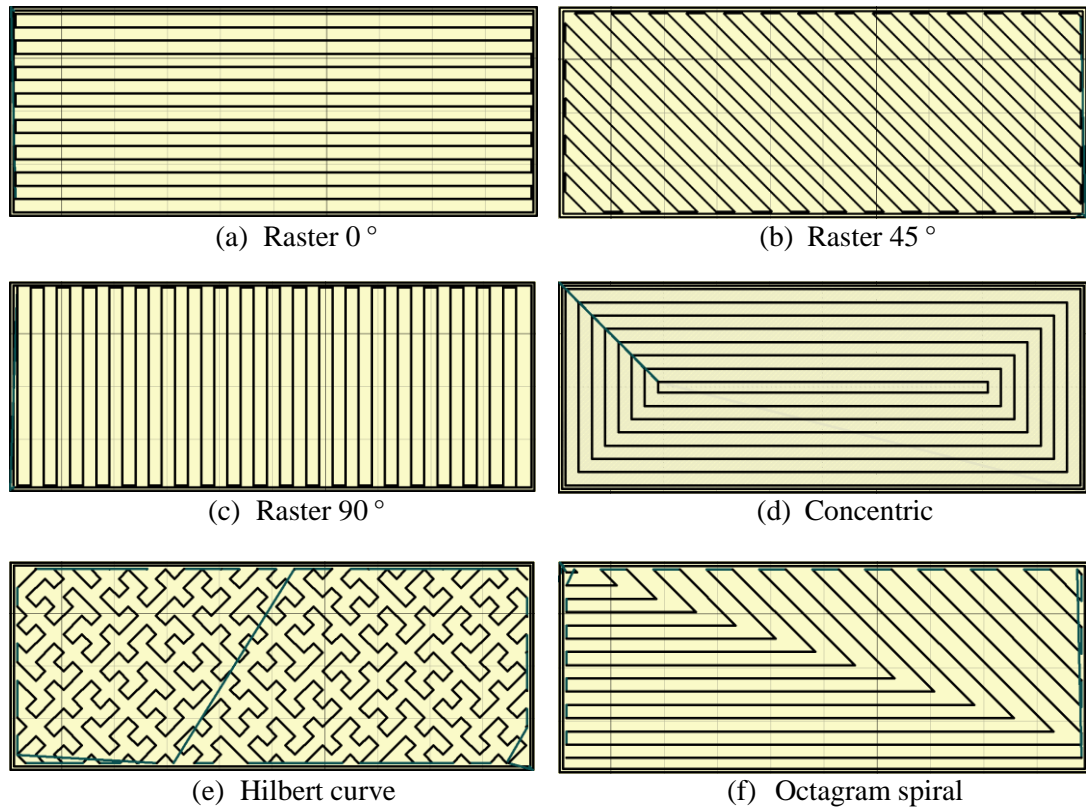
Figure 5.36 – Deposition patterns for printing a layer of the rectangular block

- *Part geometry*: distortion is also geometry dependent, which is virtually impossible to quantify. A typical example is given in Figure 5.37, which is the top view of the cross-section of the parts. The part distortion in Figure 5.37(a) is relatively easier to predict if all the above mentioned parameters are constant. However, the part distortion in Figure 5.37(b) is far more complicated since this relates to the deposition patterns. Using the raster $45\,°$ pattern, for example, the shape edge highlighted in the red circle can have (i) long continuous tool path; or (ii) short continuous tool path (see Figure 5.38, in which white lines are tool paths), depending on the position of the shape edge. As discussed above, long tool paths are likely to produce greater degrees of deflection. In addition, the tool path also varies while changing the magnitude of angle θ, leading to the variation of the residual stress distributions. Furthermore, the

build direction of the existing part may be different from that of the new part being built upon the existing part, which means the deposition patterns of these two parts are possibly different. For simplifying the experimental design and obtaining expected results, a rectangular block is adopted as the part geometry in the experiments, which will be introduced in the proceeding section.

| (a) | (b) |
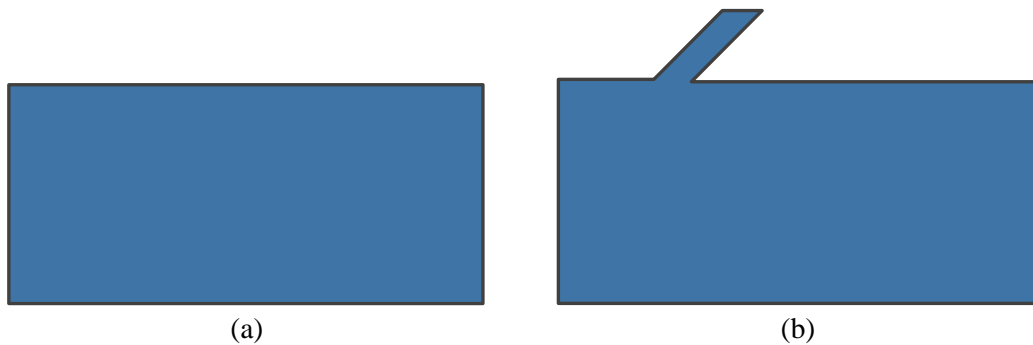
Figure 5.37 – The difference resulted from two part geometries in part distortions

| (i) | (ii) |
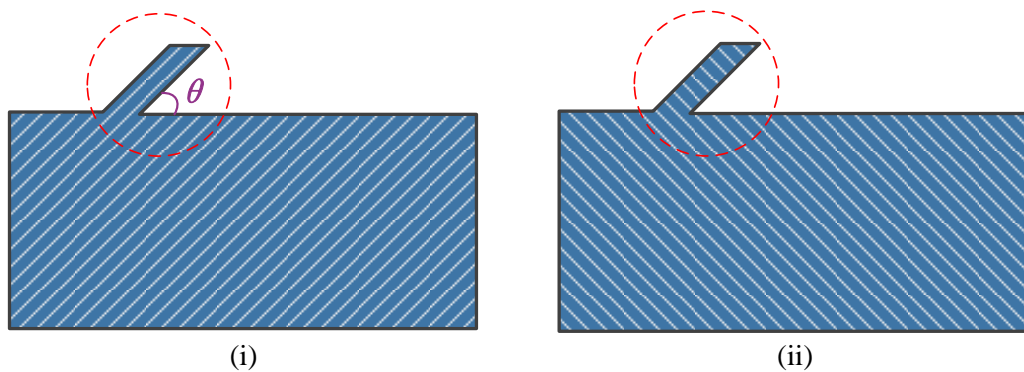
Figure 5.38 – The tool path for printing part (b) in Figure 5.37

- *Section length of the existing part (L_s), heights of the existing part (h_e) and the newly deposited part (h_n)*: these three parameters have already been identified as important parameters (in Equation 5.9) that have direct effect on part distortions. These three parameters are also the most accessible geometrical information for GRP^{2}A.

To this end, the influential parameters to be investigated together with the other parameters to be used in the experiments have been defined. It is worth mentioning that all of the above parameters are interrelated. Nevertheless, given that part distortion analysis will be used as a component for GRP^{2}A, only L_s, h_e and h_n and t were selected.

5.7.4.2 Design of test parts

Two rectangular blocks were designed, as shown in Figure 5.39. Part D is an existing part and part E is deposited directly onto the top of part D.
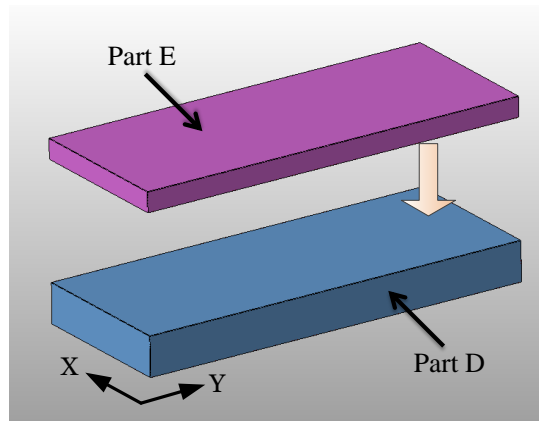
Figure 5.39 – Test part design for part distortion analysis

5.7.4.3 Taguchi design of experiments

If three levels for each control factor are adopted, the study of four factors requires 81 (3^4) experimental runs in the full factorial DoE. The Taguchi design of experiments strategy has been proved to be a powerful tool for effectively reducing the number of experiments to be conducted whilst obtaining similar statistically valid results as compared to that of using the full factorial method (Ross, 1996). Since the aim of the experiments was to identify their effects on part distortions, the Taguchi DoE strategy was chosen as an ideal candidate for the experimentation.

Three levels were applied to each parameter, representing low, medium and high levels, respectively. By considering the working volume of the FFF machine, 60mm, 90mm and 120mm were chosen for section length (L_s). Producing a block of 100cm^3 would cost significant increase in build times, thus 3mm, 6mm and 9mm were decided to be the three levels for the heights of the existing parts (h_e). These three levels of h_e were also applied to the heights of the newly deposited parts (h_n). By doing so, the ratio of h_e to h_n can be 33%, 50%, 67%, 100%, 150%, 200%, 300%, which covers a wide range of the scenarios where the new part is added onto the existing part. The layer thicknesses of 0.2, 0.25 and 0.3mm were used, which are the most stable set up used for the FFF machine. More importantly, these three levels of layer thickness meet the requirements in the process planning stage to

be introduced in section 6.7.2. The interactions between L_s, h_e and h_n were also taken into consideration. Therefore, an L27 Taguchi orthogonal array was generated. The variables and the other process parameters to be used in the experiments are listed in Table 5.6.

Table 5.6 – Process parameters used in the part distortion experiments

Process parameter	Level			Unit	Definition
	1	2	3		
Section length (L_s)	60	90	120	mm	See Figure 5.34
Height of existing part (h_e)	3	6	9	mm	See Figure 5.34
Height of newly deposited part (h_n)	3	6	9	mm	See Figure 5.34
Layer thickness (t)	0.2	0.25	0.3	mm	See Figure 5.34

Fixed factors	Value	Unit	Definition
Extrusion temperature	205	℃	The operating temperature of the nozzle/extruder
Deposition nozzle speed	2500	mm/min	The speed at which the deposition nozzle travels
Deposition pattern	45 °raster	N/A	See Figure 5.36
Road width	0.5	mm	The width of deposition line
Perimeter to raster air gap	0.0	mm	The distance between the perimeter and raster infill
Part density	100	%	The porosity of the part
Infill overlap	0.2	mm	The distance the infill overlaps with the outline perimeter

5.7.5   Results and discussion

The top surface of each newly deposited part (Part E in Figure 5.39) was face milled with 0.5mm removed in order to achieve a flat surface as a datum for measurement. The bottom surface of each test part (in reference to the build direction) was measured using the scanning mode on a CMM, as showed in Figure 5.40. The white part is the existing part and the blue part is the newly deposited part. The part was positioned in the direction opposite to the build direction. A large number of 0.5mm equally spaced points were collected for each scanned line along the section length (Y axis). In order to obtain the results as accurately as possible, 5 lines with 4mm interval between each other along the X axis were scanned. It is noted that the shadow under the blue part is the gap resulting from

the deburring process. All the measurement results are listed in Table 5.7 together with the Taguchi DoE array output.
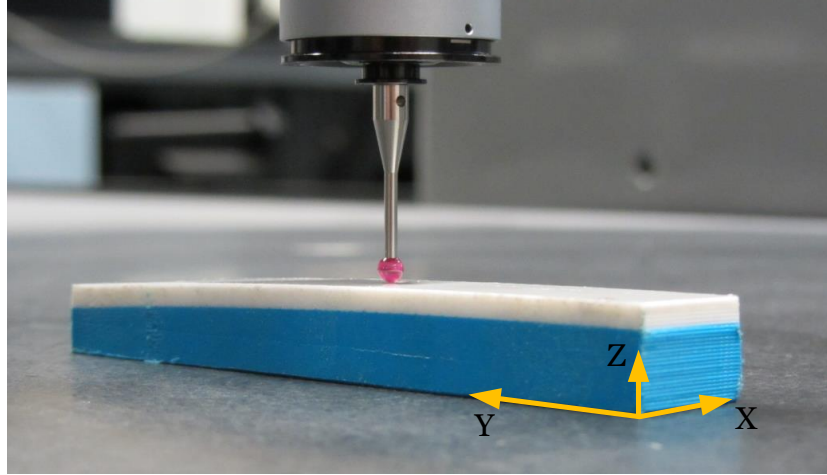
Figure 5.40 – Scanning the bottom surface of a test part

Table 5.7 – Experimental runs and the measurement results for part distortion analysis

Experimental run	Section length L_s (mm)	Height of existing part h_e (mm)	Height of new part h_n (mm)	Layer thickness t (mm)	Distortion deviation (mm)
1	60	3	3	0.2	0.465
2	60	3	6	0.25	0.380
3	60	3	9	0.3	0.521
4	60	6	3	0.25	0.192
5	60	6	6	0.3	0.267
6	60	6	9	0.2	0.155
7	60	9	3	0.3	0.190
8	60	9	6	0.2	0.066
9	60	9	9	0.25	0.166
10	90	3	3	0.25	0.714
11	90	3	6	0.3	0.710
12	90	3	9	0.2	1.285
13	90	6	3	0.3	0.278
14	90	6	6	0.2	0.314
15	90	6	9	0.25	0.186
16	90	9	3	0.2	0.316
17	90	9	6	0.25	0.364
18	90	9	9	0.3	0.389
19	120	3	3	0.3	1.158
20	120	3	6	0.2	1.438
21	120	3	9	0.25	1.263
22	120	6	3	0.2	0.250
23	120	6	6	0.25	0.487
24	120	6	9	0.3	0.720
25	120	9	3	0.25	0.086
26	120	9	6	0.3	0.426
27	120	9	9	0.2	0.285

The ANOVA approach was used to statistically analyse the results, identifying significant parameters and interactions between these parameters. The analysed results are shown in Table 5.8, indicating that the height of the existing part (h_e) is the most significant parameter, followed by the section length (L_s). The height of newly deposited part (h_n) and the layer thickness (t) are insignificant. It was found that the layer thickness of 0.25mm produces the smallest degree of distortion as compared to the layer thickness of 0.2mm and 0.3mm, as demonstrated in Figure 5.41. The three points shown in each plot of the four control factors represent the mean of the measured distortion deviation while such a factor was set at different levels (i.e. from low to high), respectively. The plots illustrate that while applying low section length and/or high value of existing part height, the degree of distortion deviation is significantly lower than that of other factors' levels. Unlike the assumptions proposed in the DoE and the analysis in the mathematical model, layer thickness and height of newly deposited part do not contribute to the majority of the changes in distortion deviation. Regarding the parameter interactions, the interaction of section length and height of the existing part is of primary significance. Therefore, the top three greatest tolerance losses were observed in the test parts, of which L_s was 120mm and h_e was 3mm. In addition, the top three smallest degree of warp deformation were found in the test parts, where L_s was 60mm and h_e was 9mm.

Table 5.8 – ANOVA table for the analysis of part distortions

Source	DOF	Sum of squares (*SS*)	Adj Mean square (*MS*)	F	P
Section length (L_s)	2	0.77	0.39	19.80	0.01
Height of existing part (h_e)	2	2.15	1.07	55.18	<0.001
Height of newly deposited part (h_n)	2	0.10	0.05	2.53	0.16
Layer thickness (t)	2	0.025	0.01	0.63	0.56
L_s*h_e	4	0.47	0.12	6.03	0.03
L_s*h_n	4	0.11	0.03	1.46	0.32
L_s*t	4	0.11	0.03	1.42	0.33
Error	6	0.12	0.02		
Total	26	3.86			
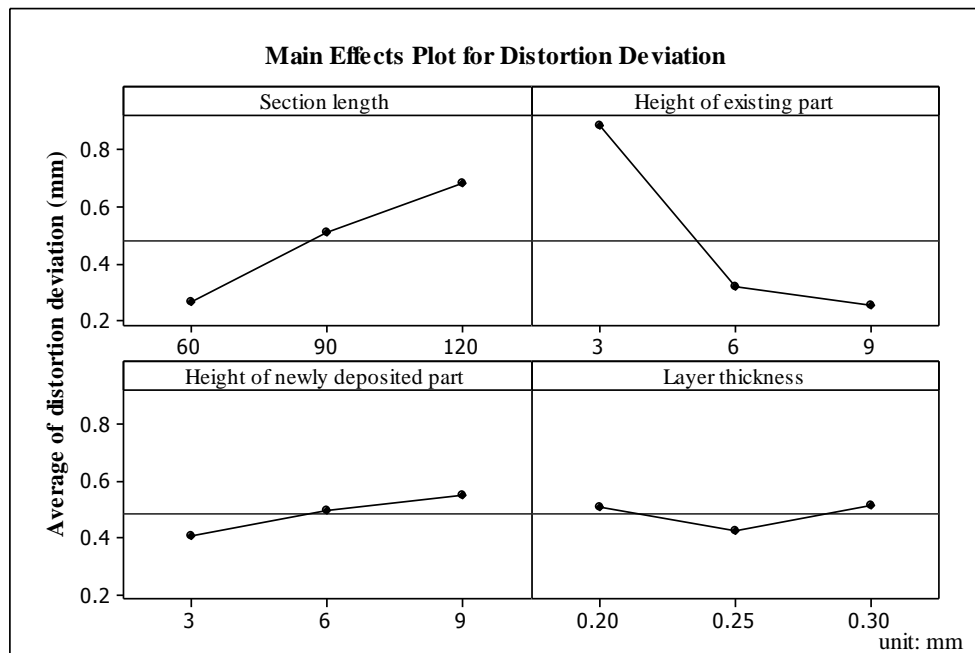
Figure 5.41 – The main effect plots for part distortions

Figure 5.42 shows significance of interaction between two factors. From blocks L1_C2, L3_C2 and L4_C2, it can be identified that increasing the height of the existing part (h_e) can significantly reduce the distortion deviation. The blocks L2_C1, L3_C1 and L4_C1 reveal that increasing section length leads to increased degree of distortion. However, the change of layer thickness (t) or height of newly deposited part (h_n) does not have significant influence on part distortion, as identified in block L3_C1 and L4_C1. In terms of the interaction between the height of existing part and other three factors (blocks L2_C1, L2_C3 and L2_C4), the height of the existing part is far more important than the other three factors, which supports the ANOVA results shown in Table 5.8. Table 5.8 also identifies that the height of newly deposited part and layer thickness are insignificant factors. As a result, there interaction is insignificant as well, as shown in block L3_C4 and L4_C3 where the distortion deviation does not fluctuate severely while changing either of the factors.
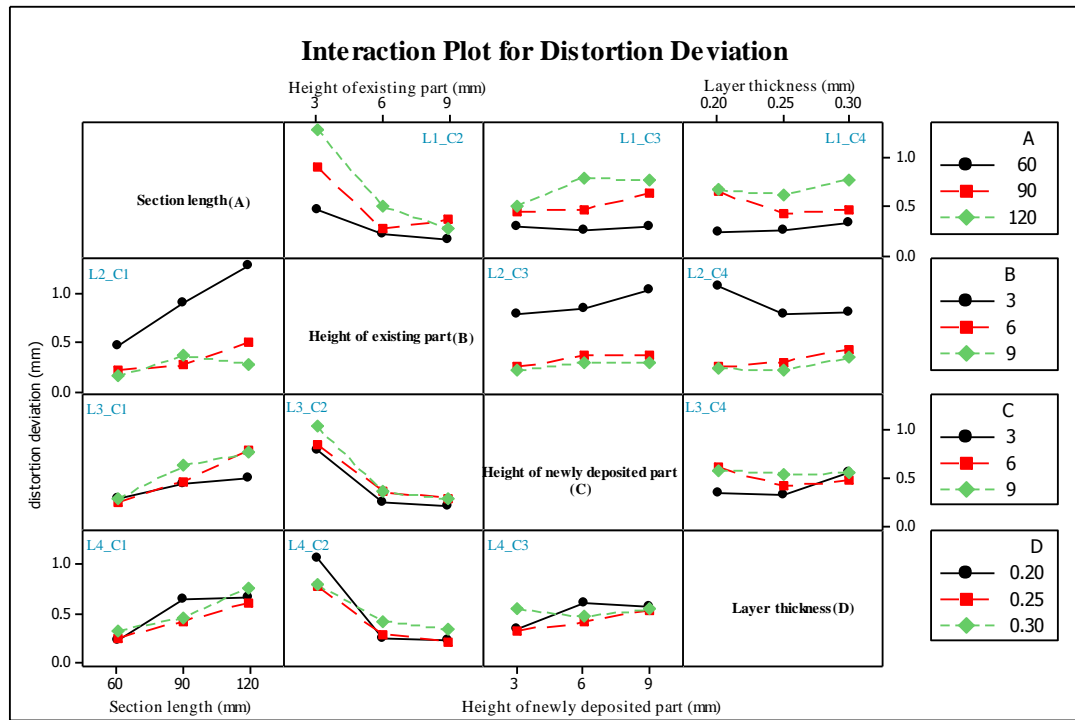
Figure 5.42 – Interaction plot for distortion deviation

The inner stresses are the main reason that results in L_s, h_e and their interaction being significant. Shrinkage along the deposition tool path may be attributed to the development of inner stresses resulting from the contraction of deposited thermoplastic fibres. The contraction is caused by the rapid cooling of the deposited material from its extrusion temperature (205 ℃) to T_g (60 ℃) in a very short period of time. However, it should be noted that, at this temperature range the deposited fibre can acquire a large deformation with less force and the capacity to resist outside force is small (Sood *et al.*, 2009). As a result, despite contraction, the inner stresses are not accumulated in this temperature range. Nevertheless, when cooling from T_g to T_r (20 ℃), stress (σ) given by Equation 5.10 is developed and continuously accumulated.

Equation 5.10 $$\sigma = -E\alpha \cdot (T_g - T_r)$$

where, E is Young's modulus of elasticity, T_g is the glass transition temperature (℃), T_r is the inspection room temperature and α is the coefficient of linear thermal expansion.

Moreover, in the FFF process, heating and rapid cooling cycles of the material results in non-uniform temperature gradients. Consequently, this leads to build up in stresses, which further causes distortions, resulting in dimensional inaccuracy and inner layer cracking or

even delamination. The reason attributed to non-uniform heating and cooling cycles is the working principle of the FFF process. That is heat dissipated by conduction and convection during the entire deposition process. The rapid reduction in temperature enables the material to quickly solidify onto the surrounding filaments (Sood *et al.*, 2009). The heat brought from the newly deposited material diffuses to the previously solidified material, generating local re-melting effects, realising strong bonding between the filaments and adjacent layers. This leads to uneven heating and cooling of material and in turn, generates non-uniform temperature gradients. As a result, uniform stress will not be developed in either the newly deposited part or the existing part. The existing part can no longer regain its original dimension completely. Furthermore, higher stresses are found along the long axis of the deposition tool path (Klingbeil *et al.*, 1998). Also, according to Equation 5.1, the longer the part that the FFF process produces, the greater the linear contraction. As a result, the longer section length directly leads to greater tolerance loss.

The scanned points were used to plot the contour of the bottom surface of each test part. The contour of the bottom of test part 19 is displayed in Figure 5.43 (L_s = 120mm, h_e = 3mm, h_n = 3mm, t = 0.3mm). However, it should be noted that the profile has been displayed in an inverted configuration. This vaulting shape is the typical distortion pattern and all the measured test parts show the similar pattern. It was found that the distortion core shifts away from the geometric centre of the bottom surface along the Y axis. This phenomenon can be explained using the conclusion obtained from the simulation results by Zhang and Chou (2008), who identified that the developed asymmetric stress is distributed during the deposition process. As a result, the position of the distortion centre is shifted. Yu *et al.*'s (2011) results derived from the finite element analysis of temperature distributions also support this finding, demonstrating that the highest temperature zone is not located in the centre of the cross-section of the part in the XY plane.
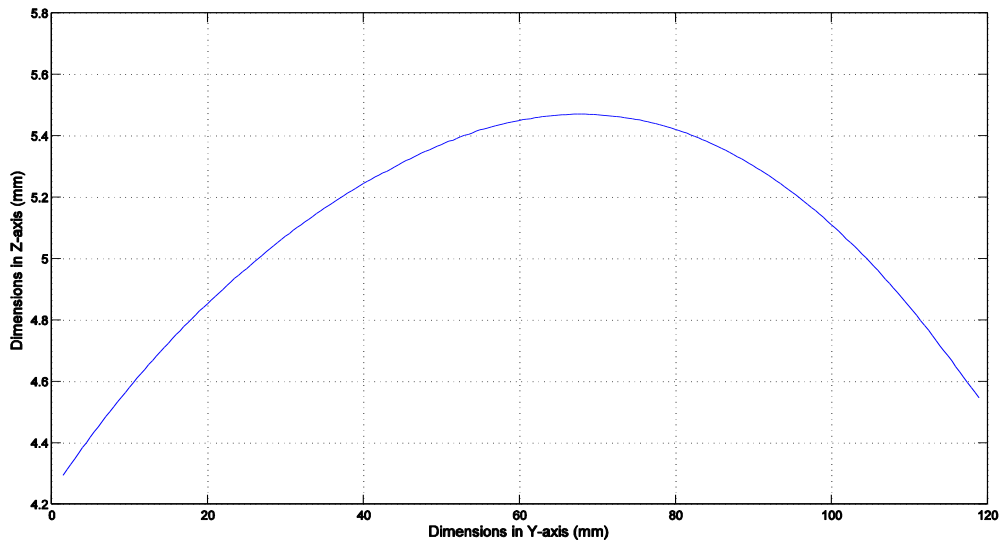
(a) Two dimensional profile
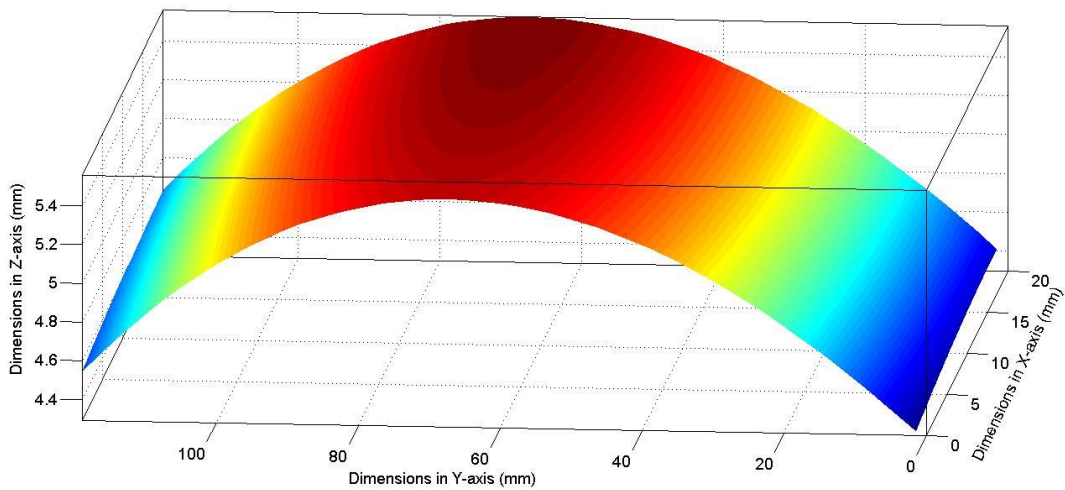
(b) Three dimensional profile

Figure 5.43 – The curvature formed at the bottom of test part 19

There are also other factors that lead to non-uniform heating and cooling cycles:

- Extrusion speed. This is the speed at which the nozzle is extruding/depositing the material. Extrusion speed may alter the heating and cooling cycle and results in different degree of thermal gradient and thus also affects the part distortions and dimensional accuracy. Apparently, at lower slice thickness (e.g. 0.2mm), the extrusion speed is slower as compared to higher slice thickness (e.g. 0.3mm). This is because, in

the same per unit length and the same unit time, more material has to be extruded while printing a 0.3mm depth layer than that of 0.2mm depth layer. In addition, in a continuous deposition process, the nozzle stops depositing material in a random manner (in depositing a layer and after completely depositing a layer), which also results in non-uniform heating and cooling cycles.

- Deposition speed/nozzle travelling speed. As introduced in the experimental design (section 5.7.4), the changes of deposition speed also results in non-uniform heating and cooling. Moreover, no matter what deposition pattern is used, the nozzle travelling speed has to be significantly decreased or even set to zero, when depositing the material at the turns near the part boundary or as the nozzle is approaching a corner on a continuous tool path. In particular, referring to Figure 5.36, the distortion degree of the part produced by using raster 45 °is greater than that of parts produced by raster 90 ° and concentric due to a considerable turns/corners around the part boundary. After passing through the turn/corner, the nozzle accelerates until it achieves the constant speed (i.e. the speed at which the deposition nozzle prints a straight line). If the length of a deposition tool path is short, this will require accelerating and decelerating the deposition nozzle in a short period of time, leading to non-uniform stress build up, particularly near the boundary of the part.

- Deposition patterns. As described in the DoE, the pattern used to deposit material has an effect on the heating and cooling cycle and furthermore the resulting stresses and part deformation. According to Equation 5.1, higher stresses are normally found along the long axis of a deposition line, as shown in Figure 5.36(a) and Figure 5.38(ii). Thus, it is advisable to adopt short raster lengths along the long axis of part to reduce the stresses. An adaptive tool path generation method is needed, which is able to generate appropriate tool paths in terms of length according to part geometries.

5.7.6   Findings and suggestions for the iAtractive process planning

A number of findings together with the suggestions for process planning are summarised as follows:

- The experimental results indicate that the section length and the height of existing part as well as their interaction are of primary significance.

- Long section length and thin existing part are detrimental to dimensional accuracy since a great degree of distortion was observed. Therefore, it is advisable to avoid decomposing long and thin subparts in the part decomposition stage.
- It is also suggested to use a layer thickness of 0.25mm if possible, as it produces the smallest degree of distortion.
- The essential reason that causes the part distortions is the accumulation of residual stresses resulting from non-uniform temperature gradients in continuous heating and cooling cycles in the deposition process.

5.8   Summary

In this chapter, the part manufacturing strategy for the iAtractive process has been investigated, developing an accuracy index for FFF manufactured parts and features; identifying the FFF process capability in producing overhangs; exploring the appropriate parameters for machining of layered parts; and analysing part distortion behaviour. This knowledge forms the basis for the GRP^{2}A and FDL presented in chapters 6 and 7, respectively, determining the generation of process plans and decision-making.

6   A generative reactionary process planning algorithm for the manufacture of complex part geometries

6.1   Introduction

The elements that compose GRP^{2}A are presented in this chapter. The developed algorithm consists of generation of static and dynamic process plans, which allows the iAtractive process to manufacture complex part geometries as well as respond promptly to quality changes during production.

6.2   An Overview of the Process Planning Algorithm

The logical GRP^{2}A is proposed and contains two major phases, namely generation of static and dynamic process plans. The overall goal of GRP^{2}A is to generate process plans from given part designs. The additive, subtractive and inspection processes are used interchangeably to produce the part in the shortest time possible. A static process plan is first generated, including the scheduled sequence of the additive, subtractive and inspection operations together with the process parameters identified in sections 5.4 – 5.7. The static process plan is ready for use in a shop floor manufacture environment, which may be further updated into dynamic plans according to the inspection feedback. A flow chart is depicted in Figure 6.1. This chapter first elaborates the elements in GRP^{2}A for generation of static process plans (sections 6.1 – 6.7), followed by the introduction of dynamic process plan generation (section 6.8).

Generation of static process plans involves three major stages, namely, pre-processing, processing and post-processing stages. The flexibility provided by the FFF process are utilised to create complex structures; CNC machining is used to finish machine FFF manufactured features, ensuring that the dimensions are within the designed tolerances. Three factors are defined as the criteria for generating static process plans, which are cutting tool accessibility, production time and dimensional accuracy.
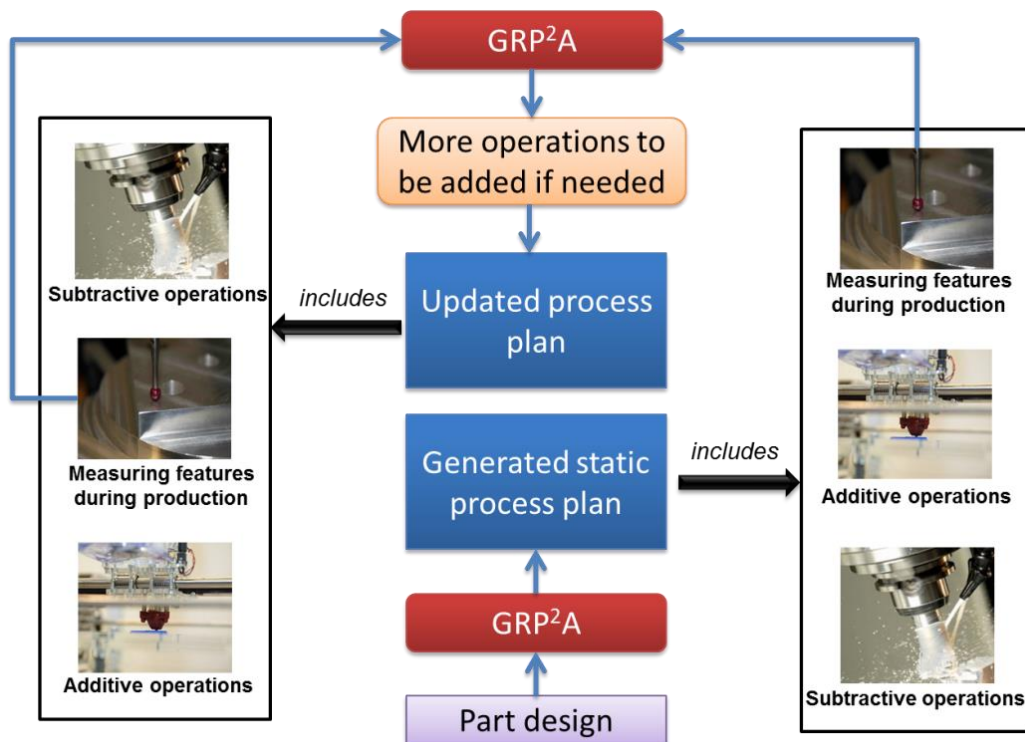
Figure 6.1 – The overview of the generative reactionary process planning algorithm

The three major stages can be further classified into nine steps. Pre-processing includes feature interpretation, manufacturability analysis and part orientation. In the processing stage, a number of operation sequences are generated and the most appropriate one is identified in terms of production time. This stage is the main focus of this chapter. The tool paths for each operation are generated in the post-processing stage based on the specified static process operation. The functional view of GRP^{2}A is depicted as an IDEF0 diagram in Figure 6.2. This figure shows the nine steps together with the relevant tools for generating the static process plan from a part design. The pre-processing stage is introduced in section 6.3. Sections 6.4 – 6.6 present the processing stage followed by post-processing as described in section 6.7.
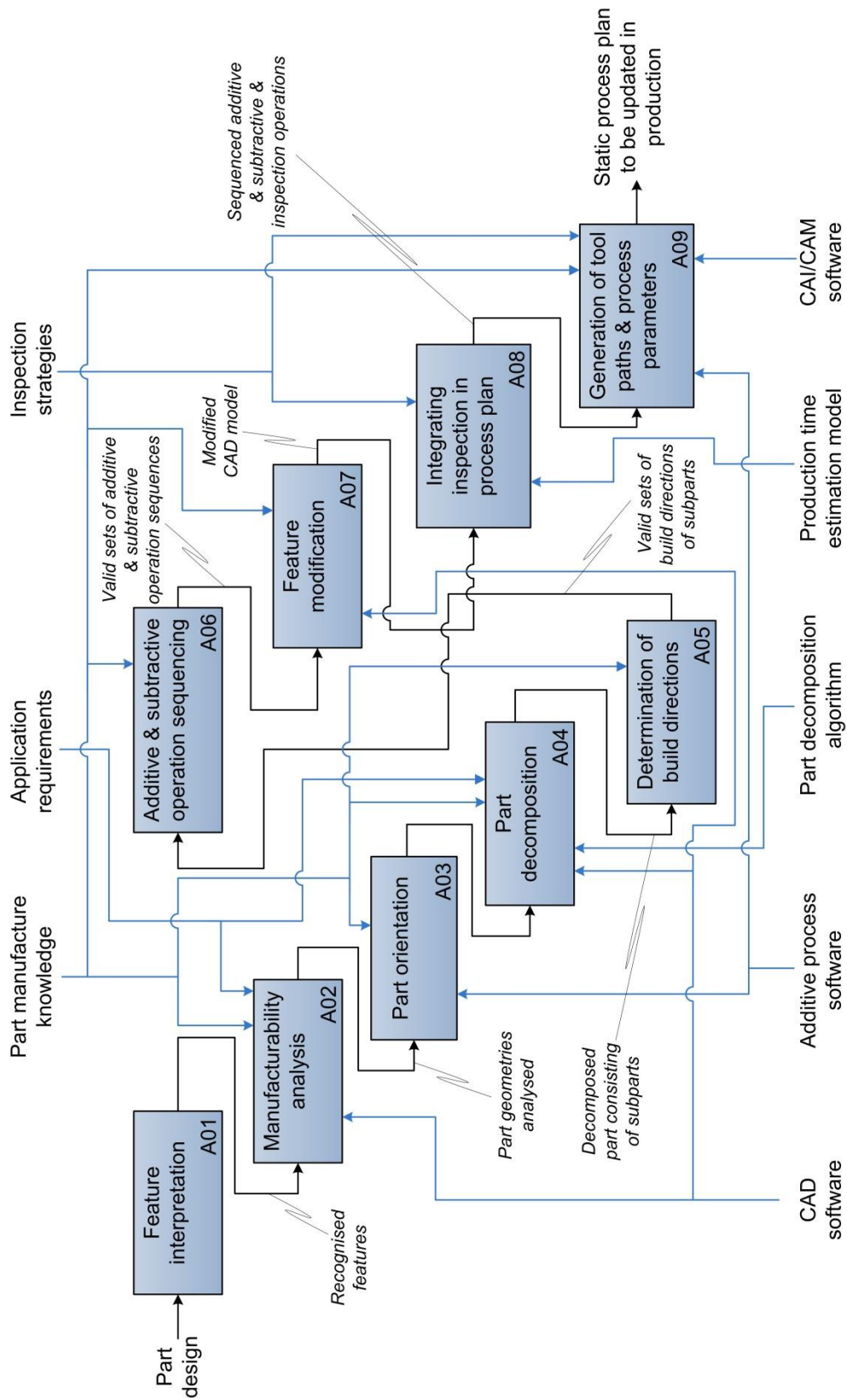
Figure 6.2 – IDEF0 view of GRP²A for the generation of static process plans

6.2.1   The overview of the method for generation of static operation sequences

As introduced above, a number of feasible manufacturing operations are generated in the processing stage. Unlike process planning for CNC machining where operation sequences largely determines production times and costs (Scallan, 2003), the operation sequences for manufacture of complex parts directly determines whether the part (internal features in particular) can be accurately manufactured. Given that the iAtractive process utilises additive, subtractive and inspection processes, the traditional process planning methods (Kulkarni *et al.*, 2000; Lee *et al.*, 2004; Guo *et al.*, 2009; Jin *et al.*, 2013) cannot be adopted since tool accessibility for internal features are not considered in these methods. As a result, the author proposes a method for generating static operation sequences, as shown in Figure 6.3, where the rectangular boxes represent the actions and the round boxes are the outputs of the actions. The final output of this method is the most appropriate operation sequence in terms of production times.
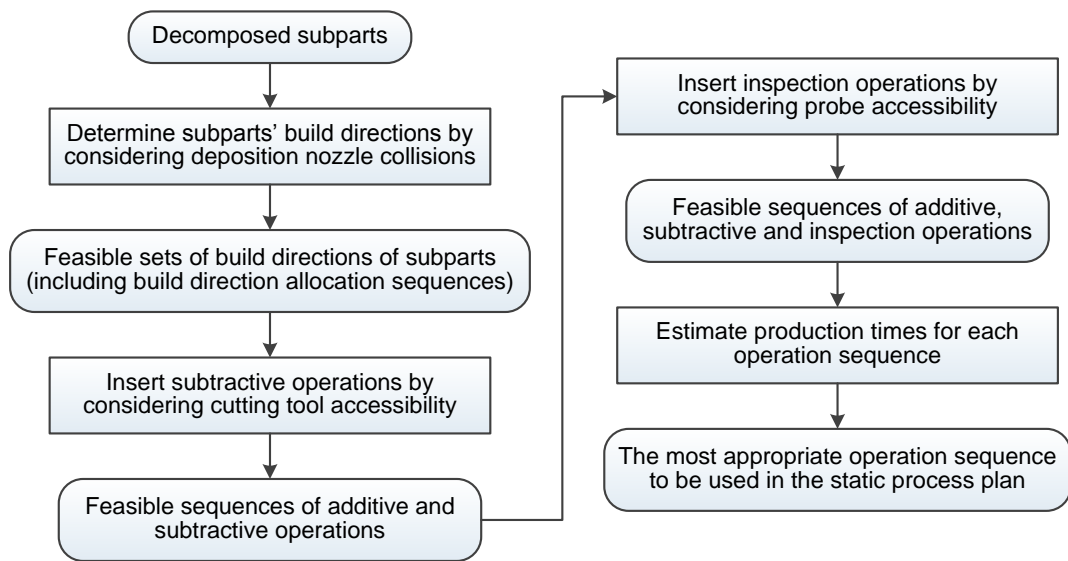
Figure 6.3 – The proposed method for the generation of the static operation sequence

In this method, the operations for additive, subtractive and inspection operations are considered independently in a certain sequence. Since a part will be produced from zero, it has to be built using the FFF process first. Due to the internal features that are required to be finish machined, the part has to be decomposed into a number of subparts, which will be introduced in section 6.4. Thus, the operation sequences for producing these subparts are determined by taking the deposition nozzle collisions into consideration (sections 6.5.2

and 6.5.3). Having obtained the sequences for building the subparts, the machining operations are inserted into the sequenced additive operations for machining the subparts where high surface quality and accuracy are required (sections 6.5.4 and 6.5.5). The cutting tool accessibility is also considered. Finally, the inspection operations are added into the generated additive and subtractive operations to ensure the internal features are measured before they become inaccessible (section 6.7.1). By doing so, a number of feasible sets of operation sequences are scheduled. The most appropriate operation sequence is then identified using the production time and build time estimation models (sections 6.9 and 6.10).

6.3   Pre-processing Stage

6.3.1   Feature interpretation and manufacturability analysis

CAD model format is one of the most frequently used input formats for the majority of the existing process planning systems (Zhang *et al.*, 2013). Pre-processing CAD models i.e. interpreting features and analysing the feature structures, requires significant effort to be made. The CAD model interpretation is considered to be beyond the research scope and is only briefly introduced in this section.

The first step is feature interpretation, which involves extracting and interpreting features from the defined CAD model. A large amount of research has been conducted on feature recognition since the 1970s (Shah and Mäntylä, 1995). Features and associated entities generated by different CAD/CAM systems or representation methods are recognised, which are then input into other CAD/CAM/CAPP systems. A number of feature recognition methods have been proposed and the readers are referred to the papers by Lam and Wong (2000), and Miao *et al*. (2002). It is worth mentioning that due to the fundamental differences between various manufacturing processes, the recognition methods that are available for one manufacturing process may no longer be feasible for other processes. In this research, feature interpretation is completed using human intervention.

The identified features are then analysed in the manufacturability analysis module. Manufacturability analysis falls into two activities, which are machinability and buildability analysis. Any features such as internal and concave features (as shown in Figure 6.4) that are likely to cause potential tool accessibility problems are detected as part

of the machinability analysis. Features that can only be manufactured by the additive process (e.g. a pocket with sharp corners) will also be identified.
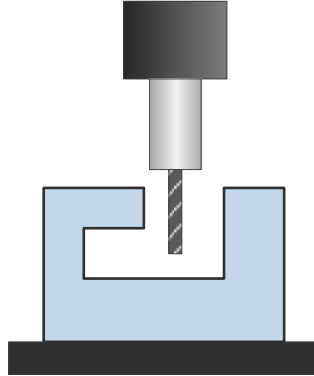
Figure 6.4 – Tool inaccessibility in machining a concave feature

Additionally, cutting tool collision detection will also be conducted even though all the surfaces of the features are exposed (i.e. no internal features). An example can be found in Figure 6.5, in which the heights of the two features exceed the maximum length of the tool, resulting in tool collision if attempting to produce the entire features by using the machining process only.
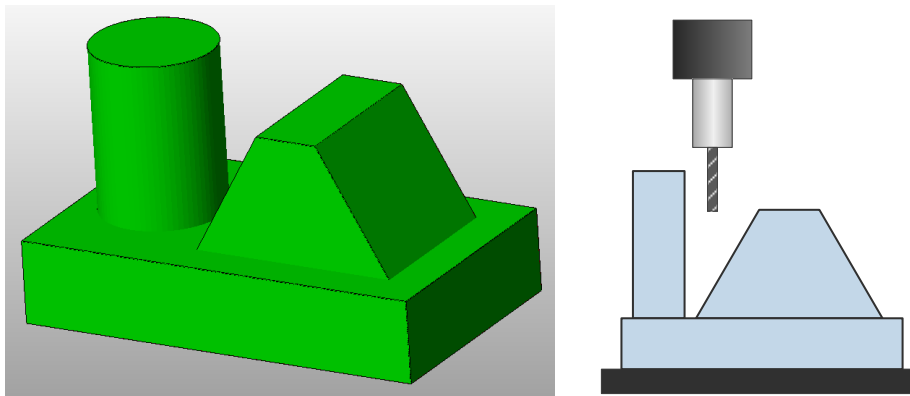
Figure 6.5 – Cutting tool collisions

Buildability analysis identifies overhanging and thin wall features. Overhangs are classified into bridges and cantilevers, as presented in section 5.5. As identified in sections 5.5.1 and 5.5.2, bridges with the length of over 23mm, and cantilevers of which the inclination angles are smaller than $60°$, have to be manufactured together with support material. As the dimensional accuracy of FFF manufactured parts shows significant deviation to the nominal values (section 5.4.2), thin wall and small features are highlighted,

indicating that a machining operation is essential. Previous printing tests have identified that the percentage dimensional error of the FFF parts has the potential to be more than 20% while producing features with less than 5mm. Any feature with the dimension of no more than 5mm is thus considered as a small feature or thin wall. In addition, nozzle collision detection will also be carried out to indicate any possible collisions between the deposition nozzle and the existing features in the case that the existing part is used. More details will be provided in chapter 7.

The aim of this step is to identify whether the given part can be solely produced by the additive or subtractive process. If this is the case, the following stages in Figure 6.2 will not have to be carried out. This is because the part can be machined directly from a block or added to the near-net shape followed by a machining operation. If there are any problems detected, this essentially means that the individual additive or subtractive process is unable to create all features due to the FFF process capability or cutting tool accessibility. The identified machinability difficulties indicate that the additive process has to be used to produce the features. Any features that cause buildability issues would require implementing machining operations. The result of the manufacturability analysis largely determines the following steps. For example, a part with internal features requiring high dimensional accuracy has to be manufactured by FFF and CNC machining interchangeably. The machining operations have to be conducted while the internal feature has not been fully built and the part features are still accessible by the cutting tool. On the other hand, if there is no specific requirement on accuracy, the internal feature can be fabricated by the additive process only, which also leads to different decomposition results while decomposing the part. It is noted that, although the manufacturability analysis has been recognised as an important element for GRP^{2}A, developing an algorithm for manufacturability analysis is considered to be outside the research boundaries. At present, the manufacturability analysis still heavily relies on operator's experience.

6.3.2   Part orientation

Part deposition orientation is a very important factor in layered manufacturing as it affects build times, part strength, dimensional accuracy, surface finish and cost of the prototype (Kulkarni *et al.*, 2000). A number of layered manufacturing process specific parameters and constraints have to be considered while deciding the part deposition orientation.

Traditionally, for individual additive processes, orientation of the part within the machine can affect part accuracy. In addition, part orientation may be in contrast with other factors such as time taken to build a part, whether a certain orientation will generate more supports, or whether certain surfaces should be built face-up to ensure good surface finish in areas that are not in contact with support structures. This is because no matter which additive process system is in use, any down-facing surface will be marginally poorer in surface quality than surfaces that point upwards and to the outside (Gibson *et al.*, 2009). Supports exacerbate this situation.

However, dimensional accuracy and surface finish are not taken into account in this step because the part will be finish machined afterwards. Sood *et al*. (2009) identified that the FDM processed ABS parts are not superior to traditionally moulded parts. The maximum tensile strength and flexural strength of the FDM parts is 16.4MPa and 35.2MPa, respectively, whereas, the moulded parts could achieve up to 65.0MPa in tensile strength and 95.1MPa in flexural strength, respectively. (Sood *et al.*, 2009). The major reasons for the decreased mechanical properties may be attributed to void formation and thermally induced stresses in the FDM parts (Sood *et al.*, 2010). FFF is a comparable process to FDM (see section 5.2). Therefore, part strength is not taken into consideration in GRP^{2}A since the part strength of FFF parts is not comparable to its moulded counterparts.

As a result, only build time is considered to be the major factor that determines part orientation. That is, amongst the different candidate orientations, the most important consideration in choosing orientation is the minimisation of the time to manufacture. A multi-factor regression model has been developed, estimating the time used in the additive process for manufacturing the part from different directions. The development of the model is presented in section 6.10. Based on the model, the following factors should be addressed:

- Part volume. The part volume will not change while orientating the part, but the amount of material to be extruded for manufacturing the part may be different as producing the part in certain orientations requires support. Furthermore, extra time will be spent in machining, setting up the CNC machine and switching between the machining and the FFF process. Thus, the CAD model is orientated in a position, in which the part can be fabricated without support material. Figure 6.6 shows three possible orientations and (c) is the recommended orientation.

(a)　　　　　　　　(b)　　　　　　　　(c)
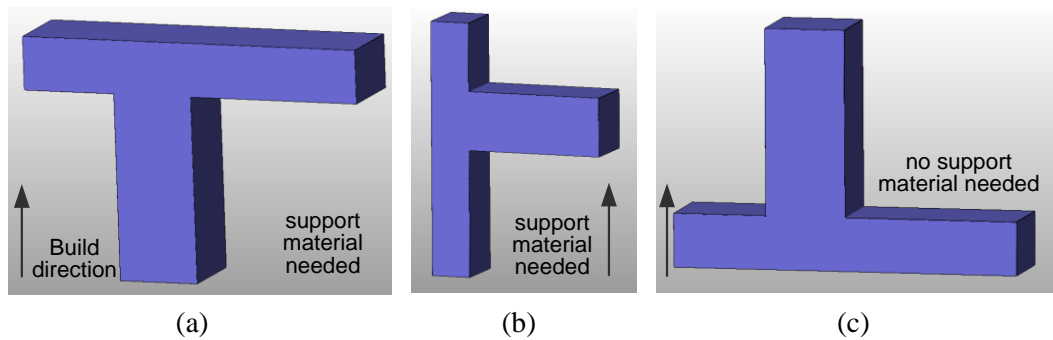
Figure 6.6 – Different part orientations

- Overhangs. It is advisable to minimise the amount of support material since more material will require longer build time, which will be demonstrated in section 6.10. In other words, printing overhanging features should be avoided if possible. In certain cases, there are always some facets that cannot withstand the overhang no matter which orientation the part is positioned. The CAD model should be orientated into a position, where the part can be produced with the least amount of support material possible.

- Height. The build time estimation model has identified that part height also relates to total build times. Taller builds take longer than shorter ones. As a result, high aspect ratio parts may be better built lying down. However, it is noted that part height may not directly correspond to build times if an adaptive slicing approach is adopted, which is considered to be the future trend for AM techniques (Gibson *et al.*, 2009).

- Base face. The area of the base on which the part rests. This area affects the stability of the object as it is being built. This base face functions as the fixture in the additive process. As the deposition nozzle is touching the part during printing, the small contact area at the bottom is not able to provide enough resistance against friction while the nozzle is moving across the part. Additionally, given that part distortions may occur, leading to potential print failure, the base face should not be too small. In initial testing, it was found that the base face should be no smaller than $20\times20\text{mm}^2$. Otherwise, the build is likely to fail. An example is given in Figure 6.7, in which both orientations are feasible and no support is needed, but orientation (b) is suggested.

(a)   (b)
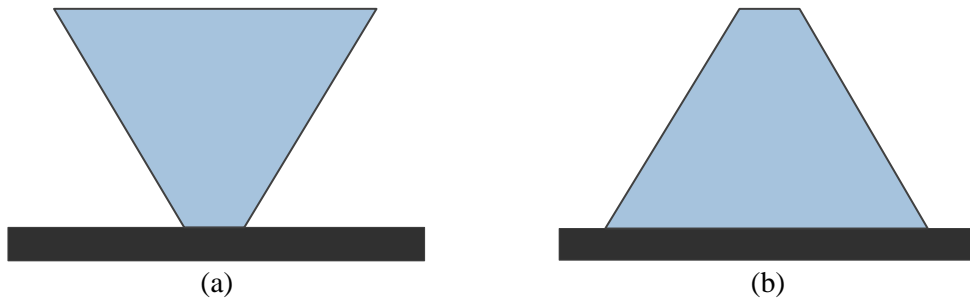
Figure 6.7 – Base face consideration

Since parts that this research deals with have internal features along multiple axes, there may not be an ideal orientation for a particular part. If high dimensional accuracy and surface quality is not specified for all internal features, it may be more important to maintain the geometry of some features when compared with others. For all features that require finish machining, orientating the part in this step is only a dummy activity since all the available orientations will be used and evaluated in order to obtain the most appropriate process sequence, which will be described in section 6.5.

6.4   Part Decomposition

If the part has internal features that cannot be machined because of cutting tool inaccessibility, it will be decomposed into a set of subparts, which allows the internal features to be first produced to the required dimensions and tolerances. Subsequent features are then added. In addition, machining certain non-internal features can also result in tool inaccessibility issue. For instance, the part shown in Figure 6.8 has to be decomposed since there is no available tool access direction for machining the hole.
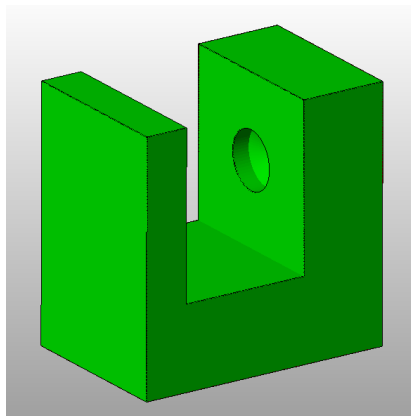
Figure 6.8 – A typical non-internal feature that causes tool inaccessibility issue

The aim of the decomposition is to enable complex parts to be manufactured as one complete unit rather than producing a number of separate pieces requiring assembly. The decomposed subparts are named original subparts. The output of part decomposition is a set of original subparts, which will be further optimised and merged in later stages. Figure 6.9 shows the decomposition results for the part in Figure 6.8. The part is decomposed into three subparts A, B and C.
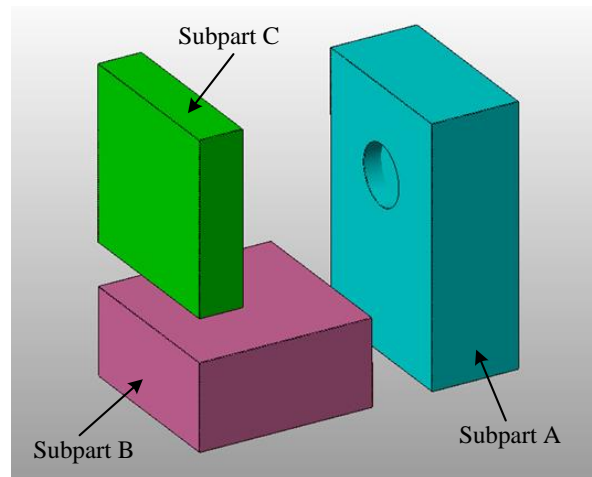
Figure 6.9 – Decomposed original subparts

As stated in chapter 4, decomposition of complex part geometries is one of the important stages in the process planning algorithm. However, this is a major area in its own right and is beyond the scope of this research and requires additional significant investigation. The decomposed subparts in this research are obtained using a method adapted from Hu and Lee (2005).

6.5   Determination of Build Directions, Operation Selection and Sequencing of Additive and Subtractive Operations

6.5.1   Methodology

Figure 6.10 illustrates the various stages in the process planning algorithm. A given part is decomposed into a number of subparts. The viable build directions for each subpart are then identified followed by subpart merging. Subsequently the sequence of the additive and subtractive operations is scheduled, which takes cutting tool accessibility into consideration. In certain scenarios the feasible sequence for producing the part cannot be found due to the limitations of the FFF and CNC machining processes. In this case, the

merged subparts that lead to the failure in operation sequencing will be re-decomposed. Having obtained one feasible sequence, other possible sequences will also be identified if the subparts have other viable build directions. This entire process is then applied to other part orientations, identifying other sequences that can potentially be used to manufacture the part.
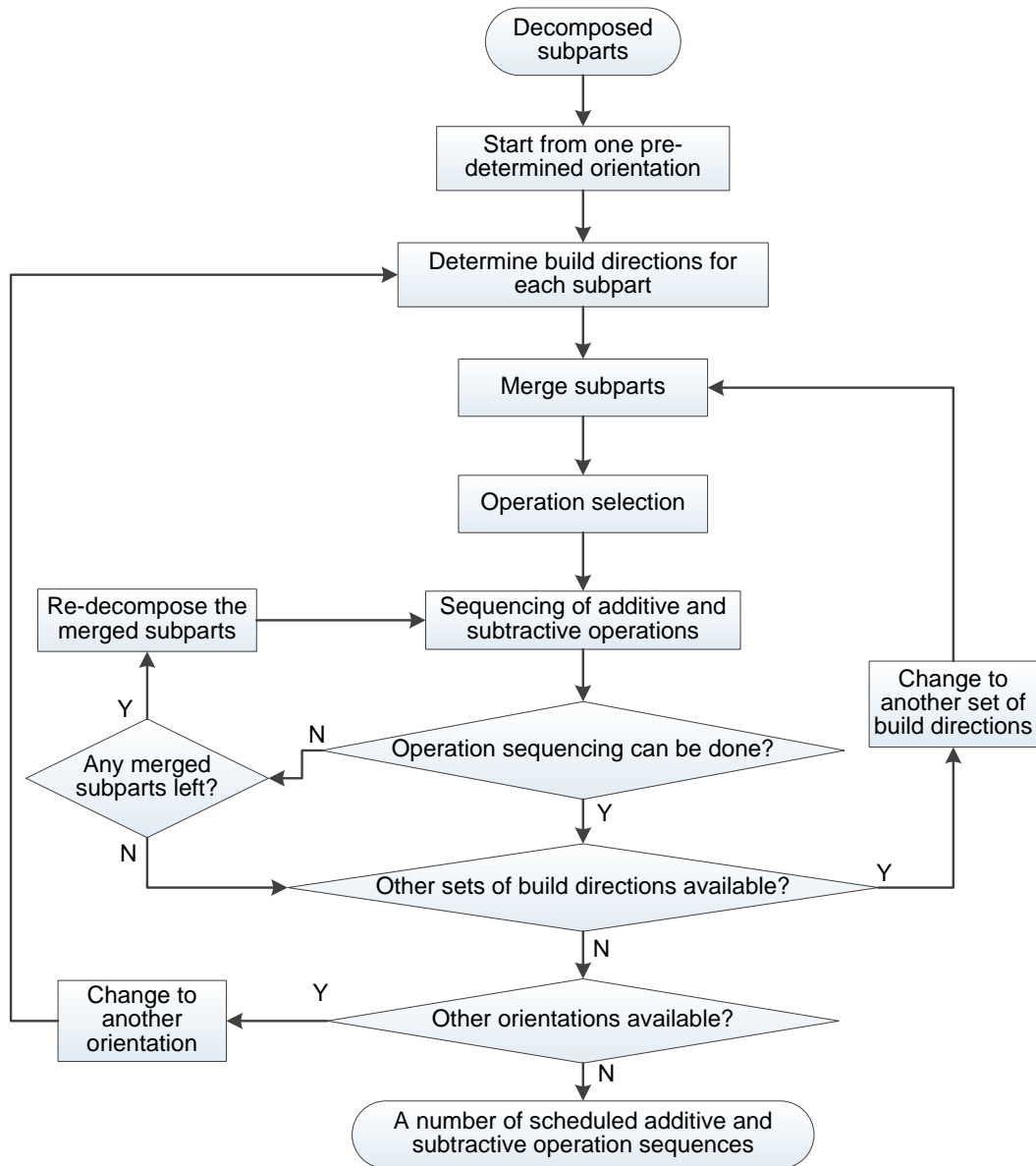
Figure 6.10 – The work flow of build direction determination, operation selection and sequencing

6.5.2 Determination of build directions

This subsection presents the method for determining build directions of decomposed subparts. The considerations and procedures in build direction determination are described in the proceeding subsections.

6.5.2.1 Considerations in determination of build directions

In determining build directions, two issues should be addressed:

(i)   Deposition nozzle collisions may happen while depositing material in certain directions.

Owing to the working principle of the material deposition process, the FFF process can only produce parts layer by layer from the bottom to the top for a given part orientation. Figure 6.11 shows the deposition nozzle on the FFF machine used in this research. Unlike the laser based additive processes, the heated block and the nozzle are the major barriers in printing a subpart on a side face of another subpart.

A typical example is as follows: a part is comprised of three subparts. Figure 6.12(a) shows the scenario where the deposition nozzle collides with subpart 2 while attempting to produce subpart 3 following the build direction indicated by the red arrow. As the build direction of subpart 3 in Figure 6.12(a) is different from that of subpart 2, there is an interruption between printing subpart 2 and 3. This means subpart 2 has already been produced before starting to produce subpart 3. In this case, using the build direction for subpart 3 in Figure 6.12(a) will undoubtedly lead to collisions. Alternatively, the build direction in Figure 6.12(b) is feasible.
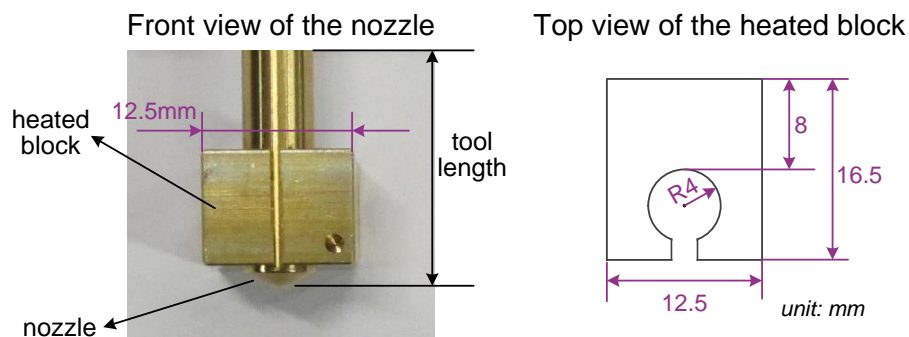
Figure 6.11 – The FFF deposition nozzle used in this research

(a)

(b)
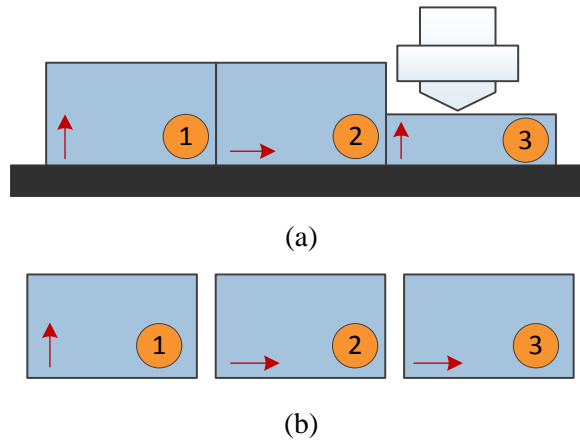
Figure 6.12 – Deposition nozzle collisions

(ii)   <u>The specific operation sequences are restricted by the limitation of the FFF process, namely, features cannot be built without support.</u>

Use the subparts in Figure 6.9 as an example. Having created subpart B using the build direction indicated in Figure 6.13, the build direction of subpart C cannot be the same as that of subpart B, not only because of the deposition nozzle collision but also the lack of support beneath subpart C. As a result, subpart B has to be orientated to act as a build platform. Subpart C can then be deposited using the build direction indicated in Figure 6.13.
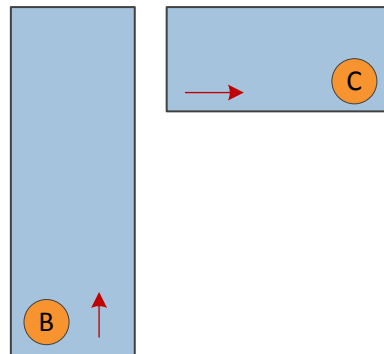
Figure 6.13 – Support is required when using certain build directions

Additionally, it should be noted that the build directions in Figure 6.12(a) may be feasible if using other additive methods, such as laser cladding, rather than the FFF deposition method. Readers are referred to the papers by Ruan *et al*. (2005) and Lanzetta and Cutkosky (2008) for more information.

6.5.2.2 Procedures in determining subpart build directions

After decomposing the part into a number of original subparts, the build directions of these subparts will be determined. The major steps are outlined as follows:

- Based on the pre-determined part orientation and the given subparts, the build direction determination module starts allocating a build direction for the leftmost subpart located at the bottom of the entire part. The build direction of this subpart (called subpart 1 or the first subpart) should be exactly the same as the part orientation specified in the previous stage.

- The adjacent subpart is then selected and the available build directions are determined. If there is more than one subpart that is adjacent next to subpart 1, the subpart (called subpart 2) that shares the same base plane with subpart 1 is chosen first. This is for facilitating subpart merging in the later stage.

- The build directions of the rest of the subparts together with their adjacent subparts will be determined accordingly. An example can be found in Figure 6.14, where two build directions are available for subpart 2, which are indicated by the red arrows. The feasible build directions of subpart 3 (adjacent to subpart 2) are then specified followed by determining the build directions for subpart 4.

- The build directions of every subpart must be specified. However, the subparts of which the build directions have been allocated will not be subject to further build direction determination in one single round. This is to avoid repetition in determining build directions. If a part is decomposed into 4 subparts, each subpart is allocated a build direction and the build direction allocation sequence is subpart 1, 2, 3 and 4. This is considered as one single round. If there is another available allocation sequence, namely subpart 1, 2, 4 and 3. It is regarded as another single round. When the build directions of all the subparts have been specified and no deposition nozzle collisions have occurred, this set of subparts' build directions is considered to be valid. Each single round can only have one or none valid set of build directions.

- Choose another subpart and set it as the first subpart to be determined a build direction until every subpart has been used as the first subpart once.

- Re-orient the entire part and implement the above steps until all the available part orientations (totally six orientations) have been performed.

Figure 6.14 shows two sets of available build directions and demonstrates the procedure in determining these build directions. The build directions of subpart 1, 2, 3 and 4 are determined in sequence. The build direction of subpart 1 is fixed, which has to be the same as the pre-determined part orientation. There are two build directions available for producing subpart 2, and for each of these directions, subpart 3 only has one available direction. Subpart 1 and 2 may have the same build direction since they share the same base plane, which implies that subpart 1 and 2 can be merged into a bigger subpart. By doing so, subpart 1 and 2 can be produced simultaneously. Similarly, the build direction of subpart 3 can also be the same as subpart 1 and 2, as shown in Figure 6.14(a). Alternatively, subpart 3's build direction may be different from that of subpart 1, as shown in Figure 6.14(b). Subpart 4 is adjacent to subpart 3, which means it cannot be produced prior to generating subpart 3. Subpart 4 is built on subpart 3 and as a result, the build direction can also be the same as subpart 3. However, once the build direction of subpart 2 is different from subpart 1, it represents that there is an interruption between producing these two subparts, namely, subpart 1 has to be created and then re-oriented. After re-orienting subpart 1, subpart 2 can be produced using the build direction shown in Figure 6.14(b). The build directions of subpart 3 and 4 have to be changed accordingly. It is noted that, having allocated the build directions of a subpart, it can be rotated 90 ° each time in order to create more available build directions for other subparts. More importantly, this provides more operation sequences for producing complex part geometries. Furthermore, for manufacturing a complete part, there might be more sets of build directions available depending on results of the part decomposition.
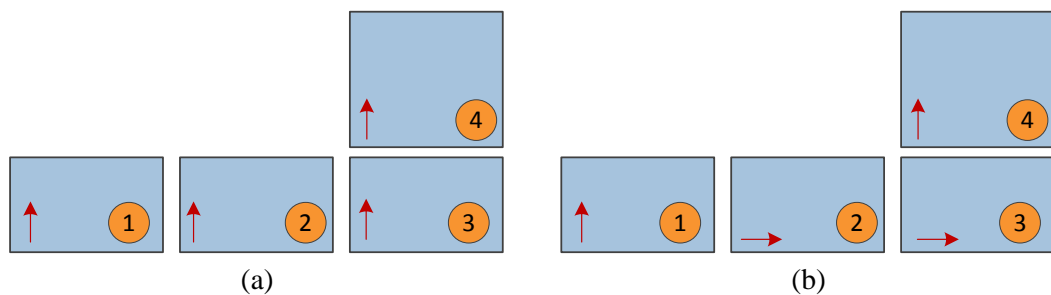
Figure 6.14 – Available build directions for adjacent subparts

Figure 6.15 illustrates the workflow for the determination of subpart build directions described above for a given part orientation. It is noted that in certain scenarios, feasible build directions might not exist due to deposition nozzle collisions and the limitation of the

FFF process described in section 6.5.2.1. When no feasible build direction can be found for any subpart in a single round, it is considered as an error. The subparts which have more than one adjacent subpart or have multiple build directions are recorded in the step (labelled by star *, see Figure 6.15) where subparts' build directions are determined one by one. Only one build direction will be specified and only one adjacent subpart will be chosen in each single round. If there are more than two subparts that have more than one available adjacent subpart or build direction, the last subpart that is allocated a build direction is recorded. For example, there are 5 subparts and the allocation sequence is subpart 1→2→3→4→5. In this sequence, both subpart 2 and 4 have two available build directions. The last subpart that has two or more adjacent subparts is subpart 4. After determining the build directions for every adjacent subpart, the build directions of the remaining subparts will also be decided if there are any subparts left. Having determined the build directions for all the subparts, if no error has ever occurred, the determination of build directions is successful and a set of subparts' build directions has been generated. The build directions determination module will then identify other possible sets of build directions starting from the recorded last subparts that have two or more adjacent subparts or available build directions. To this end, all the sets of build directions based on the build directions of the first subpart have been obtained. It is also likely that there are further sets of build directions available if using a different subpart as the first subpart that is allocated a build direction. Therefore, the module will also identify other sets of build directions using other subparts as the first subparts.

The outcome of build direction determination based on a certain part orientation can be demonstrated in the graph shown in Figure 6.16. Each branch represents a single round, which is also a set of build directions for producing the identical entire part. Each node represents an individual subpart with a certain build directions. Each black arrow represents the allocation sequence between two subparts. In each set of build directions, only one build direction is specified for each subpart. The build direction determination process moves forward (i.e. allocating build directions one by one). This means the build directions of the same subpart will not be determined again once its build direction has been specified. There are x subparts that are adjacent to subpart 2 (i.e. subpart 3, 4 and etc.). As a result, there are x branches expanding from subpart 2. The subparts in each dashed block are identical but have different available build directions. Subpart 4 has a number of build directions and thus, there are a number of corresponding branches spreading from

subpart 3. Subpart *n* has two neighbouring subparts and consequently, there are two branches expanding from it. It is noted that this graph can potentially be used to show the results of build direction determination for the iAtractive process that integrates multiple additive units in the future. Multiple additive units provide enhanced deposition capability, which increases the number of options in determining build directions such as more available build directions and adjacent subparts.
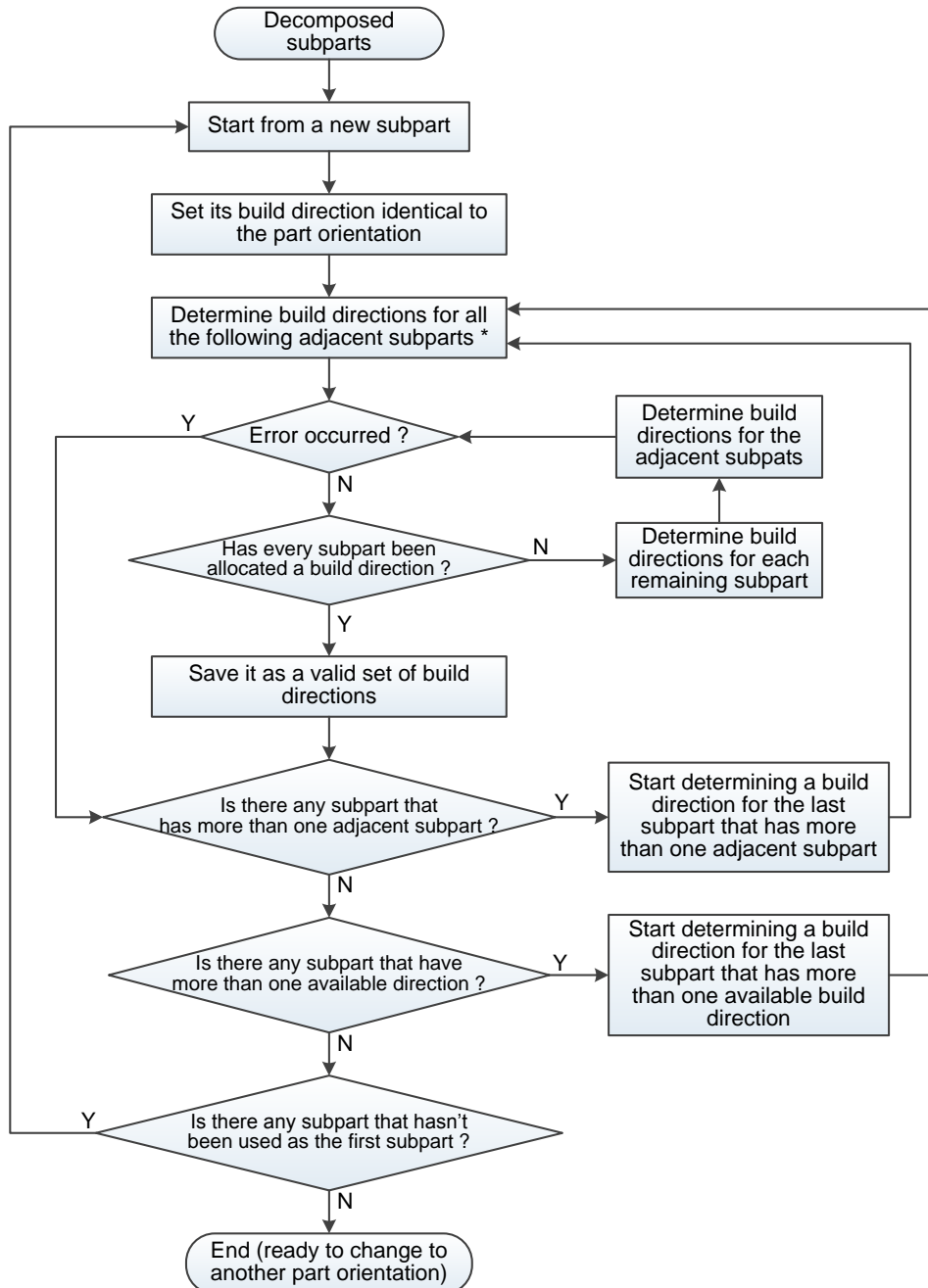
Figure 6.15 – The overall workflow for build direction determination
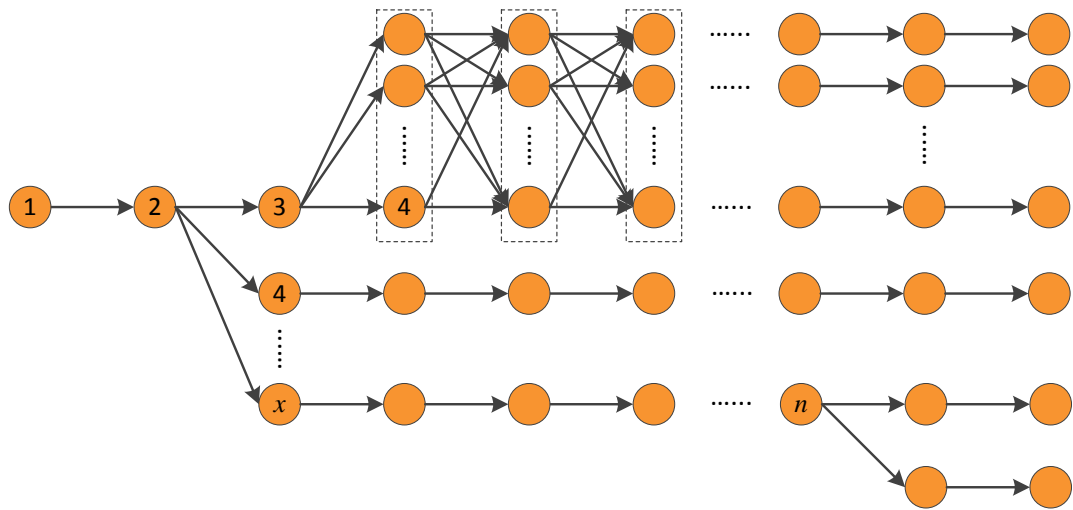
Figure 6.16 – The results obtained in build direction determination

6.5.2.3 *An example demonstrating build direction determination*

An example for the determination of build directions is provided as follows: Figure 6.18, Figure 6.19 and Figure 6.20 demonstrate a number of sets of build directions for the decomposed subparts. The part is decomposed into 9 subparts as shown in Figure 6.17. The build direction of subpart 1 has to be the same as the current part orientation.
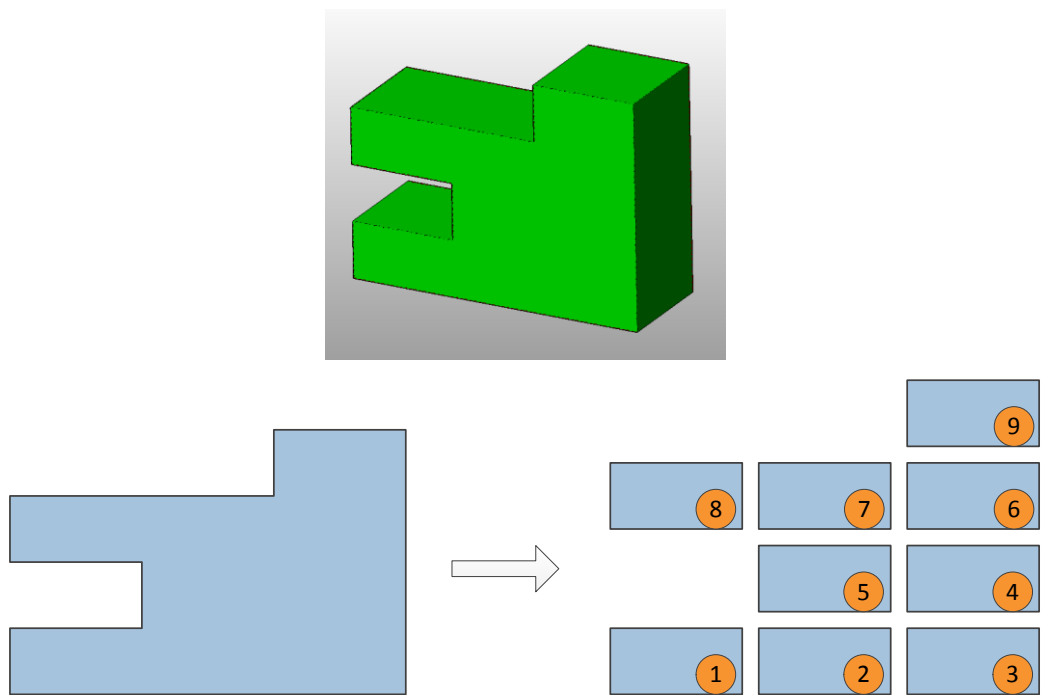
Figure 6.17 – An example part and its decomposed subparts

(i) A feasible set of build directions is shown in Figure 6.18(a). The build direction allocation sequence is: subpart $1 \rightarrow 2 \rightarrow 3 \rightarrow 4 \rightarrow 5 \rightarrow 7 \rightarrow 6 \rightarrow 9 \rightarrow 8$. Having determined the build direction for subpart 9, there is no adjacent subpart anymore. However, there is one subpart left i.e. subpart 8, of which the build direction has not been decided. According to the activity called 'allocate build directions for each remaining subpart' in Figure 6.15, subpart 8 is specified a build direction.

(ii) In the above allocation sequence, among these subparts, there are two available adjacent subparts for subpart 2, 4 and 7, respectively. Subpart 3 has two neighbours i.e. subpart 2 and 4, but the build direction of subpart 2 has already been determined before determining the build direction for subpart 3. According to the rules stated above, no repetition in build direction determination is allowed. This means subpart 4 is the only available adjacent subpart for subpart 3. Subpart 7 is the last subpart that has two adjacent subparts. As a result, another two sets of build directions are developed expanding from subpart 7, which are subpart $1 \rightarrow 2 \rightarrow 3 \rightarrow 4 \rightarrow 5 \rightarrow 7 \rightarrow 8 \rightarrow 6 \rightarrow 9$ and subpart $1 \rightarrow 2 \rightarrow 3 \rightarrow 4 \rightarrow 5 \rightarrow 7 \rightarrow 8 \rightarrow 9 \rightarrow 6$, as shown in Figure 6.18(b). In these two sets of build directions, having determined the build direction for subpart 8, subpart 6 and 9 become two remaining subparts. However, due to the deposition nozzle collisions and the FFF process limitation, these two sets of build directions are invalid. In other words, the feasible build directions based on the allocation sequence (subpart $1 \rightarrow 2 \rightarrow 3 \rightarrow 4 \rightarrow 5 \rightarrow 7 \rightarrow 8 \rightarrow$) does not exist.
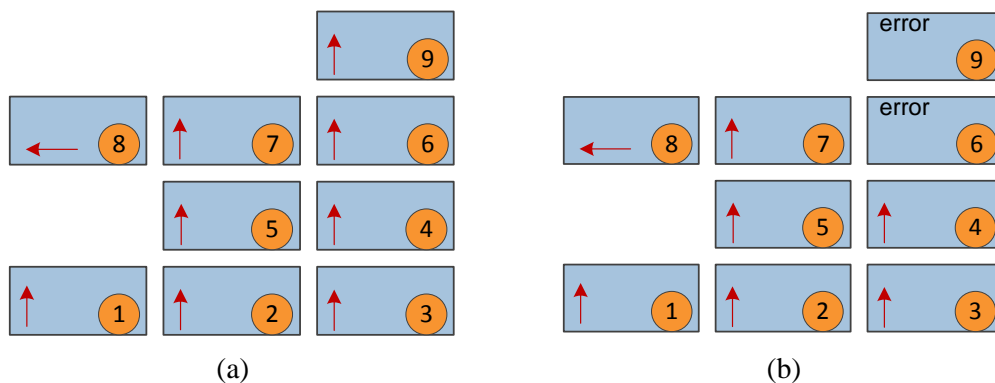
Figure 6.18 – Two sets of build directions

(iii) In determining the build directions according to the allocation sequence (subpart $1 \rightarrow 2 \rightarrow 3 \rightarrow 4 \rightarrow 5 \rightarrow 7 \rightarrow 8 \rightarrow 9 \rightarrow 6$), subpart 4 is identified as the subpart that has two available neighbouring subparts (i.e. subpart 5 and 6). Hence, a new set of

build directions are identified. More sets of build directions are found in identifying this new set of build directions. These sets are illustrated in Figure 6.20, where the cross symbol ($\times$) represents an error which has occurred in allocating the build direction of a certain subpart.

(iv) Upon obtaining all the sets of build directions based on the build direction of subpart 2 shown in Figure 6.18, more sets of build direction will be identified as a result of two build directions that exist for subpart 2. One of the feasible sets of build direction (i.e. subpart $1 \rightarrow 2 \rightarrow 3 \rightarrow 4 \rightarrow 5 \rightarrow 7 \rightarrow 6 \rightarrow 9 \rightarrow 8$) is depicted in Figure 6.19. Further sets of build directions are illustrated in Figure 6.20.
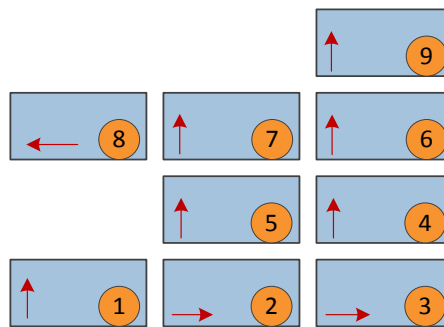
Figure 6.19 – A set of build directions based on another build direction of subpart 2

6.5.2.4 *Relationships between two successive subparts in a set of build directions*

As introduced in section 6.4, the subparts obtained from part decomposition are termed original subparts. If two original subparts in a set of build directions are allocated build directions in sequence, they are considered to be successive subparts. The relationships between two successive subparts in a set of build directions are categorised as parent, child, twin and unconnected. The parent and child relationship is generated as a result of additive operation interruption, as explained in section 6.5.2.1(i) and Figure 6.12. A subpart that has to be deposited onto another subpart is considered to be a child part. For example, subpart 3 is a parent part and subpart 4 is a child part in Figure 6.19. This is because subpart 4 is built on subpart 3 and thus, subpart 4 cannot be produced without generating subpart 3 beforehand. The twin relationship indicates these two subparts may be produced simultaneously by sharing a same build platform, such as subpart 1 and 2 in Figure 6.18. Unconnected subparts are the subparts that are not physically connected to each other. Subpart 9 and 8 in the build direction set as shown in Figure 6.18(a) are an example of a pair of unconnected subparts. However, it should be pointed out that the relationship

between two successive subparts is only valid in a certain set of build directions in a certain part orientation. In different sets of build directions, the relationship between the two successive subparts may vary. For example, in Figure 6.19, subpart 1 and 2 are parent and child part, respectively, whereas they are twin subparts in the scenario shown in Figure 6.18.
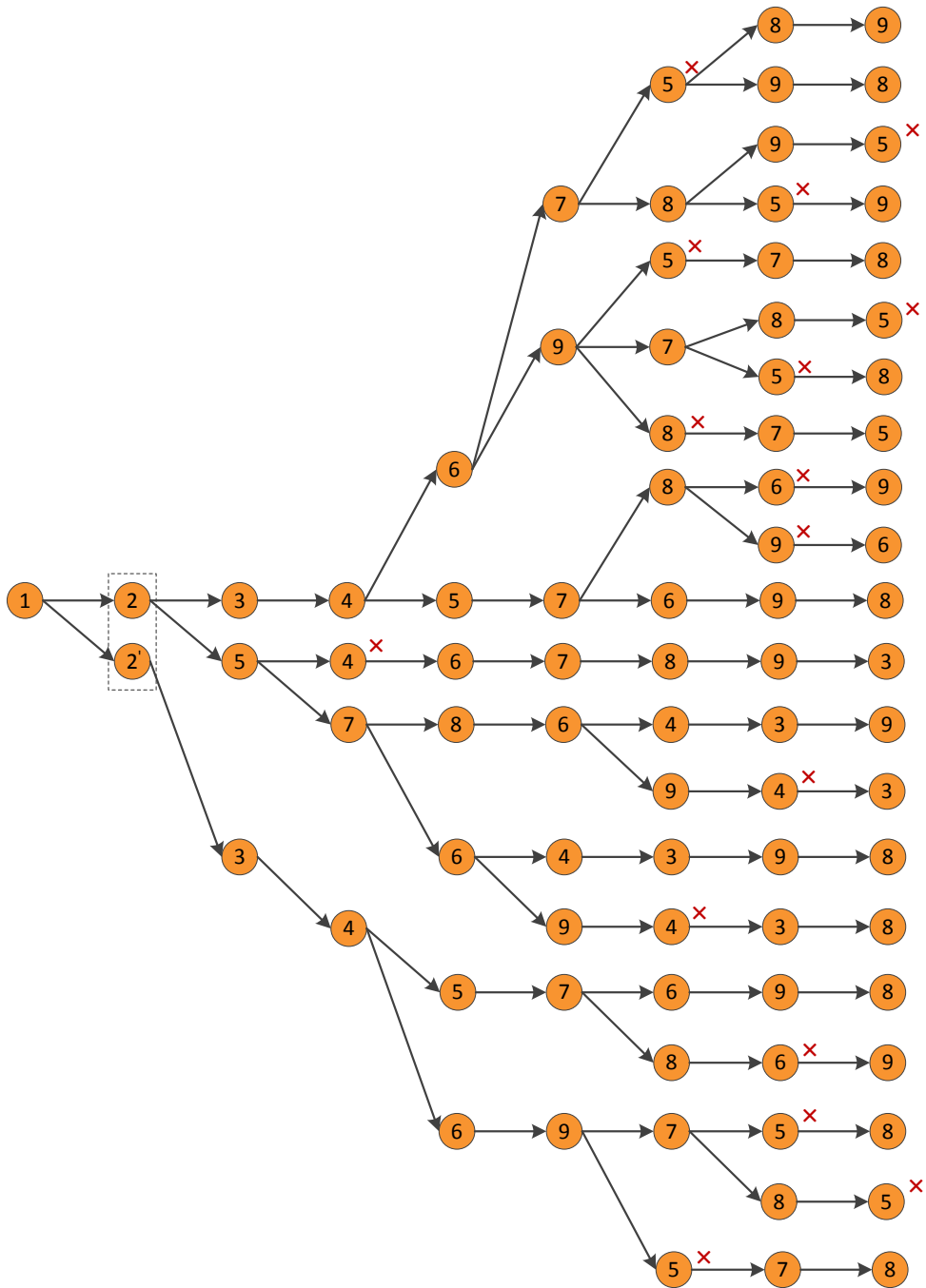
Figure 6.20 – A partial representation of the full set of build directions

6.5.3   Subpart merging

The two original subparts can be merged into one subpart if they meet the requirements below:

- They are adjacent subparts
- They are successive subparts in a set of build directions
- They have the same build direction

A merged subpart can further be merged with its adjacent original subparts if they have the same build direction. The sequence of subpart merging should follow the sequence in allocating build directions for original subparts. It is noted that the results of subpart merging may be different from one set to another set of build directions. Two examples of subpart merging are provided in Figure 6.21. The eight original subparts in Figure 6.18(a) are merged into one merged subparts as shown in Figure 6.21(a). Figure 6.21(b) shows the two merged subparts which are obtained from merging the seven original subparts in Figure 6.19.

<p align="center">(a)   (b)</p>
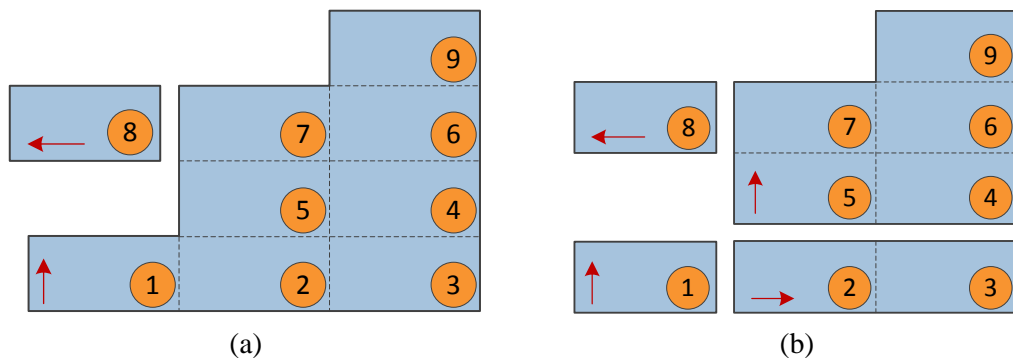
<p align="center">Figure 6.21 – Subpart merging</p>

Subpart merging is preferable when two adjacent subparts can either be produced in series or simultaneously. This is because producing merged subparts can lead to reduction in production time. Subpart merging also provides more available build directions for original subparts. For instance, in Figure 6.21(a), if subpart 2 has been produced before starting to create subpart 3, this leaves only one available build direction (i.e. →) for subpart 3. Again, once subpart 2 is built separately with the build direction indicated in Figure 6.21(a), it has to be machined and measured before subpart 3 can be deposited. This increases the production time, namely extra time used in: (i) switching from the additive operation

(building subpart 2) to the subtractive operation (machining subpart 2); (ii) setting up the machine tool (setting up fixtures, clamping built subpart 2 and etc.); (iii) machining subpart 2; (iv) switching from the subtractive operation to the inspection operation; (v) inspection (measuring machined subpart 2); (vi) switching from the inspection operation to the additive operation (building subpart 3); (vii) positioning machined subpart 2 on the build platform of the FFF machine. Moreover, there is a possibility that dimensional error is introduced in those above operations. Another issue is that the bonding strength between two subparts is much lower than one single subpart that is purely built in one additive operation. Hence, it is advisable to fabricate as many subparts as possible in one single additive operation.

6.5.4 Operation selection

Operation selection is a broad topic in process planning research, which involves a large number of factors that need to be taken into consideration, such as part geometry and cost (Xu *et al.*, 2011). In this research, operation selection is restricted in a very narrow area. Operations used in the iAtractive process production are classified into additive, subtractive (machining), inspection, switch operations. A brief description is given as follows:

- Additive/deposition operations are applied to manufacturing every subpart/feature if a part is produced from zero. In this study, additive operations are conducted on the FFF machine.

- Subtractive operations can be further classified into two operations, namely roughing and finishing. The additive process is used to create the near-net shape of the feature/subpart/part. Thus, finishing operations are used to finish machine the near-net shape of the feature. Machining is considered to be the way to obtain high part accuracy and surface quality. Roughing operations are largely used in manufacturing the first feature from an existing part and an example is provided in section 7.4.4.2(i). In addition, roughing operations are also used to remove sacrificial support material. The details of machining operations will not be considered. For example, the details such as face mill the top surface of the feature and drill the hole will not be specified. Instead, operations in GRP^2A are: rough machine the feature, finish machine the feature, finish machine the hole. Machining operations are carried out on a 3-axis vertical CNC milling centre.

- Inspection operations are used to obtain the actual dimensions of the features, which provides geometrical information for the process planning algorithm.

- Switch operations indicate there is a switch between either two of additive, subtractive and inspection processes. Additionally, reorientation and repositioning of the subpart are required when the build direction changes, which is also categorised as a switch operation.

For simplifying the considerations in operation selection and sequencing, it is assumed that a tool magazine with a full range of cutting tools is provided. That means the cutting tools with various diameters for producing the features are available. For example, a 3mm diameter slot mill is available if a pocket with a corner of 1.5mm radius is required to be produced. Additionally, even though the determination of cutting tools is an important step in process planning of CNC machining production, it is not within the boundaries of this research. The reason is: for machining a 50mm wide face feature, all the tools whose diameter is less than 75mm can be used, such as 75mm, 50mm and 20mm diameter tools. Using a 20mm diameter tool to machine the face will take approximately three times longer than that of using a 75mm tool due to the tool being over three times bigger. In this case, the 20mm diameter tool should not be used in terms of production time and costs. This example shows that involving the cutting tool determination brings more complexity in process planning. Tool selection has been well researched for CNC machining processes (Fernandes and Raja, 2000; You *et al.*, 2007; Xu *et al.*, 2011). In order to focus on the major considerations outlined in section 4.3.1, cutting tool selection will not be considered in this research but appropriate cutting tools are selected based on the features to be machined.

6.5.5   Sequencing of additive and subtractive operations

This subsection first presents the constraints that are applied in sequencing of additive and subtractive operations. The overall work flow of operation sequencing is then presented.

6.5.5.1 Precedence Constraints

Three types of precedence constraints are considered, which are dimensional accuracy constraints, build direction allocation sequence constraints, and machining constraints.

(i)   Dimensional accuracy constraints

For the features where low surface roughness and high accuracy are specified in the part design, a machining operation must be used to ensure the surface quality and dimensional accuracy. Table 5.1 provides the dimensional accuracy deviation of parts produced by the FFF process, which provides the accuracy information for GRP^{2}A to make decisions on whether to conduct a machining operation for the feature. In this chapter, the iAtractive process aims to accurately produce complex parts and thus, the dimensions of every feature are required to be accurate and only a finish machining operation is able to achieve this high accuracy.

(ii)   Build direction allocation sequence constraints

This type of constraint means that machining operations should be inserted into the build direction allocation sequence. For example, the operations for machining the child part have to be scheduled after the additive operations that are used to create the parent part. This is also logical since the child part cannot be machined before the parent part is built. Moreover, the operations to produce two unconnected subparts should also follow the allocation sequence of build directions.
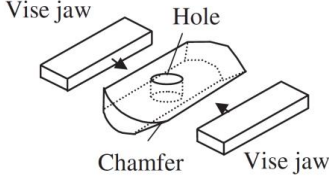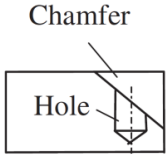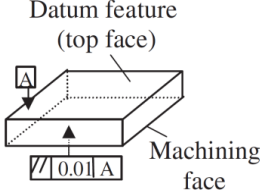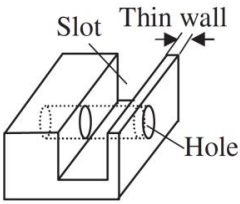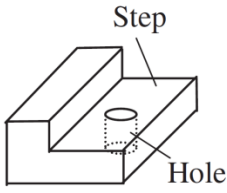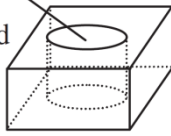
(iii)   Machining constraints

A feasible operation sequence should also comply with the machining constraints that come from geometrical and technological considerations. The machining precedence constraints between machining operations are usually classified into six types, which are fixture interaction, tool interaction, datum interaction, thin-wall interaction, material-removal interaction and fixed order of machining operations (Li *et al.*, 2004). The illustrative examples of these machining constraints are provided in Table 6.1.

6.5.5.2 Tool accessibility Constraints

Tool accessibility is one of the most important factors to be considered in the process planning algorithm as this directly determines whether or not a feature, especially an internal feature, can be built and machined. Tool accessibility constraints consist of cutting tool accessibility and deposition nozzle accessibility. The deposition nozzle accessibility has already been illustrated in section 6.5.2.1. Cutting tool accessibility is concerned with TAD.

Table 6.1 – Examples of precedence constraints (Li *et al.*, 2004)

Constraint	Example	Explanation
Fixture interactions		The hole should be machined before the chamfer, otherwise it cannot be fixed.
Tool interactions		In order to position a drilling tool correctly, the drilling of the hole should precede the machining of the chamfer.
Datum interaction		The top face (the datum feature) should be machined prior to the base face.
Thin-wall interactions		Good practice should involve drilling the hole, then machining the slot to avoid deformation of the thin wall.
Material-removal interactions		The step should be machined prior to the hole for achieving high machining efficiency (milling is faster than drilling) and surface quality.
Fixed order of machining operations	Operations for a hole: (1) Drilling (2) Boring and (3) Reaming	A typical sequence of machining a hole is drilling, boring and reaming.

In a 3-axis machining environment, there are six TADs, i.e. +x, −x, +y, −y, +z and −z. In a 5-axis machining environment, different TADs can be achieved by the extra two degrees of freedom movements using the same fixture. However, for 3-axis machining, using different TADs requires changing the fixture accordingly. This means additional time will be spent in setting up fixtures. Selection of TADs involves a number of factors to be

considered such as machining costs, fixture elements, availability of cutters, tolerance and surface roughness requirements (Guo *et al.*, 2009). Although the author has recognised that TADs selection is important in the process planning stage, it is beyond the scope of this research (see sections 2.5 and 2.6). Therefore, the most appropriate TAD is always chosen and the operation sequencing deals with whether a cutting tool or deposition nozzle can have the correct feature access.

Figure 6.22 shows two available TADs for machining a through step feature, which are –x and –z directions. As stated above, as long as the feature (the step) is accessible, it is considered to be machinable and/or buildable. In GRP^{2}A, the operations to create the step can be to build the near-net shape of the step using the FFF process (with a determined build direction) and machine it in a finishing operation. Further to the TADs, negative z may be an appropriate candidate if the workpiece was set up in a position as shown in Figure 6.22 in the previous operation.
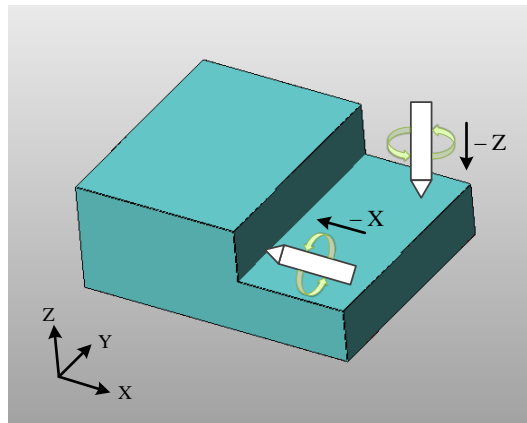
Figure 6.22 – A through step with two valid tool approach directions

6.5.5.3 *Considerations in operation sequencing*

In addition to the constraints introduced in the sections 6.5.5.1 and 6.5.5.2, there are other considerations to be taken into account in sequencing additive and subtractive operations:

(i)   A subtractive operation should be scheduled to finish machine the bottom surface of the part/subpart/feature due to part distortions.

Figure 6.23 shows the front view of three rectangular subparts A, B and C. Subpart A is the first subpart to be built. After adding subpart B onto subpart A, the bottom surface of

subpart A is warped. Therefore, the bottom surface of subpart A should be machined in order to obtain a flat surface. The reasons for doing this are: (1) obviously, the dimensional accuracy of the warped part is out of tolerance as identified in section 5.7; (2) subpart C is to be added onto the combined/fabricated subpart A and B. In the meantime, subpart A has to be positioned on the heated bed using the same part orientation in depositing subpart C, as shown in Figure 6.23(a). A flat surface is required when positioning a part on the heated bed; (3) if subpart C is to be added onto the warped bottom surface of subpart A (see Figure 6.23(b)), this surface has to be flat because material has to be deposited on a flat surface in order to obtain strong bonding strength between two subparts; (4) if the following subparts require finish machining, the warped surface cannot be clamped steadily on the machine tool bed.

(a)   (b)
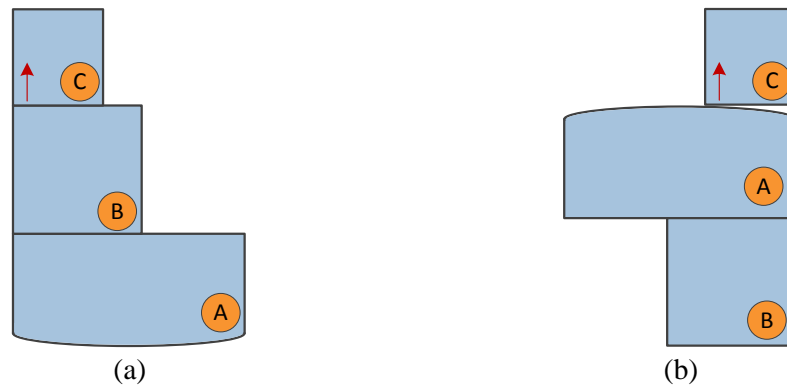
Figure 6.23 – Scheduling a machining operation for a warped surface

(ii)   Multiple and repetitive machining operations for the same feature should be avoided.

(iii)   Certain machined features/surfaces on a subpart will become un-machined again if there is more material to be added onto the subpart.

An example can be found in Figure 6.24, where each surface of the part is required to be machined to achieve the correct surface quality and tolerances. Figure 6.24(b) is the internal view of the part, which has five connected pockets. For better representation, round corners are intentionally ignored in Figure 6.24(b). The decomposed result is also shown in Figure 6.24(c). Twenty three subparts are merged into 5 as some of them have the same build directions whilst satisfying the criteria described in section 6.5.3. The merged subparts together with their build directions are shown in Figure 6.24(d). It should be noted that the result of subpart merging shown in Figure 6.24(d) is only valid for a certain set of build directions. Subpart 1 and 2 can also be merged, but for demonstrating

the considerations in operation sequencing, they are considered as separate subparts. The overall sequence is to manufacture subparts from 1 to 5 by interchangeable FFF and CNC machining processes. Even though subpart 1 has been finish machined, the surface highlighted by the black arrow in Figure 6.24(d) becomes rough (un-machined) again once subpart 2 is added. This is because printing subpart 2 onto the pocket on subpart 1 is equivalent to printing a bridge. Due to the recovery layers (see Figure 5.22), the highlighted surface requires finish machining again. Similarly, finishing operations are needed for the two highlighted pockets on subpart 2 once subpart 3 and 4 are added, respectively.

It is noted that, since these highlighted surfaces are subject to repetitive machining operations, there is no need to machine them until new subparts are added resulting in cutting tool inaccessibility. In other words, subpart 1 does not have to be finish machined prior to adding subpart 2. Having added subpart 2, subpart 1 can then be machined since the pockets on subpart 1 are still accessible. As a result, the total number of repetitive machining operations is reduced. It is also noted that the majority of the failure in operation sequencing is attributed to the machined features that become un-machined when more subparts are stacked up. Figure 6.24(e) shows the merged subparts obtained from another set of build directions based on a certain part orientation. The operation sequence is to manufacture subpart 1, 2 and 3. However, the surface pointed by the black arrow in Figure 6.24(e) becomes rough again once subpart 3 is built. In this case, the surface cannot be machined anymore as the cutting tool can no longer access the pocket on subpart 1.
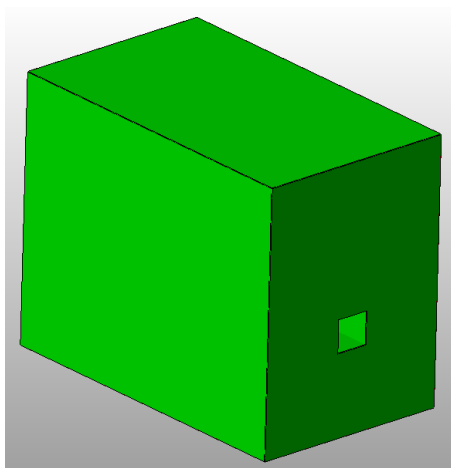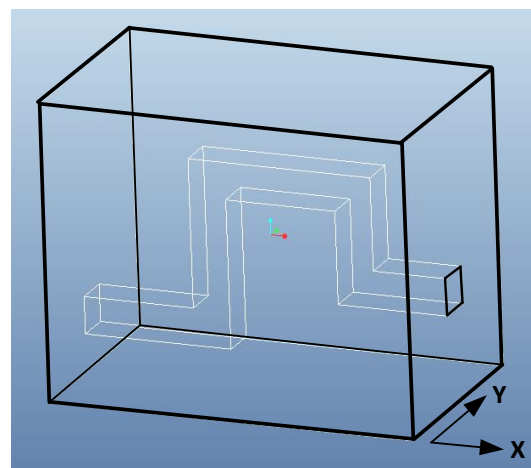
(a) example part   (b) internal view
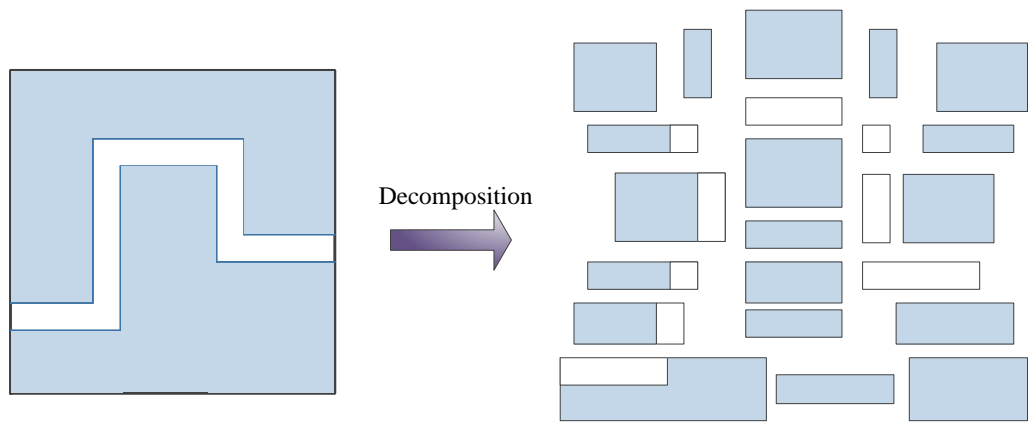
(c) cross-sectional view and part decomposition results
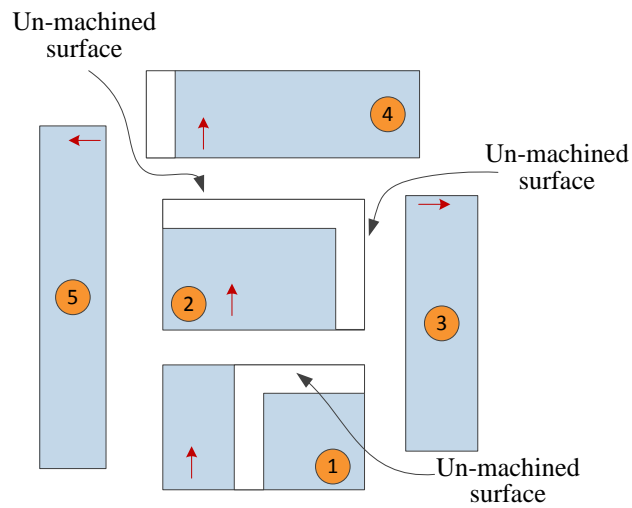
(d) build directions and merged subparts
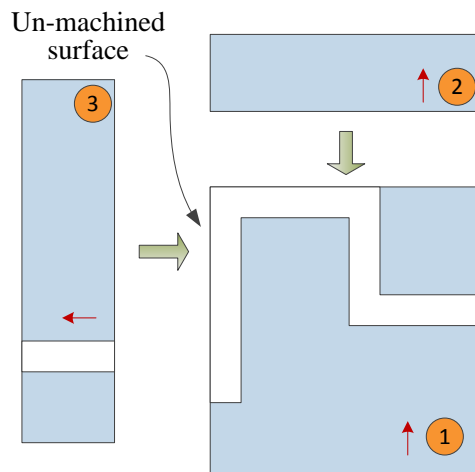
(e) failure in operation sequencing

Figure 6.24 – Repetitive machining operations and un-machined surfaces

6.5.5.4 Re-decomposition of merged subparts

Due to cutting tool and deposition nozzle accessibility that has been considered in part decomposition, the original subparts are free to be produced without any tool accessibility constraints. However, more constraints are induced as a result of a number of original subparts that have been merged, which leads to further tool accessibility issues. In this case, the merged subparts that lead to the failure in operation sequencing will be re-decomposed into the original subparts, releasing the constraints. The build directions of these re-decomposed subparts should be the same as the directions that are specified in the build direction determination stage. These re-decomposed subparts will not be combined in the subsequent stages again because combining them is likely to bring the constraints back leading to the operation sequencing failure. Figure 6.25 shows the sectional view of a part that has internal pockets. If subpart 1 and 2 were merged as they had the same build directions (denoted by the red arrows), the blind pocket would not have been machined. Therefore, the combination of subpart 1 and 2 has to be separated.
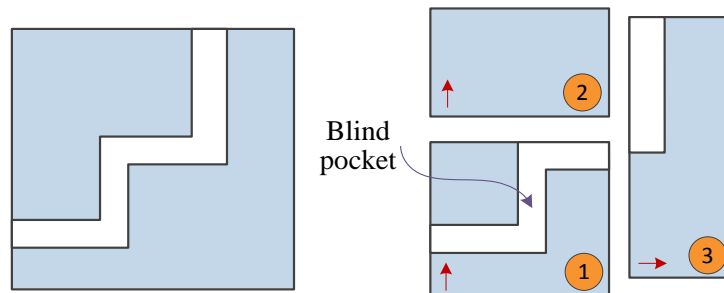
Figure 6.25 – Re-decomposing merged subparts

It is noticed that the last merged subparts that causes the tool accessibility issue will be re-decomposed first. Take the subparts in Figure 6.9 as an example. One available set of build directions is shown in Figure 6.26(a) and the build direction allocation sequence is subpart A, B, and C. Subpart A and B were merged first and then subpart C was combined with the merged subpart A and B (called subpart A-B). However, in operation sequencing, the drilling tool cannot access the hole. Since subpart C was the last subpart merged, it was separated from the combined subpart A-B-C. As a result, the combined subpart A-B will be built first followed by a machining operation for drilling the hole. Subpart C is then created after the hole is drilled. Another set of build directions is also shown in Figure 6.26(a), but with a different build direction allocation sequence, which is subpart B, C and

A. Certainly, these three subparts meet the requirements of subpart merging and were thus merged. In this case, subpart A was the last merged subpart which led to the cutting tool inaccessibility after it was merged with the already combined subpart B-C. Nevertheless, having re-decomposed subpart A, the machinability of the hole still cannot be solved. As subpart C was the last merged subpart after subpart A was taken off from the combined subpart B-C-A, subpart C was therefore separated from the merged subpart B-C. If all the merged subparts have been re-decomposed into their original subparts and the tool inaccessibility issue cannot be solved, this indicates that the available operation sequence does not exist for this set of build directions with a certain build direction allocation sequence based on a certain part orientation. It is also worth mentioning that, for certain sets of build directions, merged subpart re-decomposition might not be needed and an example is demonstrated in Figure 6.26(b), where the build direction allocation sequence is subpart A, B and C, and subpart A-B are the merged subpart.

(a)   (b)
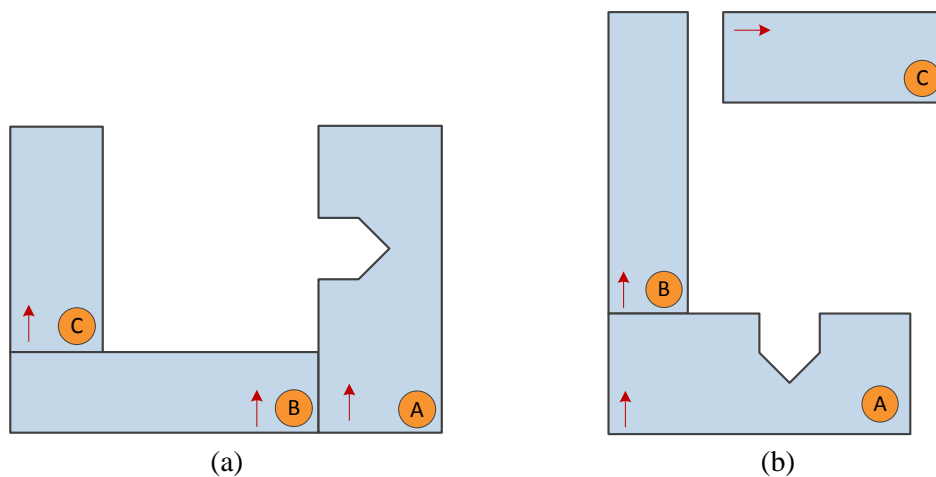
Figure 6.26 – Re-decomposing different merged subparts

6.5.5.5 *Procedures in sequencing additive and subtractive operations*

After determining build directions for each subpart and obtaining merged subparts, the sequence of addition and subtractive operations will be scheduled for each valid set of build directions. It is noted that for a given part orientation, a certain number of feasible sequences may exist due to some subparts that have multiple build directions and adjacent subparts. Other possible sequences that result from different orientations will also be identified. The procedures for sequencing additive and subtractive operations for a single set of build directions are illustrated in Figure 6.27. As presented in section 6.5.5.4, a

viable sequence might not be found for a certain set of build directions when the part is positioned in certain orientations (an error occurs in Figure 6.27).
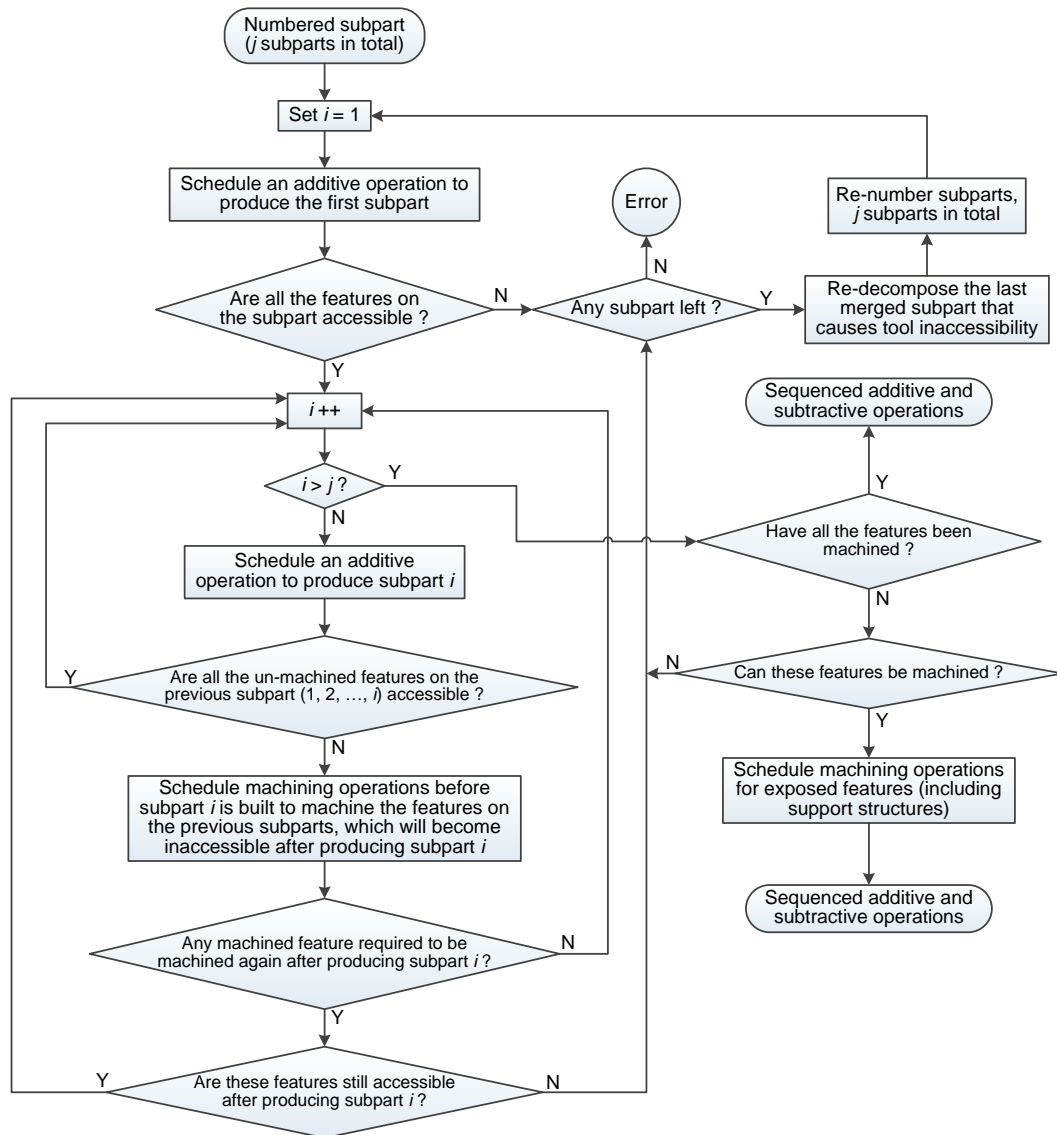
Figure 6.27 – The procedures for sequencing additive and subtractive operations

The major steps are outlined as follows:

- The subparts (including original and merged subparts) to be produced are numbered. These subparts do not have to be numbered, but for better demonstration in Figure 6.27, the subparts are numbered according to the build direction allocation sequence. The first subpart/merged subpart to be produced is subpart 1, the second subpart/merged

subpart to be produced is subpart 2 and the rest can be done in the same manner. There are j subparts in total.

- The first subpart (i.e. subpart 1) will be built followed by adding more subparts until the features on the subparts cannot be machined due to cutting tool inaccessibility. As long as there is one available TAD, the features are considered to be accessible. This step aims to reduce the number of repetitive subtractive operations conducted for machining the same features.

- After scheduling a subtractive operation for machining a feature on a subpart, it is necessary to identify whether or not the feature (or any surface on the feature) will become rough again once the subsequent subpart is added onto the machined subparts. If this is the case, it has to be identified whether or not the feature is still accessible when the subsequent subpart is added. If the cutting tool still has access to the feature, the subsequent subpart can be built onto the machined subparts.

- If the feature is not accessible anymore, the last merged subpart that causes this tool inaccessibility issue will be re-decomposed into the original subparts, which releases the cutting tool constraints arising from subpart merging. More merged subparts will be re-decomposed until there is at least one TAD that can be obtained.

- Once merged subparts are re-decomposed, all the current subparts will be renumbered. The numbers should follow the build direction allocation sequence and the build directions of the subparts should be the same as the build directions determined in the build direction determination stage.

- The re-decomposed subparts should meet the deposition nozzle accessibility requirements when sequencing an additive operation to fabricate them. This is because they were scheduled to be built simultaneously with other merged subparts. As they have now been re-decomposed and the other merged subparts have been produced, deposition nozzle collisions may occur when attempting to build the re-decomposed subparts onto the produced merged subparts.

- Once the build direction of the re-decomposed subparts allocated in the build direction determination stage causes the deposition nozzle collision, it can be concluded that a feasible operation sequence based on this set of build directions cannot be obtained. On the other hand, when all the merged subparts have been re-decomposed into the original subparts, the feasible operation sequence does not exist if the un-machined surfaces still suffer cutting tool inaccessibility.

- The subtractive operations for machining the exposed features are scheduled in the end of the process sequence because these features can always be machined.

- Subtractive operations will also be scheduled for removing the support material if needed.

- Finally, as mentioned in section 6.5.5.3, subtractive operations will be arranged in order to get a flat surface to be used as a build platform for the subsequent additive operations or a datum for the subsequent subtractive operations. In addition to part distortions, a subtractive operation is needed for the side surface of a subpart when there is another subpart to be built onto the side surface of the subpart.

6.6   Feature Modification for Different Operations

For CNC machining processes, NC programs to be used in the shop floor production environment are generated from the drawings (or CAD models) where part nominal dimensions are specified. However, for the iAtractive process, due to the interactions between individual processes, the features in the part designs (the CAD models) cannot be directly used for the individual additive and subtractive operations. The following features have to be modified:

(i)   Features to be produced in additive operations

Due to the various errors caused by the FFF machine gearings, process parameters (e.g. layer thickness, diameter of deposition nozzle) and material shrinkage, the dimensional accuracy of fabricated plastic parts are normally not as high as that of CNC machined parts. Figure 5.20 gives an example (top view) of an actual fabricated feature (denoted by the blue lines) as compared to the nominal feature (red dashed line), when a boss is added onto a block. A series of measurement tests were conducted as detailed in section 5.4.2, to identify the variability in dimensional, positioning and geometric accuracy of FFF manufactured parts. An accuracy index has been developed and readers are referred to section 5.4.4. The dimensions to be used in additive operations can be obtained by using Equation 5.4 and Table 5.1. Based on the accuracy index of the FFF process, the CAD model is modified, ensuring (1) a real positive feature fabricated is slightly bigger than its nominal dimensions (e.g. the modified length is 2.5% longer than its nominal value); (2) a real negative feature fabricated is slightly smaller than its nominal dimensions (e.g. the

modified length is 2.5% shorter than its nominal value). This allows the machining process to finish machine the part, achieving the required surface quality and accuracy.

(ii)   Parent subpart on which the child subpart will be built

As identified in section 5.7, part distortions occur when a child part is built onto a parent part or material is added onto an existing part. This essentially indicates that more material has to be removed, namely, the bottom surface of the warped part has to be face milled. Thus, the related features have to be modified accordingly for the distortion deviations, ensuring that the real part fabricated is higher than its nominal height, which allows the machining process to finish machine the warped bottom surface. Figure 6.28 shows the warped bottom surface of subpart A in Figure 6.23.
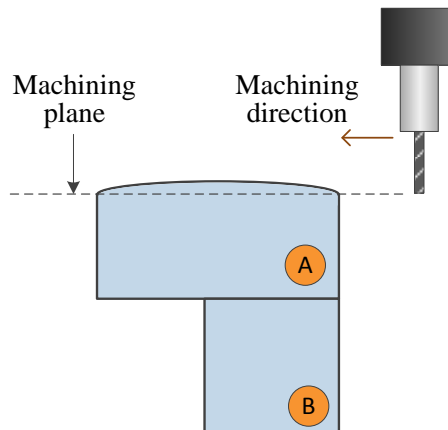
Figure 6.28 – Machining a warped parent part

(iii)   Support material

Support structures will be added to the CAD model if overhangs have been identified in the buildability analysis stage (see section 6.3.1). Additionally, in certain scenarios where a subpart is added onto another subpart, a support structure is needed. In Figure 6.29(a), subpart 2 cannot be built without support and thus, the CAD model is modified and the support structure will be constructed together with subpart 1. However, for the subparts depicted in Figure 6.29(b), the CAD model will not be modified. Even though the support structure can be created together with subpart 1, subpart 2 cannot be produced after subpart 1 is built due to deposition nozzle collisions. It is worth pointing out that the build direction of subpart 2 as shown in Figure 6.29(b) is considered to be invalid in the build direction determination stage.

(a)

(b)
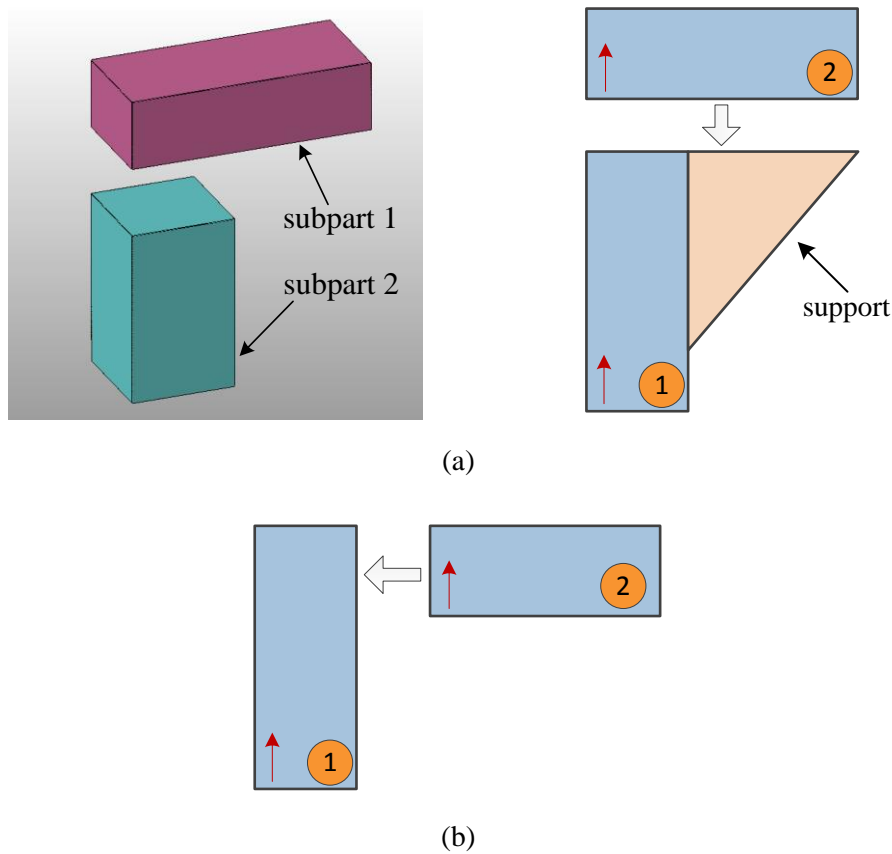
Figure 6.29 – Modifying the CAD model to support an overhanging feature

(iv)   Bridges

This scenario arises from producing subparts. While a subpart is added onto another subpart, the iAtractive process is actually producing a bridge even though neither of these two subparts has overhanging features or bridge structures. In Figure 6.30(a), subpart B is added onto subpart A. Since there is a slot on subpart A, while the FFF process is creating subpart B, it is actually manufacturing a bridge. According to Table 5.2 and Figure 5.21, the surface quality and part density is of poor quality until a number of recovery layers are laid down. The aim of feature modification is to decrease the height of the bridge in the CAD model, ensuring that the print quality comes back to normal FFF print quality before the deposition nozzle reaches the nominal bridge height, as shown in Figure 6.30(c). The orange area consists of a number of recovery layers, which will be removed using the machining process afterwards. All corners are round and are ignored in Figure 6.30 for better demonstration.

(a) two subparts, A and B

(b) original features   (c) modified features
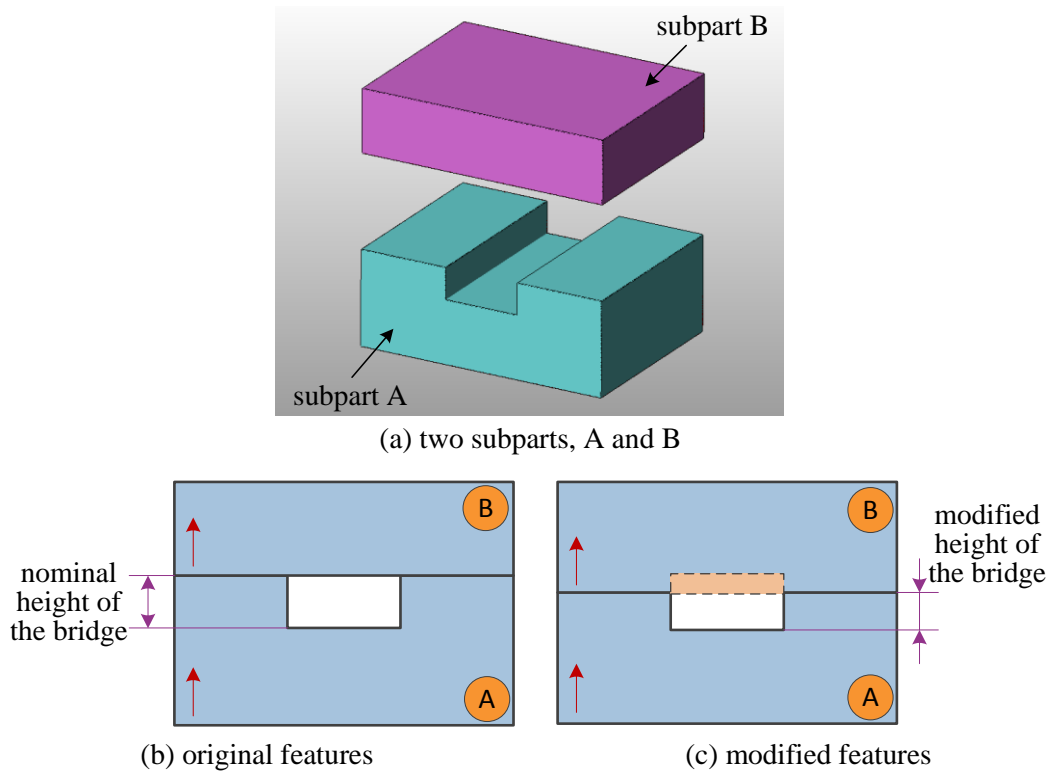
Figure 6.30 – Producing a bridge while adding a subpart onto another subpart

(v)   Creating new CAD models for dynamic process plans

In generating a dynamic process plan, new subparts (features) are added onto the subparts that have already been produced. Therefore, the CAD models of these new subparts will be created.

6.7   Post-processing Stage

6.7.1   Integration of inspection operations and generation of static process plans

Integrating inspection into the iAtractive process means that it becomes a value adding process. Inspection is considered to be the enabler for transforming a static process plan into a dynamic process plan, which will be presented in section 6.8. The inspection operations are added into the scheduled additive and subtractive operation sequences and the most appropriate operation sequence in terms of production time is then identified. To this end, the static operation sequence is now completely organised.

The inspection process should be used before the following operations take place:

(i)   The first additive or subtractive operation.

This strategy only applies to the scenarios where parts are manufactured from existing parts. Inspection operations are used at the beginning of the iAtractive process to identify the shape and dimensions of the existing part.

(ii)   Machining operations.

An inspection operation is scheduled before a machining operation starts, identifying the amount of material that should be removed from the deposited feature. In traditional machining of 2½D parts, the size of the raw material (normally a block) is bigger than that of the finished part. However, as subparts are continuously added onto previous subparts, each subpart fabricated is slightly bigger and higher than the corresponding nominal subparts. Additionally, due to the dimensional deviation in the Z axis, it is necessary to obtain the actual height and width of the subpart/feature before machining can commence. If the deposited feature is smaller than its nominal size, as identified in the inspection operation, further deposition operations will be added before the machining operation is executed.

(iii)   Additive operations for creating child parts.

Inspection operations are conducted before depositing a child part onto an un-machined parent part due to the differing heights of the parent part that could result in the change of depositing parameters. This is concerned with bonding strength between the two subparts. A thickness of 0.25mm is the most widely used layer thickness for the FFF process for printing various part structures (RepRap, 2012b). However, it is not always feasible to print child parts. A typical example is: the height of a parent part is 10.2mm, however 10.2mm cannot be divided exactly by 0.25mm. In this case, the FFF process will start printing the child part from 10.5mm because 10.25mm is the closest layer to 10.2mm. As a result, there is a 0.3mm gap between the build plane of the first layer of the child part, leading to weaker bonding strength between the parent and child subparts. In this example, layer thicknesses of 0.2mm and 0.3mm can be used. It should be noted that for a different layer thickness, the amount of melted material extruded per unit time is different. It should also be noted that the settings for 0.25mm layer thickness cannot be used to deposit

material starting from 10.25mm in height due to the narrow gap that will block the material extrusion from the nozzle. If the user insists on printing from 10.25mm, a layer thickness of less than 0.05mm may be potentially suitable, but it requires further investigations on layer thickness, print settings and part accuracy etc.

(iv)   Additive operations that lead to the cutting tool inaccessibility.

In order to measure internal features, inspection has to be carried out when the features are still accessible. In this research, the touch trigger probe measuring method is used. The probe accessibility is the same as the cutting tool accessibility. Referring to the example shown in Figure 6.24(d), the actual dimensions of the internal pocket on subpart 1 have to be measured before adding subpart 3. Similarly, the two highlighted pockets on subpart 2 have to be measured prior to producing subpart 4 and 5, respectively.

(v)   The final inspection operation is scheduled at the end of the complete operation sequence, ensuring that the part dimensions are within the part tolerances.

Based on the rules described above, the overall workflow for integrating inspection operations in the scheduled sequences of additive and subtractive operations is depicted in Figure 6.31.

6.7.2   Generation of tool path and process parameters for additive and subtractive operations, and measurement programs

This is the last stage in generation of a static process plan. In this stage, the appropriate process parameters are selected and tool paths are generated for additive and subtractive operations. In addition, the measurement programs including the number of points to be collected and the probe movement paths for measuring the subparts are prepared.

(i)   Machining process parameters

A number of selected combinations of the machining process parameters for various machining applications are provided in Table 5.5. The main effects plots for surface roughness shown in Figure 5.28 indicate that increasing feedrate is a feasible way of significantly reducing machining times, particularly for machining subparts. As a result, for roughing operations, feedrate is normally faster than that of finishing operations, in order to reduce machining time whilst maintaining high surface quality. The effects of

factor interactions depicted in Figure 5.29 indicate the appropriate parameter combinations if operators attempt to use a DoC of 1mm or 2mm for the purpose of further reducing machining time.

In the iAtractive process, finishing operations are divided into two, namely finish machining subparts and final parts (or final features). For finish machining final parts and features, the feedrate to be used should be slower than that of finishing subparts. Additionally, better surface quality ($Ra < 2 \, \mu m$) can be achieved when using a depth of cut of 0.25mm. For other application requirements, Figure 5.29 can be used to identify the suitable parameter combinations for the specific applications.
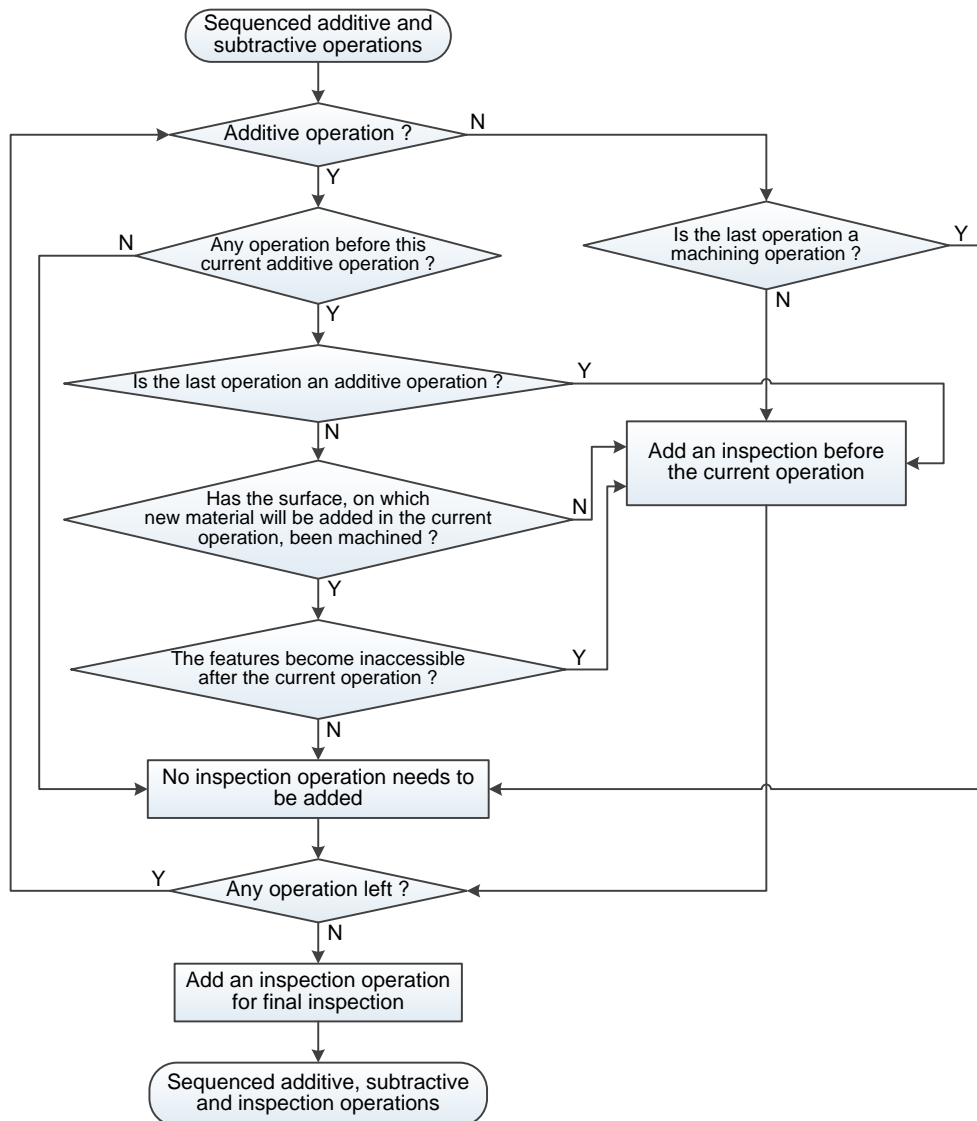
Figure 6.31 – Workflow of integrating inspection plans in the operation sequences

(ii)   Additive process parameters

In general, the additive process parameters (e.g. extrusion temperature, infill width, infill pattern and deposition speed etc.) are consistent throughout this research. The only one parameter that may vary is the layer thickness. Differing heights of the parent part may require specific layer thicknesses. The changes of layer thickness could also cause changes in the total amount of material to be deposited per unit time, resulting in changes in material shrinkage per unit time. This will further lead to the deviation variations of the dimensional accuracy of the FFF manufactured part and the degree of part distortion. Once the dimensional accuracy and the degree of part distortion have changed, the features on the subparts should be modified accordingly in order to compensate for these changes. The relationships of deposition parameters are illustrated in Figure 6.32, showing the interrelated parameters. It is noted that identifying the dimensional accuracy, the capability of printing overhangs, and part distortions based on different layer thicknesses are beyond the research scope. All above described information was gathered using the layer thicknesses of 0.2mm, 0.25mm and 0.3mm.
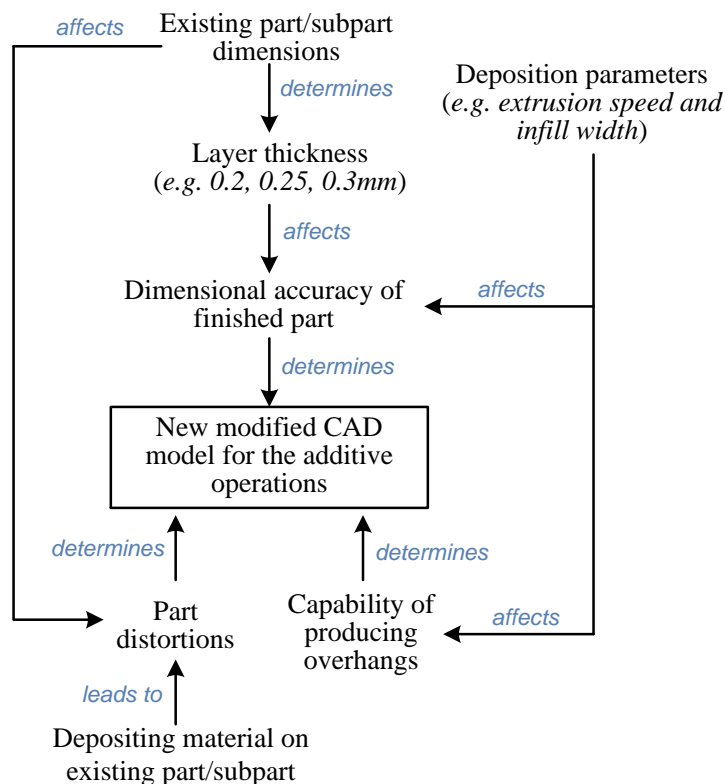
Figure 6.32 – Relationships between additive process parameters

(iii)   Tool paths for additive and subtractive operations

The tool paths for additive and subtractive operations are generated by the using different open source and commercial software, such as RepRap host (RepRap, 2012b), Slic3r (Slic3r, 2013), and Delcam Powermill (Delcam, 2012). It should be noted that the additive process tool path strategy should be developed to cope with deposition of adaptive layers and dematerialised structures in the future, which will be presented in section 10.4.2.

To this end, a static process plan has been fully developed and it will be updated during the production phase by adding new operations to the plan.

6.8   Generation of Dynamic Process Plans

Due to the integration of inspection, the iAtractive process is able to react promptly to quality changes. Dynamic process plans are generated during the production of the part based on the knowledge of the static plan generation, according to the feedback of inspection information. Operations are adjusted and added into the static process plan if necessary. By doing so, quality changes can be identified in an early stage of production rather than in the final inspection.

Given that there is only one static process plan where a number of subparts together with the specific build directions and operation sequence are specified, it is inferred that the updated dynamic process plan will not disorganise the initial static process plan. The operation that leads to the dimensions of the subpart being out of tolerance is considered to be a failed operation. The subpart produced in the failed operation is called an unqualified subpart. The aim of generating dynamic process plans is to add extra operations to ensure the dimensions of the subpart are in tolerance before continuously implementing the operations scheduled after the failed operation. This can be achieved by adding and/or removing material from the subpart. The amount of material to be deposited and/or removed depends on inspection feedback.

Figure 6.33 illustrates a dynamic process plan, where each block represents one single operation. The symbol '+' denotes additive operation, '-' denotes subtractive operation and 'I' denotes inspection operation. The blue blocks are the operations that are sequenced in the static process plan; the grey blocks are the new operations added in the dynamic process plan; the arrows denote the operation sequence and the cross ($\times$) denotes the

cancelled static operation sequence. Every output of the inspection operations could be the
start of the dynamic plan if the inspection results indicate that the subpart manufactured
does not achieve the designed requirements in terms of dimensions and tolerance. New
additive, subtractive and inspection operations will be added after the failed operation. The
end output of the dynamic process plan leads to the operation sequenced after the failed
operation in the static process plan. The next start of the dynamic plan will be the next
inspection operation that identifies the unqualified features. It should be noted that, when
new operations are scheduled, the new CAD model is generated, showing the new features
that will be added and/or removed from the failed subpart. Subsequently these new
features will be modified according to the requirements presented in section 6.6.
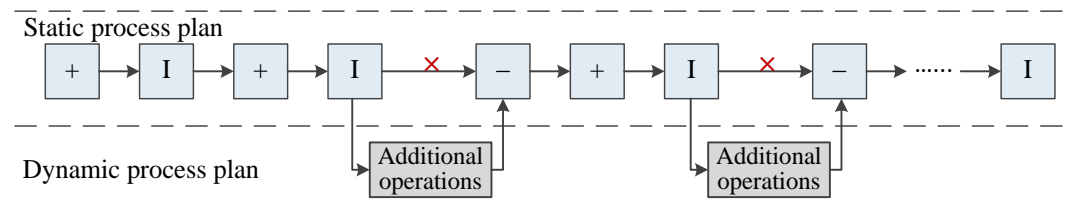
Figure 6.33 – A dynamic process plan

An example is given in Figure 6.34, where a part is decomposed into three rectangular
subparts. Subpart 1 is manufactured first followed by subpart 2 and 3, as shown in Figure
6.34(a). However, it was found that the height of the actual subpart 2 fabricated by the
additive operation was lower than its height specified in the modified CAD model obtained
in the feature modification stage (see Figure 6.34(b)). In this case, subpart 3 cannot be
directly added onto the unqualified subpart 2. As a result, three new operations are added
and inserted into the original static operation sequence. These three new operations are (i)
adding the material onto the unqualified subpart 2, as shown in Figure 6.34(c); (ii) finish
machining subpart 2; (iii) measuring the dimensions of subpart 2. After conducting the
three new operations, subpart 3 can then be added.

If the unqualified subpart contains a number of internal features causing potential tool
inaccessibility issues when conducting new operations in the dynamic plan, the entire
unqualified subpart should be removed. New operations can then be added to produce a
new subpart. Future work should be carried out, investigating various solutions in the
generation of dynamic process plan to deal with quality changes in production.
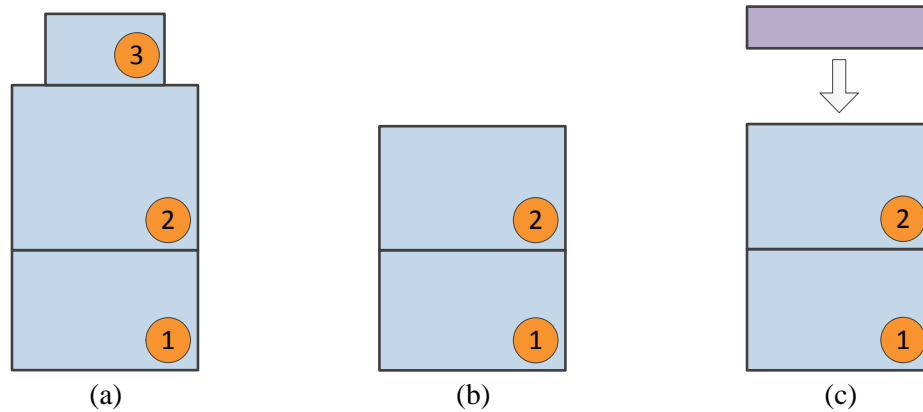
Figure 6.34 – An example of scheduling new operations in a dynamic process plan

Another possible method for generating dynamic process plans is to:

- remove all the operations sequenced after the failed operation in the static process plan.
- run through the process planning stages detailed in sections 6.4 – 6.7.
- utilise the subparts that have already been produced and generate new operations to further manufacture the subparts until the final part is manufactured.
- if unqualified subparts are identified in the new operations, remove all the operations sequenced after the failed operation in the dynamic process plan, and repeat the above three steps.

This alternative method is illustrated in Figure 6.35. The red arrows represent the actual operations sequence implemented in the production; the black arrows represent the operations that were going to be conducted, but were abandoned in the production; the blue blocks are the operations in the static process plan; the grey blocks are the new operations scheduled in the dynamic process plan; and the purple blocks are the failed operations.
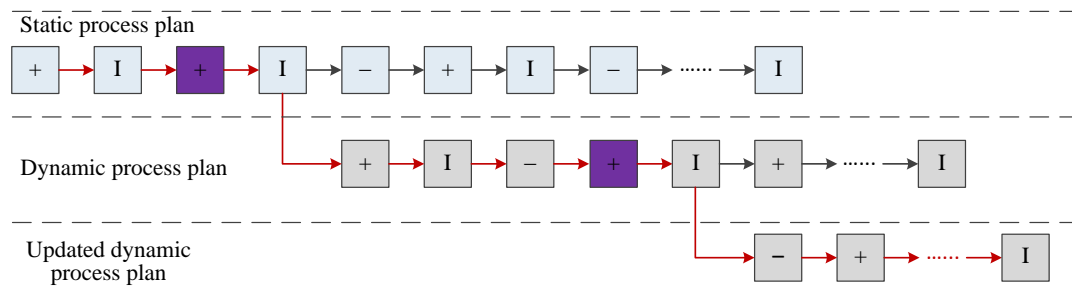
Figure 6.35 – An alternative method for dynamic process plan generation

One of the important things found in the practical machining tests is that more material should be removed if an actual part is just shorter than its nominal height (e.g. 2mm shorter). The 2mm thick material cannot simply be added onto the actual part because the bonding strength between the two parts (the actual part and the 2mm thick newly deposited part) is weak. In the finishing operation, the weak bonding strength will result in a final part that falls apart along the plane where the two parts are connected to each other. Thus, it is advisable to remove 3mm from the actual part and then add 5mm of material thickness back.

6.9   Production Times

Having gone through all the stages in Figure 6.2, a number of feasible operation sequences have thus been obtained. The criterion defined in this research for identifying the most appropriate operation sequence is production time, as shown Figure 6.36.
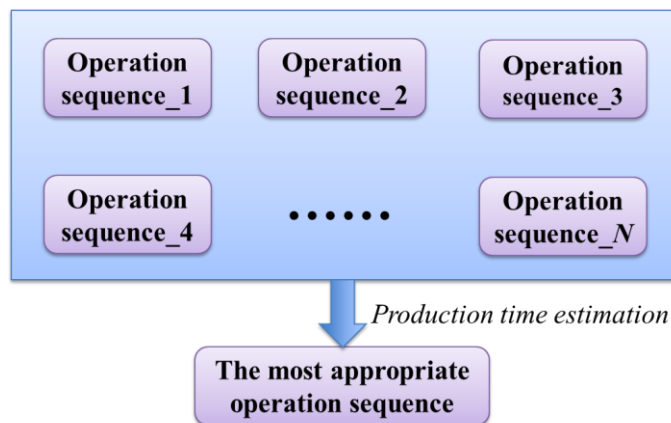
Figure 6.36 – The most appropriate operation sequence in terms of production time

The iAtractive process aims to manufacture products in the least amount of time possible. The total production time for manufacturing a part is defined as:

Equation 6.1
$$T = T_a + T_s + T_c + T_m$$

where T is the overall production time, T_a is the time for the additive process, namely build time; T_s is the time used in the subtractive process; T_c is the switching time between the additive and subtractive operations, which includes machine set-up time; T_m is the inspection time.

From Equation 6.1, it can be identified that the fewer the number of interchanges between the machining process and deposition process the better. Each switch requires retreating and relocating of the deposition nozzle as well as the machining tools, which may cost extra time, even though the deposition unit is integrated within the machine tool. The time used in each switch is considered to be constant. Since the part is decomposed into a number of subparts with reduced features, the inspection time can be considered to be constant.

Machining time estimation has been extensively researched and different estimation methods have been developed (Scallan, 2003). As the machining parameters, i.e. speed, feed and DoC, have been selected in section 6.7.2, a method proposed by Maropoulos *et al.* (2000) is adopted in GRP^{2}A, which estimates tool travel distance and calculates machining times using the above three machining parameters.

By contrast, the additive process takes longer to implement than other processes utilised. For example, the build time for producing a feature with volume of 50cm^3 could be up to 20 times more than the machining time for machining such a feature. There is a need to develop a model for estimating build times, as this directly determines operation sequencing. In addition to the time estimation accuracy, the major requirement of the model is the efficiency, i.e. being capable of predicting build times from a CAD model or 2D drawings which is considered to be the most accessible geometrical information for the process planning algorithm.

6.10   Development of a Build Time Estimation Model

This section reports on the development of a method for establishing a build time estimation model to be used at the process planning stage for the iAtractive process. A series of test parts with various combinations of features have been designed for developing and validating the model. Statistical analysis was carried out and the influential factors related to part geometries and material deposition tool path have been identified.

6.10.1 The method for developing a build time estimation model

Build times of the actual additive processes depend on part geometries, part orientation and the parameters of the additive processes involved. The parameters affecting build times may vary depending on the specific additive processes. A brief review was conducted,

identifying the existing approaches in build time estimation of additive processes such as SLA and LOM. In order to develop a build time estimation model for the FFF process, an analytic analysis was first carried out to theoretically analyse the influential parameters. Two test parts were designed and the initial tests were conducted, identifying and determining the most significant parameters that were to be used in the model. Subsequently, four test parts with varying combinations of features were designed and a fractional factorial design strategy was employed to design a series of experiments. The statistical analysis techniques, namely multi-factor regression analysis and ANOVA were used iteratively to develop the model. Finally, three test parts with specific features and volumes, combined with the *t*-tests method were used to evaluate and validate the developed model. Figure 6.37 illustrates the method used for developing such an estimation model.
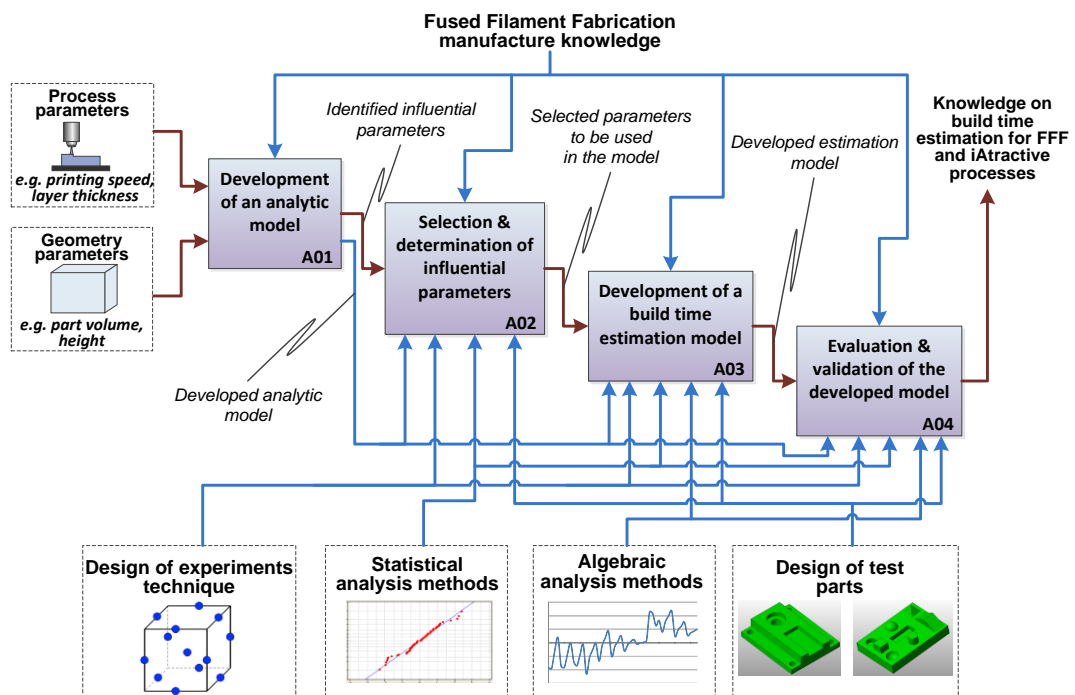
Figure 6.37 – The method for developing the build time estimation model

6.10.2 Development of an analytical model

In this subsection, an analytical model for accurately calculating build times has been developed. This model is used in the development of the build time estimation model, comparing errors between actual and estimated build times.

6.10.2.1 FFF process parameters

Build time (T_a) is defined by the author as the amount of time that is required to fabricate a single or a group of parts by using the FFF process. The estimation of build time involves a number of parameters to be taken into consideration. These parameters can be split into process parameters and geometry parameters, which are summarised in Table 6.2. These parameters are used in the development of the analytical model.

Table 6.2 – Process and geometry parameters of the FFF process

Process parameter	Notation	Unit
Layer thickness	t	mm
Boundary locations in the XY plane	BL_x, BL_y	mm
Hatch spacing	λ	mm
Road width	RW	mm
Printing speed in the XY plane	V_{pr}	mm/s
Repositioning speed in the XY plane	V_{xy}	mm/s
Repositioning speed in the Z axis	V_z	mm/s
Number of repositioning times	NR	scalar
Acceleration/deceleration in the XY plane	A_{xy}/D_{xy}	mm/s^2
Acceleration/deceleration in the Z axis	A_z/D_z	mm/s^2
Filament retraction speed	V_{ret}	mm/s
Deposition head heating time	T_{heater}	s
Bed heating time	T_{bed}	s
Delay time per print	T_{delay}	s
Geometry parameter	**Notation**	**Unit**
Part volume	V	cm^3
Support material volume	V_s	cm^3
Surface area of the part	Sa	mm^2
Number of parts to be built	NP	scalar
Part height	H	mm

Geometry parameters are the primary variables to be considered prior to the FFF process as they have direct effect on build times. Process parameters are the controllable factors, and changing them can lead to the increase/decrease in build time. For example, increasing printing speed directly results in the reduction in build time.

However, it has been reported that the change of process parameters affects the output quality of the printed parts, such as surface quality, dimensional accuracy and tensile strength (Anitha *et al.*, 2001). The purpose of predicting build times is to identify the most appropriate operation sequence which requires the least amount of build time. Despite the fact that changing the process parameters will most likely lead to the increase/decrease in build times, the aforementioned purpose cannot be achieved. This is because increasing or decreasing any or all of the speeds and accelerations/decelerations, affects the entire FFF process resulting in the increase or decrease in build times for producing the prototypes, respectively. This cannot be used to identify the appropriate operation sequence. Therefore, the process parameters are kept constant during the development of the build time estimation model. In order to avoid ambiguity in the analytical model, certain important parameters are defined as follows:

Layer thickness: the thickness of each slice of the part deposited by the nozzle and built on the previous layer. In this stage a layer thickness of 0.25mm is used.

Hatch spacing: the distance between the centrelines of adjacent parallel hatch vectors.

Road width: the width of the deposition path.

Boundary locations in the XY plane: this is the location of the part on the build platform, in which the nozzle has to operate during deposition.

Printing speed: the speed of the deposition head travels during the deposition process.

Repositioning: the deposition head moves from the point where the first path deposition ends to the point where the second path deposition starts. No material is deposited during repositioning operation.

Repositioning speed: the speed of the deposition head travels while it is being repositioned.

Acceleration: the acceleration enables the nozzle or bed to accelerate from 0 to printing speed/repositioning speed.

Filament retraction speed: before depositing material on each individual continuous path, the filament is fed back and subsequently fed into the liquefier chamber. This is because PLA tends to 'string' slightly, leaving filaments sticking out from builds where the deposition head has left the build for a repositioning movement. This problem can be eliminated by reversing the extruder by a short distance at the end of each completed deposition before the repositioning movement (Jones *et al.*, 2011). This retraction speed is thus defined as the speed that filament is fed back and fed into the liquefier chamber.

Delay time per print: before depositing material on each individual continuous path, there is a delay (delay before material deposition and head movement), which can be seen as constant.

6.10.2.2 The analytical model

Assuming that a part is sliced into *N* layers ($N = |H/t|^+$ and $|\ |^+$ represents the round up to the next integer number), the overall build time of producing the part can be described as

Equation 6.2
$$T_a = \sum_{n=1}^{N} T_n + T_{bed} + T_{heater}$$

where T_{bed} is the time for warming up the bed to T_g of the material to be deposited (for PLA, it is 60 ℃) at which point the part stops warping; T_{heater} is the time used in turning on the heater until it reaches the temperature that is 10 ℃ higher than the material melting temperature (for PLA, the melting temperature is 195 ℃); T_n is the time used in printing n^{th} layer, $n \in [1, N]$.

For each layer, the build time T_n is divided into two parts, namely,

Equation 6.3
$$T_n = T_{dep\_n} + T_{idle\_n}$$

where, T_{dep_n} is the deposition time for n^{th} layer; T_{idel_n} is the idle time for the nth layer. Idle time includes deposition head repositioning time in the XY plane and Z axis ($T_{rep\_n\_xy}$ and $T_{rep\_n\_z}$), which can be calculated using Equation 6.4 below:

Equation 6.4
$$T_{idle\_n} = T_{rep\_n\_xy} + T_{rep\_n\_z} = \frac{t}{V_z} + \sum_{j=1}^{J}\left(\frac{S_{rep\_j\_xy}}{V_{xy}} - \frac{V_{xy}}{A_{xy}}\right)$$

where, $S_{rep\_j\_xy}$ is the jth ($j \in [1, J]$) repositioning displacement (unit: mm) before depositing the jth continuous deposition path.

Deposition time (T_{dep}) is the time when the material is being extruded, which is expressed in Equation 6.5:

Equation 6.5
$$T_{dep\_n} = \sum_{k=1}^{K}\left(\frac{2L_{ret\_k}}{V_{ret}} + \frac{S_{pr\_k}}{V_{pr}} - \frac{V_{pr}}{A_{xy}} + T_{delay}\right)$$

where, S_{pr_k} is the length of the kth ($k \in [1, K]$) continuous deposition path; L_{ret_k} is the length of the filament retracted before depositing the kth deposition path. T_{delay} is the delay time before depositing material on each individual continuous path.

Based on the analysis outlined in the proceeding Equations 6.2, 6.3, 6.4 and 6.5, a full representation of the build time for a single part is derived, namely

Equation 6.6
$$T_a = T_{bed} + T_{heater}$$
$$+ \sum_{i=1}^{I}\left[\sum_{j=1}^{J}\left(\frac{S_{rep\_j\_xy}}{V_{xy}} - \frac{V_{xy}}{A_{xy}}\right) + \sum_{k=1}^{K}\left(\frac{2\cdot L_{ret\_k}}{V_{ret}} + \frac{S_{pr\_k}}{V_{pr}} - \frac{V_{pr}}{A_{xy}} + T_{delay}\right) + \frac{t}{V_Z}\right]$$

6.10.3 Selection and determination of parameters

In this subsection, the process parameters to be investigated and included in the build time estimation model are selected.

6.10.3.1 Initial selection of the parameters

Based on the analysis above, the following statements can be made:

- Calculation of the build time using an analytical approach (Equation 6.6) is generally not practical or viable in the proposed process planning approach when only CAD models or 2D drawings are given. In particular, the generation of tool paths highly depends on the part geometry and the slicing strategy. Therefore, the appropriate parameters need to be selected for developing the build time estimation model.

- Length of continuous deposition path (S_{pr}) primarily determines build times when certain printing speed and acceleration/deceleration are applied. The length of continuous deposition path is proportional to build times. Therefore, part volume (V) is considered as one of the major parameters that directly contributes to the total amount of build time.

- The time spent in heating the bed and the heater is constant for producing any given parts. Thus they are not included in the estimation model.

- Hatch spacing (λ) is not represented in Equation 6.6, but it plays an important role in terms of build time. Normally, parts are not fabricated in a fully dense pattern in the FFF process. A high value of hatch spacing indicates low density of the part (i.e. the part is more porous), which in turn reduces the total length of the deposition path. As a result, part density (ρ) is introduced in the build time estimation model. Density is also defined as: density = 100% − part porosity.

- Reducing the time taken to reposition as well as length of repositioning tool path (S_{rep}) can lead to decreases in build time. For each time the deposition head repositions, filament retraction and print delay (T_{delay}) are required, resulting in increased time. The reasons that cause the head reposition are (*i*) start printing next layer; and (*ii*) certain areas do not require material, such as printing pockets. The importance of head repositioning needs to be investigated further in order to decide whether or not to include this parameter in the model.

- Part height (H) has potential effect on build time. Since the layer thickness is being kept unchanged, different heights of the part resulting from part orientation could possibly require different build times ($N = |H/t|^{+}$). However, different orientations also lead to changes in the lengths of the deposition tool path and the tool path of the deposition head repositioning as well as the number of repositioning times etc. It is unclear whether part height should be considered in the complete estimation model. As a result, in the next subsection, a series of simplified experiments were conducted in order to finalise the parameters to be investigated in the development of the build time estimation model.

6.10.3.2 Determination of the parameters

The number of experiments to be conducted increases exponentially when further parameters are introduced in the build time estimation model. Moreover, the representation

of the model will become complicated, which is unsuitable for predicting build times in the process planning algorithm. Hence, it is suggested to exclude less important independent variables in the experiments since these variables do not significantly affect the predicted results but do make the model more complicated and thus significantly increase experimental runs. The volume and the density of the part directly determine the amount of material that is about to be deposited. In other words, high volume and high density require longer build times and thus they are included in the model.

(I)   Design of experiments:

According to the statements made in section 6.10.3.1, the following two tests have been designed to evaluate the importance of two interrelated parameters, namely, part height and deposition head repositioning. Test parts F and G are shown in Figure 6.38(a) and (b), respectively.

| (a) test part F | (b) test part G |
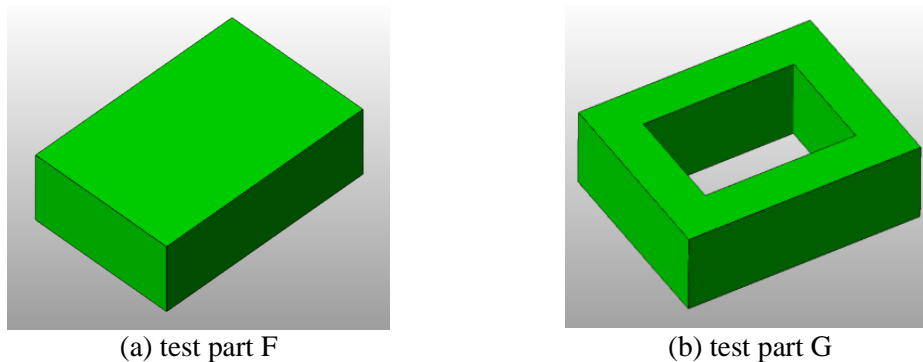
Figure 6.38 – Test part F and G

The 2^k full factorial DoE strategy was used for the tests.

Test 1: for the same rectangular blocks (test part F) with the same porosity, changing the block orientations meant changing the height values. Thus, four sets of rectangular blocks were used in Test 1. For each set of blocks, the volumes were kept the same but the height values varied. Three heights were used, namely, 10mm, 30mm and 50mm. Each height value was applied to all sets of blocks.

Test 2: Five sets of parts with four different sizes of through pockets were designed. Producing rectangular blocks with pockets requires repositioning the deposition head repeatedly and frequently since the pockets do not need material. Every time the head travels across the pocket, it can be seen as a repositioning action. In order to avoid the

effects caused by the varying volumes and heights, all of the parts in each set had the same volume and height but different pocket sizes as compared to the other parts in the same set. A density of 25% was also applied to all the parts in Test 2.

(II)   Results and analysis:

The build times were calculated by using the developed analytical model (Equation 6.6), which can be considered as the actual build times. The results for Test 1 and 2 are listed in Table 6.3 and Table 6.4.

Table 6.3 – Build times used in producing the test parts in Test 1 (unit: second)

Height Volume	Height 1 (10mm)	Height 2 (30mm)	Height 3 (50mm)
Volume 1 (15 cm^3)	1239	1530	1593
Volume 2 (32.4 cm^3)	2444	2598	2958
Volume 3 (58.8 cm^3)	4236	4219	4535
Volume 4 (96 cm^3)	6754	6453	6762

Table 6.4 – Build times used in producing the test parts in Test 2 (unit: second)

Pocket size Volume	Pocket 1 (0×0mm^2)*	Pocket 2 (10×20mm^2)	Pocket 3 (30×40mm^2)	Pocket 4 (40×50mm^2)
Volume 1 (24cm^3)	2093	2982	3826	5073
Volume 2 (35cm^3)	2837	3717	4875	5204
Volume 3 (56cm^3)	4178	5094	6293	6931
Volume 4 (72cm^3)	5164	6003	7026	7881
Volume 5 (90cm^3)	6249	7164	8119	8830

The results (i.e. build times) were analysed using ANOVA, revealing that part height and deposition head repositioning are significant parameters in relation to the total build times. The ANOVA results are shown in Table 6.5 and Table 6.6.

---

* pocket 1 (0×0mm^2) represents there was no pocket

Table 6.5 – ANOVA table for part height

Source	*SS*	*df*	*MS*	*F*	*P-value*	*F credit*
Volume	45676615	3	15225538	714.80	<0.0001	4.34
Height	207921.5	2	103960.8	4.88	0.06	4.66
Error	127801.8	6	21300.31			
Total	46012338	11				

Table 6.6 – ANOVA table for length of repositioning tool path

Source	*SS*	*df*	*MS*	*F*	*P-value*	*F credit*
Volume	44986349	4	11246587	517.53	<0.0001	3.26
Pocket	20654559	3	6884853	316.82	<0.0001	3.49
Error	260773.2	12	21731.1			
Total	65901681	19				

Due to *F credit* = 4.66 < *F* = 4.88 in Table 6.5, significant difference in build times has been identified while changing the part height. Similarly, in Table 6.6, *F credit* = 3.49 < *F* = 316.82 indicates that length of repositioning tool path is also an important factor. Test 2 demonstrates that build time is not only dependent on total part volume, but also the distribution of material. Based on the tests and the ANOVA results, part height and length of repositioning tool path should be included in the build time estimation model. In addition, it is worth mentioning that the effect of part volume is of more significance than that of part height and length of repositioning tool path.

(III) **Intermittent factor:**

In order to make the build time estimation model easy to use in the process planning algorithm, the parameters in the build time estimation model can be directly or indirectly obtained from the CAD model and/or 2D drawings. From the experiments presented above, the length of the repositioning tool path cannot be used as a variable in the estimation model despite the fact that it is a significant factor. This is because the distance travelled in repositioning and the number of times for repositioning cannot be obtained from the CAD model and/or drawings, which also depends on the part geometry and slicing strategy employed.

A term entitled intermittent factor (*I*) is therefore proposed to reflect the influence of the above two variables against total build times. A high intermittent factor implies that a

significant amount of time is used in repositioning the deposition head and other relevant actions such as filament retraction and print delay (T_{delay}). The parameters related to repositioning actions include two variable and four constant parameters, in which length of repositioning tool path and number of repositioning times are variable/inconstant. Although repositioning speed, acceleration/deceleration, filament retraction speed and delay time per print are kept constant throughout the estimation model development, they are still included in the intermittent factor as the constant and variable parameters individually and interactively affect build times. A typical example is the increase in the number of repositioning times results in a longer build time since the resulting delay time and filament retraction time increase accordingly. Assume that a feature (e.g. feature A) is sliced into a number of layers where discrete deposition areas exist. The intermittent factor can be calculated as the product of the ratio of discrete areas and STL boundary areas, and the ratio of feature A's height and the height of outer feature that contains feature A.

As stated above, high intermittent factor implies that a significant amount of time is consumed in repositioning related activities, particularly in zig-zag deposition tool path strategies. As illustrated in Figure 6.39, the build time for printing this single layer is divided into two parts, namely, productive time during which the material is being deposited (i.e. deposition time), and idle time. During idle time, the nozzle is switched off, the head quickly moves to the next deposition position and the material is being prepared to be deposited (i.e. repositioning time, filament retraction time and delay time). An example part is shown Figure 6.39(a), and the tool paths are shown Figure 6.39(b) where the black lines represent the material deposition tool paths; and the red lines highlight the tool paths for the deposition head movement in the idle time.

(a) the CAD model of the part   (b) tool path for printing a layer
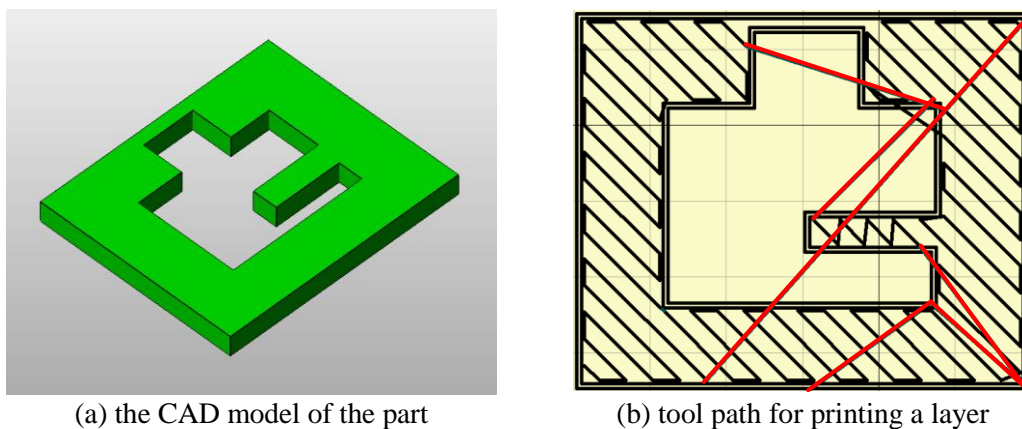
Figure 6.39 – Zig-zag tool path strategy for printing a layer

Table 6.7 shows the classifications of the sliced layers of 2.5D features while the features/subparts are oriented in different directions. In this table, *D* stands for the layers in which there are discrete deposition areas. Similarly, the layers where only continuum deposition areas exist are denoted as *C*. *NC* represents the layers where there is a non-material deposition area located within the continuum deposition areas (e.g. a pocket or the part shown in Figure 6.39). Table 6.7 indicates that the intermittent factor has been defined appropriately since it covers all the scenarios in the determination of part orientation and operation sequencing where the part/subpart/feature is built along different build directions. By changing the build directions, the new intermittent factor can be calculated accordingly.

Table 6.7 – The classification of sliced layers of 2.5D features in different orientations

Rotation / Feature	0°	90° in X axis	180° in X axis	270° in X axis	90° in Y axis	180° in Y axis	270° in Y axis
Planar face	C	C	C	C	C	C	C
Boss	C	C	C	C	C	C	C
Open pocket	C	C	C	C	C	C	C
Closed pocket	NC	C	NC	C	C	NC	C
Through pocket	NC	D	NC	D	D	NC	D
Open slot	D	C	D	C	C	D	C
One open end slot	C	C	C	C	C	C	C
Step	C	C	C	C	C	C	C
Through hole	NC	D	NC	D	D	NC	D
Non-through hole	NC	C	NC	C	C	NC	C

To this end, part volume (V), part density (ρ), part height (H) and intermittent factor (I) were selected and defined to be investigated in the experiments for developing the build time estimation model. Among these four parameters, part volume and height can be directly obtained from the CAD model and/or 2D drawings; part density is specified by the operator; the intermittent factor can be calculated based on the dimensions of the features. This facilitates the calculations in the process planning stage as compared to other build time estimation methods (Han *et al.*, 2003; Kechagias *et al.*, 2004).

6.10.4 Test part designs

There have already been several existing test parts for additive manufacturing machines but most of these parts were designed for accuracy evaluation only (Brajlih *et al.*, 2011). Therefore, four new test parts (test part H – K) were designed by the author, containing various combinations of features, volumes, heights and intermittent factors. Due to factor interactions, four variables can be expanded to 14 different combinations. Thus, these four test parts were scaled proportionally, generating more test parts with varying volumes and heights but constant intermittent factors. The four test parts are shown in Figure 6.40.

(a) Test part H

(b) Test part I

(c) Test part J
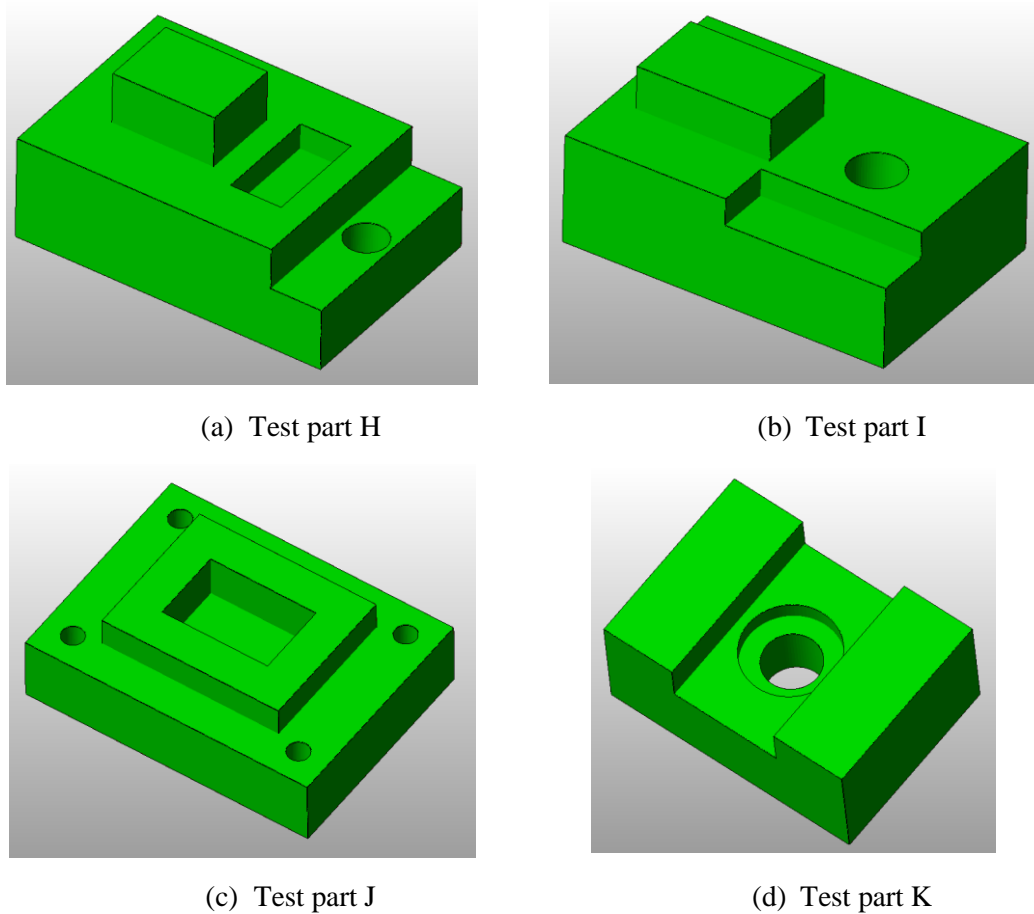
(d) Test part K

Figure 6.40 – Test parts H, I, J and K

6.10.5 Design of experiments

In the development of the build time estimation model, reducing experimental runs was critical since the theoretical model (Equation 6.6) had identified 12 variables, leading to a

large number of experiments. In order to significantly reduce experimental runs, the number of control factors and interactions to be examined was minimised. The first step in designing experiments was to select and determine the factors, which have been elaborated in section 6.10.3.

Having determined the parameters to be involved in the model, the next step was to determine the number of levels to be investigated for each factor. Given that those four factors are multi-level variables and their outcome effects are not linearly related, four levels were thus chosen to apply to part volume, height and density for each test part design. As the aim of the experiments was to develop a build time estimation model rather than identify the influence of important factors only, the Taguchi method (Ross, 1996) was not considered to be appropriate for this experimental design. Another standard approach for DoE is to use full factorial method. However, this method is only acceptable and feasible when a few (usually no more than three) factors are to be explored. In this regard a 3^4 experimental plan would have been required if the full factorial method was to be used. Furthermore, involving four variables implies there are ten interactions between them, requiring even more experimental runs. In addition, the intermittent factor represents the geometrical attributes, which are constant and unique for each test part. However, the full factorial methods require different levels for each variable.

However, for predicting build times, the more experimental data obtained the more accurate the prediction results. As a result, the levels of the parameters need to cover a wide range of values. For instance, it is better to investigate the influences caused by both a small volume part and a large volume part and other volumes in between. Based on the above reasons, the four test parts were scaled up 1.2, 1.4 and 1.6 times, by which the part volume, height vary accordingly. It is also noted that the length of repositioning tool path in the XY plane and Z axis were changed accordingly as well. Four levels of part density, namely 25%, 50%, 75% and 100% were used for each part volume and height variables. As a result, 64 experimental runs were required. Table 6.8 shows the parameters for 16 experiments for test part H. Note that the intermittent factor was constant for the identical build direction.

Table 6.8 – The designed experiments for test part H

Volume (cm3)	Porosity (%)	Height (mm)	Intermittent factor
46.2	25	30	0.115
46.2	50	30	0.115
46.2	75	30	0.115
46.2	100	30	0.115
79.8	25	36	0.115
79.8	50	36	0.115
79.8	75	36	0.115
79.8	100	36	0.115
126.8	25	42	0.115
126.8	50	42	0.115
126.8	75	42	0.115
126.8	100	42	0.115
189.2	25	48	0.115
189.2	50	48	0.115
189.2	75	48	0.115
189.2	100	48	0.115

6.10.6 Experimental results, analysis and discussion

To obtain the build time estimation model, regression analysis and ANOVA was carried out iteratively. The errors were analysed by comparing the actual and the predicted build times to identify the importance of the interactions among the four control factors. By feeding back the error analysis, the final estimation model was obtained, where unimportant interactions were removed.

In detail, the actual build times of a total of 64 test parts were accurately calculated using Equation 6.6. Having obtained the actual times, a multi-factor regression analysis technique was used to obtain a full factorial estimation model. This model was subsequently applied to the same test parts to estimate the build times. The estimated and actual results were compared and the errors were analysed. The development of the estimation model and the deviation analysis were carried out iteratively. The deviation analysis identified the importance of each parameter and the interactions. In turn, the parameters that were of secondary importance were removed in the next step of the development process. The deviation in the new model was analysed again, identifying the least important parameters which were ignored in the following regression analysis. By doing so, the original 14 factors (including individuals and interactions) were reduced to four.

The actual build time (T_a) and the estimated build time (T_a^*) can be depicted in Equation 6.7 and Equation 6.8, respectively.

Equation 6.7
$$T_a = f_1(V,H,\rho,I) + f_2(V,H,\rho,I) + \cdots + \sum_{p=1}^{P} f_i(V,H,\rho,I)$$

Equation 6.8
$$T_a^* = C + f_1^*(V,H,\rho,I) + f_2^*(V,H,\rho,I) + \cdots + \sum_{q=1}^{Q} f_i^*(V,H,\rho,I)$$

where, f_i and f_i^* are the functions related to part volume, height, density and intermittent factor in the actual and the build time estimation model, respectively. C is the intercept. Thus, the deviation (ζ_m) for each individual experiment can be simply expressed using Equation 6.9.

Equation 6.9
$$\zeta_m = \left| T_{total.m} - T_{total.m}^* \right|$$

The root mean square of the deviation (RMS_ζ) and each function (RMS_{fi}) in the estimation model can be calculated using Equation 6.10 and Equation 6.11, where, m denotes experiment number m.

Equation 6.10
$$RMS_\zeta = \sqrt{\frac{\sum_m^{M=64} \zeta_m}{M}}$$

Equation 6.11
$$RMS_{f_i} = \sqrt{\frac{\sum_m^{M=64} f_{i.m}}{M}}$$

Given that producing a middle size prototype (i.e. $1.25 \times 10^2 \text{cm}^3$) requires up to 7 hours, the acceptable deviation between the actual and estimated build times was set to be five minutes. Therefore, for those RMS_{fi} that were one or more orders of magnitude greater than RMS_ζ, the corresponding functions were kept in the next run of the estimation model development process. Other functions were taken off from the model. After five iterations, the final build time estimation model was obtained as depicted in Equation 6.12.

Equation 6.12
$$T_a = 168.33 + 23.56V + 9.44H + 160.19V\rho + 78.17HI + \varepsilon$$

where, ε is the uncertainty in the actual experiments.

The selected analysis results are shown in Table 6.9, which were obtained by fitting a second-order regression model (Equation 6.12). Due to the square terms of the four variables and other interactions that were either unimportant or not considered in the DoE, they are not shown in Table 6.9. The *t*-stat represents the statistic *t*-test value for individual regression coefficients. A large absolute value of the *t*-stat implies the significance of the variables and interactions. *P*-value represents the probability value. The smaller the value the more significant it represents. Since the *P*-values of part volume, the interaction of volume and density, height, and intermittent factor are significantly smaller than the threshold value of 5% in the analysis, they are of primary significance. Among them, the interaction of volume and density is the most significant factor, followed by part volume. With respect to the regression confidence and the adjusted regression confidence, R^2, $(R^2)_{adj}$ and the difference between them indicates that the regression model is satisfactory.

Table 6.9 – Summary of the selected regression analysis results

Variables	Standard deviation	t-stat	P-value	R square	Adjusted R square	
Intercept	27.76	0.61	0.55			
Part volume (V)	0.94	25.07	<0.001			significant
Part height (H)	8.35	1.13	0.26			
V×ρ	0.50	318.60	<0.001			significant
H×I	17.08	4.58	<0.001			significant
Regression model				99.98%	99.98%	

The residual analysis was carried out for checking the adequacy of the developed estimation model. Figure 6.41 is the normal probability plot of the standardised residuals of the model. It is considered as satisfactory due to the standardised residuals that are evenly distributed along the straight line. Figure 6.42 shows the distribution of the standardised residuals versus the experiment numbers. No distinct pattern has been observed, revealing that the current model is appropriate and no further factors are required for describing the relationship between the input factors and the estimated times. Approximately 98.4% of the standardized residuals fall in the interval (-2, +2), demonstrating that the errors are normally distributed. Nevertheless, it should also be noted that there are two points that are outside the interval. The standardised residual of one of the points is 2.01, which can still be considered as normal, but another standardised residual of 3.02 indicates the presence of an outlier. Thus, the parameters in the corresponding influential observation (experiment number 45) were traced back and the

distance of the point from the average of all the points in the data set was recalculated. The results show that the outlier does not have a dramatic impact on the regression model. Figure 6.43 also supports this statement, which plots the errors curve showing that the error of 2.2% in experiment 45 is acceptable. Due to an unknown reason that caused the high-standardised residual, more tests are required to validate and evaluate the performance of the model, which will be presented in the next section.
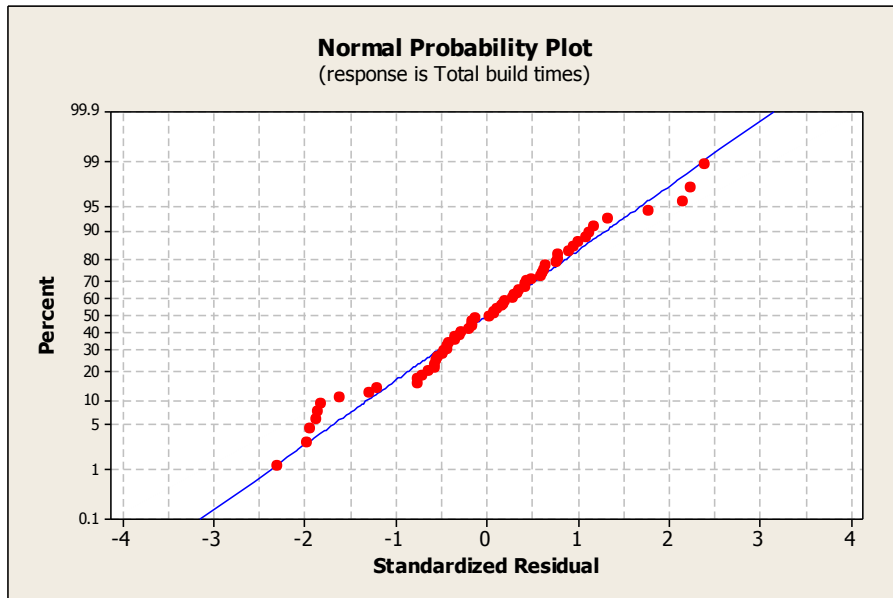
Figure 6.41 – Normal probability plot of standardised residuals
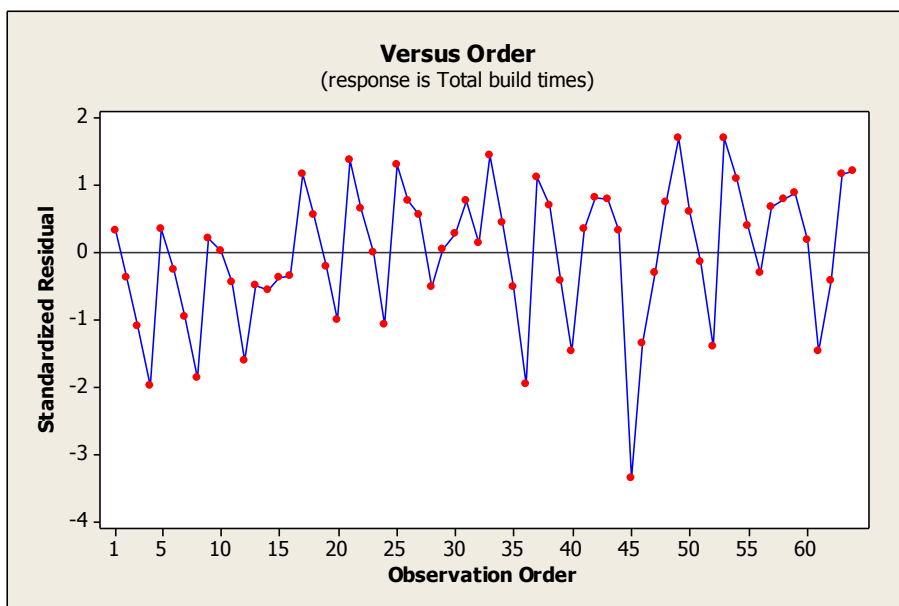
Figure 6.42 – Distribution of standardised residuals versus experiment number

It is noted that the errors tend to increase while the part volume is small, as identified in Figure 6.43. While the four test parts were not scaled up (experiment 1-4, 17-20, 33-36 and 49-52), the errors are relatively larger than the errors in other experiments. In addition, the original volumes of test part H and I are small (less than 50 cm^3). As a result, the errors do not decrease significantly while the parts were scaled up 1.2 times. An exact reason cannot be provided, however for small parts where the volume does not exceed 100 cm^3, even though the number of repositioning and filament retraction times is kept unchanged, the length of the repositioning tool path is significantly shorter than that of the larger volume parts, while the intermittent factors are identical. This may lead to an increase in estimation error. Furthermore, it is worth mentioning that errors can be simply reduced to lower than 1% by expanding Equation 6.12 with more factors (e.g. adding interactions between V, H, ρ and I, as shown in Equation 6.13 as an example).

Equation 6.13

$$T_a^* = 51.32 + 26.71V + 8.62H + 160.19V\rho - 0.07VH + 69.83HI + 0.10H^2 + \varepsilon^*$$
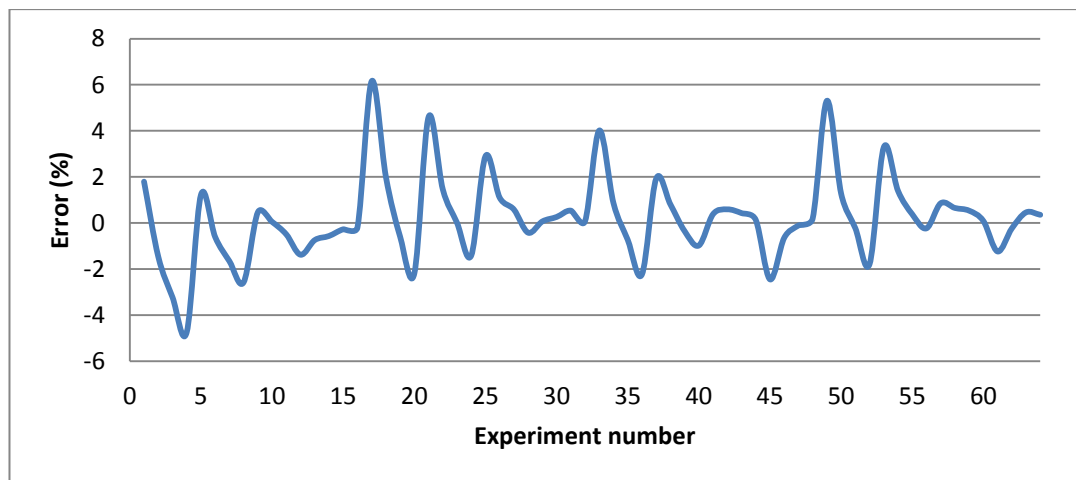
Figure 6.43 – Percentage errors between the actual and estimated build times for the test parts in the estimation model development

6.10.7   Evaluation of the developed build time estimation model – case study

After obtaining positive results from the previous experiments, three case studies were conducted for the evaluation and validation of the developed build time estimation model, and are described below.

6.10.7.1Design of experiments for the estimation model evaluation

Given that the aim of the evaluation experiments was to evaluate and validate the developed model, the Taguchi design strategy was not appropriate and full factorial experiments were unnecessary. The designed test parts needed to include various prismatic features. More importantly, fabricating these features requires varying length of repositioning tool paths and differing number of repositioning and filament retraction times. This research focuses on prismatic part manufacture, but it is still worth understanding the performance of the build time estimation model in relation to the manufacture of sculptured surfaces. This is because the iAtractive process is likely to be further developed for sculptured surface manufacture. Based on the above reasons, three test parts (as shown in Figure 6.44) have been designed and modified, covering the typical prismatic features and two 3D features. Test part M was modified from the NAS 979 (National Aerospace Standard 979, 1969) test part; and test part N was selected and modified from Zhou *et al.*'s (2000) test part which contains nine features including planar face, boss, pocket, sphere and chamfer.
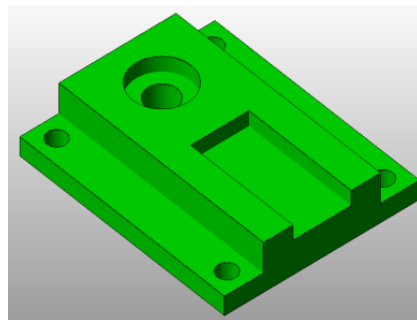
(a) Test part L
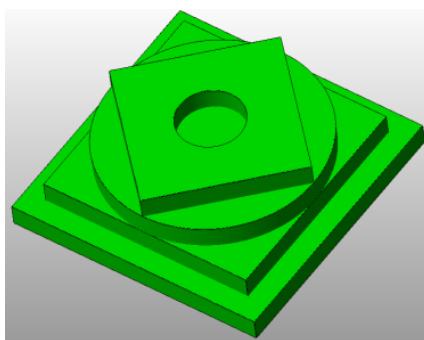
(b) Test part M
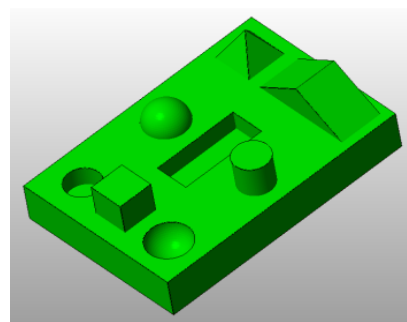
(c) Test part N

Figure 6.44 – Test parts L, M and N

It was found that the majority of the estimation inaccuracy lies in producing parts with a volume of less than 50 cm^3. Therefore, the volumes of test part L and test part N were specially designed to be less than 50 cm^3. Subsequently the three original test parts were scaled up 1.2, 1.4 and 1.6 times, generating 12 test parts with differing part volumes and heights. Due to the interaction of volume and porosity that is the most significant factor, 25%, 50%, 75% and 100% levels of porosity were applied to these 12 test parts. The properties of the original test parts L, M and N are summarised in Table 6.10. A total of 48 test parts were defined.

Table 6.10 – Properties of the test parts L, M and N

Properties / Part	Volume (cm^3)	Height (mm)	Porosity (%)	Intermittent factor
Test part L	26.05	13	N/A	0.245
Test part M	45.68	20	N/A	0.141
Test part N	25	18	N/A	0.689

6.10.7.2 Experimental results and discussion

The actual build times of the above 48 test parts were obtained using Equation 6.6 and the estimated build times were calculated using Equation 6.12. Table 6.11 presents the results obtained in the experimental runs 17 – 32. The errors between the predicted and the actual build times are also presented. It is observed that the errors for the part volume of 45 cm^3 could be up to -6.73%, whereas the largest error is only 0.75% for the part volume of 187.11 cm^3. With the increase in part volume, the mean error gradually reduces from 3.44% to 0.36%.

The percentage errors between the predicted and actual build times are plotted in Figure 6.45. The best results were obtained in the experimental runs 17-32 and there is no obvious fluctuation (less than 12% error) in the experimental runs 1-16 and 33-48. As the estimation model (Equation 6.12) only has four factors rather than 6 factors (Equation 6.13), it is not as sensitive as Equation 6.13 in terms of the accuracy in predicting times for the actions relating to repositioning. The test parts in the experiments 17-32 (test part M and variations) have a low intermittent factor (less than 0.2), indicating the short length of repositioning tool path, relatively low number of repositionings and filament retraction times, as well as a short resulting delay time during production. As a result, the resulting

errors were reduced. In other words, the developed build time estimation model has better performance for parts with a low intermittent factor (< 0.2). The predicted times tend to be longer than the actual times while the model is applied to parts with a high intermittent factor (> 0.5).

Table 6.11 – The predicted build times using the developed estimation model

| Experiment number	Volume (cm^3)	Height (mm)	Porosity (%)	Intermittent factor	Actual build times (seconds)	Estimated build times (seconds)	Errors (%)
17	45.68	20	25	0.14	3735	3483.58	-6.73
18	45.68	20	50	0.14	5365	5312.99	-0.97
19	45.68	20	75	0.14	7012	7142.40	1.86
20	45.68	20	100	0.14	8609	8971.81	4.21
21	78.94	24	25	0.14	5981	5680.68	-5.02
22	78.94	24	50	0.14	8962	8841.90	-1.34
23	78.94	24	75	0.14	11931	12003.12	0.60
24	78.94	24	100	0.14	14794	15164.34	2.50
25	125.35	28	25	0.14	8982	8714.54	-2.98
26	125.35	28	50	0.14	13866	13734.44	-0.95
27	125.35	28	75	0.14	18670	18754.34	0.45
28	125.35	28	100	0.14	23493	23774.24	1.19
29	187.11	32	25	0.14	12788	12724.62	-0.50
30	187.11	32	50	0.14	20220	20217.88	-0.01
31	187.11	32	75	0.14	27661	27711.14	0.18
32	187.11	32	100	0.14	34941	35204.40	0.75
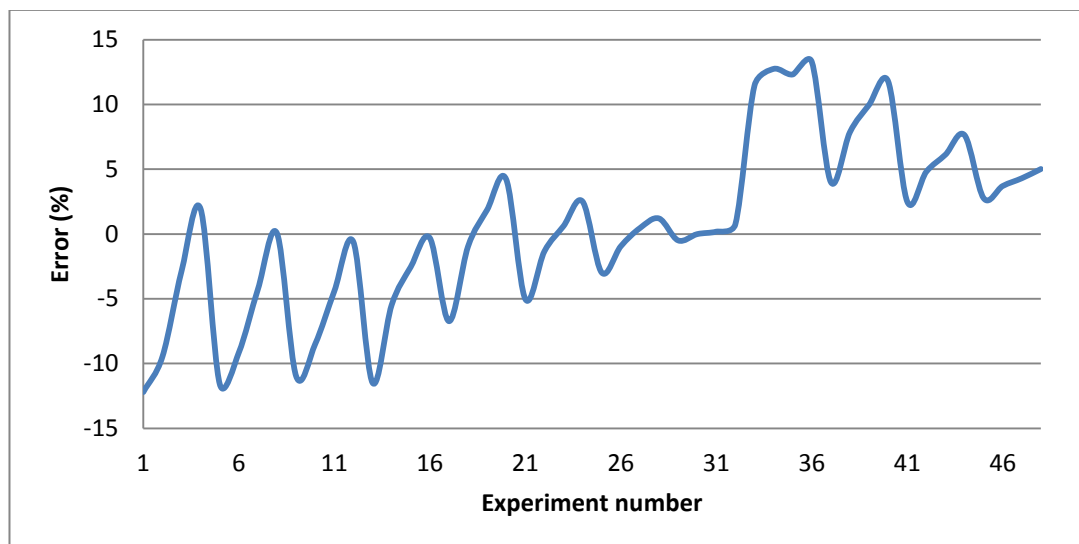
Figure 6.45 – Percentage errors between the actual and estimated build times for the test parts in the estimation model evaluation

In order to evaluate the model, a statistical method, namely, t-tests was used to analyse the results, identifying whether significant difference exists between the estimated and actual build times. Paired t-tests were carried out for all the test parts at a 95% confidence interval for the analysis of the differences between the estimated and actual times. The selected results are listed in Table 6.12, where t-stat is $0.75 < t$ two-tail critical = 2.01 ($\alpha = 0.05$). Thus, it can be concluded that the build time estimation model does not yield significantly different results when compared to the actual times.

Table 6.12 –Selected results of the paired t-test

t-test output	*Estimated*	*Actual*
Observations	48	48
Pearson correlation	0.99	
df	47	
t Stat	0.75	
P(T<=t) one-tail	0.23	
t one-tail critical	1.68	
P(T<=t) two-tail	0.46	
t two-tail critical	2.012	

6.11 Summary

In this chapter, a process planning algorithm, entitled GRP^{2}A, has been investigated, which is capable of generating static and dynamic process plans for the manufacture of complex part geometries. The procedure for generating process plans is:

- The part features are first recognised and the analysed, identifying potential cutting tool collisions and overhanging features (section 6.3.1). The part is then oriented into a position and the factors affecting orientation were addressed (section 6.3.2).
- The part is decomposed into a number of subparts, enabling the internal features to be finish machined without cutting tool collisions (section 6.4).
- Build directions are allocated to each subpart by considering the FFF process capability and deposition nozzle collisions. If every subpart has been specified a build direction and no nozzle collisions occur, this set of build directions is considered to be valid. A number of sets of build directions may exist (sections 6.5.2 and 6.5.3).

- Machining operations are inserted into the valid sets of build directions whilst taking into considerations precedence and tool accessibility constraints (section 6.5.5). Thus, the additive and subtractive operations are sequenced.

- Features are modified for the corresponding additive and subtractive operations (section 6.6).

- Inspection operations are added into the scheduled additive and subtractive operation sequences, by which feasible operations for manufacturing the part are obtained (section 6.7.1).

- The production times for feasible operations are estimated and the most appropriate operation sequence is identified (sections 6.9 and 6.10). The tool paths and process parameters are then generated and determined, respectively (section 6.7.2). To this end, the static process plan is generated.

- This static process plan will be further updated into the dynamic process plan depending on the inspection feedback (section 6.8).

7 <u>Investigation of feature-based decision-making logic for material reuse</u>

7.1 Introduction

One of the major advantages of the iAtractive process, namely accurate manufacturing of complex parts, has been presented in chapter 6. In this chapter, FDL is investigated, enabling existing parts to be further manufactured, which is considered to be another distinct advantage of the iAtractive process. Existing parts are classified into a series of groups based on features and a number of available manufacturing strategies are then proposed to utilise these existing parts.

7.2 The Overview of Feature-based Decision-making Logic

7.2.1 The definitions of material reuse and existing part

As identified in section 2.4 and Table 2.1, both FFF and CNC machining processes are constrained by raw materials in terms of shape and size. In general, additive processes start producing parts from zero, adding material layer by layer until the parts are fully generated. On the other hand, CNC machining is a subtractive process, requiring a block of material that must be at least as big as the part that is to be made. Neither of these types of manufacturing processes is able to utilise existing parts.

Referring to existing part/material, it is defined as a part/object that has already been produced, used, worn or abandoned. A finished part can be seen as an existing part; an abandoned finished part of which the dimensions are out of tolerance is also considered as an existing part; a block or an object with arbitrary shape is an existing part as well. In broad terms, an existing part may be of any shape and size. For the iAtractive process, existing parts are considered as raw material to be further manufactured and transformed into final parts. The features on the final parts are different from the features on the existing parts. This essentially means the existing parts are utilised as part of the final parts and are thus considered as being reused. It should be noted that all the existing parts in this chapter are solid objects rather than hollow.

7.2.2   An overall view of Feature-based Decision-making Logic

An existing part is first inspected on a CMM in order to obtain its dimensional and geometric information, which is the input for FDL. By considering the geometry and the dimensions of the existing part as well as the designed features on the final part, feasible manufacturing strategies are selected, specifying available operations for remanufacturing the existing part. The existing part will then be further manufactured by using the additive, subtractive and inspection processes interchangeably. By doing so, the final part is obtained. It is noted that each manufacturing strategy can be applied to a number of existing parts with various features and in turn, there are a number of manufacturing strategies available for the same existing part.

7.3   Classification of Existing Parts

7.3.1   Final and non-final features

Prior to defining final and non-final features, the definitions of 'qualified' and 'unqualified' part/feature are first specified. 'Qualified' represents the manufactured part/feature that achieves the designed requirements in terms of accuracy and surface quality. 'Unqualified' indicates the part/feature requires further manufacturing as it does not meet the tolerance and surface quality requirements.

Qualified final features are features that the iAtractive process aims to produce. Every feature on the finished part is a final feature. If the dimensions of the features on the final part are out of tolerance, they are considered as unqualified final features.

Non-final features are features on the existing part, but are not the desired features on the final qualified part. Non-final features require further processing by either removing and/or adding more material. By doing so, they can be transformed into the final features. In terms of dimensions, a feature, of which the dimensional deviation is more than 1mm compared to the nominal, is regarded as a non-final features. In addition, the maximum allowance of the positioning error of a final feature is defined as less than 1mm. Figure 7.1(a) shows a final feature ($8 \times 12 \times 5$mm^3) located in the designed location. However, the boss ($12 \times 14 \times 5$mm^3) shown in Figure 7.1(b) is considered to be a non-final feature. Furthermore, in Figure 7.1(c), despite the fact that the dimensions of the boss ($8 \times 12 \times 5$mm^3)

are exactly the same as the dimensions of the boss in Figure 7.1(a), it is still a non-final feature due to the positioning error being beyond the maximum allowance.

The sacrificial features on a subpart can be seen as semi-final features. For example, the support material on a subpart has to be created and then removed. In this scenario the support material is classified as a semi-final feature required to be created when producing the subpart (see Figures 6.29 and 6.30).

| (a) | (b) | (c) |
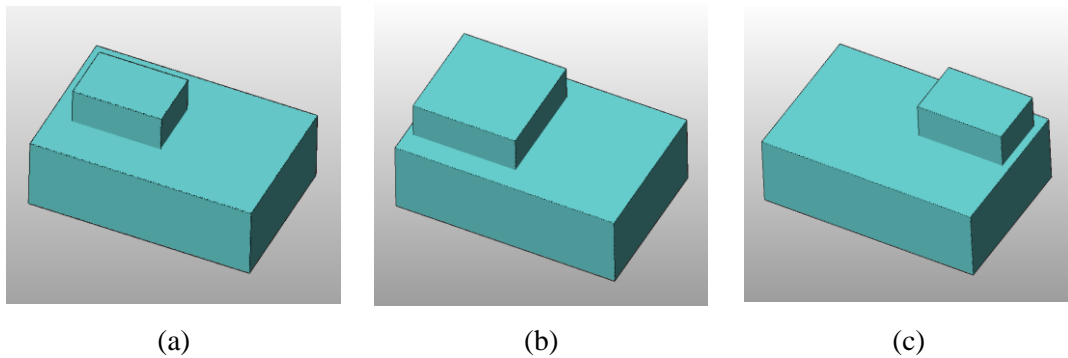
Figure 7.1 – A final feature and non-final features

7.3.2   Existing parts classification

Existing parts are classified into three types, namely, existing part with non-final features, with final features, and with both non-final and final features. As this research is only focused on prismatic part manufacture, six types of features are considered in FDL, namely, boss, pocket, step, slot, hole and planar face. Thus, each of these six types of existing parts is further classified based on features, which are existing part with a single feature, and with combinations of any of these single features. In terms of feature combination, it can be categorised as combinations of interacting features, and combination of separate individual features. The existing part in Figure 7.1(a) is an example of an existing part with a single feature. Figure 7.2 shows an existing part with a separate pocket and a boss. Figure 7.3(a) shows an existing part with a pocket containing a boss. To avoid confusion, for representing interacting features, the first feature contains the second feature. For example, an existing part with an interacting boss and pocket is shown in Figure 7.3(b). Furthermore, for a feature that contains two separate individual features, the notation is: an existing part with interacting [1st feature] and ([2nd feature] and [3rd feature]), e.g. an existing part with an interacting pocket and (a boss and a hole) in Figure 7.3(c).
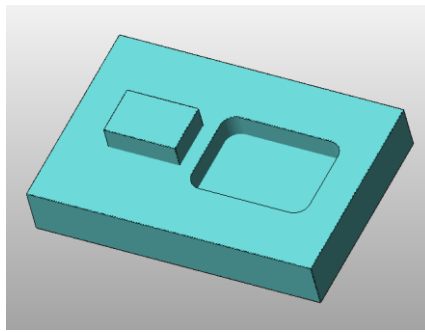
Figure 7.2 – An existing part with a separate boss and a pocket
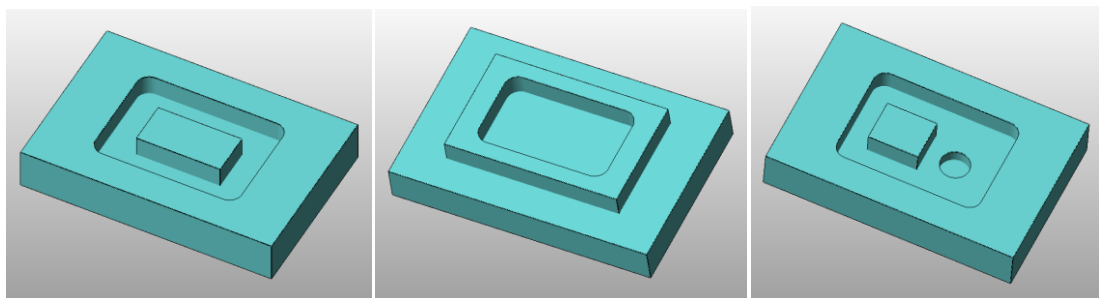
(a)	(b)	(c)

Figure 7.3 – Existing parts with interacting features

7.4   Manufacturing Strategies for Producing Parts Based on Existing Parts

This section presents a series of manufacturing strategies capable of transforming various existing parts into final parts. The global and local constraints are specified, which are used to select appropriate manufacturing strategies based on the geometries of the existing and final parts.

7.4.1   Global and local constraints

Prior to developing manufacturing strategies for reusing existing parts, the differing constraints have to be specified. Two types of constraints, namely global and local constraints that affect the selection of manufacturing strategies are defined as follows.

(i)   Local constraints

Local constraints are referred to geometrical and positioning dimensions of the features on both the existing and final parts. Local constraints only deal with the selection of manufacturing strategies based on the dimensions of the features on the existing part identified in the initial inspection operation. The initial inspection operation, as shown in

Figure 4.4, is the first operation to be conducted, which measures the given existing part and thus identifies the geometrical attributes.

A typical example of local constraints is as follows: an existing part is given as shown in Figure 7.4. The final part is a rectangular block, of which the length and width are the same as the existing part on the XY plane. The height of the block is higher than that of the existing part. It is assumed that the pocket width (W_p) is shorter than the pocket length (L_p), i.e. $W_p < L_p$. Thus, when $\sqrt{2}W_p \leq 23$mm, (23mm is the longest bridge length that can be produced, as identified in Table 5.2), one of the available strategies is to directly add material onto the top face of the existing part until the near-net shape of the block is built. On the other hand, when $\sqrt{2}W_p > 23$mm, the above strategy cannot be used since the deposition process will fail while attempting to deposit material upon the pocket. This example demonstrates that the local constraints primarily determine feasible manufacturing strategies for remanufacturing existing parts.
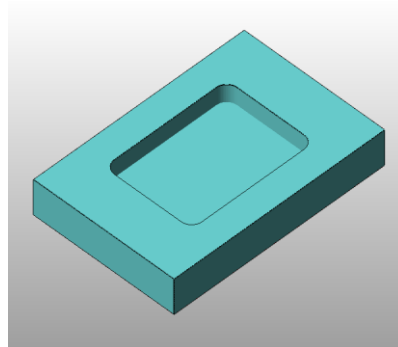
Figure 7.4 – An existing part with a pocket

(ii)   Global constraints

Global constraints focus on application requirements (in terms of tolerances and surface quality), production time, material consumption and positions of negative features in part designs. Global constraints significantly restrict the number of manufacturing strategies to be used. They are applied at the end of the decision-making process to finally determine the feasible manufacturing strategies.

For instance, for a component – which can be both manufactured by the FFF process only, and by the FFF process followed by a finishing operation – cannot be solely fabricated by the FFF process in certain application areas where high dimensional accuracy is required.

For simplifying the number of options in FDL, none of the features can be purely produced by the FFF process since high part accuracy has been specified in the scope of this research.

Determination of the final manufacturing strategy depends on the actual requirements. If the first priority is production time, the manufacturing strategy, where the least amount of production time is achievable, should be selected. Similarly, if material consumption or production costs is the most important factor, the manufacturing strategy that matches this factor should be chosen accordingly.

Further to positions of negative features in part designs, it is explained as follows: Figure 7.5 shows a final part with two through holes (negative features). If the existing part in Figure 7.4 is going to be reused and $\sqrt{2}W_p \leq 23$mm, two examples of manufacturing strategies are:

(I)   Directly add material onto the top of the existing part until the near-net shape of the final part is built; then finish machine the entire part (including drilling two holes and finish machining all the surfaces of the final part).

(II)   Remove the existing pocket on the exiting part in a machining operation; continuously deposit layers onto the top of the machined surface until the near-net shape of the final part is built; then finish machine the entire part (including drilling two holes and finish machining all the surfaces of the final part).
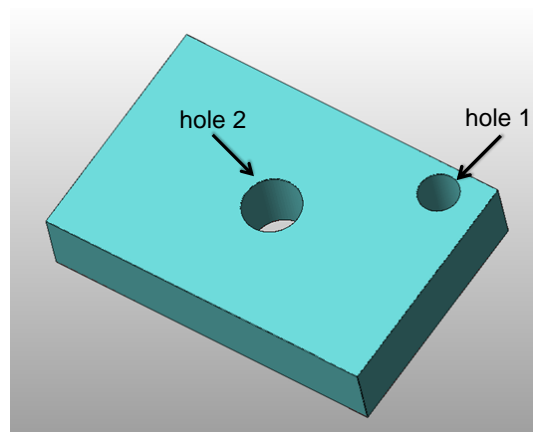
Figure 7.5 – Positions of holes in a part design

Both manufacturing strategies would have been feasible if hole 2 was not designed in the position shown in Figure 7.5. As hole 2 (on the final part) and the pocket (on the existing

part) are overlapping in the Z axis and the pocket is bigger than hole 2, the first manufacturing strategy is not feasible in this scenario. Figure 7.6 shows the final part produced using strategy I. The transparent view reveals that hole 2 cannot be fully created in the overlapping area of hole 2 and the pocket. The red lines highlight the profiles of the two holes. As a result, only strategy II is available. It is also noted that the existence of hole 1 does not affect the manufacturing strategy selection in this example.
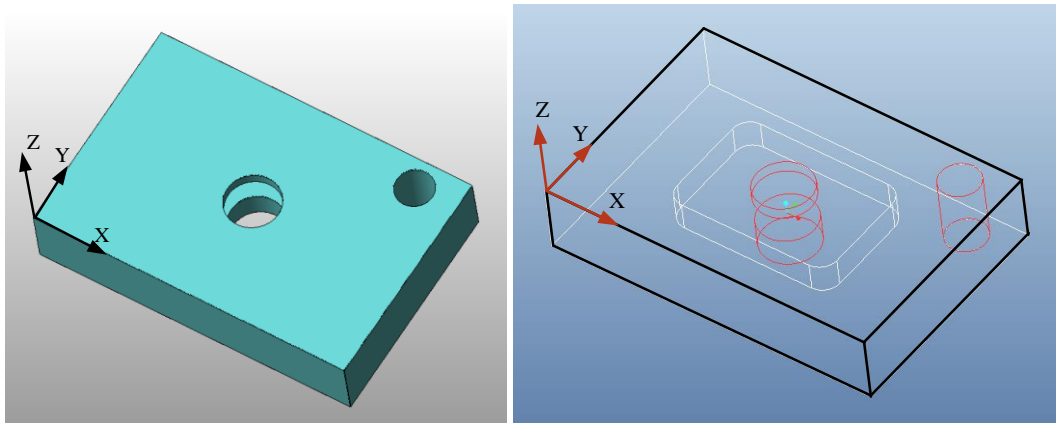
Figure 7.6 – The final part is manufactured using an inappropriate manufacturing strategy

7.4.2   Deposition nozzle constraints

In fact, the deposition nozzle constraints are included in the local constraints. The reason that the deposition nozzle constraints are emphasised is that, unlike the traditional AM methods which create physical models from zero on a build platform (in which case no deposition nozzle collision occurs), in this scenario material is directly added onto existing parts. As a result, the potential deposition nozzle collisions in this first instance need to be considered. Nozzle collisions are likely to occur between the deposition nozzle and the existing features.

The deposition nozzle is shown in Figure 6.11. Due to the nozzle configuration, existing pockets, holes, slots and steps cannot be completely filled by depositing new melted material. However, the deposition nozzle can still access pockets and holes, and then deposit material providing their dimensions are greater than the nozzle's dimensions. For deep pockets and blind holes, the current nozzle may not be able to access their surfaces because of the limited length of the deposition tool used.

7.4.3   Manufacturing strategies for remanufacturing existing part

This section introduces eight available manufacturing strategies that can be used to further manufacture existing parts. These strategies are outlined in Table 7.1.

Table 7.1 – Available manufacturing strategies for material reuse

Strategy number	Available manufacturing strategy
①	Directly add material onto the existing part, then interchangeably add & subtract & inspect (iASI) until the part is finished.
②	Remove the existing feature(s), then iASI.
③	For an existing feature that is included in another existing feature, remove the outer feature, then iASI.
④	For an existing feature that is included in another existing feature, remove the inner feature, then iASI.
⑤	Machine the existing features to the final dimensions directly.
⑥	Add material inside the existing feature until the height of the newly deposited material reaches the same height as the existing feature, then iASI.
⑦	Add material outside the existing feature until the height of the newly deposited material reaches the same height as the existing feature, then iASI.
⑧	Produce a mating part separately, which matches the features on the existing part; assemble the mating part and the existing part, then iASI.

Strategies ② and ⑧ are considered as universal manufacturing strategies since they can be applied to all kinds of existing parts with various features. The above eight strategies by no means cover all the available manufacturing strategies and it is likely that more strategies exist, which will be discussed in sections 9.7 and 10.4.3.

The aim of the manufacturing strategies is to provide feasible manufacturing operations to further manufacture the given existing part, transforming it into the final part. If the final part contains internal features, the manufacturing strategy will only focus on the first few operations to transform the existing part into the ith subpart identified in GRP^{2}A (assuming that the $(i+1)^{th}$ subpart leads to a cutting tool inaccessibility issue). Regarding the following operations (i.e. iASI), they should be the same as the operations specified in GRP^{2}A. The number of 'first few operations' depends on existing part geometry, which will be described in the proceeding sections.

For example, a rectangular block is given as an existing part and the final part to be produced is shown in Figure 6.25. The operation sequence generated by GRP^2A is as follows:

(i)   build subpart 1;

(ii)   measure subpart 1;

(iii)   finish machine the blind pocket on subpart 1;

(iv)   build subpart 2;

(v)   measure the produced subpart 1&2;

(vi)   machine the other pockets in subpart 1&2;

(vii)   measure the finish machined pockets on subpart 1&2;

(viii) build subpart 3;

(ix)   finish machine the exposed pockets;

(x)   measure the finish part and the exposed pockets.

It is virtually impossible to directly machine the existing part to the combined subpart 1&2 (the subpart 1&2 is produced in operation vi) because the cutting tool cannot access the blind pocket. As a result, the existing part has to be transformed into subpart 1 first no matter what the shape and size the existing part is. The following iASI operations should follow the operations defined in (ii) – (x). In addition, subpart 2 is the $(i+1)^{th}$ subpart that causes cutting tool inaccessibility.

Another consideration that makes the first few operations very important arises from deposition nozzle collisions as well as the FFF process capability in producing overhangs. Figure 7.7(a) shows an existing part with a boss. The deposition nozzle collisions should be avoided when printing material (green part) onto the existing part (blue part), as shown in Figure 7.7(b). This is because the absolute height of the green part being printed in Figure 7.7(b) is lower than that of the existing boss. Once the height of the green part reaches the same height as the existing boss as shown in Figure 7.7(c), no tool collisions will occur and the printing process becomes the same as that of the traditional FFF process, namely printing from bottom to top. Therefore, subsequent operations may follow the operations generated from GRP^2A if there are other subparts to be manufactured.

In addition, due to cutting tool and deposition nozzle accessibility that is also taken into consideration in GRP^2A, subsequent subparts can be produced and there is no need for

FDL to provide further manufacturing strategies. Moreover, if the deposition nozzle is printing a bridge as shown in Figure 7.7(d), the bridge length should not exceed the longest length that FFF is capable of producing. This factor has been considered in FDL before starting to produce the green part in Figure 7.7(b). Thus, the FFF process capability is taken into account before remanufacturing the existing part and the highest risk of deposition nozzle collisions is most likely to occur in the first few operations.

(a)

(b)

(c)

(d)
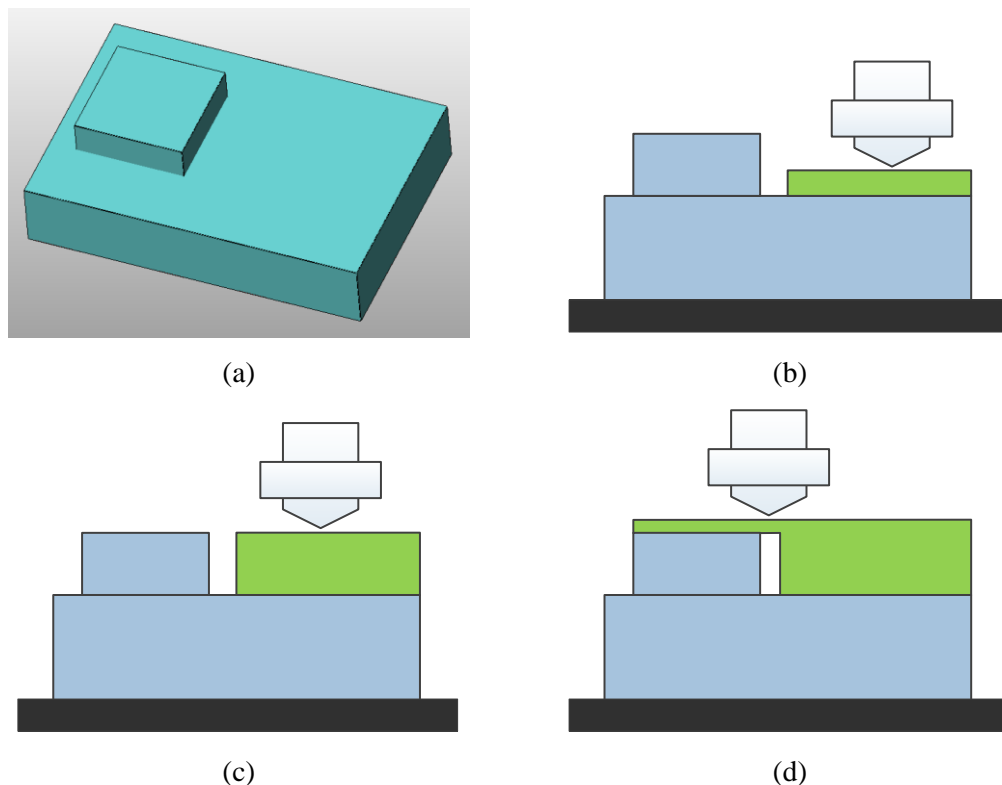
Figure 7.7 – Depositing material onto an existing part with a boss

In order to concentrate on the manufacturing strategies themselves, in this chapter, no internal features are designed in the final parts. That means the final parts do not have to be decomposed and there is only one subpart for each final part, which is actually the final part itself. FDL will provide feasible manufacturing strategies to further manufacture the existing parts, reincarnating them into final parts.

7.4.4 Existing part with single non-final feature

Sections 7.4.4 to 7.4.8 illustrate the selection of manufacturing strategies based on existing parts with various features by applying the local constraints. In this section, the available

strategies for manufacturing existing parts consisting of a wide range of combinations of non-final features are described. The notations for the dimensional parameters are summarised in Table 7.2. These parameters will be explained along with the manufacturing strategies in the subsequent sections.

Table 7.2 – Notations of the dimensional parameters in manufacture of existing parts

Parameter	Notation	Parameter	Notation
Length (in the X axis)	L	Slot	s
Width (in the Y axis)	W	Hole	h
Depth (in the Z axis)	D	Step	st
Height (in the Z axis)	H	Existing part	e
Diameter of the hole	ϕ	Positioning dimension in X axis	PL
Nominal dimension	Nd	Positioning dimension in Y axis	PW
Boss	b	Vertical distance between the existing feature to its adjacent final feature	D_f
Pocket	p	Total thickness of all the recovery layers	D_r

Both final and non-final features are further split into two groups, namely positive and negative features. Boss is considered to be a positive feature. Negative features are pocket, slot, step and hole. For the classification of positive and negative features, readers are referred to section 5.3.

The final part P is shown in Figure 7.8, which is modified from test part C in Figure 5.10, consisting of a boss, a closed pocket and a step. The reason that the two holes in test part C are ignored is that the positions of holes are global constraints, which do not affect the initial stage of manufacturing strategy selection.
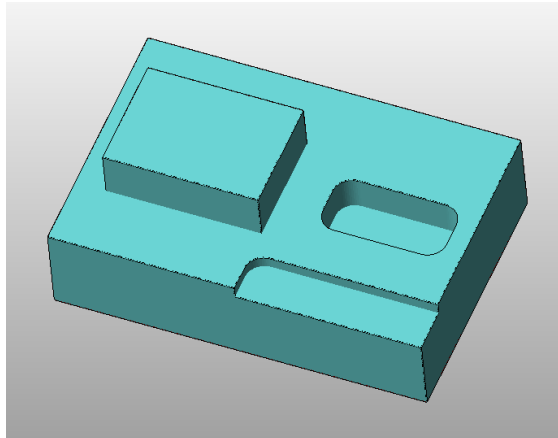
Figure 7.8 – Final part P to be produced from different existing parts

The typical combinations of non-final features together with the manufacturing strategies are illustrated in section 7.4.5 and Table 7.4.

7.4.4.1 Block

A block is considered as a single boss (non-final feature). The local constraints are: the total length, width and height of the final part (L, W and H), and the length, width and height of the block (L_e, W_e and H_e).

(i) $L_e \geq L$, $W_e \geq W$ and $H_e \geq H$

This means the block size is bigger than that of the final part P. Thus, strategy ⑤ can be used to directly machine the block to the final part. This scenario is exactly the same as the scenario where a part is solely CNC machined.

(ii) $L_e \geq L$, $W_e \geq W$ and $H_e < H$

This means the block height is lower than the total height of the final part P. Therefore, strategy ① can be used to directly add material onto the block until the near-net shape of the final part is built (see Figure 7.9) followed by a finishing operation.
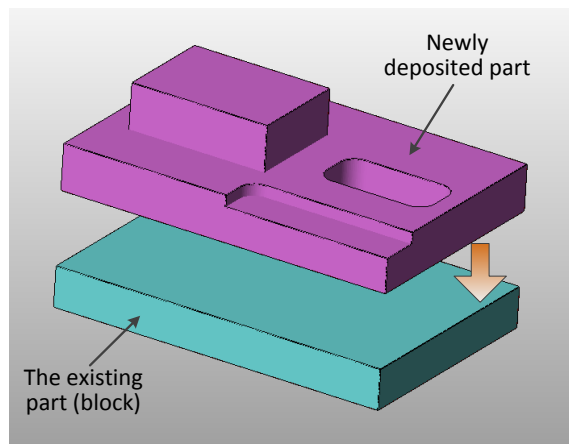
Figure 7.9 – Further manufacture a block

(iii) $L_e < L$, $W_e < W$ and $H_e < H$

This scenario is similar to other relevant scenarios which will be introduced in proceeding sections.

7.4.4.2 *Existing part with a boss*

Figure 7.10 shows an existing part with a boss. In this scenario, the existing boss is located in the centre of the existing part on the horizontal plane. In order to focus on the scenario of having a boss, the total length and width of the existing part (L_e and W_b) are assumed to be equivalent to the total length and width of the final part (L and W), respectively. In addition, the final part is higher than the existing part (i.e. $H > H_e$).

Thus, the local constraints are: the length, width and height of the boss (L_b, W_b and H_b), and the position of the boss (PL and PW).
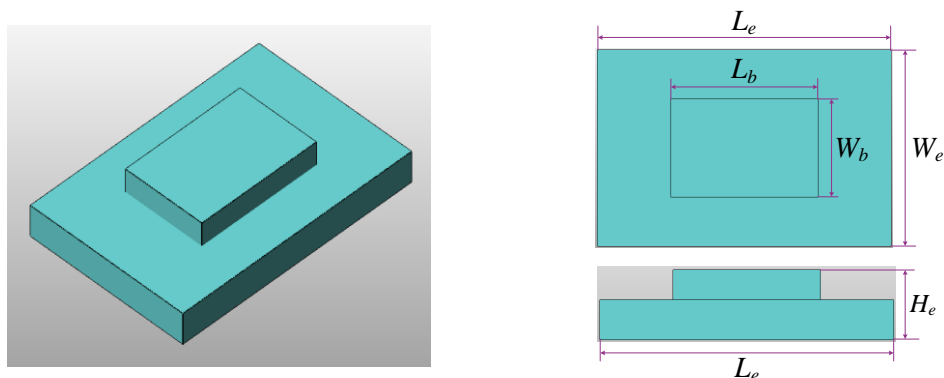
Figure 7.10 – An existing part with a boss

(i)   The universal manufacturing strategy ②

This strategy can be used to remove the boss. By doing so, the existing part becomes a rectangular block as shown in Figure 7.9. Subsequently, more material will be added until the near-net shape of the final part P is generated. A machining operation will then be conducted to obtain the desired dimensional accuracy and surface quality. It is noted that, in order to reduce machining times whilst obtaining a surface with acceptable surface roughness (i.e. Ra < 12 μm) to act as a build platform for further depositing material, the machining parameters can be determined by referring to Table 5.5. Feed 3000mm/min, speed 4000rpm and DoC 2mm are recommended for removing the existing boss.

(ii)   The universal manufacturing strategy ⑧

As illustrated in Figure 7.11, a mating part (black) is first produced, consisting of final features and a female feature (i.e. a pocket) against the male feature (i.e. the boss) on the existing part. The existing part and the mating part are then assembled followed by a finishing operation. However, given that assembly operations have to be carried out, this strategy is not recommended unless there are no other methods to process the existing part.
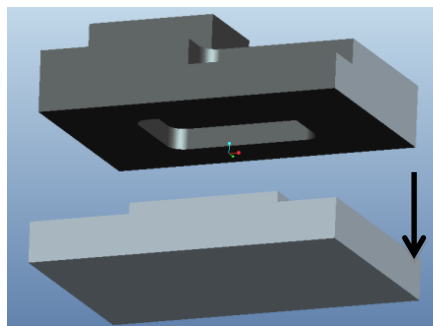
Figure 7.11 – Assemble a mating feature and an existing part

(iii) $\dfrac{L_e - L_b}{2} \geq 9$ mm and $\dfrac{W_e - W_b}{2} \geq 15$ mm, $D_f > D_r$

The material (newly deposited part_1) is added around the boss until the height of the newly deposited material reaches the same height of the existing boss, as shown in Figure 7.12(a). More material (i.e. newly deposited part_2 and 3) will be continuously added, producing the near-net shape of the final part (see Figure 7.12(b)). This is manufacturing strategy ⑦. Figure 7.12(c) shows a real existing part with a boss; the combined existing part and newly deposited part_1 is shown in Figure 7.12(d); in Figure 7.12(e), the newly

deposited part_2 is being printed. Figure 7.12(f) shows the first recovery layer printed on part_1 and the finished combined existing part, part_1 and 2 is shown in Figure 7.12(g). As the top surface of the combined existing part, part_1 and 2 is flat, part_3 can then be built.
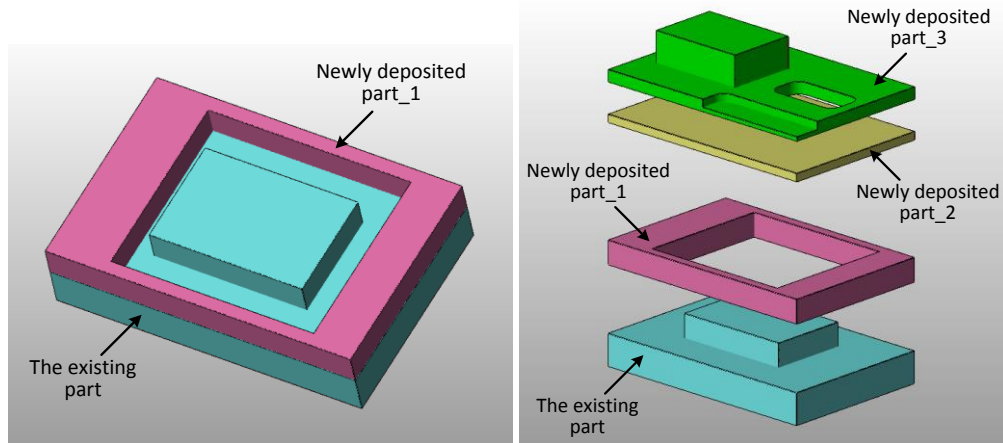
(a) add part_1

(b) overview of adding new parts
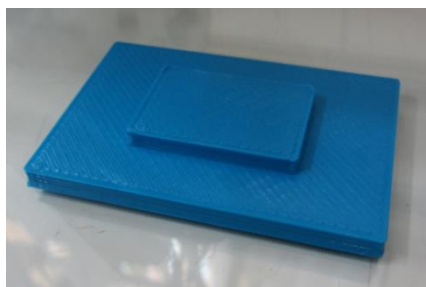
(c) the existing part

(d) the combined existing part&part_1
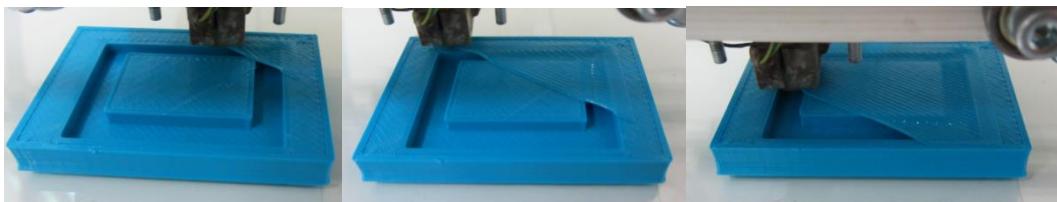
(e) newly deposited part_2 is being printed
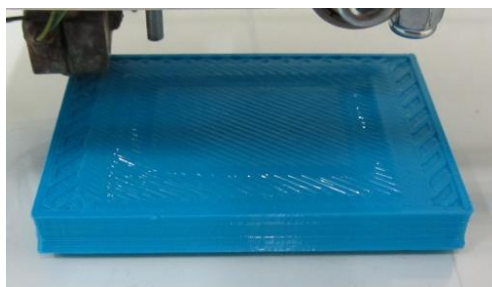
(f) a few layers of part_2 has been printed   (g) the combined existing part&part_1&2

Figure 7.12 – Manufacturing strategy (7) for manufacturing an existing part with a boss

The local constraint relationships (i.e. $\dfrac{L_e - L_b}{2} \geq 9$ mm and $\dfrac{W_e - W_b}{2} \geq 15$ mm, $D_f > D_r$) are used to determine whether the newly deposited part_1 can be produced by taking the potential deposition nozzle collisions into consideration (see Figures 6.11 and 6.12). The newly deposited part_2 is the recovery layers since the iAtractive process is actually producing bridges while part_2 is being printed. In this example, the step on newly deposited part_3 can be fully generated, whereas the pocket cannot be fully produced. The depth of the pocket ($D_p = 6$mm) is deeper than the depth of the step ($D_s = 2$mm). However, the print quality has not come back to normal when the bottom surface of the pocket is required to be created. In here, 'normal print quality' refers to the print quality illustrated in Figure 5.22.

Figure 7.13 illustrates the relationship between the recovery layers and the most adjacent final feature. The pocket in this example is the most adjacent final feature since its bottom surface is the surface closest to the existing boss in terms of vertical distance. Given that the recovery layers are of poor quality (porous), high surface quality (Ra < 1 μm) cannot be obtained even though the recovery layers are finish machined. Therefore, manufacturing strategy ⑦ is only feasible when $D_f > D_r$. Alternatively, the existing part can be face milled with a certain depth of material removed in order to get D_f greater than D_r.
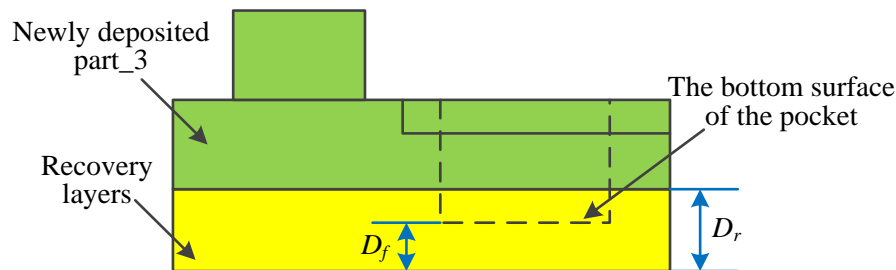
Figure 7.13 – Recovery layers and the most adjacent final feature

For more general scenarios where the boss is located in a random area on the surface as shown in Figure 7.7(a), the local constrains (i.e. $PL_b\_1 \geq 9$mm, $PL_b\_2 \geq 9$mm, $PW_b\_1 \geq 9$mm, $PW_b\_2 \geq 15$mm, and $D_f > D_r$) should be applied. Figure 7.14 is the top view of the existing part, which shows the positioning dimensions of the boss in the X and Y axes, respectively. In order to deposit material around the boss and avoid nozzle collision, the positioning dimensions of the boss need to meet the requirements of the local constraints.
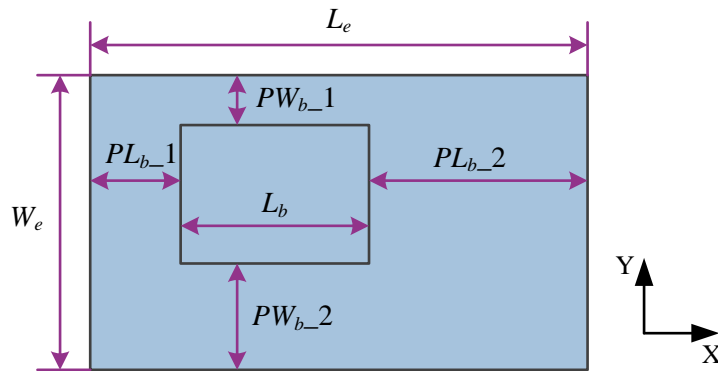
Figure 7.14 – Positioning dimensions of an existing boss

7.4.4.3 Existing part with a pocket

Figure 7.4 shows an existing part with a non-final pocket. In order to focus on the situation of having a pocket, the total length and width of the existing part (L_e and W_e) are assumed to be equivalent to the total length and width of the final part (L and W), respectively. Additionally, the final part is higher than the existing part (i.e. $H > H_e$). Thus, the local constraints are: the length and width of the pocket (L_p and W_p).

(i) $\sqrt{2}W_p \leq 23\text{mm}$ and $D_f > D_r$

The manufacturing strategy that can be used in this scenario has been briefly introduced in section 7.4.1. The material can be directly printed onto the top surface of the existing part. The deposition nozzle moves across the pocket whilst extruding material. This additive operation is the same as printing a bridge. The reason for requiring $D_f > D_r$ is similar to that of the scenario described in section 7.4.4.2(iii).

(ii) $\sqrt{2}W_p > 23\text{mm}$ and $D_f > D_r$

Manufacturing strategy ⑥ is feasible for this scenario. A boss (the newly deposited part_1) is first added in a layer by layer manner inside the pocket, as shown in Figure 7.15(a). The height of the boss should be the same as the depth of the pocket. The length and width of the boss are dependent on the size of the pocket as well as the configuration of the heated block as shown in Figure 6.11. The priority is to ensure the deposition nozzle does not hit the existing pocket. Further material is deposited as depicted in Figure 7.15(b). The newly deposited part_2 is the recovery layers. The existing part with a pocket, and the combined

existing part & part_1 are shown in Figure 7.15(c) and Figure 7.15(d), respectively. The combined existing part & part_1 & 2 is shown in Figure 7.15(e). Subsequently, part_3 was continuously built on the combined existing part & part_1 & 2.
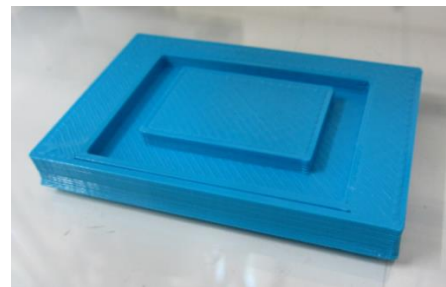

(a) add part_1   (b) overview of adding new parts

(c) the existing part   (d) the combined existing part & part_1   (e) the combined existing part & part_1 & 2
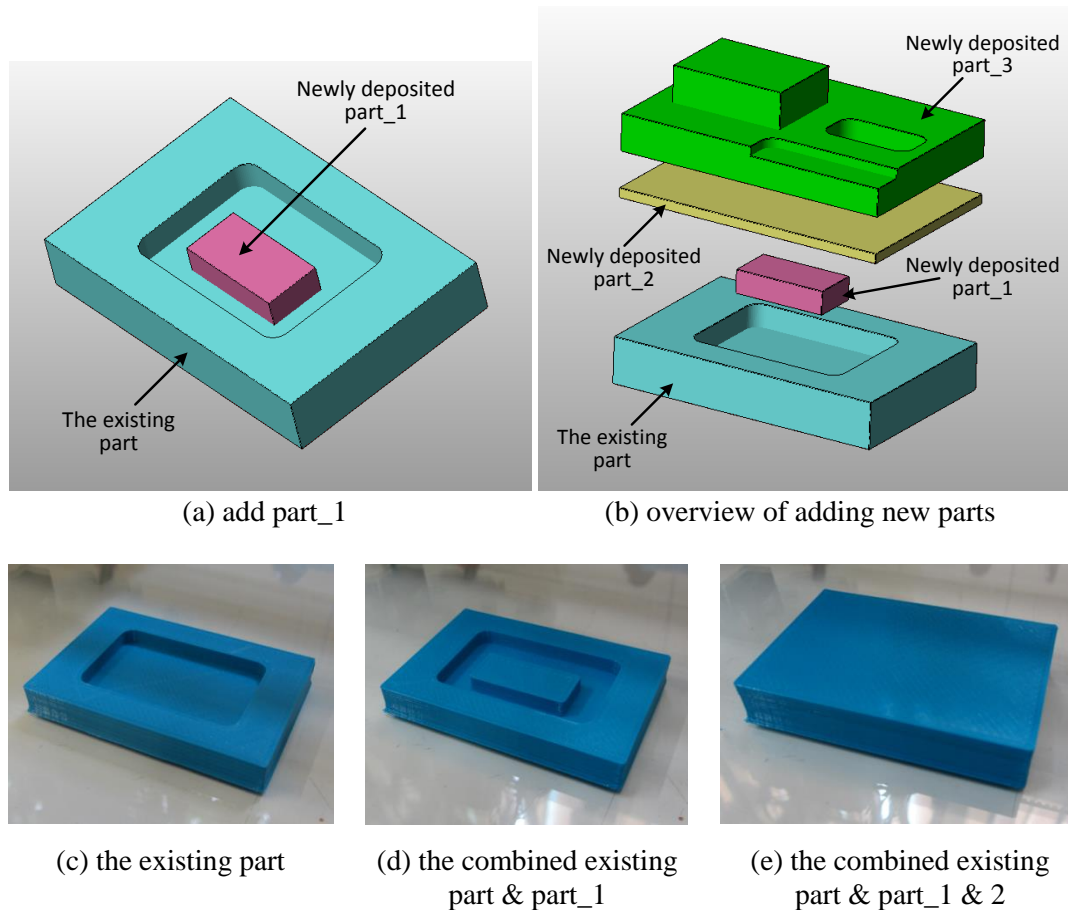
Figure 7.15 – Manufacturing strategy (6) for manufacturing an existing part with a pocket

7.4.4.4 Existing part with a through hole

It is assumed that the existing part's length and width (L_e and W_e) are no shorter than the final part's length and width (L and W), i.e. $L_e \geq L$ and $W_e \geq W$. The final part is higher than the existing part, i.e. $H > H_e$. The existing part is shown in Figure 7.16. The local constraints are the diameter of the hole (ϕ) and the position of the hole (PL_h and PW_h). The positioning dimensions of the hole are illustrated in Figure 7.17, which is the top view of the existing part.
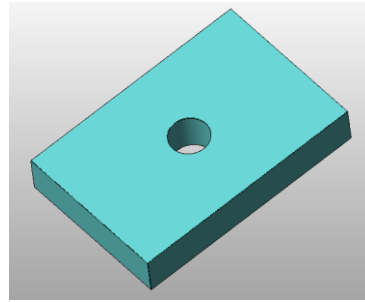
Figure 7.16 – An existing part with a through hole
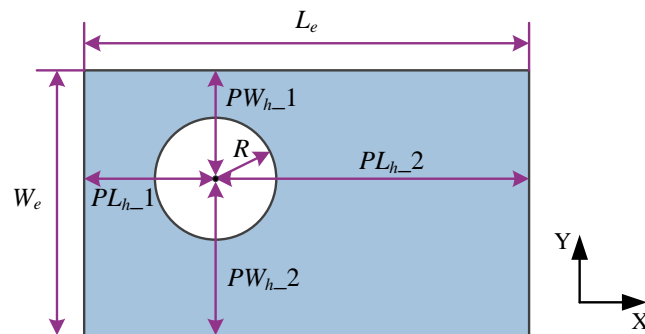
Figure 7.17 – Positioning dimensions of an existing hole

(i) $\phi > 23$mm

In this case, the hole has to be removed first since the bridge cannot be created upon the existing hole. Figure 7.18(a) shows that the grey part is machined off from the existing part. More material is then added onto the machined existing part as illustrated in Figure 7.18(b). By doing so, the near-net shape of the final part is produced. It is noted that the manufacturing strategy ② for the scenario shown in Figure 7.18(b) can be applied to existing blocks with the local constraints ($L_e < L$, $W_e < W$ and $H_e < H$) in section 7.4.4.1(iii).

(a) remove the existing hole   (b) more material is added
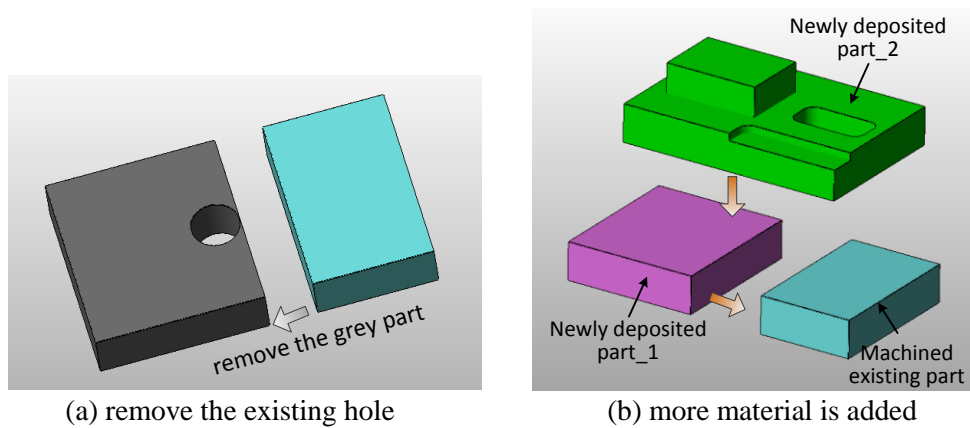
Figure 7.18 – Manufacturing strategy (2) for manufacturing an existing part with a hole

(ii) $\phi \leq 23$mm, $\phi < W < L$ and $D_f > 2D_r$

A hole diameter of less than 23mm indicates that the new material can be directly deposited onto the existing part without support. Hence, the material is deposited on both top and bottom faces of the existing part in order to cover the existing hole, as depicted in Figure 7.19, where $L_e = L$, $W_e = W$ and $H_e < H$. The newly deposited part_1 is first added onto the existing part. The thickness of part_1 should be thicker than that of the recovery layers since it will be finished machined. The newly deposited part_2 and 3 are then added onto the other side of the existing part.
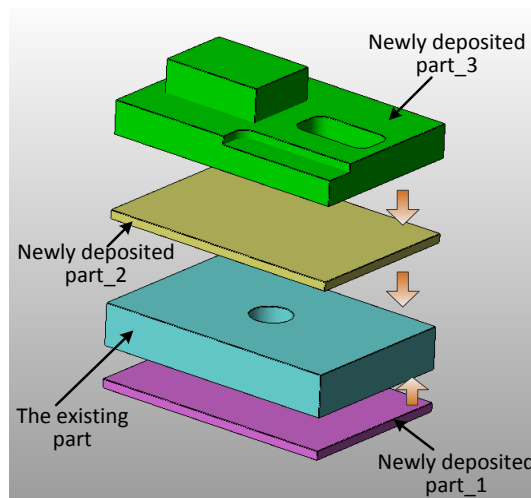
Figure 7.19 – Manufacturing strategy (1) for manufacturing an
existing part with a through hole

Figure 7.20 shows the application of strategy ① in a more general scenario where $L_e < L$, $W_e < W$ and $H_e < H$. In Figure 7.20(b) and (c), the purple dashed lines represent the newly deposited part_1 to be printed. The considerations that should be addressed in positioning of the deposition nozzle to create the newly deposited part_1 are:

•   Firstly, it would be ideal if the newly deposited part_1 can be fully printed on the existing part whilst not covering the existing hole, as illustrated in Figure 7.20(a).

•   Secondly, if the first condition cannot be achieved, the newly deposited part should cover the existing hole, as shown in Figure 7.20(b). The position of the newly deposited part_1 in Figure 7.20(c) is not acceptable and the reason will be expanded in section 7.4.4.4(iii).

- In the above conditions, the existing part is first machined to obtain the length and width that are slightly bigger than those of the final part, i.e. $L_e = L + 2$ and $W_e = W + 2$, unit: mm.

- Finally, for the scenario shown in Figure 7.20(b), the global constraints (i.e. the positions of negative features) have to be considered, ensuring that the existing hole and the final negative features do not overlap (see Figure 7.6). Then, the existing part can be remanufactured using manufacturing strategy ① as illustrated in Figure 7.19.

(a) add part_1 onto the existing part

(b) feasible location of part_1   (c) infeasible location of part_1
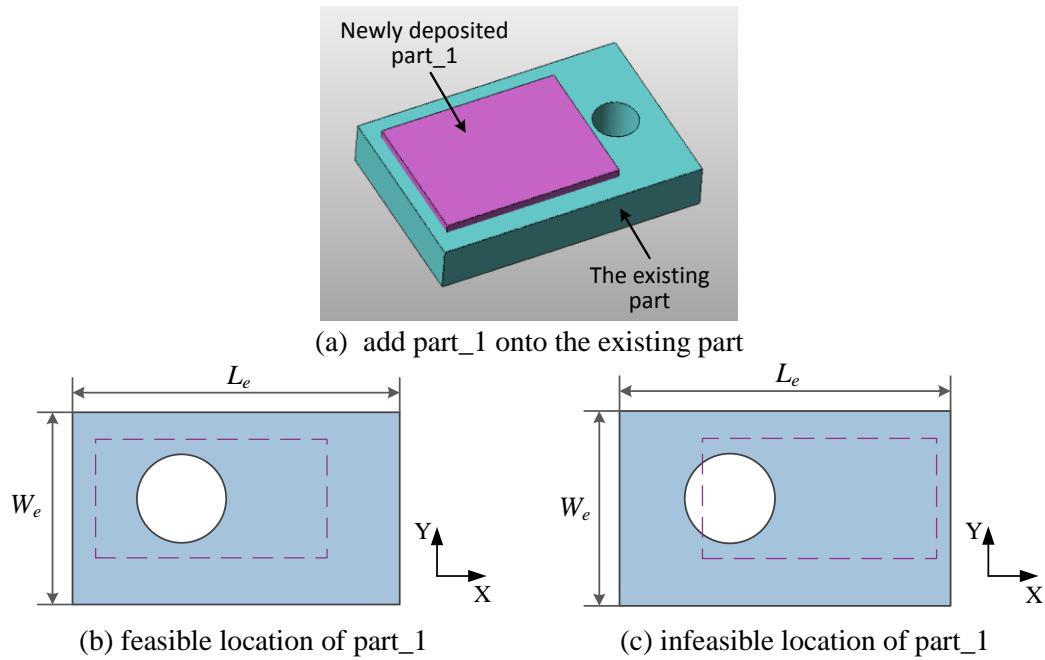
Figure 7.20 – Positioning deposition nozzle for printing the newly deposited part_1

(iii) $L \leq \phi \leq 23mm$, and none of the constraints meets the following relationships:

$$L_e - PL_h\_1 - \frac{1}{2}\phi > L \quad , \quad L_e - PL_h\_2 - \frac{1}{2}\phi > L \quad , \quad W_e - PW_h\_1 - \frac{1}{2}\phi > W \quad \text{and}$$

$$W_e - PW_h\_2 - \frac{1}{2}\phi > W .$$

In this scenario, the lengths and widths of the existing and final parts are shown in Figure 7.21. The red dashed lines represent the total length and width of the final part. No matter where the deposition nozzle is positioned to start depositing new material on the XY plane, the final part P overlaps the existing hole in the Z direction. In this case, the existing hole will appear when finish machining the final part. Therefore, the first operation is to remove the existing hole using strategy ② as demonstrated in Figure 7.18.
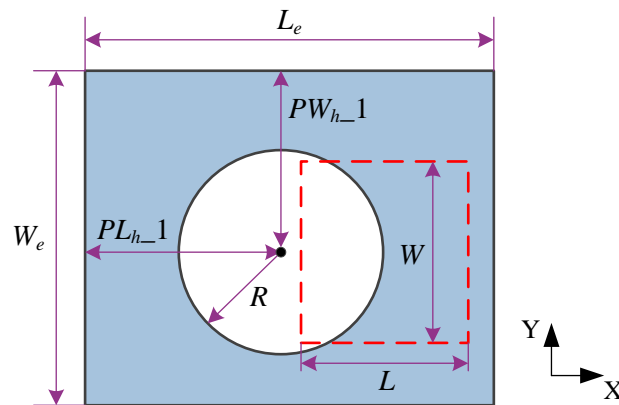
Figure 7.21 – The positions of the existing hole and the final part's length and width

7.4.4.5 Existing part with a blind hole

For a simplified demonstration it is assumed that the existing part's length and width are equivalent to the final part's length and width, respectively, i.e. $L_e = L$ and $W_e = W$. The final part is higher than the existing part, i.e. $H > H_e$. For the constraints and manufacturing strategies specified in the scenarios where $L_e > L$ and $W_e > W$, readers are referred to section 7.4.4.4. A blind hole can be further classified as a blind hole with a flat bottom face and with a sharp bottom face.

(1) A blind hole with a flat bottom face

This type of hole is normally produced using a slot mill cutter. The local constraint is the diameter of the hole (ϕ).

- $\phi \leq 23$mm and $D_f > D_r$. New layers can be directly laid down upon the existing part until the near-net shape of the final part P is obtained (strategy ①). This scenario is similar to the scenario introduced in section 7.4.4.3 (i). If $D_f \leq D_r$, the existing hole will have to be removed (strategy ②), as demonstrated in section 7.4.4.2 (i) and section 7.4.4.4 (i).

- $\phi > 23$mm. This means the gap (the existing hole) is too big to afford a bridge hanging upon it. As the bottom face of the hole is flat, new material can be extruded onto it as long as the deposition nozzle does not collide with the hole. However, this requires further design improvement and a specific tool path generation approach to be conducted as part of the future work, which will be discussed in sections 10.4.3 and 10.4.5.

(2) A blind hole with a sharp bottom face (see Figure 7.22)
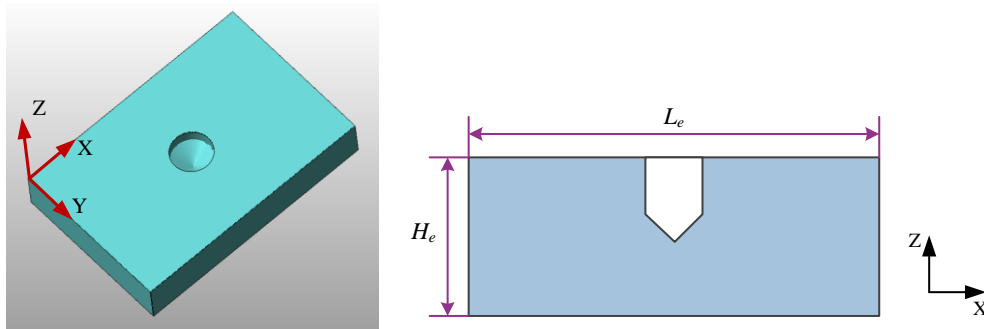
Figure 7.22 – An existing blind hole with a sharp bottom face

This type of holes is normally produced using a drill. The local constraint is the diameter of the hole (ϕ).

- $\phi \leq 23$mm and $D_f > D_r$. The manufacturing strategies used to remanufacture an existing hole ($\phi < 23$mm) with a flat bottom face can be applied to these two scenarios.

- $\phi \leq 23$mm and $D_f \leq D_r$ or $\phi > 23$mm. Restricted by the FFF process capability and in particular current nozzle design, new material cannot be directly deposited on the sharp face. As a result, manufacturing strategy ② is chosen to remove the existing hole and produce a planar face. Removing the hole from the XY plane (as illustrated in section 7.4.4.2 (i)) or from the YZ plane (as illustrated in section 7.4.4.4 (i) and Figure 7.18) depends on the production times.

7.4.4.6 Existing part with a slot

The existing part is shown in Figure 7.23. If the part dimensions are: the existing part's length and width (L_e and W_e) are not shorter than the final part's length and width (L and W), respectively, only the two universal manufacturing strategies (i.e. ② and ⑧) are feasible for further processing the existing part.
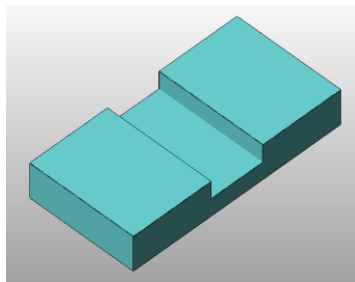
Figure 7.23 – An existing part with a slot

If the part dimensions are: $L > L_e$, $W > W_e$, and $H > H_e$, the local constraints will be the width of the slot (W_s), D_f and D_r. Two scenarios are discussed below:

(i) $\sqrt{2}W_s > 23$mm; or $\sqrt{2}W_s \leq 23$mm and $D_f \leq D_r$ (in the Z axis); or $\sqrt{2}W_s \leq 23$mm and $W_e + 2D_r' < W$ (on the XY plane)

In this scenario, the strategies ② and ⑧ can be used to produce the final part P.

(ii) $\sqrt{2}W_s \leq 23$mm, $D_f > D_r$ (in the Z axis) and $W_e + 2D_r' < W$ (on the XY plane)

The material will be deposited onto the both side faces of the existing part as shown in Figure 7.24(a). The widths of both newly deposited part_1 and 2 (in the Y axis) should be thicker than the recovery layers since they will be subject to finishing operations. In the meantime, for the same reason, the sum of widths of the existing part, part_1 and 2 should not be greater than the final part width (W). Having generated part_1 and 2, part_3 and 4 are then added onto the combined existing part & part_1 & 2. Figure 7.24(b) depicts the four new parts to be added onto the existing part. Part_3 and 4 are actually one newly deposited part. For demonstrating the recovery layers in the Z axis, part_3 and 4 are shown separately.

(a)	(b)
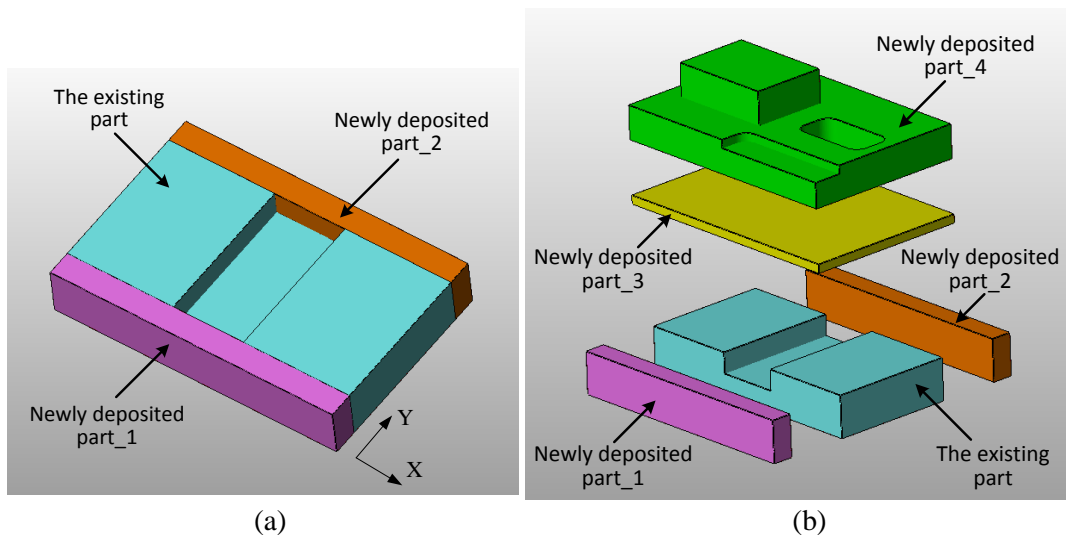
Figure 7.24 – Manufacturing strategy (1) for manufacturing an existing part with a slot

It is worth mentioning that these four new parts cannot be directly added onto the existing part one by one in consecutive operations. The rules in operation sequencing (presented in sections 6.5.2 and 6.5.5), which specify the circumstances where machining operations are

required, are still valid for the remanufacture of existing parts. For the above example in Figure 7.24, part_1 should be finish machined after it is built. Then the other side face of the existing part on which part_2 is about to be built, should also be machined to remove built up part distortions which have occurred while creating part_1. Part_2 requires machining prior to printing part_3.

7.4.4.7 Existing part with a step

For this type of existing part, due to deposition nozzle collisions, the existing step cannot be fully filled to obtain a planar face. As a result, the step has to be removed first. More material will then be added onto the machined existing part (strategy ②). Alternatively, a mating part can be produced to match the existing part geometry (strategy ⑧).

7.4.4.8 Existing part with a feature located on a vertical plane (XZ or YZ plane)

In fact, the manufacturing strategies for existing parts with features located on a vertical plane are similar to the ones presented in the foregoing sections for the existing parts with features on a horizontal plane. This is because the existing parts can be rotated, by which the horizontal planes may become vertical planes and vice versa. An example is given below to demonstrate the available manufacturing strategies for this type of existing parts.

Figure 7.25 shows an existing part with a slot on the vertical plane (i.e. the YZ plane), of which the length (L_e, in the X axis) is shorter than the final part length (L), the width and height (W_e and H_e) are not shorter than the final part width and height (W and H). Thus, the local constraints are the slot width (W_s), D_f and D_r.
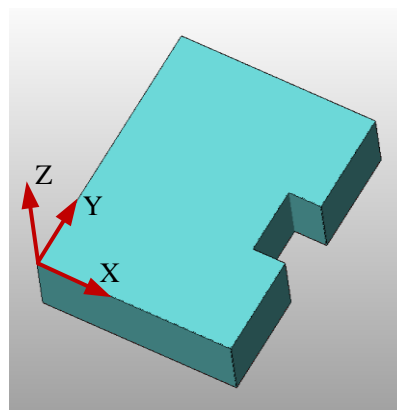
Figure 7.25 – An existing part with a slot on the vertical plane

(i) $\sqrt{2}W_s > 23$mm; or $\sqrt{2}W_s \le 23$mm and $D_f \le D_r$.

The relationship (i.e. $\sqrt{2}W_s > 23$mm) implies that the FFF process cannot directly deposit material onto the top of the slot on the YZ plane. The relationship (i.e. $\sqrt{2}W_s \le 23$mm) demonstrates that the material can be deposited on the XY plane without the need for support. The relationship (i.e. $D_f \le D_r$) indicates that, even though the material can be deposited on the YZ and XY planes, the porous structure is still widely distributed in the most adjacent final feature. As a result, the slot has to be removed first, which is similar to the scenario illustrated in Figure 7.18. Alternatively, a mating feature can be manufactured to match the existing part and more material is subsequently added, as shown in Figure 7.26.
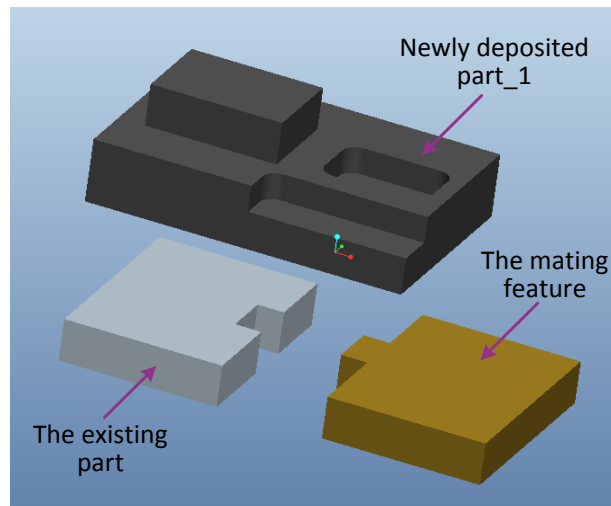
Figure 7.26 – Manufacturing strategy (8) for manufacturing an existing part with a slot

(ii) $\sqrt{2}W_s \le 23$mm and $D_f > D_r$.

Manufacturing strategy (1) can be applied to this scenario. The newly deposited part_1 is built onto the top of the slot on the YZ plane (as shown in Figure 7.27) followed by a machining operation. The subsequent operations can be referred to the example in section 7.4.4.4(ii) and Figure 7.19.
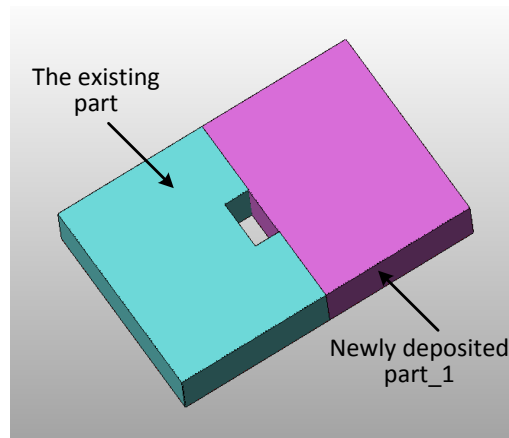
Figure 7.27 – Build a part onto the top of a slot

7.4.5   Existing part with multiple separate non-final features

This type of existing part is the combination of the separate non-final features. Therefore, the local constraints for existing parts with multiple separate non-final features are similar to the local constraints for the existing parts with single non-final features. The available manufacturing strategies are the combinations of the individual strategies.

The existing part with a separate boss and a pocket in Figure 7.2 is used as an example. Assume that $L_e > L$, $W_e > W$, $H_e < H$. The local constraints for the boss are: PL_b_1, PL_b_2, PW_b_1, PW_b_2, D_{f_b} and D_{r_b}; the local constraints for the pocket are: W_p, D_{f_p} and D_{r_p}. D_{f_b} is the vertical distance between the existing boss to its adjacent final feature. In this example, the adjacent final feature is the final pocket on the final part P. D_{f_p} is the vertical distance between the existing pocket to the final pocket on the final part P. D_{r_b} and D_{r_p} are the total thickness of all the recovery layers for the existing boss and pocket, respectively, which will be explained in the proceeding section.

As strategy ⑦ is only feasible when $PL_b\_1 \geq 9mm$, $PL_b\_2 \geq 9mm$, $PW_b\_1 \geq 9mm$, $PW_b\_2 \geq 15mm$ and $D_{f\_b} > D_{r\_b}$, the local constraints which do not meet the above relationships will lead to strategy ⑦ becoming invalid. If all the constraints for the boss meet the relationships, it is denoted as '√' in Table 7.3. Otherwise, it is denoted as '×'. Similarly, strategy ⑥ can only applied to the existing part if $\sqrt{2}W_p > 23mm$ and $D_{f\_p} > D_{r\_p}$. The available manufacturing strategies for this existing part are listed in Table 7.3, which classifies a number of scenarios based on the local constraints. In this table, the symbol '+' (e.g. ⑥+⑦) represents that both manufacturing strategies have to be used in sequence.

Table 7.3 – Available manufacturing strategies for an existing part with a separate boss and a pocket

	whether or not the local constraints meet the relationships			
Boss	√	√	×	×
Pocket	√	×	√	×
Manufacturing strategy	⑥$_p$+⑦$_b$, ②, ⑧,	①$_p$+⑦$_b$, ②, ⑧	②$_b$+⑥$_p$, ②, ⑧,	②, ⑧,
Example	see Figure 7.28, Figure 7.9, Figure 7.11	see Figure 7.12, Figure 7.9, Figure 7.11	see Figure 7.15, Figure 7.9, Figure 7.11	see Figure 7.9, Figure 7.11

In addition, in Table 7.3, ⑥$_p$ represents that strategy ⑥ is only applied to the existing pocket, and ⑦$_b$ represents that material is added outside the existing boss. If there is no subscript, it means that the manufacturing strategies are applied to the entire existing part.

For an existing part in Table 7.3 where the combination of the strategies ⑥$_p$ + ⑦$_b$ is feasible, it can be manufactured in the way depicted in Figure 7.28. As $\sqrt{2}W_p > 23$mm, the newly deposited part_1 can be created inside the pocket (⑥$_p$). The newly deposited part_2 will then be added around the boss (⑦$_b$), as shown in Figure 7.28(a). Subsequently, part_3 and 4 are built on part_2 to create the near-net shape of the final part P. The entire deposition operations are demonstrated in Figure 7.28(b). In here, D_{r_b} is the total thickness of the recovery layers printed on the newly deposited part_2. Similarly, D_{r_p} is the total thickness of the recovery layers printed on the newly deposited part_1.

It should be noted that, for an existing part with a single non-final pocket, the position of the pocket does not affect the selection of manufacturing strategies when $L_e = L$ and $W_e = W$. However, the pocket's positions on the existing part with multiple separate non-final features determine the available strategies to be used. More generally, the selection of manufacturing strategies for existing parts with multiple separate non-final positive and negative features is also dependent on the positions of non-final negative features.

(a)   (b)
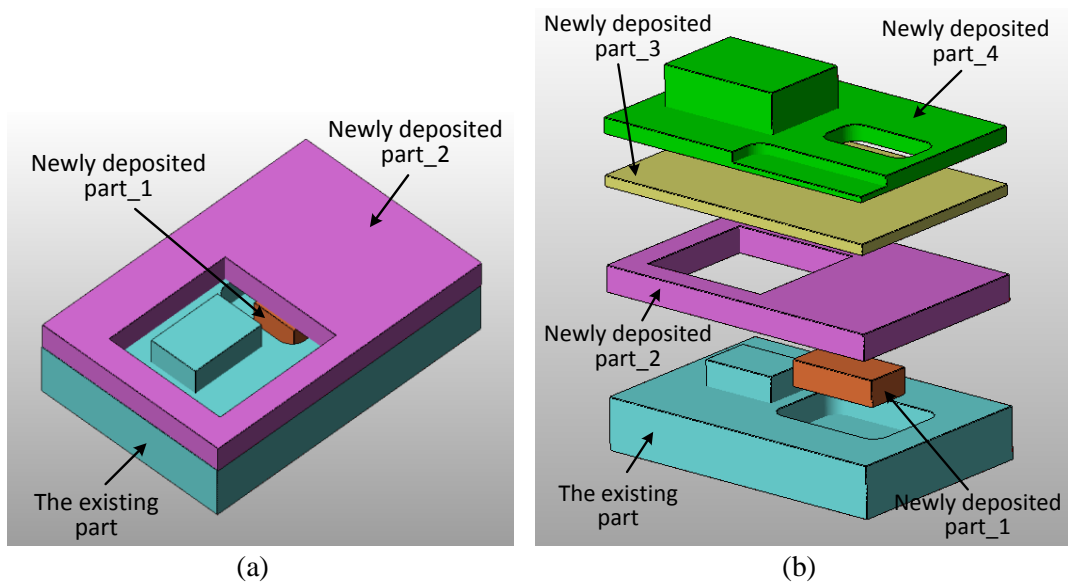
Figure 7.28 – Manufacturing strategy (6) and (7) for further manufacturing an existing part with a separate boss and a pocket

For example, a non-final pocket (e.g. L_p = 50mm and W_p = 10mm) is located in a position shown in Figure 7.29(a). Due to deposition nozzle collision, no material can be deposited inside the pocket. The newly deposited part_1 is built as shown in Figure 7.29(b). However, one of its edges has to be produced without support, as highlighted in Figure 7.29(c). As a result, print failure is highly likely to occur, and therefore strategy ⑦ cannot be applied to this existing part. It is advisable to remove the boss (strategy ②) followed by depositing material onto the machined surface whilst not filling in the pocket (strategy ①).

(a) the existing part with a separate boss and a pocket

(b) add part_1

(c) top view of the combined existing part & part_1
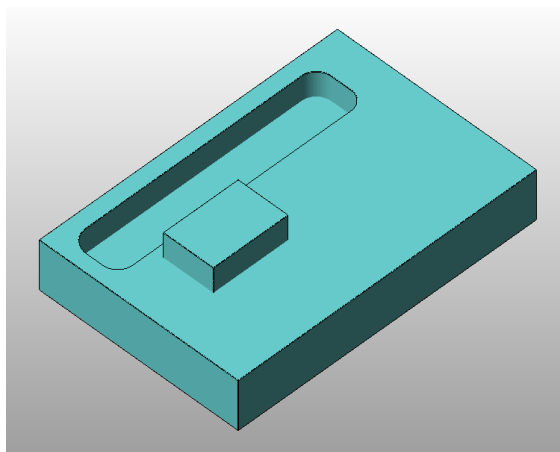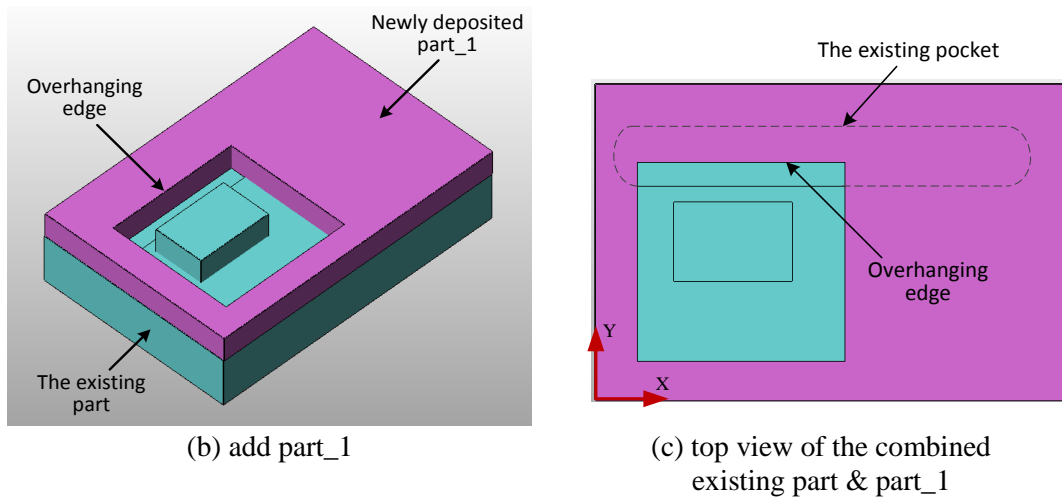
Figure 7.29 – The position of a pocket on an existing part

In addition, the manufacturing strategies for existing parts with single non-final features can also be used in the scenarios, in which existing parts with separate non-final features on different planes are required to be remanufactured. In Figure 7.30, there are two non-final features i.e. a boss and a slot located on a horizontal and a vertical plane (i.e. the XY and YZ planes), respectively. A possible method to transform this existing part into the final part P is to use strategy ① to directly add material onto the top of the slot on the YZ plane, which is similar to the existing part shown in Figure 7.27. Subsequently, strategy ⑦ is applied to building a pocket around the boss, which is similar to the existing part shown in Figure 7.12 and Figure 7.28. More material will then be deposited onto the bottom surface of the existing part (this bottom surface is opposite to the horizontal surface on which the existing boss is located). This is similar to the newly deposited part_1 added onto the existing part shown in Figure 7.19. It is noted that strategy ① for existing parts with holes is available when $\phi \leq 23$mm and $D_{f\_h} > 2D_{r\_h}$. However, for the existing part in this example, strategy ① is valid when $\phi \leq 23$mm and $D_{f\_s} > D_{r\_s}$.
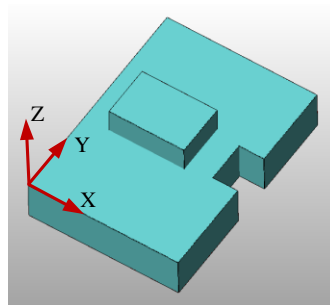
Figure 7.30 – An existing part with a boss and a slot located on different planes

From the two examples illustrated above, it can be identified that the methods to further manufacture this type of existing part are to utilise the manufacturing strategies for existing parts with single non-final features. Thus, the details of the available manufacturing strategies for this type of existing parts will not be elaborated on and they are summarised in Table 7.4. Since there are no other ways to deal with existing steps except removing them, this table only includes the existing part with combinations of boss, pocket, slot and hole. The examples of using these manufacturing strategies can be found from Figure 7.9 to Figure 7.28.

As stated in section 7.4.3, strategies ② and ⑧ are universal manufacturing strategies. As a result, they can be applied to every type of existing part in Table 7.4. A typical example of using strategy ⑧ can be found in Figure 7.31, where an existing part (red) with a non-final boss and four holes is given. A mating part (white) was produced, of which the features match the existing boss and holes. Thus, the existing and mating parts can be assembled and then finish machined.
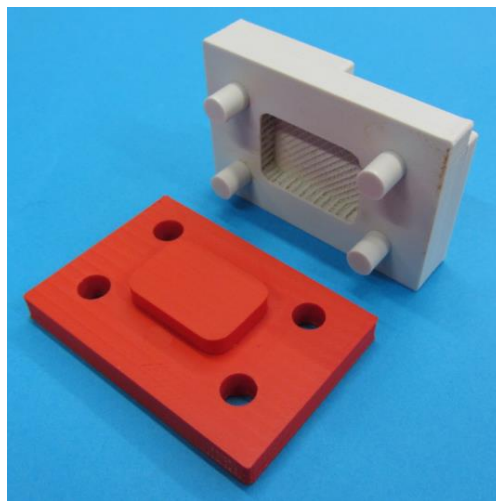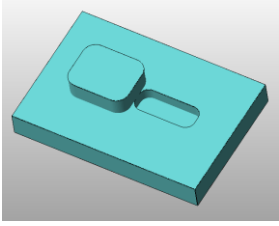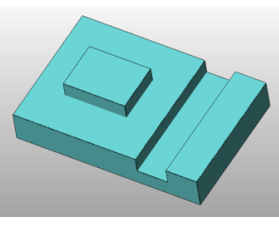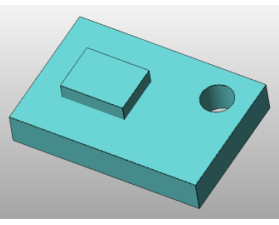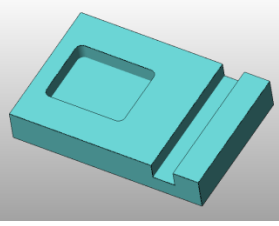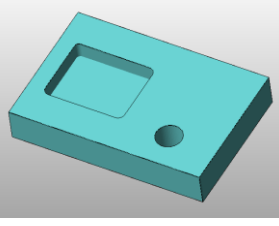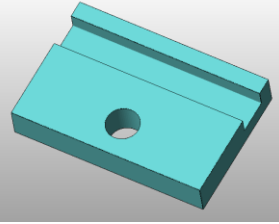
Figure 7.31 – An existing part and a mating part

7.4.6 Existing part with interacting non-final features

This section describes manufacturing strategies ③ and ④, which can be used to transform existing parts with interacting non-final features into final parts.

Table 7.4 – Manufacturing strategies for further manufacturing existing parts with multiple separate non-final features

Features on the existing part	Example part	Local constraint	Available manufacturing strategy
Boss and pocket		For boss: L_b, W_b, PL_b_1, PW_b_1, D_{f_b}, D_{r_b} For pocket: L_p, W_p, PL_p_1, PW_p_1, D_{f_p}, D_{r_p},	②$_b$ + ②$_p$, ⑥$_p$ + ⑦$_b$, ②$_b$ + ⑥$_p$, ⑧,
Boss and slot		For boss: L_b, W_b, PL_b_1, PW_b_1, D_{f_b}, D_{r_b} For slot: L_e, W_e, W_s, D_{f_s}, D_{r_s}, PL_s_1, PW_s_1	②$_b$ + ②$_s$, ②$_b$ + ①$_s$, ①$_s$ + ⑦$_b$, ⑧
Boss and hole		For boss: L_b, W_b, PL_b_1, PW_b_1, D_{f_b}, D_{r_b} For hole: ϕ, PL_h_1, PW_h_1, D_{f_h}, D_{r_h}	①$_h$ + ⑦$_b$, ②$_b$ + ①$_h$, ②$_h$ + ⑦$_b$, ②$_b$ + ②$_h$, ⑧
Pocket and slot		For pocket: W_e, W_s, D_{f_p}, D_{r_p} For slot: L_e, W_e, W_s, D_{f_s}, D_{r_s}	⑥$_p$ + ①$_s$, ②$_p$ + ②$_s$, ②$_p$ + ①$_s$, ②$_s$ + ⑥$_p$, ⑧
Pocket and hole		For pocket: W_e, W_s, D_{f_p}, D_{r_p} For hole: ϕ, D_{f_h}, D_{r_h}	①$_h$ + ⑥$_p$, ②$_p$ + ①$_h$, ②$_h$ + ⑥$_p$, ②$_p$ + ②$_h$, ⑧
Slot and hole		For slot: L_e, W_e, W_s, D_{f_s}, D_{r_s} For hole: ϕ, D_{f_h}, D_{r_h}	②$_s$ + ①$_h$, ①$_s$ + ①$_h$, ②$_h$ + ①$_s$, ②$_s$ + ②$_h$, ⑧

Features that interact introduce more local constraints to be taken into consideration. For example, the pocket depth is a constraint, which does not have to be considered when there are only separate non-final features on the existing part. Moreover, there are a large number of combinations of non-final features in terms of feature dimensions and quantities. As a result, more manufacturing strategies are potentially available to deal with these existing parts, and further investigations are needed, which will be presented in sections 9.7 and 10.4.3. In addition, advances in the FFF process, in particular nozzle designs will also contribute to the development of new manufacturing strategies. Therefore, in this section, only existing parts that can be manufactured by using manufacturing ③ and ④, or the combinations of strategies in Table 7.1 are discussed.

7.4.6.1 Interacting positive and negative features

An existing part with an interacting boss and pocket is shown Figure 7.3(b). Assume that $L_e > L$, $W_e > W$, $H_e < H$. The local constraints for the boss are: H_b, PL_b_1, PL_b_2, PW_b_1, PW_b_2, D_{f_b} and D_{r_b}; the local constraints for the pocket are: L_p, W_p, D_p, D_{f_p} and D_{r_p}. To avoid repetitive discussion, it is considered that $D_{f\_b} > D_{r\_b}$ and $D_{f\_p} > D_{r\_p}$.

(i)   Constraints do not meet the relationships: $PL_b\_1 \geq 9$mm, $PL_b\_2 \geq 9$mm, $PW_b\_1 \geq 9$mm, $PW_b\_2 \geq 15$mm

The manufacturing strategy ⑦ is not applicable in this scenario because the edges of the existing boss are close to the edges of the existing part leading to deposition nozzle collisions if attempting to deposit material around the existing boss. Thus, the existing boss has to be removed (using strategy ③). After removing the boss, the existing part becomes a rectangular block or a rectangular block with a pocket, depending on the depth of the pocket (D_p).

*   If $D_p > H_b$, the machined existing part will be a rectangular block with a pocket, which is similar to the part shown in Figure 7.4. The new pocket depth (D_p') will be $D_p' = D_p - H_b$. According to the criteria stated in section 7.4.4.3(i) and (ii), it can be determined whether to add material inside the pocket (strategy ⑥) or directly add material onto the top surface of the machined existing part whilst not filling in the pocket (strategy ①).

- If $D_p \leq H_b$, after machining the boss, the existing part will become a rectangular block. The strategy ① can be applied as illustrated in Figure 7.9, by which the near-net shape of the final part P is obtained.

(ii) Constraints meet the relationships: $PL_b\_1 \geq 9$mm, $PL_b\_2 \geq 9$mm, $PW_b\_1 \geq 9$mm, $PW_b\_2 \geq 15$mm

This indicates the material can be deposited around the existing boss (strategy ⑦). This is similar to the scenario in section 7.4.4.2 and Figure 7.12. If the pocket size meets the local constraints relationship i.e. $\sqrt{2}W_p > 23$mm, strategy ⑥ can be used to deposit a boss inside the existing pocket, as depicted in Figure 7.32 below.

Figure 7.32(a) and (b) illustrates the use of combining strategy ⑦ and ⑥ to remanufacture an existing part. The newly deposited part_1 and 2 are successively added outside the boss and inside the pocket, respectively. It does not matter which part is created first since the production times and the following operation sequences are identical. In other words, the order of strategy ⑦ and ⑥ can be interchanged. The newly deposited parts_3 and 4 are built until the approximate geometry of the final part P is generated. Figure 7.32(c), (d), (e) and (f) provide a real example. An existing part with an interacting boss and a pocket is shown in Figure 7.32(c). Part_1 and 2 were built on the existing part as shown in Figure 7.32(d). In Figure 7.32(e), the deposition of the 4th layer of part_3 has been completed. As material was continuously deposited, the near-net shape of the final part P was obtained (see Figure 7.32(f)). In addition, if $\sqrt{2}W_p \leq 23$mm, part_2 will not have to be produced since the pocket is small enough to allow the features to be directly created without support.

7.4.6.2 Interacting negative and positive features

An example of existing parts with interacting negative and positive features can be found in Figure 7.3(a), which shows a boss that is included inside an existing pocket. The position of the existing pocket is described by the four parameters (i.e. PL_p_1, PL_p_2, PW_p_1 and PW_p_2). The description of these four parameters is similar to that of the position of an existing boss, and readers can be referred to Figure 7.14.

(a) add part_1 and 2

(b) overview of adding new parts

(c) the existing part

(d) the combined existing part & part_1 & 2

(e) a few layers of part_3
has been deposited

(f) the near-net shape of
the final part P
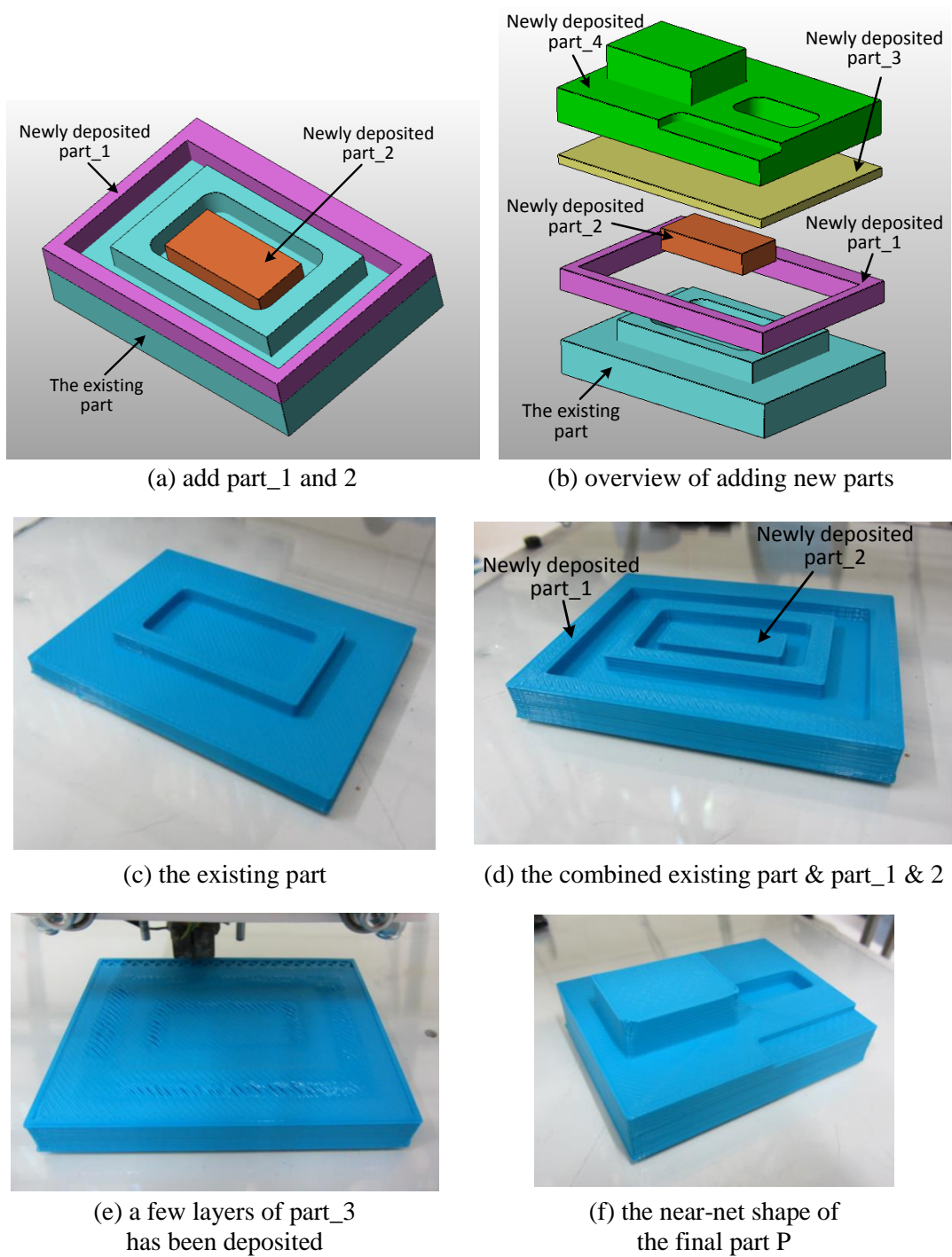
Figure 7.32 – Manufacturing strategy (7) and (6) for further manufacturing an existing part
with an interacting boss and a pocket

It is assumed that the pocket depth is equivalent to the boss height, i.e. $H_b = D_p$. Other assumptions are referred to in section 7.4.6.1.

(i) $\sqrt{(PL_b\_1 - PL_p\_1)^2 + (PW_b\_1 - PW_p\_1)^2} > 23\,\text{mm}$ or

$\sqrt{(PL_b\_2 - PL_p\_2)^2 + (PW_b\_2 - PW_p\_2)^2} > 23\,\text{mm}$

In this scenario, the existing boss is not big enough for the FFF process to produce a bridge that crosses the pocket and the boss. As a result, the original existing boss has to be removed (strategy ④, see Figure 7.33(a) and (b)) and a new boss will then be added inside the pocket (strategy ⑥, see Figure 7.33(c) and (d)). Subsequently, more material will be deposited, which is similar to the scenario depicted in Figure 7.15(b).

(a) the existing part   (b) remove the existing boss

(c) add a new boss   (d) a new boss has been deposited
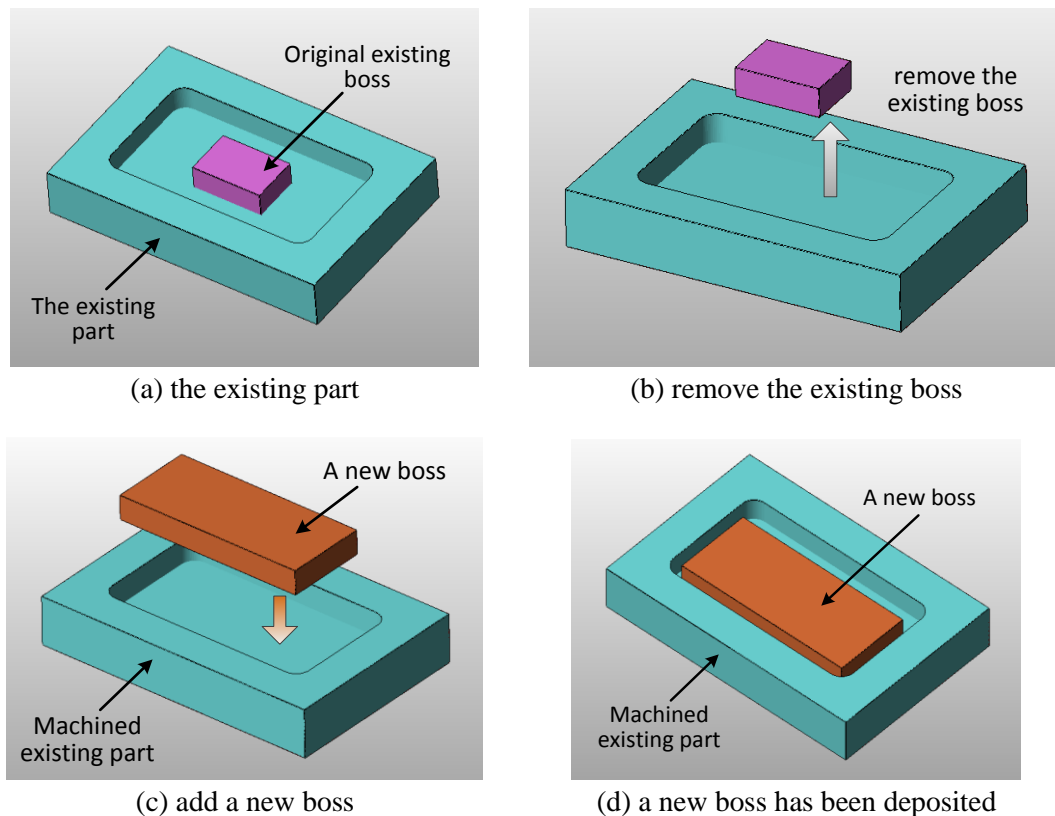
Figure 7.33 – Manufacturing strategy (4) and (6) for further manufacturing an existing part with an interacting pocket and a boss

(ii) $\sqrt{(PL_b\_1 - PL_p\_1)^2 + (PW_b\_1 - PW_p\_1)^2} < 23\,\text{mm}$ and

$\sqrt{(PL_b\_2 - PL_p\_2)^2 + (PW_b\_2 - PW_p\_2)^2} < 23\,\text{mm}$

This means the distance between each two side faces of the existing boss and pocket does not exceed the longest bridge length that can be produced. As a result, material is directly added onto the top surface of the existing part, as illustrated in Figure 7.15(b) (strategy ①).

For the scenario where $H_b > D_p$ or $H_b < D_p$, according to the positions of the existing boss and pocket discussed above, available manufacturing strategies can be found in Figure 7.35.

It is noted that there are other types of interacting features, which are:

- Existing parts with interacting negative features, e.g. an interacting pocket and a hole.
- Existing parts with interacting positive features, e.g. multiple interacting bosses.
- Existing parts with interacting features and individual features, e.g. an existing part with an interacting pocket and (a boss and a hole) in Figure 7.3(c).

7.4.7 Existing part with final features

It is assumed that the final features on the existing parts in this section are out of tolerance. If they are in the desired tolerance, no action is needed. This type of existing part is also classified into three groups, i.e. existing parts with final positive features; with final negative features; and with combination of final positive and negative features. The manufacturing strategies for the first two groups can be directly applied to existing parts with both final positive and negative features.

7.4.7.1 Existing part with final positive features

The strategies ② and ⑤ can be used to deal with the scenarios where the existing parts contain a number of final bosses. Assume that the height of the existing boss is equivalent to its nominal height. Referring to Figure 7.14, the nominal positioning dimensions of a boss in the X and Y axes are denoted as $PL_b\_1\_n$, $PL_b\_2\_n$, $PW_b\_1\_n$ and $PW_b\_2\_n$. These nominal dimensions together with the actual dimensions are the local constraints.

(i)   Constraints meet the relationships:

$PL_b\_1\_n \geq PL_b\_1$, $PL_b\_2\_n \geq PL_b\_2$, $PW_b\_1\_n \geq PW_b\_1$, and $PW_b\_2\_n \geq PW_b\_2$.

This scenario is depicted in Figure 7.34(a), which shows an existing part with a final boss (top view). The blue lines represent the actual position of the boss and the red dashed lines represent the nominal position of the boss. In this figure, only one of the positioning dimensions in the X axis (i.e. $PL_b\_1\_n$ and PL_b_1) is shown but the principle can be applied to other positioning dimensional parameters (e.g. $PL_b\_2\_n$ and PL_b_2). Only when all the actual positioning dimensions are smaller than the nominal ones, strategy ⑤ can be employed to directly machine the existing boss to its final dimensions.
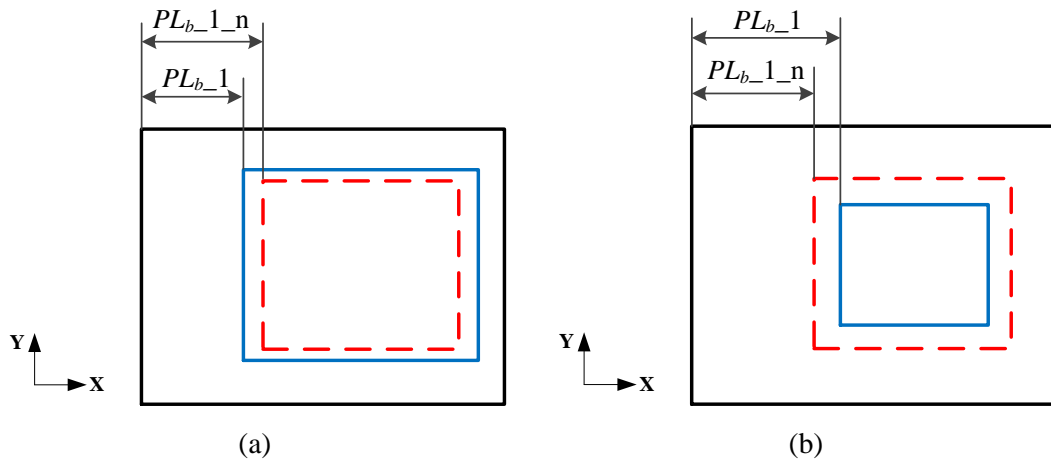
Figure 7.34 – The position of a boss on an existing part (top view)

(ii)   Constraints do not meet the relationships:

$PL_b\_1\_n \geq PL_b\_1$, $PL_b\_2\_n \geq PL_b\_2$, $PW_b\_1\_n \geq PW_b\_1$, and $PW_b\_2\_n \geq PW_b\_2$.

Figure 7.34(b) shows an example in which all the actual positioning dimensions are smaller than the nominal ones. In fact, the boss has to be removed (strategy ②) as long as one of the actual positioning dimensions is smaller than the nominal one. This is because deposition nozzle collisions will occur when trying to directly add material onto the boss's side faces to increase the boss's size. As a result, the boss has to be first removed followed by an additive operation to create a new boss which will be subsequently finish machined.

7.4.7.2 Existing part with final negative features

The aforementioned strategy ② and ⑤ are also available for existing parts with final negative features. However, the constraints relationships for these two strategies are slightly different to those of existing parts with positive features. The positive features, which are larger than they should be, can be directly machined to their final dimensions, whereas, the negative features which are larger than the nominal sizes cannot be machined.

(i)   Using an existing final pocket as an example, strategy ② can be used if the local constraints do not meet the relationships below:

$PL_{p\_}1\_n \leq PL_{p\_}1, PL_{p\_}2\_n \leq PL_{p\_}2, PW_{p\_}1\_n \leq PW_{p\_}1,$
$PW_{p\_}2\_n \leq PW_{p\_}2, D_p \leq D_{p\_}n$

Referring to Figure 7.34(a), one or more edges of the existing pocket cannot be machined as the pocket is bigger than its designed size. Again, material cannot be added along the pocket's side faces owing to deposition nozzle collisions. As a result, strategy ② is applied, by which the entire existing pocket is taken off and the thickness of the material removed is equivalent to the pocket depth. Thus, a planar face is obtained. The succeeding operations are to print a new pocket as well as other features that were removed together with the existing pocket. For the subsequent operations, readers are referred to section 7.4.4.1(ii) and Figure 7.9.

(ii)   Strategy ⑤ can be applied is all the local constraints meet the relationships below:

$PL_{p\_}1\_n \leq PL_{p\_}1, PL_{p\_}2\_n \leq PL_{p\_}2, PW_{p\_}1\_n \leq PW_{p\_}1,$
$PW_{p\_}2\_n \leq PW_{p\_}2, D_p \leq D_{p\_}n$

The pocket is smaller than the required size, which means it can be directly finish machined to obtain the final dimensions.

For other final negative features, the conditions to which strategy ② can be applied are: the local constraints do not meet the relationships as listed in Table 7.5 below. By contrast, strategy ⑤ can be used when all the local constraints meet the relationships.

Table 7.5 – The local constraints relationships for using strategy (2) and (5) for existing parts with final negative features

Feature	Local constraint relationship
Slot	$PL_s\_1\_n \leq PL_s\_1$, $PL_s\_2\_n \leq PL_s\_2$, $D_s \leq D_s\_n$, or $PW_s\_1\_n \leq PW_s\_1$, $PW_s\_2\_n \leq PW_s\_2$, $D_s \leq D_s\_n$
Through hole	$\phi\_n > \phi$, the position of the hole centre in the X and Y axes: $PL_h\_n = PL_h$ or $PW_h\_n = PW_h$
Blind hole	$\phi\_n > \phi$, $D_s \leq D_s\_n$, $PL_h\_n = PL_h$ or $PW_h\_n = PW_h$
Step	$PL_{st}\_n \leq PL_{st}$, $PW_{st}\_n \leq PW_{st}$ and $D_{st} \leq D_{st}\_n$
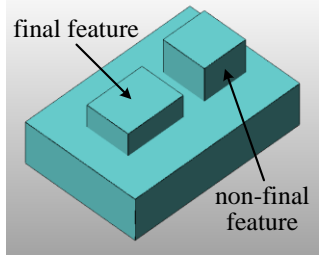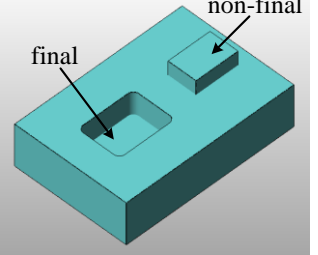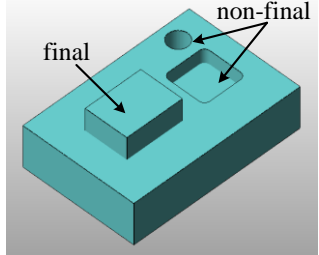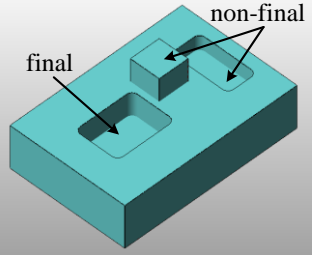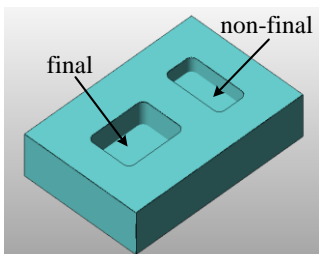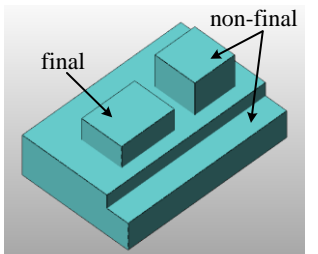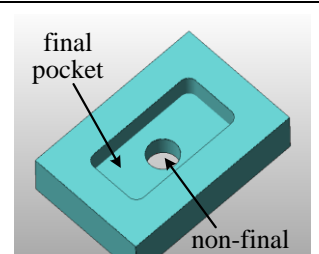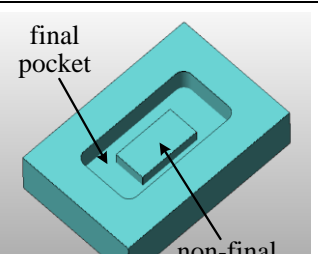
7.4.7.3 Existing part with both final positive and negative features

The local constraints relationships and the corresponding manufacturing strategies introduced in sections 7.4.7.1 and 7.4.7.2 can be applied to this type of existing part, including multiple separate and interacting final features. It should be mentioned that the strategy ② is not recognised as a time-effective strategy since existing features have to be removed and added back again.

7.4.8   Existing part with final and non-final features

Due to the limitations of the FFF process, particularly the deposition nozzle accessibility, non-final features on the existing part have to be removed (i.e. using strategy ②). Again, this strategy is time-ineffective and is not recommended since a large amount of material has to be removed and subsequently added back just because of the existence of the undesired non-final features. Further discussion for these types of existing part is not highly valuable until the iAtractive process integrates other AM techniques whilst improving the extrusion nozzle designs. Therefore, this section only classifies this type of existing part into 7 groups, and aims to provide the basis for the development and discussion of manufacturing strategies that can be potentially employed in the future. These 7 groups of existing parts with final and non-final features are summarised in Table 7.6.

Table 7.6 – The classification of existing parts with final and non-final features

Existing part classification	Example part demonstration	Existing part classification	Example part demonstration
Positive (final) and positive (non-final) features		Negative (final) and positive (non-final) features	
Positive (final) and negative (non-final) features		Negative (final), and positive & negative (non-final) features	
Negative (final) and negative (non-final) features		Positive (final), and positive & negative (non-final) features	
Interacting final negative feature and non-final negative features		Interacting final negative feature and non-final positive features	

7.5 Decision Tree for Material Reuse

A decision tree has been developed, as shown in Figure 7.35. The root is the existing part geometry and dimensions which are obtained from the initial inspection. Each branch carries expressions (i.e. local constraints relationships). The manufacturing strategies that are feasible to further manufacture the existing part are listed at the junction of each terminal branch.

A full representation of the decision tree is not constructed because certain scenarios only increase the complexity of the decision tree, but do not introduce new strategies for producing final parts. In Figure 7.35, it is assumed that $D_f > D_r$ and all the units are in mm.

7.6   Summary

This chapter defined existing parts and features under the background of material reuse. Features are classified into three types, namely, final, semi-final and non-final features. Based on this feature classification as well as prismatic feature types, existing parts are categorised into a number of groups. FDL has been developed, including 8 manufacturing strategies. Global and local constraints were specified and are used to select feasible manufacturing strategies. These strategies interchangeably utilise FFF, CNC machining and inspection to further manufacture the existing parts based on the features and dimensions of the existing and final parts.
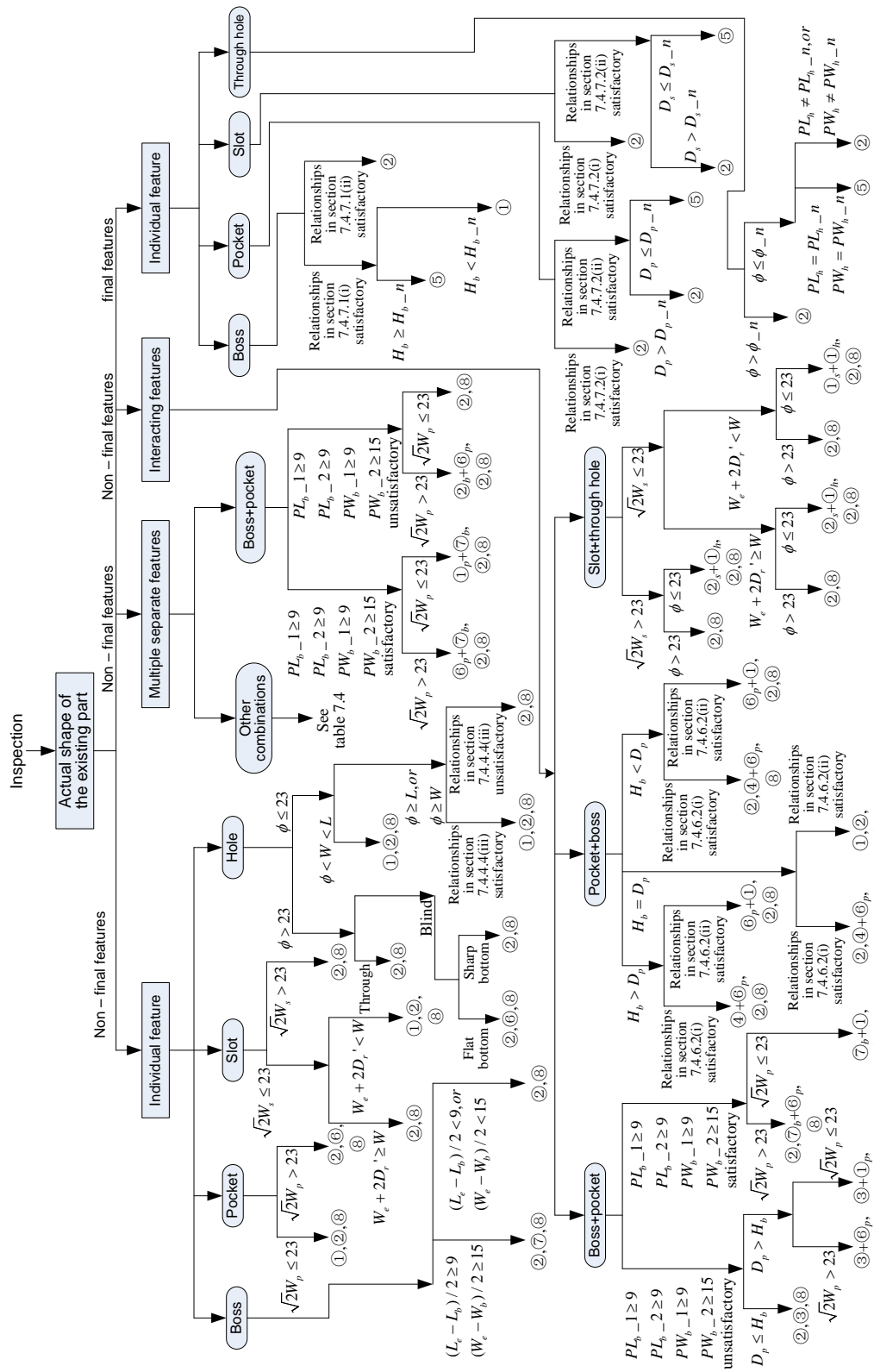
Figure 7.35 – The decision tree for remanufacturing existing parts

8 Evaluation of the hybrid manufacturing process

8.1 Introduction

In order to evaluate the iAtractive process together with GRP^{2}A and FDL, a series of case studies have been developed. This chapter documents a number of case study examples manufactured using the iAtractive process. The process plans implemented in this chapter were generated from GRP^{2}A and FDL, demonstrating the efficacy of GRP^{2}A and FDL in the manufacture of complex part geometries and the remanufacture of existing parts, respectively.

8.2 Case Study 1

8.2.1 Design of test part I

This case study aims to evaluate the capability of the iAtractive process in the manufacture of difficult to machine structures, which are virtually impossible to machine due to cutting tool inaccessibility. Thus, a test part (test part I) consisting of four connected pockets and a hole, was designed and is shown in Figure 8.1(a).

(a)   (b)
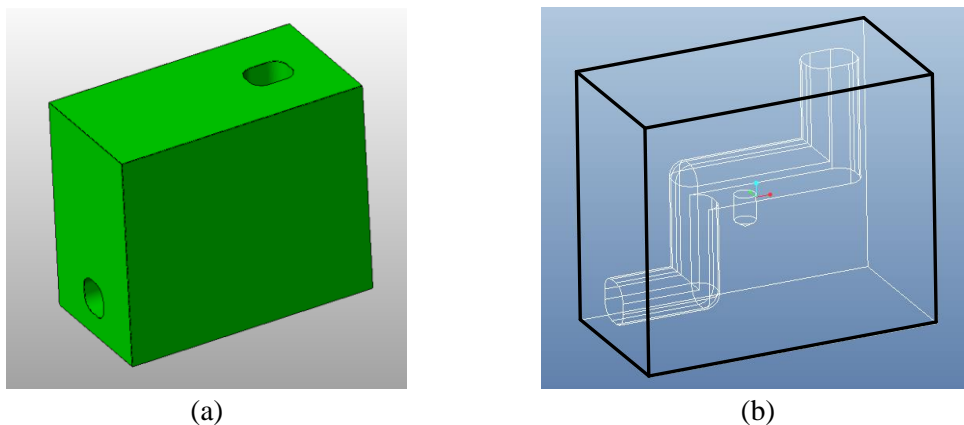
Figure 8.1 – The CAD model of test part I

Figure 8.1(b) shows the internal view of test part I. All corners (except the corner where the hole is located) are round corners with 3mm radii. Among these four pockets, only two of them are exposed features. These two exposed pockets can be directly machined. However, the other two unexposed pockets and the hole are internal features that cannot be solely produced by the CNC machining process. For better representation, the round

corners are intentionally ignored in Figure 8.2. All surfaces required finish machining in order to achieve the correct surface quality and tolerances.
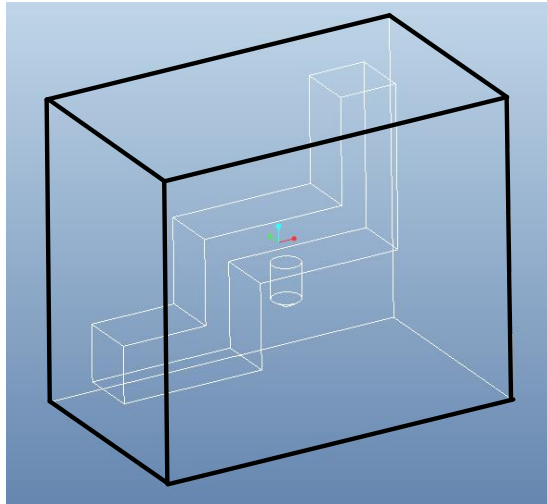
Figure 8.2 – The internal view of test part I without round corners

8.2.2   Part decomposition results

As the internal features cannot be machined from a block, the part has to be decomposed in order to accurately create the two internal pockets and the hole. One possible decomposition result is shown in Figure 8.3(a) and Figure 8.3(b). Test part I has been decomposed into 5 subparts and a sectional view is shown in Figure 8.4. It is noted that the decomposition results may vary depending on the decomposition methods employed.

(a)   (b)
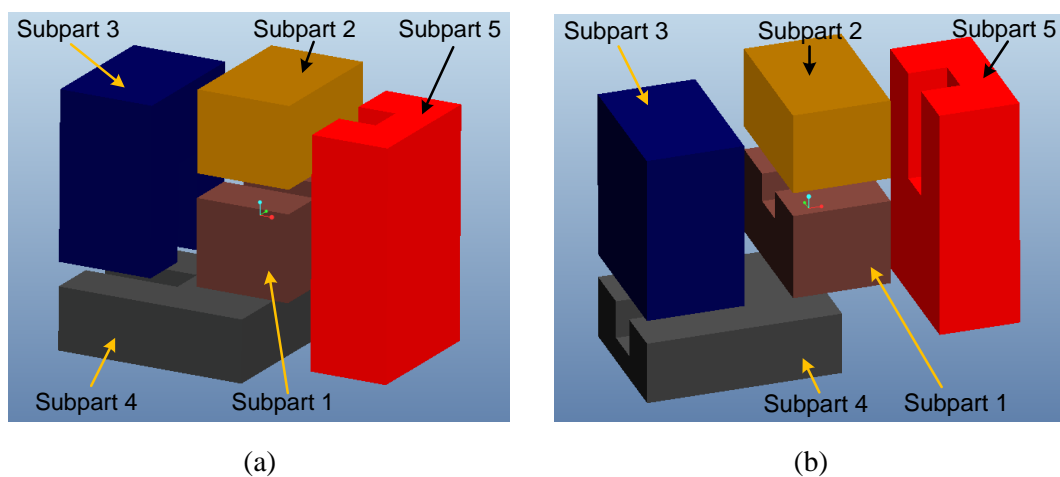
Figure 8.3 – The decomposed subparts for test part I
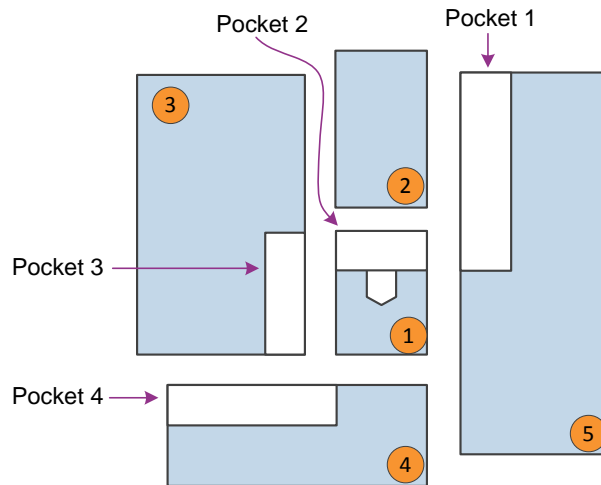
Figure 8.4 – A sectional view of the decomposed subparts for test part I

8.2.3   Determination of build directions of subparts

Since test part I is comprised of internal features resulting in cutting tool inaccessibility, the part orientation is a dummy activity and every part orientation has to be used in order to identify all the available build directions for the different subparts. Figure 8.5 demonstrates a partial representation of the complete subparts' build directions starting from allocating a build direction for subpart 1 with the part orientation shown in Figure 8.3. The build direction of each subpart in the feasible set of build directions is also indicated in Figure 8.5. The cross ($\times$) denotes that the failure of build direction allocation occurs in determining a build direction for the subpart.
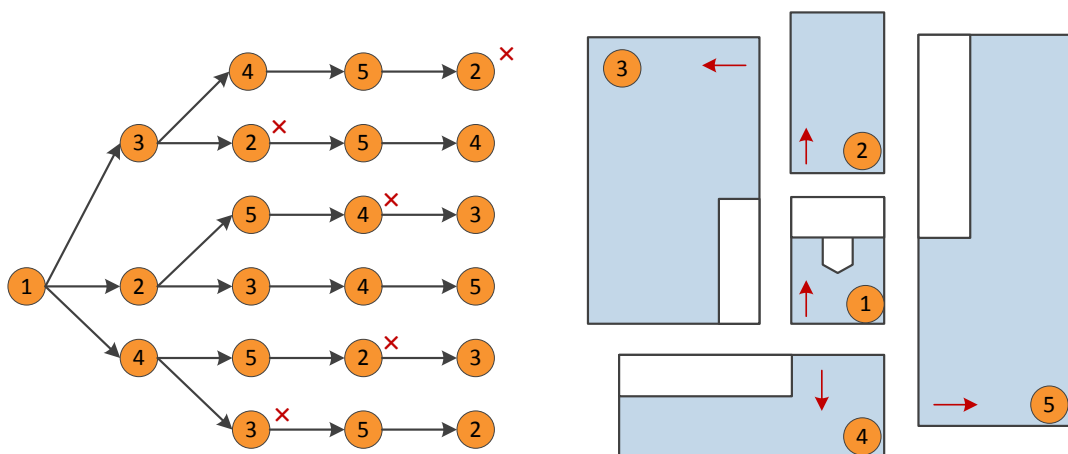
Figure 8.5 – A partial representation of the complete sets of build directions starting from subpart 1 with a certain part orientation

In this example, the feasible set of subparts' build directions (including allocation sequence of build directions) is subpart 1→2→3→4→5. Other build directions and allocation sequences are not available due to deposition nozzle collisions.

Figure 8.6 and Figure 8.7 shows two example sets of build directions, in which the build directions of subpart 4 and 2 are determined first, respectively. The feasible sets of build directions are also indicated in Figure 8.6 and Figure 8.7, which are: subpart 4→1→2→3→5, and subpart 2→1→3→4→5.

It is noted that the identified three sets of build directions are only feasible in this stage. They might not be available when adding machining operations into them. This is because adding machining operations will introduce cutting tool accessibility constraints, which is likely to result in operation sequencing failure.
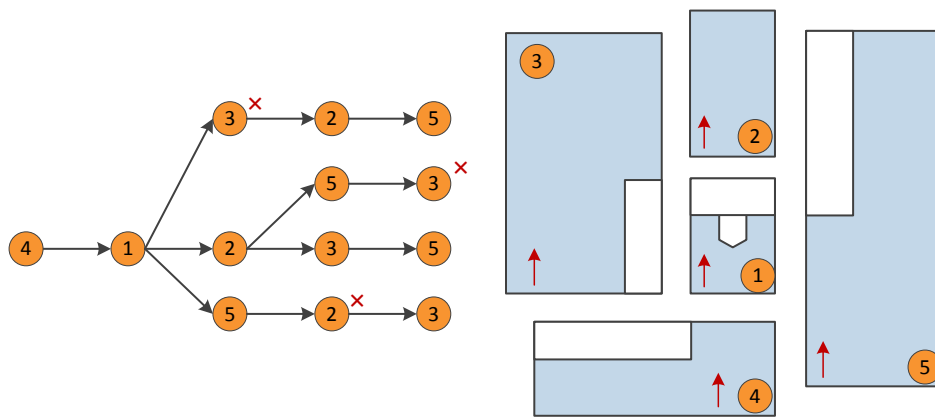
Figure 8.6 – A partial representation of the complete sets of build directions starting from subpart 4 with a certain part orientation
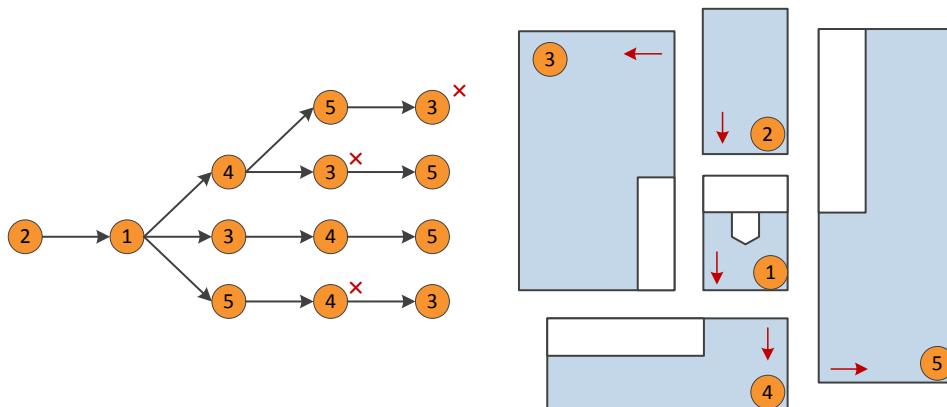
Figure 8.7 – A partial representation of the complete sets of build directions starting from subpart 2 with a certain part orientation

8.2.4   Sequencing additive and subtractive operations

The machining operations are inserted into those three feasible sets of build directions identified in section 8.2.3.

(i)   Subpart 2→1→3→4→5 in Figure 8.7

Given that test part I will be produced from zero, an additive operation is scheduled first to create subpart 2. The next subpart to be produced is subpart 1. However, the hole cannot be finished machined once subpart 1 is added onto subpart 2 since there are no available TADs, as illustrated in Figure 8.8. As a result, no viable additive and subtractive operation sequence can be obtained from this set of build directions.
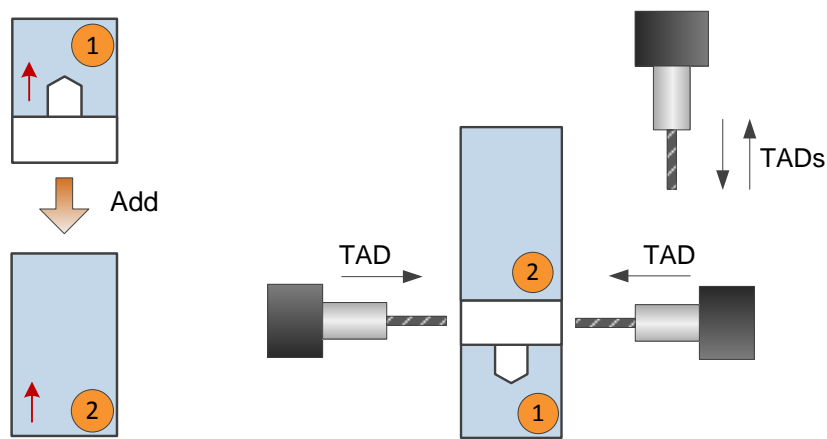
Figure 8.8 – The inaccessible hole

(ii)   Subpart 4→1→2→3→5 in Figure 8.6

As shown in Figure 8.6, subpart 4 and subpart 1 have the same build direction. As a result, they are merged into one subpart, which is called the combined subpart 4&1. Similarly, subpart 2 is merged into the combined subpart 4&1 because they have the same build direction as well. Finally, all the subparts are merged together, which is subpart 4&1&2&3&5.

Machining all the features on subpart 4&1&2&3&5 will definitely lead to cutting tool collisions. As subpart 5 is the last merged subpart that results in regions of cutting tool inaccessibility, it is re-decomposed into the original subpart 5 as shown in Figure 8.9(a). However, the pocket on subpart 3 cannot be machined and thus, subpart 3 is re-

decomposed as shown in Figure 8.9(b). In order to drill the hole on subpart 1, subpart 2 has to be re-decomposed back into its original shape. The final result is shown in Figure 8.9(c). Every feature is accessible for the cutting tool.

(a) Re-decomposition step 1

(b) Re-decomposition step 2   (c) Re-decomposition step 3
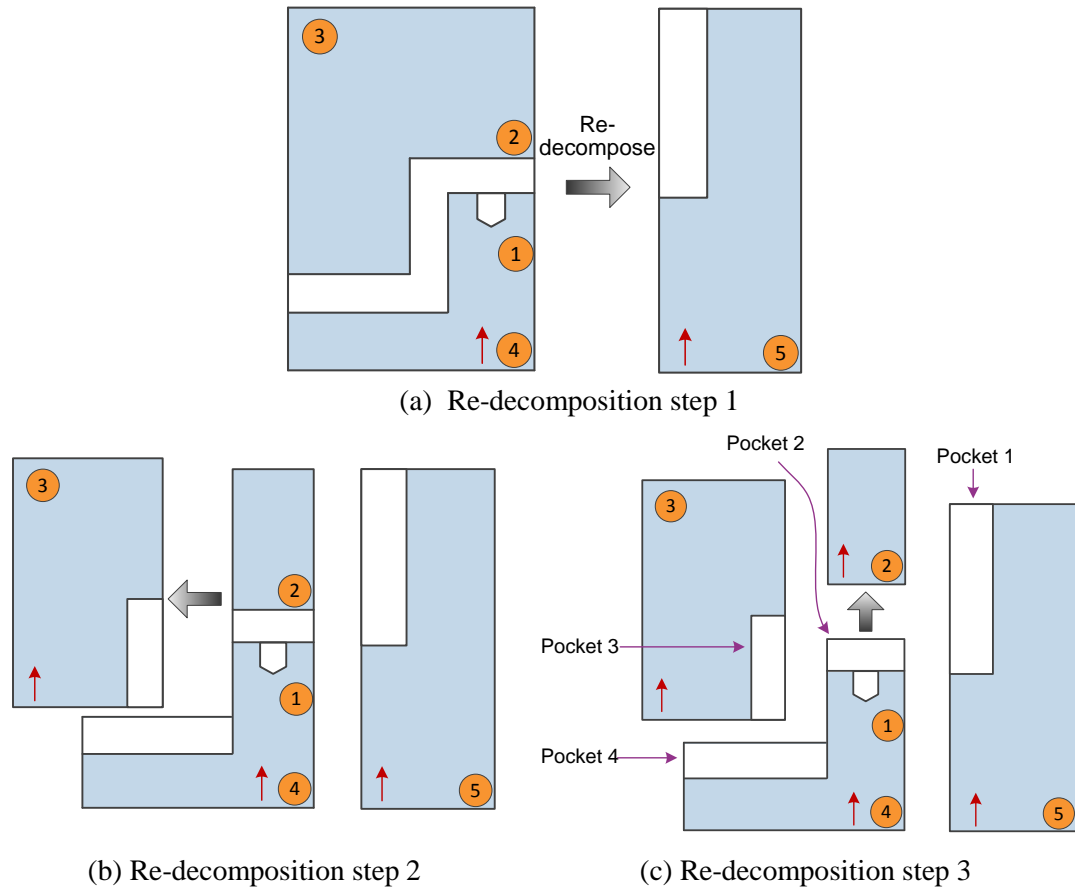
Figure 8.9 – Re-decomposing merged subparts

Based on the result as shown in Figure 8.9(c), subpart 4&1 is built first by using the FFF process. The pocket on subpart 4&1 (i.e. pocket 2) and the hole are finish machined. Pocket 4 will not be subject to finish machining because it is an exposed feature. Subpart 2 is then added onto the machined subpart 4&1, by which subpart 4&1&2 is obtained. Nevertheless, subpart 3 cannot be created with the determined build direction (i.e. ↑) due to deposition nozzle collisions. This indicates that this set of build direction specified in the 'determination of build directions' stage is no longer feasible. In addition, deposition nozzle collisions will occur if attempting to deposit subpart 5 with the build direction specified in Figure 8.9(c).

According to the rules of GRP^{2}A as presented in section 6.5, a set of build directions is considered to be invalid as long as one subpart cannot be created by using either the additive or subtractive processes. Using subpart 5 as an example: as it cannot be created with the build direction (↑), this set of build directions is invalid and will be abandoned. The build direction of subpart 5 will not be re-determined. Using the build direction (→) can enable subpart 5 to be successfully built, but this build direction (→) does not belong to the current set of build directions (Subpart 4→1→2→3→5, shown in Figure 8.9(c)). The build direction of subpart 5 (→) belongs to another set of build directions illustrated in Figure 8.10, namely, subpart 4→1→2→3→5'.
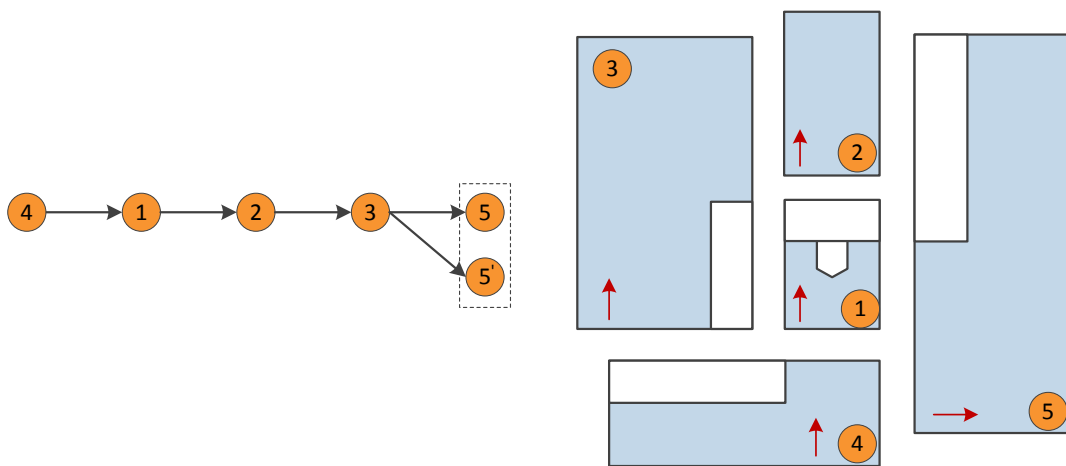
Figure 8.10 – Another set of build directions for test part I

(iii)   Subpart 1→2→3→4→5 in Figure 8.5

According to this additive operation sequence and the subparts' build directions as shown in Figure 8.5, no deposition nozzle collision has been detected. In order to obtain high accuracy and surface quality, machining operations are inserted into the additive operation sequence. Figure 8.11 illustrates the sequencing of additive and subtractive operations, where the machining operations are added according to the rules and procedures presented in section 6.5.5 and Figure 6.27. The sequence for building the subparts is shown in the box with the blue dashed lines. The reasons that the machining operations are inserted will be explained in section 8.2.6. The CAD model of each subpart for the additive process is also modified accordingly. The modified subpart for the specific additive operation is denoted as 'subpart nA'. For example, the modified CAD model of subpart 1 to be fabricated by the additive operation is called subpart 1A.
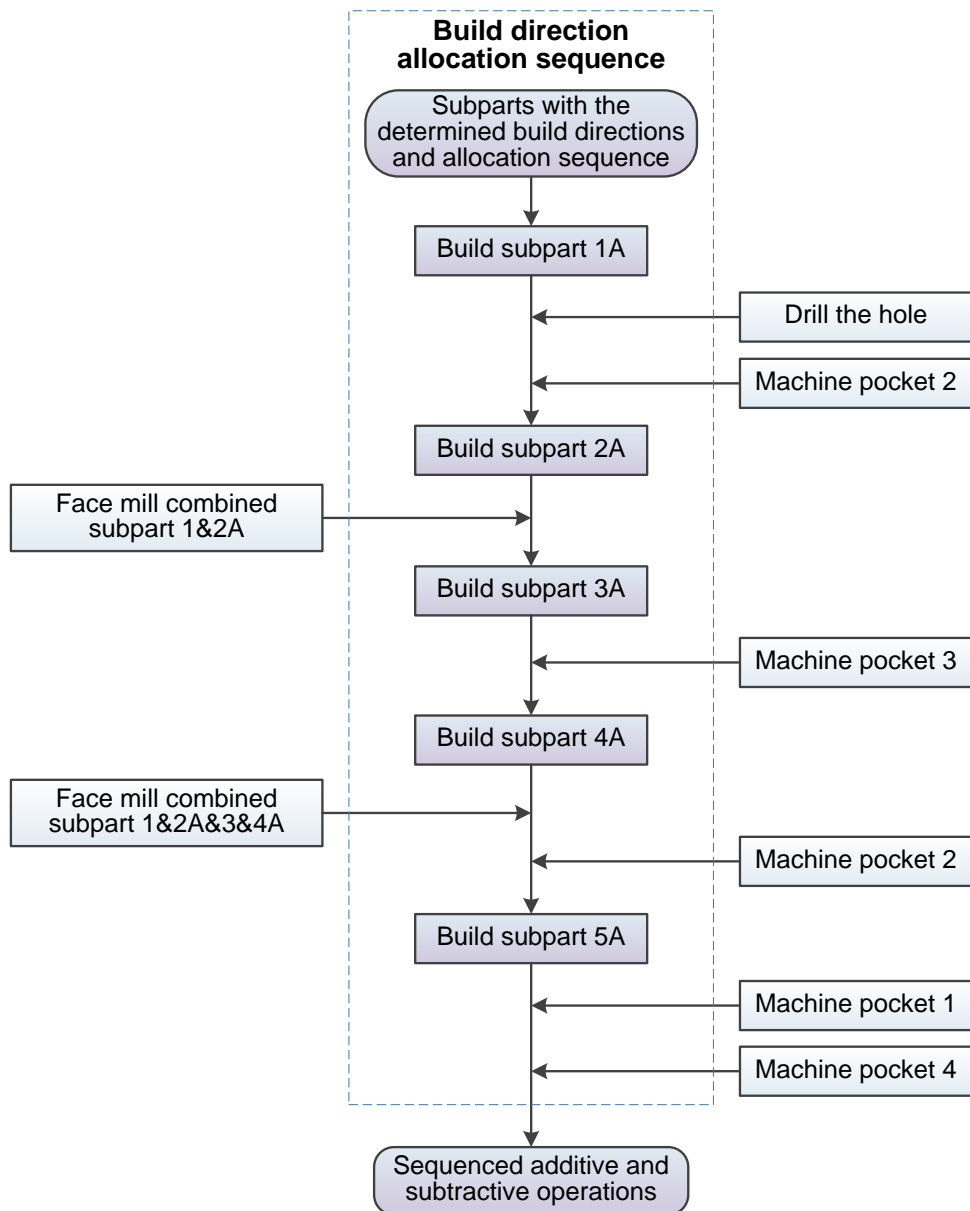
Figure 8.11 – Inserting machining operations into the additive operation sequence

8.2.5 Integration of inspection operations and generation of the static process plan

Based on the procedures described in section 6.7.1 and Figure 6.31, the inspection operations were added into the developed additive and subtractive operation. The additive process parameters were determined according to the relationships depicted in Figure 6.32. The machining process parameters i.e. Feed, speed and DoC were selected from Table 5.5. To this end, the static process plan has been generated, which is outlined in Table 8.1. It is noted that for the drilling operation, the parameters used were obtained from the practical

machining tests. The tool paths for the additive operations were generated from slic3r software (Slic3r, 2013), and the machining tool paths were obtained from Delcam Powermill software (Delcam, 2012). It is also noted that, since deposition speed, deposition pattern and part density etc. were constant throughout the entire production, they are not listed for every additive operation. For the produced subparts, they are represented as 'subpart $n\&(n+1)$'. For instance, subpart 2A is added onto subpart 1, and thus, the finished subpart is called subpart 1&2A. If subpart 1&2A has been finished machined, it is then called subpart 1&2.

Table 8.1 – The developed static process plan for manufacturing test part I

Operation sequence	Operation	Process parameter
1	Build subpart 1A by using the additive process	Extrusion temperature: 205 ℃ Deposition speed: 35mm/s Layer thickness: 0.25mm Part density: 100% Deposition pattern: raster 45 ° Extrusion size: 0.5mm
2	Measure the length, width and height of subpart 1A to obtain the dimensions of subpart 1A because subpart 1A is considered as raw material for the next operation	N/A
3	Machine pocket 2 on subpart 1A	Feed: 2000mm/min Speed: 4000rpm DoC: 0.25mm
4	Drill the hole on subpart 1A to obtain subpart 1	Feed: 500mm/min Speed: 2000rpm DoC: 1mm
5	Measure the dimensions of the hole on subpart 1	N/A
6	Build subpart 2A onto subpart 1 to obtain subpart 1&2A	See operation 1
7	Measure the length, width and height of subpart 1&2A to determine the amount of material to be removed in the next operation (face milling)	N/A
8	Face mill the combined subpart 1&2A	Feed: 3000mm/min Speed: 4000rpm DoC: 2mm
9	Build subpart 3A onto the face milled subpart 1&2A to obtain subpart 1&2A&3A	See operation 1

Table 8.1 – The developed static process plan for manufacturing test part I (continued)

10	Finish machine pocket 3 on subpart 3A (note: subpart 3A is already included in subpart 1&2A&3A). By doing so, subpart 1&2A&3 is produced	Feed: 2000mm/min Speed: 4000rpm DoC: 0.25mm
11	Measure the dimensions of pocket 3 as it will become inaccessible once subpart 4A is deposited onto subpart 1&2A&3	N/A
12	Build subpart 4A onto subpart 1&2A&3 to obtain subpart 1&2A&3&4A	See operation 1
13	Measure the length, width and height of subpart 1&2A&3&4A to determine the amount of material to be removed in the next operation (face milling)	N/A
14	Face mill the combined subpart 1&2A&3&4A	Feed: 3000mm/min Speed: 4000rpm DoC: 2mm
15	Finish machine pocket 2 on subpart 2A to obtain subpart 1&2&3&4A since machining pocket 2 will result in cutting tool inaccessibility issue if subpart 5A is produced	Feed: 2000mm/min Speed: 4000rpm DoC: 0.25mm
16	Measure the dimensions of pocket 2 on subpart 2 as it will become inaccessible after subpart 5A	N/A
17	Build subpart 5A onto subpart 1&2&3&4A to obtain subpart 1&2&3&4A&5A	See operation 1
18	Measure the length, width and height of subpart 1&2&3&4A&5A to determine the amount of material to be removed in the next operation	N/A
19	Finish machine pocket 1 on subpart 5A, including face milling of subpart 5A, to obtain subpart 1&2&3&4A&5	For face milling: see operation 13 For finish machining: Feed: 2000mm/min Speed: 4000rpm DoC: 0.25mm
20	Finish machine pocket 4 on subpart 4A to finally obtain subpart 1&2&3&4&5, which is test part I	Feed: 2000mm/min Speed: 4000rpm DoC: 0.25mm
21	Measure the final part size and pocket 1 and 4	N/A

8.2.6   Part production and the generation of the dynamic process plan

This section describes some of the important operations in the static process plan and presents the generation of a dynamic process plan.

(1) Operation 1: built subpart 1A

Subpart 1A was built from zero, as shown in Figure 8.12. It was the first subpart to be created, and it can be seen that a finish machining operation was required to obtain high surface quality and part accuracy.
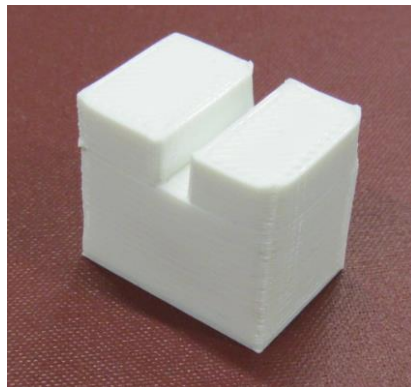
Figure 8.12 – The fabricated subpart 1A

(2) Operation 3 and 4: machined pocket 2 and drilled the hole to obtain subpart 1

As the surface where the hole is located does not have round corners, it has to be vertically machined together with the hole, as shown in Figure 8.13(a). The finished subpart 1 can be found in Figure 8.13(b).
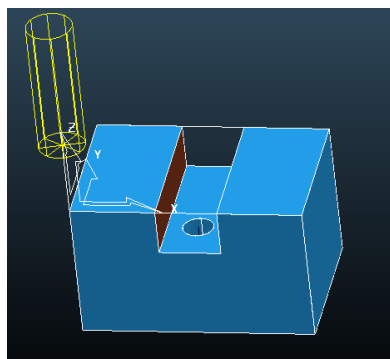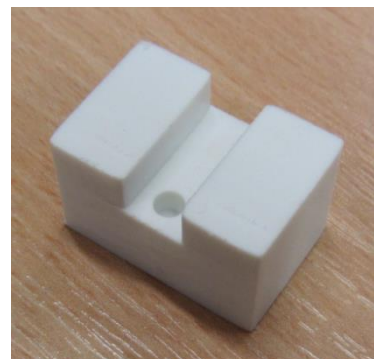
(a)   (b)

Figure 8.13 – The finished subpart 1

(3) Operation 6: built subpart 2A onto subpart 1, by which subpart 1&2A was obtained

Subpart 2A was directly added onto the machined subpart 1, as illustrated in Figure 8.14(a). As the FFF process was actually producing a bridge, the surface highlighted by the arrow in Figure 8.14(b) had to be finish machined afterwards.

(a)　　　　　　　　　　　　　(b)
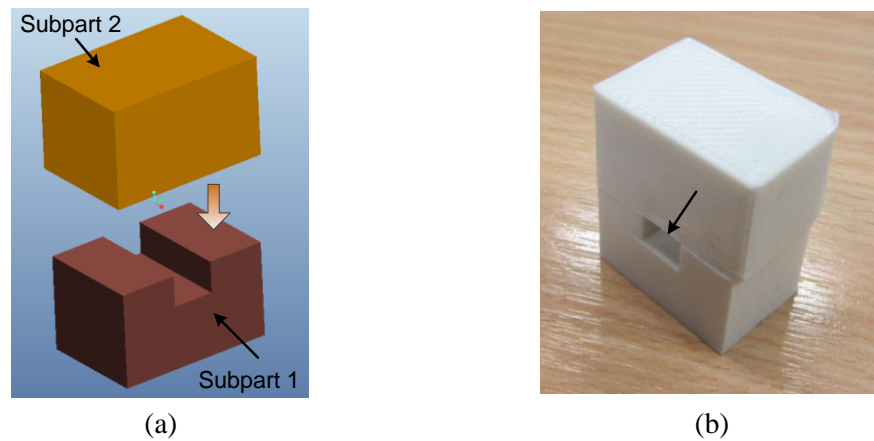
Figure 8.14 – The fabricated subpart 1&2A

(4) Operation 8 and 9: face milled subpart 1&2A and then deposited subpart 3A onto the face milled subpart 1&2A to obtain subpart 1&2A&3A

Subpart 3A was added onto subpart 1&2A as depicted in Figure 8.15(a). However, subpart 2A had not been machined (see Figure 8.14(b)), which means subpart 3A cannot be directly deposited onto the un-machined surface indicated in Figure 8.15(a). As a result, subpart 1&2A was face machined followed by adding subpart 3A. The produced subpart 1&2A&3A is shown in Figure 8.15(b).

(a)　　　　　　　　　　　　　(b)
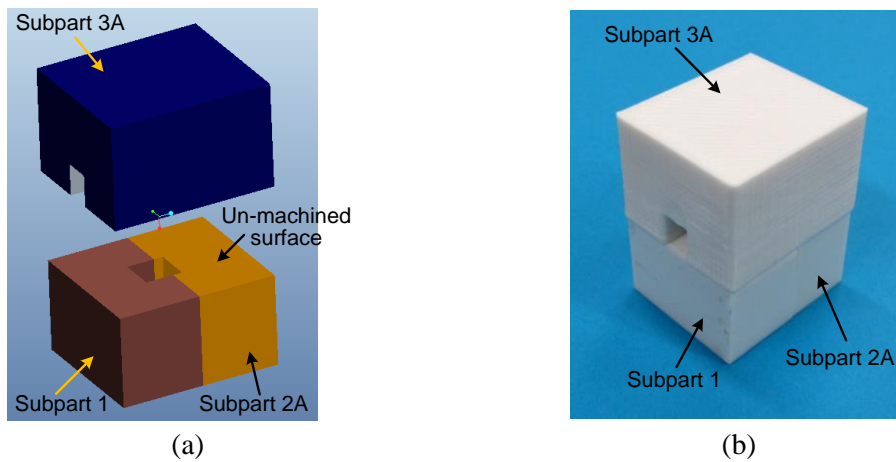
Figure 8.15 – The fabricated subpart 1&2A&3A

(5) Operation 10: finish machined pocket 3 on subpart 1&2A&3A to obtain subpart 1&2A&3

Since subpart 4A was about to be created, pocket 3 on subpart 1&2A&3A had to be finish machined otherwise the pocket would have been inaccessible if subpart 4A was built prior to finish machining pocket 3. Figure 8.16 shows the machined subpart1&2A&3.
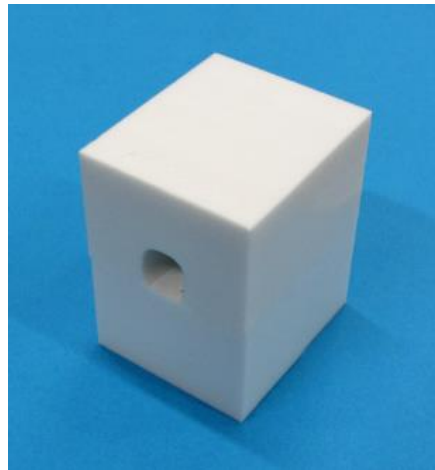
Figure 8.16 – The machined subpart 1&2A&3

(6) Operation 12: built subpart 4A to obtain subpart 1&2A&3&4A, as illustrated in Figure 8.17(a). The fabricated subpart 1&2A&3&4A is shown in Figure 8.17(b).

(a)   (b)
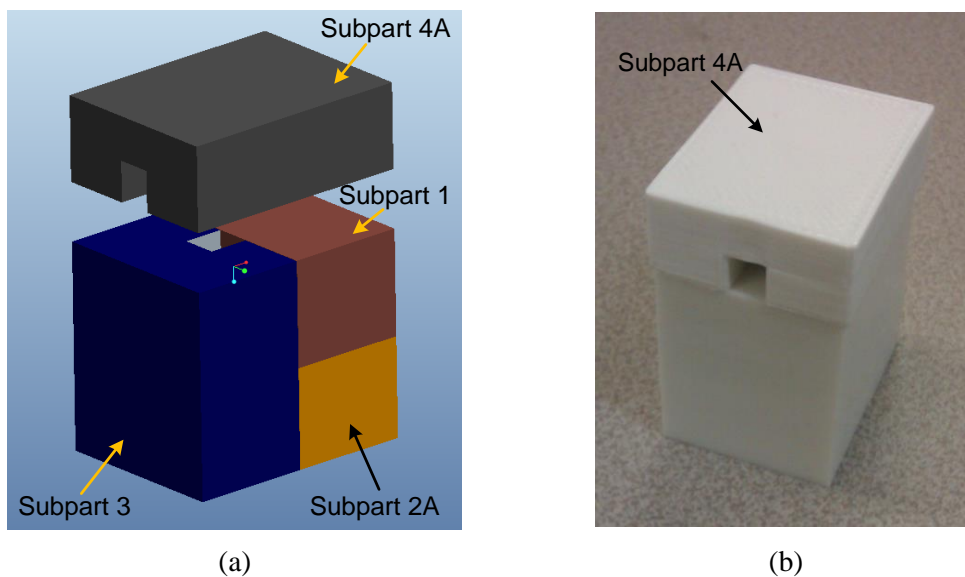
Figure 8.17 – Illustration of adding subpart 4A onto subpart 1&2A&3

(7) Operation 15: finish machined pocket 2 on subpart 1&2A&3&4A to obtain subpart 1&2&3&4A.

The reason that pocket 2 was subject to finish machining again is that the surface highlighted in Figure 8.14(b) became rough when subpart 2A was added onto the machined subpart 1.

(8) Operation 17: built subpart 5A (the red subpart in Figure 8.18(a)) on subpart 1&2&3&4A.

In this operation, subpart 1&2&3&4A&5A was created, as shown in Figure 8.18(b), where each subpart was indicated by the frame with the corresponding colour in Figure 8.18(a).

(a)   (b)
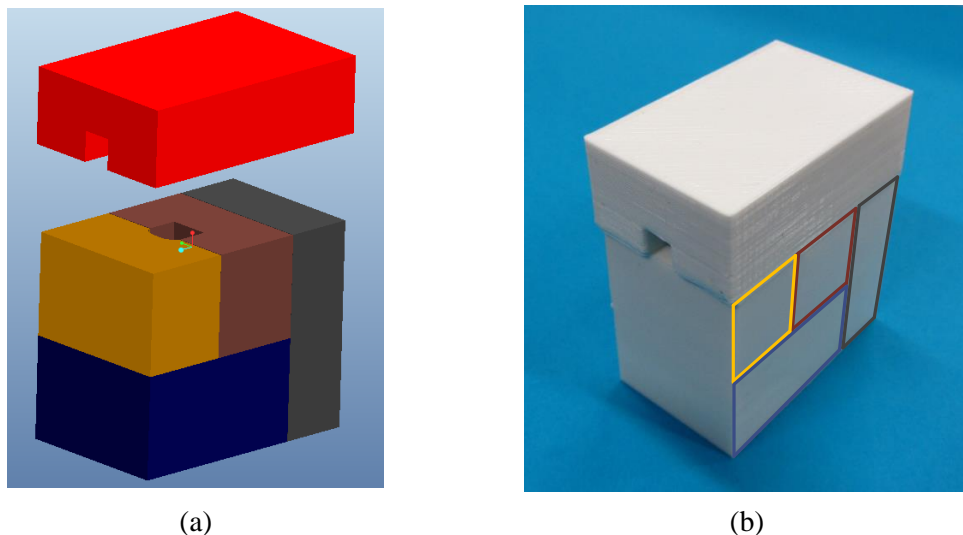
Figure 8.18 – The manufactured subpart 1&2&3&4A&5A

(9) Operation 18 and the generation of a dynamic process plan

The aim of operation 18 was to determine the amount of material to be removed by measuring the length, width and height of subpart 1&2&3&4A&5A. As subpart 5A was just built by the additive process in operation 17, the degree of accuracy is much lower than that of an entirely CNC machined subpart. Subpart 5A was considered as the raw material to be finish machined. Thus, its dimensions had to be measured. However, it was identified that subpart 5A was not positioned correctly as shown in Figure 8.19. As a result, a dynamic process plan had to be generated.
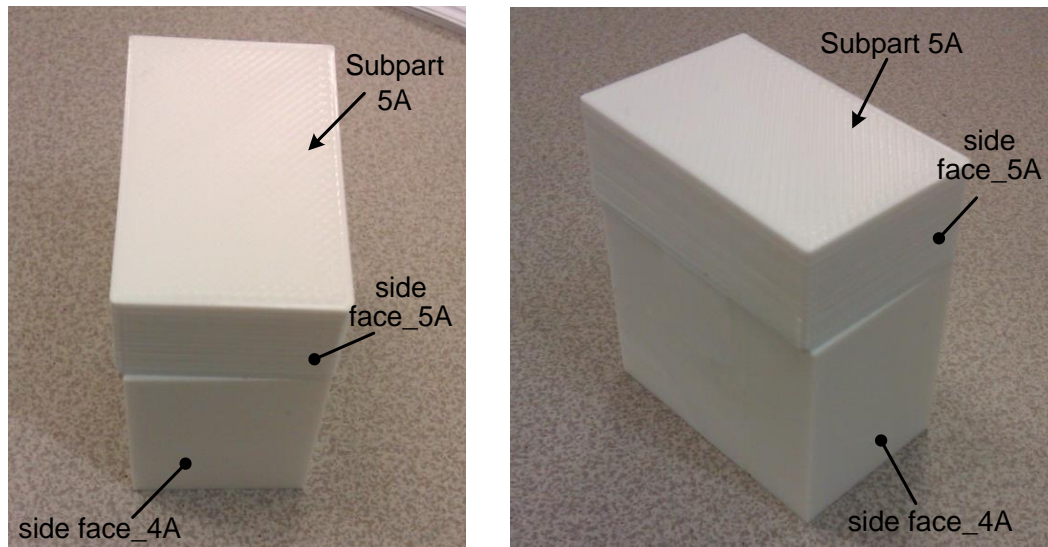
Figure 8.19 – The subpart 5A was not positioned correctly

The author has identified two available dynamic process plans. The first one was to completely remove subpart 5A followed by adding a new subpart 5A, and then carry on operation 18 and onwards in the static process plan. Alternatively, the side face (called side face_5A) highlighted in Figure 8.19 and one of the side faces of subpart 4A (called side face_4A) can be face milled 2mm off, by which a planar face is obtained. This allows the 4mm thick material to be added onto the machined side face_4A and 5A, and then operation 19 and onwards can be correctly conducted. At this stage, the second dynamic process plan was chosen since it required less production time. The operations added into the static process plan are depicted in Figure 8.20, where the operations included in the blue dashed lines are the sequenced operations in the static process plan. Four new operations were added into the static process plan, generating a dynamic process plan.
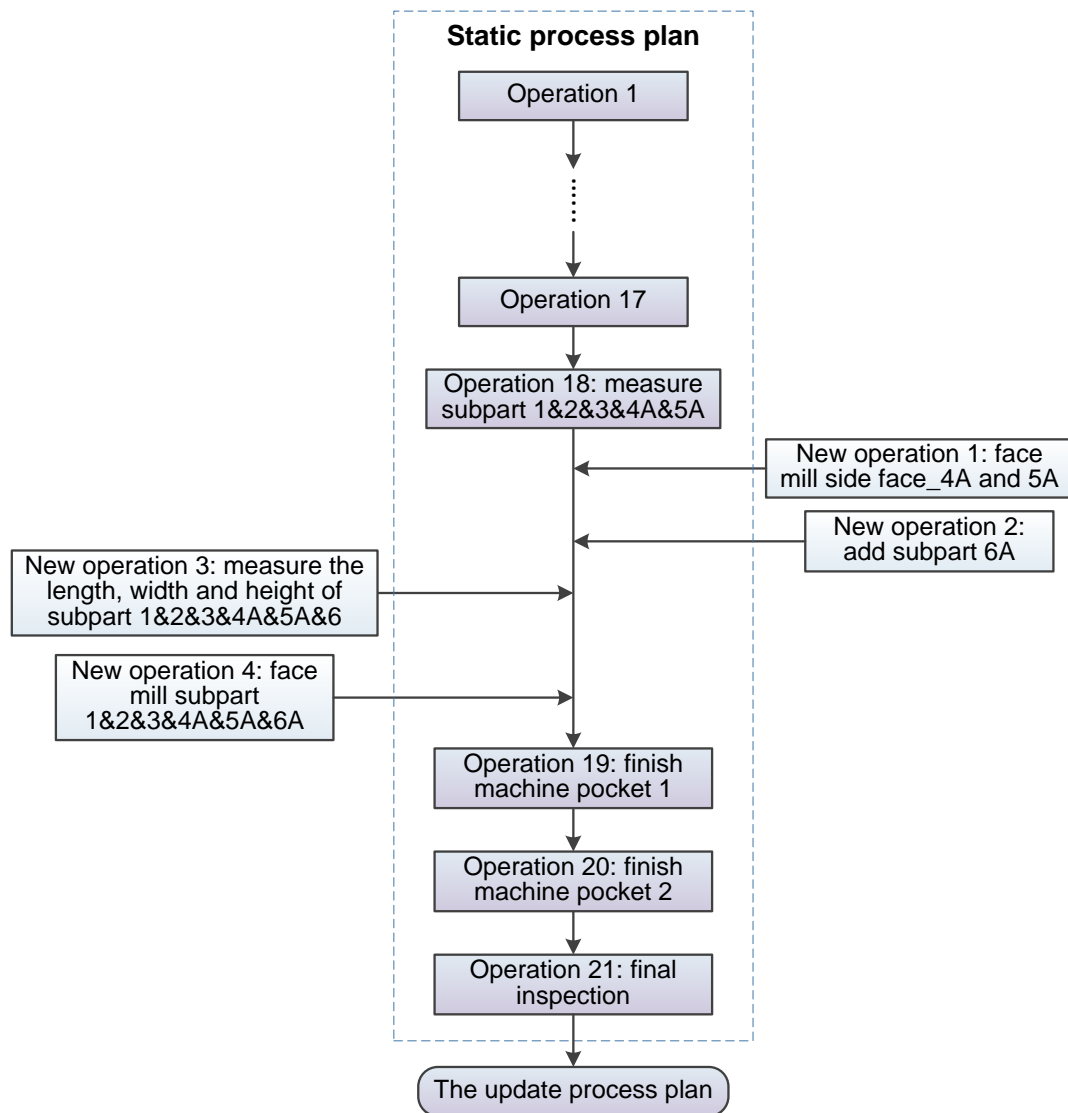
Figure 8.20 – Generation of the dynamic process plan

Figure 8.21(a) shows subpart 1&2&3&4A&5A clamped on a 3-axis vertical machine tool. The side face_4A and side face_5A was face milled 2mm off, as shown in Figure 8.21(b).

(a)   (b)
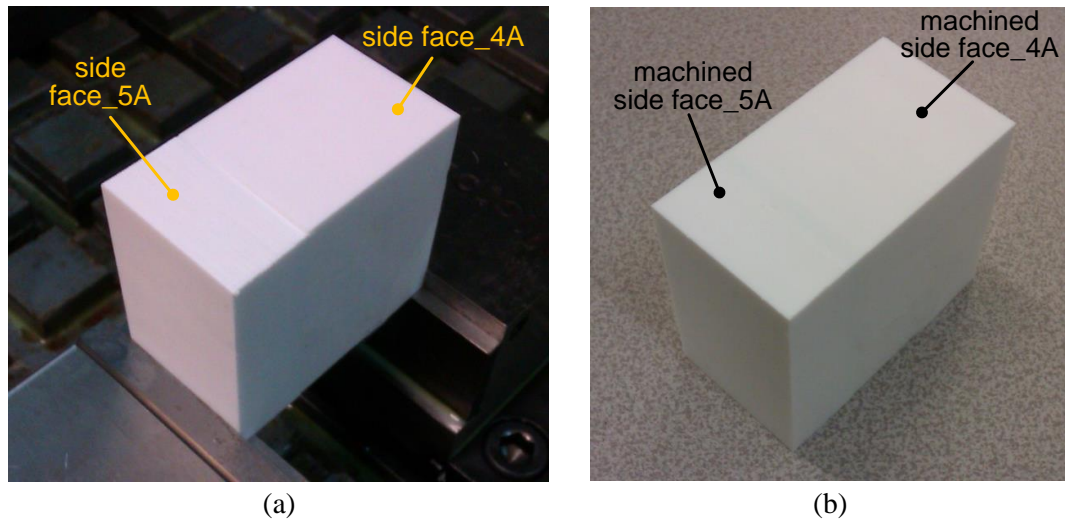
Figure 8.21 – Machining side face_4A and side face_5A

Figure 8.22(a) illustrates that the 4mm thick material (called subpart 6A, green) was added onto the machined side face_4A and 5A. The reason that subpart 6A with a 4mm thickness (rather than a 2mm thickness) was added was because more material was required to be removed in the finishing operations. The fabricated subpart 1&2&3&4A&5A&6A is shown in Figure 8.22(b).

(a)   (b)
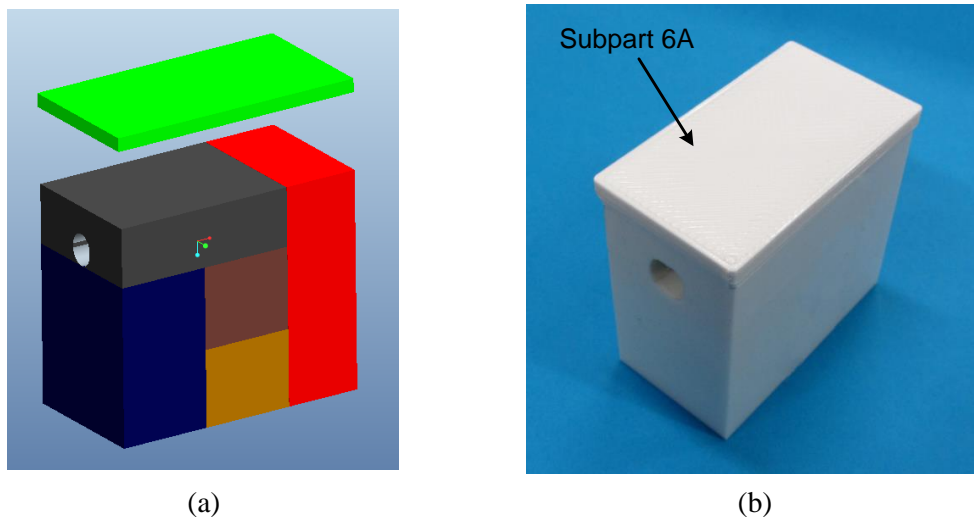
Figure 8.22 – Adding 4mm thick material onto the machined side face_4A and 5A

(10)   Finish machine pocket 1 and 4.

Having completed the newly generated operations in the dynamic process plan, the iAtractive process returned to the static process plan and kept conducting the originally

scheduled operation 19 and 20, which were to finish machine pocket 1 and 4. These two machining operations were sequenced at the end of the process plan since they are exposed features and machining them will not lead to cutting tool inaccessibility. Finally, the dimensions of the finished part and pocket 1 and 4 were measured. The manufactured test part I is shown in Figure 8.23(a) (pocket 4 is in this figure) and Figure 8.23(b) (the upper pocket is pocket 1). For showing the internal features, the part has been sectioned (40% material was removed) in Figure 8.23(c).
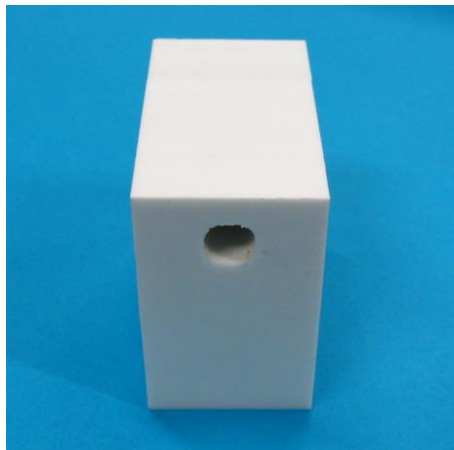
(a) pocket 4
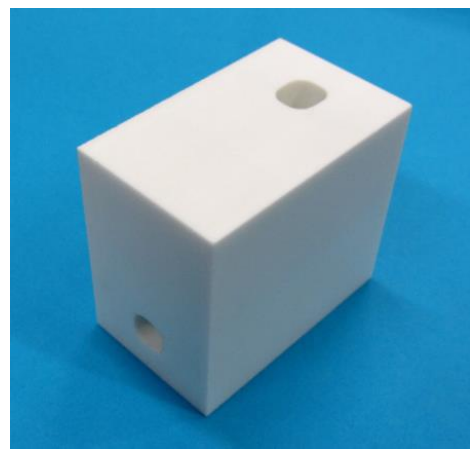
(b) pocket 1 (on the top face) and pocket 4
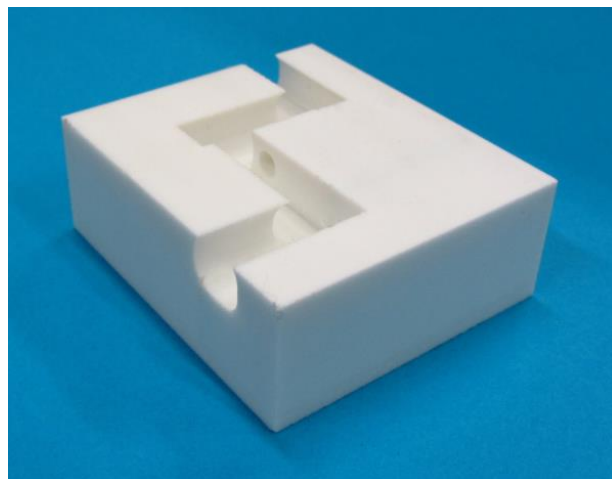
(c) sectioned view

Figure 8.23 – The finished test part I

8.3 Case Study 2

8.3.1 Design of test part II

The aim of this case study was to demonstrate the capability of the iAtractive process in producing complex part geometries as defined in the research scope. Test part II has been designed and the part geometry is shown in Figure 8.24. The majority of the difficulty in manufacturing this part lies in the machining of the blind pocket. This test part consists of three pockets and one of them is a blind pocket. This pocket is likely to lead to cutting tool accessibility issues if attempting to machine it from a block. The internal view of the pockets is shown in Figure 8.25.
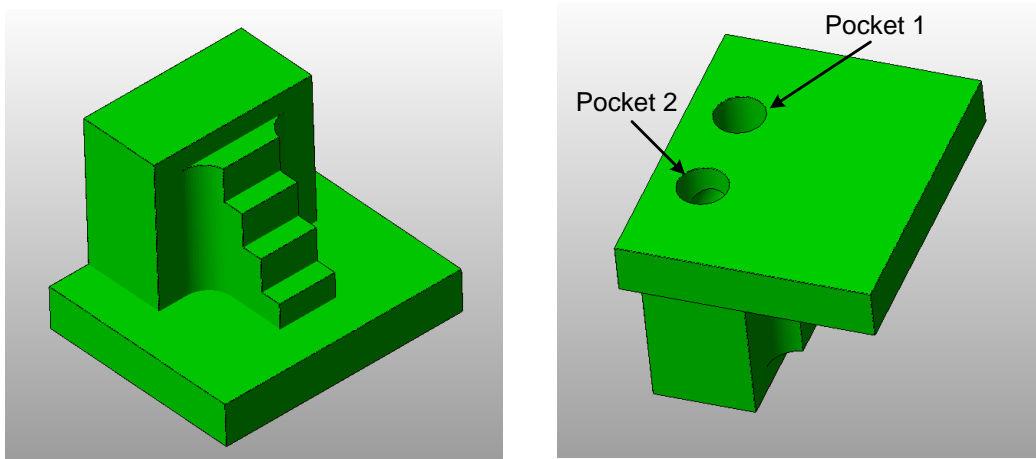
Figure 8.24 – Test part II
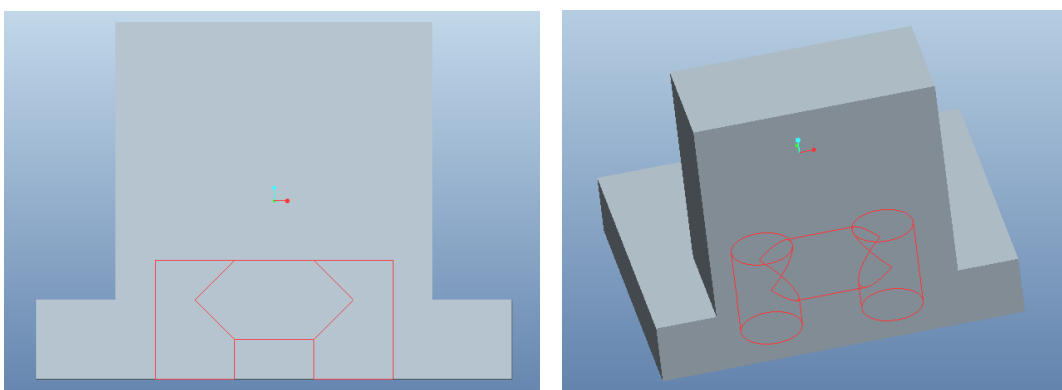
Figure 8.25 – The internal view of the pockets on test part II

8.3.2   Part decomposition results

In order to machine the blind pocket shown in Figure 8.25, test part II was decomposed into three subparts, enabling the blind pocket (called pocket 3) to be accessible for the cutting tools in certain machining operations. These three subparts are shown in Figure 8.26.
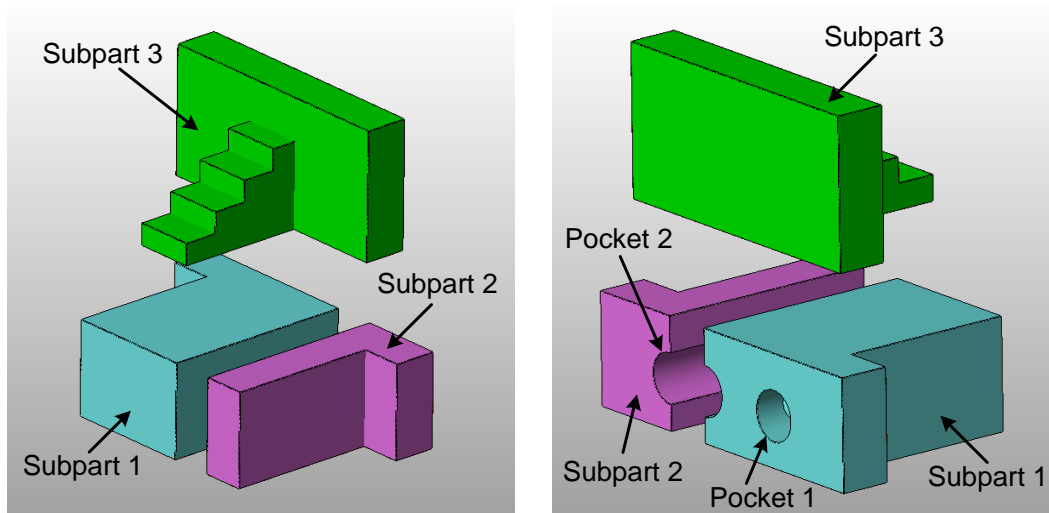
Figure 8.26 – The subparts decomposed from test part II

8.3.3   Determination of build directions of subparts, sequencing of additive and subtractive operations and integration of inspection operations

The full graph of build directions of subparts will not be elaborated upon in this section. Certain sets of build directions are discussed as follows:

(1) Determine a build direction starting from subpart 2

Assume that subpart 2 is the first subpart to be built in a possible build direction and then finish machined. Given that the blind pocket (i.e. pocket 3) is on subpart 1, it is still cutting tool inaccessible when subpart 1 is added onto subpart 2. Therefore, the build direction allocation sequence subpart 2→1→3 is not feasible.

Regarding the sets of build directions in which the allocation sequence is subpart 2→3→1, assume that subpart 2 has already been fabricated in an additive operation in a possible build direction. Since adding subpart 3 does not lead to cutting tool inaccessibility of pocket 2, subpart 3 can be built onto subpart 1. However, having produced subpart 3 to

obtain subpart 2&3, subpart 1 cannot added onto subpart 2&3 due to deposition nozzle collisions. In other words, no feasible build direction can be identified for subpart 1. As a result, all the sets of subparts' build directions where the allocation sequence is <u>subpart 2→3→1</u> are not valid. This indicates it is impossible to obtain a feasible set of build directions if determining a build direction starting from subpart 2.

(2) Determine a build direction starting from subpart 3

If subpart 3 is the first subpart to be fabricated, there are two possible build direction allocation sequences to be considered, which are <u>subpart 3→1→2</u> and <u>subpart 3→2→1</u>. However, having built and finish machined subpart 1, subpart 2 cannot be built owing to deposition nozzle collisions. Similarly, subpart 1 cannot be created in the circumstances where subpart 2 has been generated. In addition, it is virtually impossible to finish machine pocket 3 if subpart 2 is manufactured prior to subpart 1 because the only available tool approach direction for pocket 3 is blocked by subpart 2. As a result, it can be concluded that feasible operation sequences cannot be identified when determining a build direction starting from subpart 3.

(3) Determine a build direction starting from subpart 1

There are two possible build direction allocation sequences to be considered. One of them is <u>subpart 1→3→2</u>. Nevertheless, for the same reason (i.e. deposition nozzle collisions), subpart 2 cannot be created if subpart 3 has already been produced.

Another allocation sequence is <u>subpart 1→2→3</u>. The build directions for each subpart are indicated by the red arrow in Figure 8.27. Once subpart 1 is created, the build direction for subpart 2 has to be along the –X direction. As a result, the only option of build direction for printing subpart 3 is along the +Z direction. As for the build directions of subpart 1, there are six available directions (i.e. +X, –X, +Y, –Y, +Z and –Z). As a result, there are six sequences of additive, subtractive and inspection operations. These six operation sequences are almost identical and the majority of the difference lies in the build directions of subpart 1. In this case, the build time estimation model (developed in section 6.10) was applied to estimating the build times used in printing subpart 1 with different build directions. The results are listed in Table 8.2. The star (*) represents that support material is needed while printing subpart 1 along the –X and –Y directions. Additionally, the build directions of +Z and –Z do not make any difference when printing subpart 1 on the FFF

machine since subpart 1 is a symmetric part on the XY plane. This essentially means the sliced #n layers are identical to the #(N–n) when the subpart is sliced into N layers along +Z and –Z directions, respectively. As a result, the +Z direction was selected.
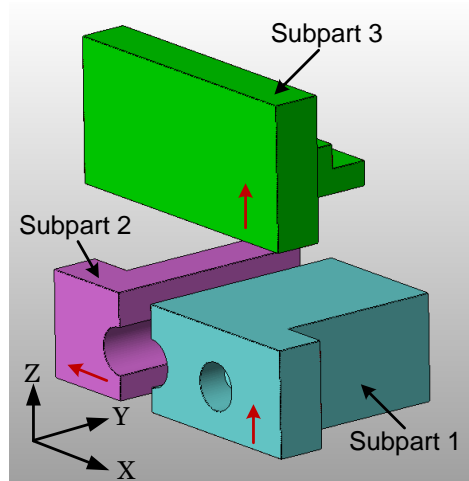
Figure 8.27 – The build directions of subparts

Table 8.2 – Build times for manufacturing subpart 1 by the FFF process

	+X	–X	+Y	–Y	+Z	–Z
Build times (h:m:s)	1:50:30	2:11:24*	1:54:14	2:02:31*	1:46:39	1:46:39

Upon consideration of cutting tool accessibility, the machining and inspection operations were inserted into the build direction allocation sequence. The overall operation sequence is shown in Table 8.3.

Table 8.3 –The developed static process plan for manufacturing test part II

Operation sequence	Operation	Process parameter
1	Build subpart 1A by using the additive process	Extrusion temperature: 205 ℃ Deposition speed: 35mm/s Layer thickness: 0.25mm Part density: 100% Deposition pattern: raster 45 º Extrusion size: 0.5mm
2	Measure subpart 1A to obtain its actual dimensions because subpart 1A is considered as raw material for the machining operations (i.e. operation 3, 4 and 5)	N/A
3	Face mill subpart 1A	Feed: 3000mm/min Speed: 4000rpm DoC: 2mm
4	Finish machine pocket 1	Feed: 2000mm/min Speed: 4000rpm DoC: 0.25mm
5	Finish machine pocket 3 (the blind pocket) to obtain subpart 1	Feed: 2000mm/min Speed: 4000rpm DoC: 0.25mm
7	Measure the dimensions of pocket 3 since it will become inaccessible once subpart 2A is added	N/A
6	Build subpart 2A onto subpart 1 to obtain subpart 1&2A	See operation 1
7	Measure the length, width and height of subpart 1&2A	N/A
8	Face mill subpart 1&2A in order to obtain a planar face for depositing subpart 3A	Feed: 3000mm/min Speed: 4000rpm DoC: 1mm
9	Build subpart 3A onto subpart 1&2A, by which subpart 1&2A&3A is obtained	See operation 1
10	Measure the length, width and height of subpart 1&2A&3A	N/A
11	Finish machine subpart 3 to obtain subpart 1&2A&3	Feed: 2000mm/min Speed: 4000rpm DoC: 0.25mm
12	Finish machine pocket 2 to finally obtain subpart 1&2&3, which is test part II	Feed: 2000mm/min Speed: 4000rpm DoC: 0.25mm
13	Measure the dimensions of the finished test part II	N/A

The final test part II has been produced, as shown in Figure 8.28.
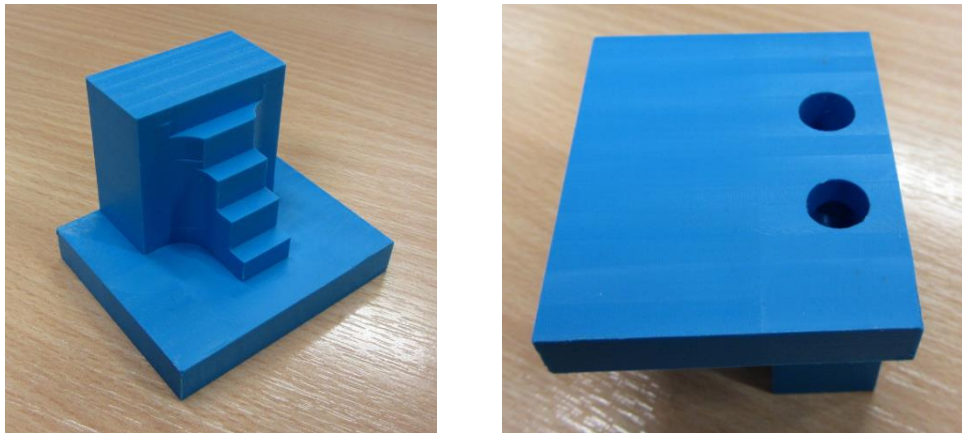
(a) front view   (b) base view

Figure 8.28 – The finished test part II

8.4 Case Study 3

8.4.1 Design of test part III

This case study is aimed at demonstrating the feasibility of the iAtractive process together with FDL in reusing existing parts. Test part III was designed and is depicted in Figure 8.29. It was modified from test part C as illustrated in Figure 5.10. Test part III consists of a boss, a pocket, a step and two holes, which are considered to be typical 2½D features. No internal features were designed, indicating that test part III does not have to be decomposed. There is only one subpart, which is test part III itself.
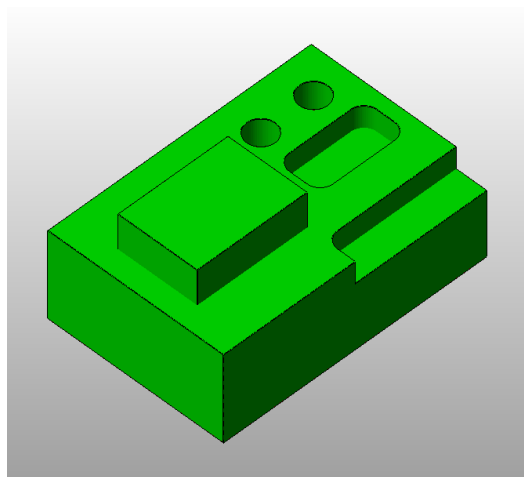
Figure 8.29 – Test part III

Three existing parts were provided, which were a part with a boss (Figure 8.30) and a pocket (Figure 8.31), respectively, and a finished part. The finished part has been identified in the final inspection process as being out of tolerance since the actual dimensions of the boss feature was $24.2 \times 17.8 \times 8.3mm^3$, whereas the nominal values are $25 \times 18 \times 8mm^3$. Readers are referred to Appendix B for the drawings of test part III and the three given existing parts.
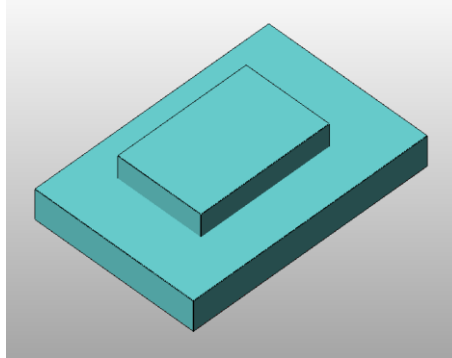
Figure 8.30 – The existing part with a boss
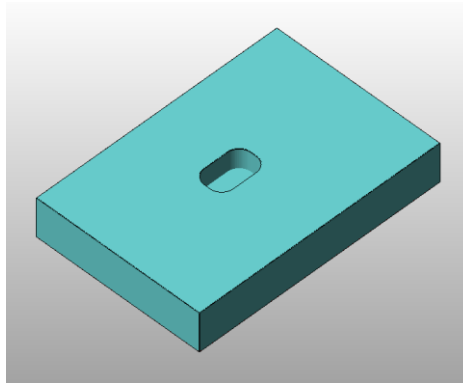
Figure 8.31 – The existing part with a pocket

8.4.2 Global and local constraints

(1) The global constraints for all the three existing parts are:
- Tolerance and surface quality
- Positions of the negative features (i.e. two holes, a pocket and a step)

It is assumed that high surface quality and accuracy is required for test part III, indicating that every feature is required to be finish machined. Moreover, hollow structures and recovery layers that are overlapping with negative features are not allowed, as illustrated in

Figure 7.6 and Figure 7.13. It is noted that production time and material consumption are not considered in this case study, but they are recognised as important factors to be considered in the decision-making logic in the future.

(2) The local constraints for the existing part with a boss:

The total length (L), width (W) and height (H) of the final part (test part III); the total length (L_e), width (W_e) and height (H_e) of the existing part; the length, width and height of the boss (L_b, W_b and H_b); the position of the boss (PL and PW); the total thickness of the recovery layers (D_r); the vertical distance between the existing boss to its adjacent final feature (D_f). These notations are referred to Table 7.2 and section 7.4.4.2.

(3) The local constraints for the existing part with a pocket:

The total length (L), width (W) and height (H) of test part III; the total length (L_e), width (W_e) and height (H_e) of the existing part; the length and width of the pocket (L_p and W_p); the total thickness of the recovery layers (D_r); the vertical distance between the existing pocket to its adjacent final feature (D_f). These notations are referred to Table 7.2 and section 7.4.4.3.

(4) The local constraints for the finished part where the dimensions of the boss are out of tolerance:

The length, width and height of the boss (L_b, W_b and H_b); the position of the boss (PL_b and PW_b);

These local constraints together with their values obtained from Appendix B are summarised in Table 8.4.

Table 8.4 – The local constraints for the given existing parts

Existing part	Local constraint (unit: mm)
Existing part with a boss	$L = 60$, $W = 40$, $H = 28$, $L_e = 62$, $W_e = 42$, $H_e = 14$, $L_b = 34$, $W_b = 22$, $H_b = 6$, $PL_b\_1 = 13$, $PL_b\_2 = 15$, $PW_b\_1 = 9$, $PW_b\_2 = 11$, $D_f = 1$
Existing part with a pocket	$L = 60$, $W = 40$, $H = 28$, $L_e = 62$, $W_e = 42$, $H_e = 10$, $L_p = 12$, $W_p = 7.5$, $D_f = 5$, $D_r = 1$
Existing part with a final boss	Nominal boss dimensions: $L_b\_n = 25$, $W_b\_n = 18$, $H_b\_n = 8$, $PL_b\_1\_n = 5$, $PL_b\_2\_n = 30$, $PW_b\_1\_n = 11$, $PW_b\_2\_n = 11$ Actual boss dimensions: $L_b = 24.2$, $W_b = 17.8$, $H_b = 8.3$, $PL_b\_1 = 5$, $PL_b\_2 = 30.8$, $PW_b\_1 = 11.3$, $PW_b\_2 = 10.9$

8.4.3 The manufacturing strategies and the finished parts

The manufacturing strategies used in this case study for further manufacturing the above three existing parts are presented as follows:

(1) Manufacturing strategy ② for the existing part with a boss

One of the local constraints, i.e. $PW_b\_2 = 11$mm, does not meet the local constraints relationships as specified in section 7.4.4.2 (i.e. $PL_b\_1 \geq 9$mm, $PL_b\_2 \geq 9$mm, $PW_b\_1 \geq 9$mm, $PW_b\_2 \geq 15$mm, and $D_f > D_r$). As a result, the manufacturing strategy ⑦ cannot be applied to this existing part and D_r is not applicable.

In this case, the manufacturing strategy ② was used to further manufacture the existing part. The existing boss was first removed, by which a planar face was obtained. More material was added onto the machined existing part followed by a finishing operation to ensure that the dimensions of the final features were in the desired tolerances. The operations are illustrated in Figure 8.32.
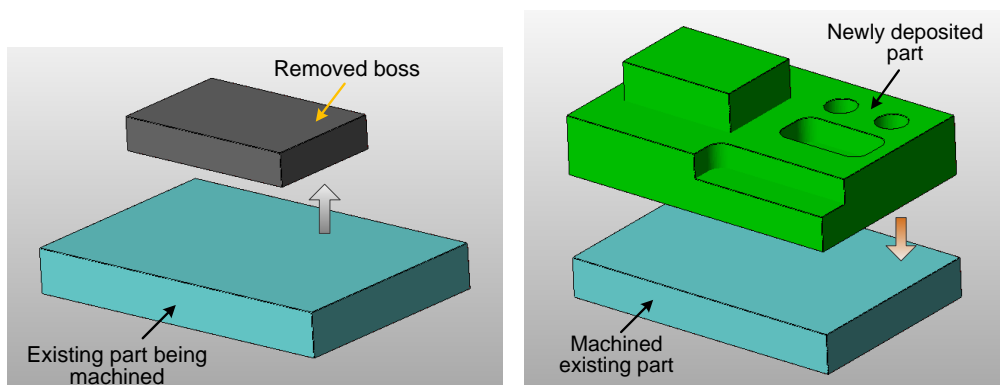
Figure 8.32 – Manufacturing strategy (2) used in case study 3

(2) Manufacturing strategy ① for the existing part with a pocket

Given that $\sqrt{2}W_p = 10.6\text{mm} < 23\text{mm}$ and $D_f = 5\text{mm} > D_r = 1\text{mm}$, material can be directly deposited onto the top surface of the existing part. Figure 8.33 depicts the newly deposited part together with the recovery layers being added onto the existing part to create the near-net shape of test part III, which was finish machined as part of the last operation.
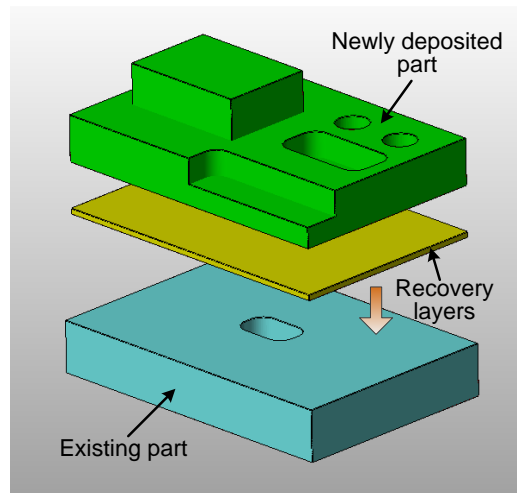
Figure 8.33 – Manufacturing strategy (1) used in case study 3

(3) Manufacturing strategy ② for the existing part on which the dimensions of the final boss were out of tolerance

Referring to section 7.4.7.1, the manufacturing strategy ⑤ (machine the existing features to the final dimensions directly) can be used when all the local constraints meet the relationships below:

- $PL_b\_1\_n \geq PL_b\_1$, $PL_b\_2\_n \geq PL_b\_2$, $PW_b\_1\_n \geq PW_b\_1$, and $PW_b\_2\_n \geq PW_b\_2$ (see Figure 7.34)

However, two of the positioning dimensions of the existing boss did not meet the relationships, which were: $PL_b\_2 = 30.8\text{mm} > PL_b\_2\_n = 30\text{mm}$, $PW_b\_1 = 11.3\text{mm} > PW_b\_1\_n = 11\text{mm}$. As illustrated in Figure 7.34, the existing boss had to be removed by using the subtractive process. Therefore, a new boss was added onto the machined existing part and the new boss was subsequently machined to its designed dimensions.

Three identical test part III have been produced from the three given existing parts, as shown in Figure 8.34. The blue material represents the existing parts and the white material represents the new material that was added and finish machined.
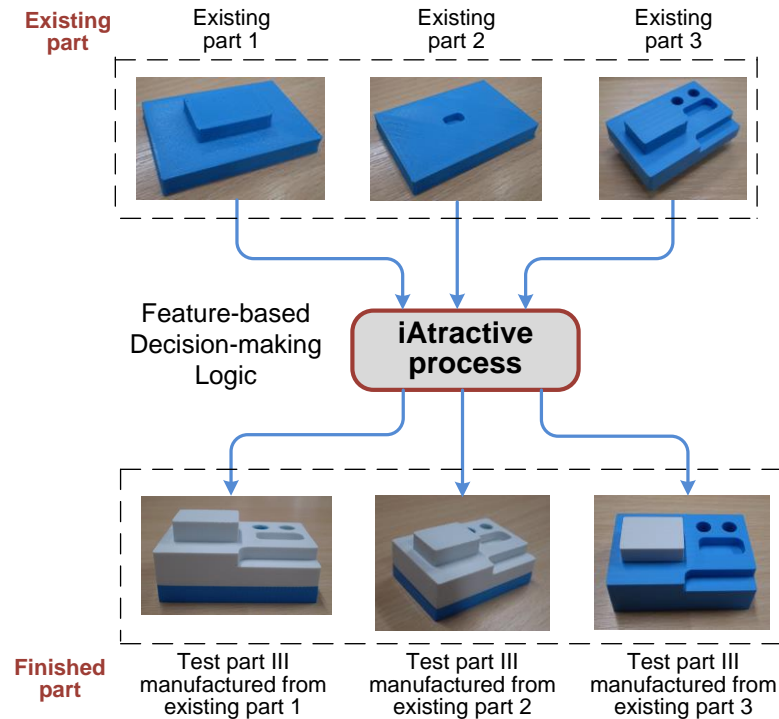
Figure 8.34 – Further manufacturing existing parts to test part III

8.5   Review of the Case Studies

The present state of the art manufacturing processes are still significantly constrained by their capabilities either from technical limitations, such as complex part geometries, and raw materials. The iAtractive process together with GRP^{2}A and FDL, has been proposed, developed and documented in this thesis. The three case studies have demonstrated the ability of the iAtractive process to:

- Manufacture accurate complex part structures, which are traditionally impossible to produce by single individual manufacturing processes alone.
- React promptly to quality changes to continuously manufacture the part until it achieves the designed requirements. In traditional manufacturing methods, the parts that do not meet the specified quality are scrapped.

- Reuse existing parts and transform them into new final parts, whereas, conventionally, CNC machining processes have to start with a block of which the size has to be bigger than the final part; additive processes are only designed to start manufacturing parts from zero.

9 <u>Concluding discussion</u>

9.1 Introduction

This chapter presents a discussion of the areas related to the scope of this research and brings together a number of major issues of the research reported in this thesis.

9.2 State-of-the-art in Hybrid Manufacturing Technology

The author has identified that there is no consensus definition of hybrid manufacturing processes (see sections 3.6.1 and 3.6.8). The author has proposed a definition and the term 'hybrid processes' is defined as an approach that combines two or more manufacturing processes, each of which is from different manufacturing technology. Through the review, it is also revealed that the most of the hybrid processes only focus on enhancing capability of the constituent processes, such as increasing tool life, improving surface quality and accuracy, and reducing production times. However, it has not been reported that complex features can be accurately produced by using any of the developed hybrid processes. The combination of additive and subtractive processes have been recognised as a potential candidate to manufacture complex parts, but no process planning approach has been developed to effectively utilise the capability of this type of hybrid process. The developed hybrid processes are only able to deal with very specific applications and their validity fails while applying these hybrid processes to manufacturing other parts with various structures. The review has also indicated that the current manufacturing processes are always constrained by the available raw materials in terms of shape and size. The application of such hybrid processes on the application of material reuse has not been thoroughly explored due to the lack of process planning techniques. These identified research gaps were the principle drivers to formulate the basis of the author's research.

9.3 The iAtractive Process and the Design of Experimental Methodology

The hybrid process termed iAtractive, presented in chapter 4, has been proposed, which is aimed at accurately manufacturing complex part geometries as well as utilising existing parts. The overall workflow of the iAtractive process together with the major considerations as described in sections 4.3.1 and Figure 4.4, was used to design a structured experimental methodology to generate new knowledge on hybrid manufacturing

and process planning. The methodology consists of 3 stages, focusing on the following three major aspects:

- Investigation of the part manufacturing strategy, in particular process interactions, when combining the capability of the additive, subtractive and inspection processes.
- Development of GRP^{2}A for manufacture of complex part geometries. Based on the part manufacture knowledge gained from the last stage, GRP^{2}A has been explored and developed, which is able to generate static and dynamic process plans from given part designs.
- Investigation of FDL for reusing of existing parts. The existing parts are classified based on features. Two types of constraints are proposed and considered in FDL, which are local and global constraints. Eight manufacturing strategies have been investigated, which can be used to further manufacture various types of existing parts with different constraints relationships.

There is potential to further extend this experimental methodology to develop the knowledge for the iAtractive process that can incorporate more additive, subtractive and inspection units, such as multi-material deposition units, laser-based deposition units and optical scanning measurement devices. The capability and constraints of potentially incorporated units will be taken into consideration in GRP^{2}A and FDL.

9.4 The Part Manufacturing Strategy for the iAtractive Process

The part manufacturing strategy (presented in chapter 5) was investigated, forming the basis for GRP^{2}A and FDL. Manufacturing strategies for the individual FFF and CNC machining processes has been extensively researched. However, a number of new issues have arisen when these two processes are interacting. This investigation was conducted in the following four areas.

9.4.1 Evaluation of dimensional and geometric accuracy of FFF manufactured parts

It has been widely recognised that the accuracy of parts manufactured by FFF is much lower than that of CNC machined parts (Jones *et al.*, 2011). Therefore, additively manufactured features require finish machining in the iAtractive process production. This requires that the printed positive features to be slightly bigger than their nominal sizes (e.g.

the printed dimensions are 1 to 2mm greater than the nominal ones) and positioned in the correct location. In addition, the printed negative features are required to be slightly smaller than their nominal sizes (e.g. the printed dimensions are 1 to 2mm shorter than the nominal ones) and positioned in the correct location, as presented in section 5.4.4. An accuracy index for the FFF process has been developed, which is integrated in GRP^{2}A and FDL, taking dimensional and positioning accuracy into account. The designed dimensions and coordinates for the additive operations are calculated and modified according to the accuracy index, enabling the FFF fabricated features to be finish machined. It should be noted that the experiments in the accuracy evaluation were specifically designed for developing the accuracy index for process planning of the iAtractive process.

The geometric accuracy evaluation results indicate that face milling operations for each layer are not necessary for manufacturing fully dense parts. This finding is also used in the development of the elements (i.e. subpart merging and operation sequencing) in GRP^{2}A. Thus, production times can be significantly reduced compared to the state of the art methods presented by Jeng and Lin (2001), and Karunakaran *et al*. (2010), since the redundant face milling operations for each layer have been removed.

9.4.2 Investigation of FFF capability in producing overhanging features

Overhanging features have been defined in section 5.3.4, which are classified as bridge and cantilever in section 5.5. The capability of the FFF process to produce overhangs has been investigated. A bridge length of 23mm and inclination angle of 60 °has been identified as the longest length and smallest angle that the FFF process can create without support, respectively. Recovery layers have also been defined and explored. These establish the criteria for GRP^{2}A to determine whether or not to use support structures, and to modify features for different operations. The FFF capability and recovery layers are also used in FDL to specify local constraints for selecting feasible manufacturing strategies.

9.4.3 Machinability of plastic layered parts

The machinability of FFF manufactured parts has been explored in section 5.6. A full factorial DoE strategy was employed to design the experiments. A number of slot milling experiments in both dry and wet cutting environments were conducted and the surface roughness was measured. The appropriate machining parameters and their combinations have been identified. The results indicate that selecting lower DoC (e.g. 0.25mm) is more

likely to obtain less surface roughness. Spindle speeds of between 4000 – 5000rpm are recommended alongside high feedrates for reducing machining times whilst not significantly diminishing surface quality. Different parameter combinations are provided in Table 5.5 for machining parts in various stages in the iAtractive process sequence, such as finish machining final parts and subparts, rough machining existing parts and support material. These identified combinations of process parameters are selected in the post-processing stage of GRP^{2}A. Moreover, it was found that friction induced heat is the major factor that affects surface roughness and thus using coolant in finishing operations is required.

9.4.4   Analysis of part distortions

The degree of part distortions has been significantly reduced in commercial additive machines. However, in the iAtractive process, due to temperature gradients involved in the deposition process, thermal stresses develop. These stresses arise from the contraction associated with the deposition of each layer, resulting in distortions or even failure of the deposition process. In addition, the heating and rapid cooling cycles of the material lead to non-uniform thermal gradients that cause continuous stress accumulations, leading to further distortions between the existing part and the part built upon it. The distorted parts require additional machining operations to eliminate the dimensional effects of distortions.

The distortion behaviour was experimentally investigated. A mathematical model was first developed, identifying important process parameters related to warp deformation. A Taguchi DoE strategy was used to design the experiments. The experimental results reveal that:

- The section length and the height of existing part as well as their interaction are of primary significance.
- Long section length and thin existing part are detrimental to dimensional accuracy since a great degree of distortion was observed.
- It is advisable to avoid decomposing long and thin subparts in the part decomposition stage. A layer thickness of 0.25mm if possible, is recommended as it produces the smallest amount of distortion.

It is noted that the distortion behaviours of other materials, such as metals, requires further investigations. This enables GRP^{2}A to be extended for other applications where the

iAtractive process is expected to be applied to. As the surface of the warped part has to be removed, the iAtractive process could be beneficial for developing a model, which is capable of predicting part distortion behaviour, enabling GRP^{2}A to estimate the total amount of material to deposit. This model has the potential to reduce the number of manufacturing operations.

9.5   The Generative Reactionary Process Planning Algorithm

One of the key challenges in the development of GRP^{2}A was to establish a method to sequence additive, subtractive and inspection operations, whilst taking into consideration, the constraints of the individual processes and production times. The developed algorithm, presented in chapter 6, contains two major phases, namely, generation of static and dynamic process plans. A specific static process plan is first generated based on the given part design. The algorithm addresses the cutting tool accessibility, deposition nozzle collisions and production times when generating operation sequences. The method that was proposed to sequence operations, considers individual additive, subtractive and inspection operations in sequence. The additive operations sequences are first determined followed by inserting subtractive operations. The inspection operations are finally added into the sequenced additive and subtractive operations. The three major stages formulate this process planning algorithm.

(i)   Pre-process stage. A CAD model is input into GRP^{2}A and the part geometry is analysed, identifying the potential features that are likely to cause cutting tool collisions.

(ii)   Processing stage. The available operation sequences are scheduled in this stage, which can be further split into the following steps:

- Part decomposition. It has been recognised that the part decomposition results may lead to completely different operation sequences. For example, if test part I in section 8.2 was decomposed into 3 subparts instead of 5, as shown in Figure 9.1, the operation sequences would be different from the sequences generated in section 8.2.5. Part decomposition requires further investigations, which will be presented in section 10.4.2, future work.
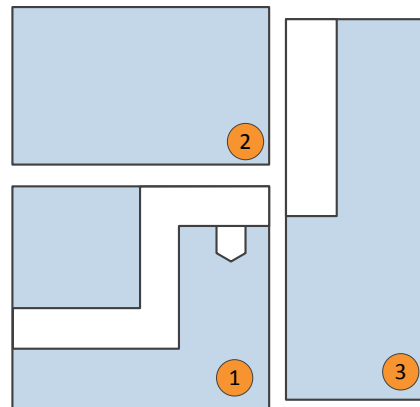
Figure 9.1 – Another possible decomposition result for test part I in section 8.2

- A number of sets of subparts' build directions are determined and each set of build directions contains a unique combination of subparts' build directions and the build direction allocation sequence. The machining operations will then be inserted to these allocation sequences. A valid set of build directions should not include any build directions that are likely to cause deposition nozzle collisions. However, it is noted that the valid sets of build directions may no longer be feasible after inserting machining operations into them.

- Machining operations are required when the features are still accessible by the cutting tool. This enables the manufactured products to be achieved with a high level of accuracy and surface quality comparable to that of an entirely CNC machined parts. Whereas, certain features manufactured by adopting the method developed by Kerbrat *et al.* (2010), presented in section 3.4.4.1 could still remain inaccurate. As certain machined surfaces may require extra finishing operations when subsequent subparts are built, a feasible tool approach direction might not be found, in which case, the operation sequencing based on a certain set of build directions is considered to be failed.

(iii) Post-processing stage. The major activities involved in this stage are outlined as follows:

- Inspection operations are added into the scheduled additive and subtractive operations. As a result, the static operation sequences are obtained.

- Inspection is also the enabler for transforming a static process plan into a dynamic process plan, responding promptly to quality changes during production. Therefore, GRP^{2}A is reactionary. Each inspection operation is the start for the dynamic

process plan if the part is found to be out of tolerance. Implementing the dynamic process plan, which is generated during production, enables the part to be manufactured appropriately, allowing the final product to be achieved with the correct tolerances. Two methods for generating dynamic plans were proposed in section 6.8. It is unclear which method is better and further investigations are thus required.

- Production time estimation. A number of feasible operation sequences to produce a part may exist. In this research, production time is considered to be the major factor that determines the final operation sequence. A build time estimation model has been developed and documented in section 6.10, utilising the most accessible geometrical information i.e. part volume, height, density and intermittent factor. The estimation accuracy can be further improved by involving more FFF process parameters, which will be discussed in the subsequent section.

9.6   The Build Time Estimation Model

A build time estimation model has been developed and it has been identified that the model is able to predict build times and the predicted results do not have a significant difference to the actual times. In comparison to other estimators (Han *et al.*, 2003; Pham and Wang, 2000; Kechagias *et al.*, 2004; Campbell *et al.*, 2008), this developed model offers a time-saving method, which only requires the dimensions of the part, i.e. 2D drawings. This eliminates considerable time used in generating 3D CAD models for each decomposed subpart, generating STL files, slicing and post-processing them for build time calculations. Even though, the method has been applied solely to the FFF process at present, the basic principle of using a 2D drawing to estimate build times is equally applicable to all additive processes.

However, certain issues should be addressed. Firstly, the model shows advantages only for parts in which all the features involved are prismatic features. It is currently not suitable for parts with sculptured surfaces because the intermittent factor cannot precisely represent properties of such structures. The dimensions in the horizontal plane may vary along with the vertical direction depending on the designed sculptured surface. As the iAtractive process is designed primarily for prismatic part production and the majority of engineering parts are prismatic or cylindrical, the estimated build times can be considered as being approximated to the actual times. It is also noted that two or three fully dense layers at the

bottom as well as on the top surface of a part are always required in the deposition process even though a non-fully dense part is specified. For simplifying the process in developing the estimation model, this factor is not taken into account, which, in theory, could lead to increase in incorrect predictions of build times.

In addition, it is worth pointing out that the model is only valid for a particular set up in which the process parameters are kept constant. Any changes in the process parameters, such as increasing layer thickness, printing speed and road width, could result in significant errors since the new set up may require different factors and coefficient for achieving the optimal results. A possible solution to enhance the functionality and accuracy of the model is to employ a correction factor as used by Pham and Wang (2000), which is partly dependent upon the ratio of the part (or parts) volume to the volume of a bounding box around the STL file. The factor thus takes into consideration, part complexity, wall thickness and the number of parts being produced on a build platform.

9.7   The Feature-based Decision-making Logic for Material Reuse

One of the most distinctive advantages of the iAtractive process is that it is not constrained by raw material in terms of shape and size. FDL has been developed and presented in chapter 7, which provides a number of manufacturing strategies to further manufacture existing parts. Existing features are categorised as final features and non-final features. Existing parts are then classified into three types, namely, existing part with non-final features, with final features, and with both non-final and final features. Eight manufacturing strategies have been proposed and investigated, which aim to effectively utilise the given existing part, transforming it into the final part, rather than simply removing the existing features and adding new features onto the machined existing part. In other words, the priority of the first step is to deposit new material onto the existing part. The newly deposited features in conjunction with the existing features enable further material to be added. The existing features are first completely removed only under the circumstances where directly depositing new material onto the existing part leads to deposition nozzle collisions. New nozzle designs will provide further enhancement to the FFF process capability, enabling material to be added onto the existing part with reduced risks of deposition nozzle collisions, providing more manufacturing strategies for reusing existing parts.

Additionally, it is noted that there are potentially unlimited variations of existing parts. For example, for an existing part with a non-final boss as shown in Figure 7.2(a), the existing boss can be of any size located in any random position on any of the six surfaces. Moreover, there can also be two bosses, three bosses and even an arbitrary quantity of bosses. Furthermore, each boss could be at any possible distance. Therefore, a robust decision-making logic is expected to be developed to take this issue into consideration.

Moreover, parts produced from existing parts may not have the same quality compared to the counterparts entirely produced by CNC machining or FFF in terms of part integrity. As discussed in section 6.5.3, the bonding strength between the two connected parts that were deposited in two individual additive operations respectively, is much lower than that of the part produced in one single additive operation. A potential solution to increase bonding strength is to apply the appropriate process parameters for depositing material onto existing parts or using chemical methods to enhance the bonding effect. This requires further investigations.

9.8   Evaluation of the iAtractive Process

The test parts in the case studies described in chapter 8 have been successfully produced by using the iAtractive process according to the process plans generated from GRP^2A and FDL. This demonstrates that the iAtractive process together with the developed GRP^2A and FDL is feasible for producing complex part geometries and reusing existing parts.

9.9   Advantages of the iAtractive Process Consisting of Additive, Subtractive and Inspection Processes

There are a number of advantages in relation to the iAtractive process. Among them, one of the principle advantages is that the iAtractive process is able to produce complex part geometries with high surface quality and accuracy. The iAtractive process is not constrained by the capabilities of the individual constituent processes. GRP^2A is the only viable algorithm developed, facilitating difficult to machine structures to be accurately produced.

Another principle advantage is that the iAtractive process is able to utilise existing parts, transforming them into final parts, which is virtually impossible to create by any other individual manufacturing process. The manufacturing strategies in FDL enable existing

parts to be fully utilised and the iAtractive process is thus not constrained by raw material in terms of shape and size.

In addition, combining the inspection technique enables the iAtractive process to respond promptly to quality changes during production, generating dynamic process plans to further manufacture in-process parts (i.e. the parts during production). Whereas, products that are out of tolerances are simply abandoned, resulting in unnecessary waste and increased production costs.

Moreover, the capabilities of FFF and CNC machining have been taken into consideration in GRP^{2}A and FDL. There is potential that GRP^{2}A and FDL can be extended by involving the capabilities of other additive processes if they are combined and utilised in the iAtractive process. Furthermore, the author believes that this novel concept of hybrid manufacturing, namely, combination of additive, subtractive and inspection processes can be applied to various application areas for manufacturing products made of a wide range of materials.

9.10   Limitations of the iAtractive Process

Despite the fact that the iAtractive process has shown a number of valuable advantages over individual processes, a number of limitations need to be addressed:

- The iAtractive process is currently not applicable to manufacturing of free form sculptured surfaces and other non-prismatic shapes. As GRP^{2}A and FDL have been developed based on prismatic part manufacture, further research needs to be carried out to extend them for manufacturing free form surfaces.
- The current GRP^{2}A still requires human intervention and thus a fully automatic process planning system needs to be developed, realising automatic part production.
- The developed FDL for material reuse does not cover all the possible scenarios where more types of existing parts and variations may exist, as stated in section 9.7. Thus further investigations are required in order to develop a robust decision-making logic capable of dealing with a wide range of existing parts.

10 <u>Conclusions and future work</u>

10.1 Introduction

In this chapter, a series of conclusions that have been derived as a result of this research are provided. The contributions of this research to knowledge are highlighted together with future areas of investigation.

10.2 Conclusions

- Through reviewing the state-of-art hybrid manufacturing processes, the author has identified that although the capability of the individual manufacturing processes have been improved, the hybrid processes are still constrained by the capabilities of the constituent processes as well as raw materials in terms of shape and size. Very limited research has been reported on process planning for hybrid processes.

- A novel concept of hybrid manufacturing process, termed iAtractive, which consists of additive, subtractive and inspection processes, has been proposed. It has been proved that it is not constrained by the capability of the individual constituent processes and raw material in terms of shape and size.

- A structured experimental methodology for the iAtractive process has been designed and verified for generating new knowledge on hybrid manufacturing.

- A Generative Reactionary Process Planning Algorithm (GRP^{2}A) has been developed, capable of organising manufacturing operations and sequences, determining appropriate process parameters, generating static and dynamic process plans for manufacture of complex parts i.e. internal features. The core of GRP^{2}A is the generation of operation sequences and a method was proposed for sequencing additive, subtractive and inspection operations.

- An accuracy index of the FFF process has been developed, which is integrated in GRP^{2}A. The modified dimensions and coordinates of the features to be additively produced can be calculated by applying the index.

- The capability of FFF process in producing overhanging features has been explored, establishing criteria for determining whether or not to construct support structures.

- The machinability of plastic layered parts has been experimentally investigated, identifying a number of sets of appropriate machining parameters that can be used in different machining operations (i.e. roughing and finishing of subparts, existing and final parts) in the iAtractive process.

- The part distortion behaviour has been explored, establishing the relationship related to existing and newly deposited parts. This provides the basis for GRP^{2}A in the operation sequencing stage.

- A build time estimation model has been specifically developed for the iAtractive process. It has been proved that the model is able to estimate build times based on the most accessible geometrical attributes which can be directly obtained from the CAD models or 2D drawings. This estimation model is included in the GRP^{2}A to determine the most appropriate operation sequence in terms of production times.

- Feature-based Decision-making Logic (FDL) has been developed, enabling existing parts to be further manufactured and reincarnated into final parts with desired shapes. It has also been identified that the decision-making logic is restricted by the capability of the FFF process and the current deposition nozzle design.

- A series of case studies have been manufactured using the iAtractive process and the process plans generated by GRP^{2}A and FDL. The designed test parts consisted of internal features and existing parts. The manufactured test parts have shown the successful ability of the iAtractive process in producing complex part geometries and reusing existing parts.

10.3   Contributions to Knowledge

The major contribution to knowledge is the new vision for a hybrid manufacturing process, powered by a Generative Reactionary Process Planning Algorithm and Feature-based Decision-making Logic. The hybrid process is not constrained by the capability of individual processes. The novelty of this research lies within the realisation of a hybrid process that can produce complex part geometries as well as provide the capability to

remanufacture existing parts from a wide range of given raw materials in terms of shape and size.

New knowledge that has been generated in this research is:

• A part manufacturing strategy for manufacturing parts in the hybrid process production scenario where process interaction is taken into consideration.

• Development of a Generative Reactionary Process Planning Algorithm that enables the hybrid process to accurately manufacture complex parts whilst having the capability to respond promptly to quality changes during production.

• Investigation of Feature-based Decision-making Logic that is able to provide viable manufacturing strategies for reusing existing parts and transforming them into final parts with desired shapes and tolerances.

10.4 Future Work

Throughout the course of this research a number of opportunities for extending the work further have been identified.

10.4.1 Extending the application areas of the hybrid process

The iAtractive process is focused on prismatic part production. Given that the manufacturing paradigm is shifting towards bespoke and customisation (Gibson *et al.*, 2009), the iAtractive process will benefit from producing various part geometries, particularly custom-designed geometries. This requires further investigation on intelligent process planning techniques, enabling parts with various structures including free-form sculptured structures to be produced based on more feasible process plans.

10.4.2 Developing a fully automatic process planning system

The current GRP^{2}A still requires human intervention and thus a fully automatic process planning system needs to be developed, realising automatic part production. This can be achieved by the following:

• A feature recognition method. The process planning system to be developed should be able to interpret the given part designs, normally in CAD formats. Due to the

fundamental differences between various manufacturing processes, the recognition methods that are available for one manufacturing process may no longer be feasible for other processes. As the iAtractive process integrates additive, subtractive and inspection processes, a unique feature interpretation approach may be advantageous, requiring further investigations.

- A robust part decomposition approach. As discussed in section 9.5, the output of the part decomposition significantly determines the following steps, particularly the operations to be used and the sequences to be scheduled. Part decomposition requires significant investigation. An ideal part decomposition approach should be capable of decomposing a complex part into a number of subparts whilst taking into consideration the capability of the individual processes. The optimal operation sequences can be realised by scheduling operations for manufacturing these subparts. For instance, the results of the decomposed subparts depicted in Figure 9.1 are better compared with the results presented in Figure 8.4 in terms of production times.

- An adaptive slicing method. An adaptive slicing method for the iAtractive process is needed, which allows varying thicknesses of layers to be deposited. Thick layers can be adopted for the area of the part where no high accuracy and surface quality is required (Kulkarni *et al.*, 2000). Thus build times can be significantly reduced. A potential candidate to be modified is the slicing method proposed by Liou *et al*. (2007), which allows the hybrid process to be used on a 5-axis machining centre where parts can be built by rotating the work table whilst using the adaptive layer thickness.

- Investigation of part distortion behaviour. As discussed in section 9.4.4, the process planning system will be beneficial for developing a model to predict part distortion behaviour. This will enable the process planning system to estimate the total amount of material to deposit and reduce the number of manufacturing operations to be conducted. For instance, in Figure 6.28, after the bottom surface of the parent subpart is machined, more material has to be added if the height of the machined parent subpart is shorter than its designed height. Having added the material onto the machined bottom surface, a finish machining operation is also needed. This significantly increases production time.

- Investigation of bonding strength between two subparts. Bonding strength between two subparts is much lower than one single subpart that is purely built in one additive operation. Parts that consist of two subparts were found to decouple when the cutting tool is close to the boundary where the two subparts are bonded to each other. Bonding strength significantly restricts the application areas of the iAtractive process, which also largely determines part decomposition results. Therefore, bonding strength should be considered in the process planning system and efforts should be made to seek feasible methods to increase bonding strength such as chemical methods.

- A production time estimation model for sculptured surfaces manufacture. As the application areas of the iAtractive process will be further extended, there is a need to develop a production time estimation model capable of predicting production times for production of sculptured surface parts. There is potential to further extend the developed build time estimation model to enhance the functionality and accuracy of the model. This can be achieved by employing a correction factor as used by Pham and Wang (2000), as presented in section 9.6. In addition, the machining time estimation algorithms developed by Heo *et al*. (2006) and So *et al*. (2007) are potential candidates that can be modified for predicting machining times.

- Generation of dynamic process plans. The iAtractive process will benefit from the exploration of a robust strategy for generating dynamic process plans. This strategy should be capable of dealing with quality changes during production. According to the different quality changes, corresponding operations will be implemented to ensure the part being manufactured meets the designed requirements in the least amount of time. This strategy can be applied to scenarios such as the one in section 8.2.6 and Figure 8.19, determining the optimal dynamic process plan.

10.4.3 Investigating robust decision-making logic for reusing materials

As discussed in section 9.7, further efforts should be made on developing a complete decision-making logic, which is capable of generating appropriate operations for further manufacturing any given existing parts that are of arbitrary geometries. The decision-making logic should include a number of criteria for making decisions on how to manufacture existing parts. At present, deposition nozzle accessibility, production time and material consumption are recognised as the three most important factors for consideration

in FDL. In the future, more factors can be included, such as production cost and part strength. Further research should be conducted on investigating bonding strength between existing and newly deposited parts in order to ensure the new part manufactured from the existing part can obtain the same or similar quality as that of a part entirely produced by CNC machining or the FFF process. This is because the bonding strength between the existing and newly deposited parts largely determines the application areas of the iAtractive process in material reuse. Furthermore, a specific deposition tool path generation approach is needed. This approach will be capable of generating tool paths by taking deposition nozzle collisions into account, enabling the nozzle to deposit material onto the existing part whilst not colliding with the existing features.

10.4.4 Exploring a part dematerialisation method

Part dematerialisation can be defined as manufacturing a product with the minimum amount of material possible, without compromising on part integrity or overall functionality. CNC machining is not capable of producing such parts due to limited tool accessibility. However, the iAtractive process enables new opportunities to dematerialise parts by using less material through material re-distribution and re-densification. The existing topology optimisation methods, such as Evolutionary Structural Optimisation (ESO) method (Huang and Xie, 2010) and Solid Isotropic Microstructure with Penalisation (SIMP) (Rozvany, 2009) are potential candidates to be adapted and modified to analyse part structures, identifying structurally efficient designs. For example, ESO is based on the concept of gradually removing inefficient material from a structure so that the residual shape evolves towards the optimum. By applying the ESO technique, the interior porous structure of the part can be obtained, consisting of different areas of material densification. This provides enhanced structural functionality and integrity only where it is actually required in the part.

Figure 10.1 provides an example of the ESO optimised structure, where the interior structure of a solid block (bearing a force F downwards) is optimised to the structure as shown on the right hand side. This example indicates that the total amount of material can be significantly reduced by using the ESO method. The iAtractive process will create the internal structure of subparts by using the FFF process. CNC machining can be applied to finish machining the exterior structure of the dematerialised subparts.
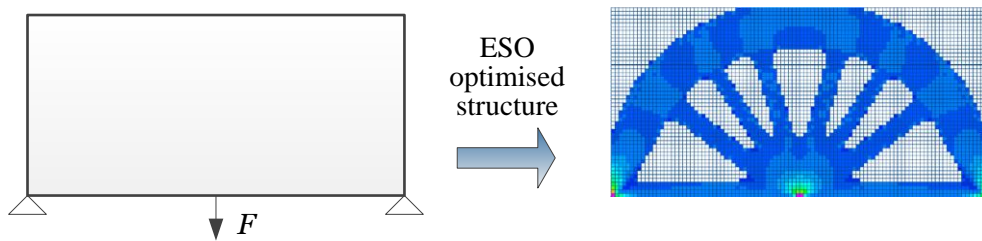
Figure 10.1 – An ESO optimised structure for a rectangular block

10.4.5 Hardware development

The capability of the iAtractive process can be further enhanced with additional hardware development. An improved deposition nozzle design will enhance the iAtractive process capability. An example can be found in Figure 3.13 where material can be directly added onto any accessible surfaces (Lanzetta and Cutkosky, 2008). This enhanced capability will enable more feasible operation sequences to be realised in scheduling additive and subtractive operations as well as providing more manufacturing strategies to remanufacture existing parts. A machine prototype consisting of a number of additive (material deposition based and laser based), subtractive and inspection units is expected to be developed, realising automatic interchangeable additive, subtractive and inspection processes. Thus, the vision of the unconstrained hybrid process presented in this thesis can be realised.

References

Akula, S. and Karunakaran, K.P., 2006. Hybrid adaptive layer manufacturing: An intelligent art of direct metal rapid tooling process. *Robotics and Computer-Integrated Manufacturing,* 22(2), pp.113-123.

Ali, L., 2005. *Development of a step-nc compliant feature-based inspection framework for prismatic parts*. Loughborough University, Loughborough, UK,

Allahverdi, M., Jadidian, B., Harper, B., Rangarajan, S., Jafari, M., Danforth, S.C. and Safari, A., 2000. Development of tube actuators with helical electrodes using fused deposition of ceramics. Proceedings of the 2000 12th Ieee International Symposium on Applications of Ferroelectrics, Vols I and Ii, Hawaii, USA. pp.381-384. 21 July - 2 August, 2010

Alting, L. and Zhang, H., 1989. Computer aided process planning: The state-of-the-art survey. *The International Journal of Production Research,* 27(4), pp.553-585.

Amstead, B.H., Ostwaid, P.F. and Begeman, M.L., 1987. *Manufacturing processes,* 8th edition. United States: John Wiley & Sons, Inc.

Anderson, M., Patwa, R. and Shin, Y.C., 2006. Laser-assisted machining of inconel 718 with an economic analysis. *International Journal of Machine Tools & Manufacture,* 46(14), pp.1879-1891.

Anderson, M.C. and Shin, Y.C., 2006. Laser-assisted machining of an austenitic stainless steel: P550. *Proceedings of the Institution of Mechanical Engineers Part B-Journal of Engineering Manufacture,* 220(12), pp.2055-2067.

Anitha, R., Arunachalam, S. and Radhakrishnan, P., 2001. Critical parameters influencing the quality of prototypes in fused deposition modelling. *Journal of Materials Processing Technology,* 118(1-3), pp.385-388.

Araghi, B.T., Manco, G.L., Bambach, M. and Hirt, G., 2009. Investigation into a new hybrid forming process: Incremental sheet forming combined with stretch forming. *CIRP Annals-Manufacturing Technology,* 58(1), pp.225-228.

Aspinwall, D.K., Dewes, R.C., Burrows, J.M. and Paul, M.A., 2001. Hybrid high speed machining (hsm): System design and experimental results for grinding/hsm and edm/hsm. *CIRP Annals-Manufacturing Technology,* 50(1), pp.145-148.

Axinte, D.A. and Gindy, N., 2004. Turning assisted with deep cold rolling - a cost efficient hybrid process for workpiece surface quality enhancement. *Proceedings of the Institution of Mechanical Engineers Part B-Journal of Engineering Manufacture,* 218(7), pp.807-811.

Azarhoushang, B. and Akbari, J., 2007. Ultrasonic-assisted drilling of inconel 738-lc. *International Journal of Machine Tools & Manufacture,* 47(7-8), pp.1027-1033.

Baesso, R. and Lucchetta, G., 2007. Fluid structure interaction analysis in manufacturing metal/polymer macro-composites, Numiform '07: Materials processing and design: Modeling, simulation and applications, pts i and ii. Melville: Amer Inst Physics.

Bagshaw, R.W., 1999. *Production data analysis for discrete component manufacture.* Loughborough University, Loughborough, UK,

Bang, H.S., Kim, Y.C. and Joo, S.M., 2010. Analysis of residual stress on ah32 butt joint by hybrid co2 laser-gma welding. *Computational Materials Science,* 49(2), pp.217-221.

Bariani, P.F., Bruschi, S., Ghiotti, A. and Lucchetta, G., 2007. An approach to modelling the forming process of sheet metal-polymer composites. *CIRP Annals-Manufacturing Technology,* 56(1), pp.261-264.

Barnes, C., Shrotriya, P. and Molian, P., 2007. Water-assisted laser thermal shock machining of alumina. *International Journal of Machine Tools & Manufacture,* 47(12-13), pp.1864-1874.

Bejjani, R., Shi, B., Attia, H. and Balazinski, M., 2011. Laser assisted turning of titanium metal matrix composite. *CIRP Annals-Manufacturing Technology,* 60(2), pp.61-64.

Bellini, A. and Guceri, S., 2003. Mechanical characterization of parts fabricated using fused deposition modeling. *Rapid Prototyping Journal,* 9(4), pp.252-264.

Ben Fredj, N., Sidhom, H. and Braham, C., 2006. Ground surface improvement of the austenitic stainless steel aisi 304 using cryogenic cooling. *Surface & Coatings Technology,* 200(16-17), pp.4846-4860.

Bhattacharyya, B., Doloi, B.N. and Sorkhel, S.K., 1999. Experimental investigations into electrochemical discharge machining (ecdm) of non-conductive ceramic materials. *Journal of Materials Processing Technology,* 95(1-3), pp.145-154.

Biermann, D. and Heilmann, M., 2011. Analysis of the laser drilling process for the combination with a single-lip deep hole drilling process with small diameters. *Physics Procedia,* 12, pp.311-319.

Biermann, T., Göttmann, A., Zettler, J., Bambach, M., Weisheit, A., Hirt, G. and Poprawe, R., 2009. Hybrid laser assisted incremental sheet forming: Improving formability of ti-and mg-based alloys. Laser in Manufacturing, Munchen, Germany. pp.pp. 273-278. 15 - 18 June 2009

Bingham, G.A., Hague, R.J.M., Tuck, C.J., Long, A.C., Crookston, J.J. and Sherburn, M.N., 2007. Rapid manufactured textiles. *International Journal of Computer Integrated Manufacturing,* 20(1), pp.96-105.

Brajlih, T., Valentan, B., Balic, J. and Drstvensek, I., 2011. Speed and accuracy evaluation of additive manufacturing machines. *Rapid Prototyping Journal,* 17(1), pp.64-75.

Brecher, C. and Emonts, M., 2010. Laser-assisted shearing: New process developments for the sheet metal industry. *International Journal of Advanced Manufacturing Technology,* 48(1-4), pp.133-141.

Brecher, C., Esser, M. and Witt, S., 2009. Interaction of manufacturing process and machine tool. *CIRP Annals-Manufacturing Technology,* 58(2), pp.588-607.

Brecher, C., Rosen, C.J. and Emonts, M., 2010a. Laser-assisted milling of advanced materials. *Physics Procedia*. Laser Assisted Net Shape Engineering 6, Proceedings of the Lane 2010, Part 2, Amsterdam. pp.259-272. 21 - 24 September, 2010

Brecher, C., Schug, R., Weber, A., Wenzel, C. and Hannig, S., 2010b. New systematic and time-saving procedure to design cup grinding wheels for the application of ultrasonic-assisted grinding. *International Journal of Advanced Manufacturing Technology,* 47(1-4), pp.153-159.

Brinksmeier, E. and Brockhoff, T., 1996. Utilization of grinding heat as a new heat treatment process. *CIRP Annals-Manufacturing Technology,* 45(1), pp.283-286.

BS ISO 5725-1:1994, 1994. Accuracy (trueness and precision) of measurement methods and results - part 1: General principles and definitions.

Campana, G., Fortunato, A., Ascari, A., Tani, G. and Tomesani, L., 2007. The influence of arc transfer mode in hybrid laser-mig welding. *Journal of Materials Processing Technology,* 191(1-3), pp.111-113.

Campanelli, S.L., Cardano, G., Giannoccaro, R., Ludovico, A.D. and Bohez, E.L.J., 2007. Statistical analysis of the stereolithographic process to improve the accuracy. *Computer-Aided Design,* 39(1), pp.80-86.

Campbell, I., Combrinck, J., de Beer, D. and Barnard, L., 2008. Stereolithography build time estimation based on volumetric calculations. *Rapid Prototyping Journal,* 14(5), pp.271-279.

Casalino, G., 2007. Statistical analysis of mig-laser co2 hybrid welding of al-mg alloy. *Journal of Materials Processing Technology,* 191(1-3), pp.106-110.

Case, K. and Gao, J., 1993. Feature technology: An overview. *International Journal of Computer Integrated Manufacturing,* 6(1-2), pp.2-12.

Chak, S.K. and Rao, P.V., 2007. Trepanning of al2o3 by electro-chemical discharge machining (ecdm) process using abrasive electrode with pulsed dc supply. *International Journal of Machine Tools & Manufacture,* 47(14), pp.2061-2070.

Chang, T.C. and Wysk, R.A., 1984. *An introduction to automated process planning systems,* New York: Prentice Hall Professional Technical Reference.

Cheah, C.M., Chua, C.K., Lee, C.W., Feng, C. and Totong, K., 2005. Rapid prototyping and tooling techniques: A review of applications for rapid investment casting. *International Journal of Advanced Manufacturing Technology,* 25(3-4), pp.308-320.

Chen, J.S.S. and Feng, H.Y., 2011. Contour generation for layered manufacturing with reduced part distortion. *International Journal of Advanced Manufacturing Technology,* 53(9-12), pp.1103-1113.

Chen, Y.H. and Song, Y., 2001. The development of a layer based machining system. *Computer-Aided Design,* 33(4), pp.331-342.

Chikamori, K., 1991. Grooving on silicon-nitride ceramics with arc discharge in electrolyte. *International journal of the Japan Society for Precision Engineering,* 25(2), pp.109-110.

Chin, R., Beuth, J. and Amon, C., 2001. Successive deposition of metals in solid freeform fabrication processes, part 1: Thermomechanical models of layers and droplet columns. *Journal of manufacturing science and engineering,* 123(4), pp.623-638.

Choi, D.S., Lee, S.H., Shin, B.S., Whang, K.H., Song, Y.A., Park, S.H. and Jee, H.S., 2001. Development of a direct metal freeform fabrication technique using co2 laser welding and milling technology. *Journal of Materials Processing Technology,* 113(1-3), pp.273-279.

Chua, C., Leong, K. and Lim, C., 2003. *Rapid prototyping: Principles and applications,* World Scientific Publishing Company.

CIRP,2011. CIRP - the internal academy for production engineering [Online]. Available from [www.cirp.net], accessed on 14 May 2011.

Colwell, L., 1956. The effects of high-frequency vibrations in grinding. *Trans. ASME,* 78, pp.837.

Cook, N.H., Foote, G.B., Jordan, P. and Kalyani, B.N., 1973. Experimental studies in electro-machining. *Journal of Engineering for Industry-Transactions of the Asme,* 95(4), pp.945-950.

Cooper, A.G., Kang, S., Kietzman, J.W., Prinz, F.B., Lombardi, J.L. and Weiss, L.E., 1999. Automated fabrication of complex molded parts using mold shape deposition manufacturing. *Materials & Design,* 20(2-3), pp.83-89.

Curtis, D.T., Soo, S.L., Aspinwall, D.K. and Sage, C., 2009. Electrochemical superabrasive machining of a nickel-based aeroengine alloy using mounted grinding points. *CIRP Annals-Manufacturing Technology,* 58(1), pp.173-176.

Dalgarno, K., Childs, T., Rowntree, I. and Rothwell, L., 1996. Finite element analysis of curl development in the selective laser sintering process. Proceedings of Solid freeform fabrication symposium, University of Texas, Austin, TX, pp.559-566.

Dandekar, C.R., Shin, Y.C. and Barnes, J., 2010. Machinability improvement of titanium alloy (ti-6al-4v) via lam and hybrid machining. *International Journal of Machine Tools & Manufacture,* 50(2), pp.174-182.

de Lacalle, L.N.L., Perez-Bilbatua, J., Sanchez, J.A., Llorente, J.I., Gutierrez, A. and Alboniga, J., 2000. Using high pressure coolant in the drilling and turning of low

machinability alloys. *International Journal of Advanced Manufacturing Technology,* 16(2), pp.85-91.

de Lacalle, L.N.L., Sanchez, J.A., Lamikiz, A. and Celaya, A., 2004. Plasma assisted milling of heat-resistant superalloys. *Journal of Manufacturing Science and Engineering-Transactions of the Asme,* 126(2), pp.274-285.

De Silva, A., Pajak, P., McGeough, J. and Harrison, D., 2011. Thermal effects in laser assisted jet electrochemical machining. *CIRP Annals-Manufacturing Technology,* 60(2), pp.243-246.

De Silva, A.K.M., Pajak, P.T., Harrison, D.K. and McGeough, J.A., 2004. Modelling and experimental investigation of laser assisted jet electrochemical machining. *CIRP Annals-Manufacturing Technology,* 53(1), pp.179-182.

Delcam,2012. Powermill cam software [Online]. Available from [http://www.delcam.co.uk/], accessed on 22 August 2012.

Dhokia, V.G., 2009. *The cryogenic CNC machining of soft materials*. Thesis (Ph.D). University of Bath, Bath, UK.

Dhokia, V.G., Kumar, S., Vichare, P., Newman, S.T. and Allen, R.D., 2008. Surface roughness prediction model for CNC machining of polypropylene. *Proceedings of the Institution of Mechanical Engineers Part B-Journal of Engineering Manufacture,* 222(2), pp.137-153.

Dhokia, V.G., Newman, S.T., Crabtree, P. and Ansell, M.P., 2010. A methodology for the determination of foamed polymer contraction rates as a result of cryogenic CNC machining. *Robotics and Computer-Integrated Manufacturing,* 26(6), pp.665-670.

Dhokia, V.G., Newman, S.T., Crabtree, P. and Ansell, M.P., 2011. Adiabatic shear band formation as a result of cryogenic CNC machining of elastomers. *Proceedings of the Institution of Mechanical Engineers, Part B: Journal of Engineering Manufacture,* 225(9), pp.1482-1492.

Dimitrov, D., van Wijck, W., Schreve, K. and de Beer, N., 2006. Investigating the achievable accuracy of three dimensional printing. *Rapid Prototyping Journal,* 12(1), pp.42-52.

Ding, H.T. and Shin, Y.C., 2010. Laser-assisted machining of hardened steel parts with surface integrity analysis. *International Journal of Machine Tools & Manufacture,* 50(1), pp.106-114.

Ding, H.T. and Shin, Y.C., 2013. Improvement of machinability of waspaloy via laser-assisted machining. *International Journal of Advanced Manufacturing Technology,* 64(1-4), pp.475-486.

DMG,2011. Lasertec [Online]. Available from [http://www.dmg.com/home,en/], accessed on 23 March 2011.

Dollar, A.M. and Howe, R.D., 2006. A robust compliant grasper via shape deposition manufacturing. *Ieee-Asme Transactions on Mechatronics,* 11(2), pp.154-161.

Dollar, A.M., Wagner, C.R., Howe, R.D. and Ieee, 2006. *Embedded sensors for biomimetic robotics via shape deposition manufacturing, 2006 1st ieee ras-embs international conference on biomedical robotics and biomechatronics, vols 1-3.*

Duflou, J.R., Callebaut, B., Verbert, J. and De Baerdemaeker, H., 2007. Laser assisted incremental forming: Formability and accuracy improvement. *CIRP Annals-Manufacturing Technology,* 56(1), pp.273-276.

Duflou, J.R., Callebaut, B., Verbert, J. and De Baerdemaeker, H., 2008. Improved spif performance through dynamic local heating. *International Journal of Machine Tools & Manufacture,* 48(5), pp.543-549.

Dumitrescu, P., Koshy, P., Stenekes, J. and Elbestawi, M.A., 2006. High-power diode laser assisted hard turning of aisi d2 tool steel. *International Journal of Machine Tools & Manufacture,* 46(15), pp.2009-2016.

ElMaraghy, H.A., 1993. Evolution and future perspectives of capp. *CIRP Annals-Manufacturing Technology,* 42(2), pp.739-751.

Emmens, W.C., Sebastiani, G. and van den Boogaard, A.H., 2010. The technology of incremental sheet forming-a brief review of the history. *Journal of Materials Processing Technology,* 210(8), pp.981-997.

Ezugwu, E.O., Da Silva, R.B., Bonney, J. and Machado, A.R., 2005. Evaluation of the performance of cbn tools when turning ti-6al-4v alloy with high pressure coolant supplies. *International Journal of Machine Tools & Manufacture,* 45(9), pp.1009-1014.

Fathima, K., Rahman, M., Kumar, A.S. and Lim, H.S., 2007. Modeling of ultra-precision elid grinding. *Journal of Manufacturing Science and Engineering-Transactions of the Asme,* 129(2), pp.296-302.

Fernandes, K.J. and Raja, V.H., 2000. Incorporated tool selection system using object technology. *International Journal of Machine Tools & Manufacture,* 40(11), pp.1547-1555.

Fessler, J., Nickel, A., Link, G., Prinz, F. and Fussell, P., 1997. Functional gradient metallic prototypes through shape deposition manufacturing, Solid freeform fabrication proceedings, september 1997. Austin: Univ Texas Austin.

Fonda, P., Nakamoto, K., Heidari, A., Yang, H.-A., Horsley, D.A., Lin, L. and Yamazaki, K., 2013. A study on the optimal fabrication method for micro-scale gyroscopes using a hybrid process consisting of electric discharge machining, chemical etching or micro-mechanical milling. *CIRP Annals-Manufacturing Technology (in press),*

Fuller, S.B., Wilhelm, E.J. and Jacobson, J.M., 2002. Ink-jet printed nanoparticle microelectromechanical systems. *Journal of Microelectromechanical Systems,* 11(1), pp.54-60.

Galdos, L., Sukia, A., Otegi, N., Ortubay, R., De La Torre, A.R., Forgas, A. and Rastellini, F., 2010. Enhancement of incremental sheet metal forming technology by means of stretch forming. *AIP Conference Proceedings*. International Conference on Advances in Materials and Processing Technologies (AMPT2010), Pts One and Two, Paris, France. pp.601-606. 24 - 27 October, 2010

Gasdaska, C., Clancy, R., Ortiz, M., Jamalabad, V., Virkar, A. and Popovitch, D., 1998. Functionally optimized ceramic structures. *Solid Freeform Fabrication Proceedings (Series)*. Solid Freeform Fabrication Proceedings, August, 1998, Austin. pp.705-712. 25 - 26 August

Geiger, M., Merklein, M. and Kerausch, M., 2004. Finite element simulation of deep drawing of tailored heat treated blanks. *CIRP Annals-Manufacturing Technology,* 53(1), pp.223-226.

Gibson, I., Rosen, D.W. and Stucker, B., 2009. *Additive manufacturing technologies: Rapid prototyping to direct digital manufacturing,* Springer.

Goujon, C., Goeuriot, P., Delcroix, P. and Le Caer, G., 2001. Mechanical alloying during cryomilling of a 5000 al alloy/aln powder: The effect of contamination. *Journal of Alloys and Compounds,* 315(1-2), pp.276-283.

Guo, Y., Li, W., Mileham, A.R. and Owen, G.W., 2009. Applications of particle swarm optimisation in integrated process planning and scheduling. *Robotics and Computer-Integrated Manufacturing,* 25(2), pp.280-288.

Halevi, G. and Weill, R.D., 1995. *Principles of process planning: A logical approach,* London: Chapman & Hall.

Han, W.B., Fafari, M.A. and Seyed, K., 2003. Process speeding up via deposition planning in fused deposition-based layered manufacturing processes. *Rapid Prototyping Journal,* 9(4), pp.212-218.

Hayes, D.J., Cox, W.R. and Grove, M.E., 1998. Micro-jet printing of polymers and solder for electronics manufacturing. *Journal of Electronics Manufacturing,* 8(3-4), pp.209-216.

Heisel, U., Wallaschek, J., Eisseler, R. and Potthast, C., 2008. Ultrasonic deep hole drilling in electrolytic copper ecu 57. *CIRP Annals-Manufacturing Technology,* 57(1), pp.53-56.

Heo, E.Y., Kim, D.W., Kim, B.H. and Chen, F.F., 2006. Estimation of nc machining time using nc block distribution for sculptured surface machining. *Robotics and Computer-Integrated Manufacturing,* 22(5-6), pp.437-446.

Holman, J.P., 2001. *Experimental methods for engineers,* 7th ed. McGraw-Hill Ltd.

Holtkamp, J., Roesner, A. and Gillner, A., 2010. Advances in hybrid laser joining. *International Journal of Advanced Manufacturing Technology,* 47(9-12), pp.923-930.

Hong, S.Y. and Ding, Y., 2001. Micro-temperature manipulation in cryogenic machining of low carbon steel. *Journal of Materials Processing Technology,* 116(1), pp.22-30.

Hong, S.Y., Markus, I. and Jeong, W., 2001. New cooling approach and tool life improvement in cryogenic machining of titanium alloy ti-6al-4v. *International Journal of Machine Tools & Manufacture,* 41(15), pp.2245-2260.

Hu, Z. and Lee, K., 2005. Concave edge-based part decomposition for hybrid rapid prototyping. *International Journal of Machine Tools & Manufacture,* 45(1), pp.35-42.

Huang, H., Zhang, H., Zhou, L. and Zheng, H.Y., 2003. Ultrasonic vibration assisted electro-discharge machining of microholes in nitinol. *Journal of Micromechanics and Microengineering,* 13(5), pp.693-700.

Huang, X. and Xie, M., 2010. *Evolutionary topology optimization of continuum structures: Methods and applications,* Wiley.

Hur, J.H., Lee, J., Zhu, h. and Kim, J., 2002. Hybrid rapid prototyping system using machining and deposition. *Computer-Aided Design,* 34(10), pp.741-754.

ISO 14649:10, 2002. Industrial automation systems and integration -- physical device control -- data model for computerized numerical controllers -- part 10: General process data.

Jafari, M.A., Han, W., Mohammadi, F., Safari, A., Danforth, S.C. and Langrana, N., 2000. A novel system for fused deposition of advanced multiple ceramics. *Rapid Prototyping Journal,* 6(3), pp.161-174.

Jahan, M.P., Saleh, T., Rahman, M. and Wong, Y.S., 2010. Development, modeling, and experimental investigation of low frequency workpiece vibration-assisted micro-edm of tungsten carbide. *Journal of Manufacturing Science and Engineering-Transactions of the Asme,* 132(5), pp.054503.1-054503.8.

Jamshidi, H. and Nategh, M.J., 2013. Theoretical and experimental investigation of the frictional behavior of the tool-chip interface in ultrasonic-vibration assisted turning. *International Journal of Machine Tools & Manufacture,* 65, pp.1-7.

Jandric, Z., Labudovic, M. and Kovacevic, R., 2004. Effect of heat sink on microstructure of three-dimensional parts built by welding-based deposition. *International Journal of Machine Tools & Manufacture,* 44(7-8), pp.785-796.

Jeng, J.Y. and Lin, M.C., 2001. Mold fabrication and modification using hybrid processes of selective laser cladding and milling. *Journal of Materials Processing Technology,* 110(1), pp.98-103.

Jia, X.H., Zhang, J.H. and Ai, X., 1997. Study on a new kind of combined machining technology of ultrasonic machining and electrical discharge machining. *International Journal of Machine Tools & Manufacture,* 37(2), pp.193-199.

Jin, G.Q., Li, W.D. and Gao, L., 2013. An adaptive process planning approach of rapid prototyping and manufacturing. *Robotics and Computer-Integrated Manufacturing,* 29(1), pp.23-38.

Jones, R., Haufe, P., Sells, E., Iravani, P., Olliver, V., Palmer, C. and Bowyer, A., 2011. Reprap - the replicating rapid prototyper. *Robotica,* 29, pp.177-191.

Jones, R.O., 2013. *Additive manufacturing of functional engineering components*. Thesis (Ph.D). University of Bath, Bath, UK.

Jung, J.W., Choi, J.Y. and Lee, C.M., 2013. A study on laser assisted machining using a laser area analysis method. *International Journal of Precision Engineering and Manufacturing,* 14(2), pp.329-332.

Kalpakjian, S. and Schmid, S., 2010. *Manufacturing engineering and technology,* 6th edition. Singapore: Pearson.

Kalyanasundaram, D., Shehata, G., Neumann, C., Shrotriya, P. and Molian, P., 2008. Design and validation of a hybrid laser/water-jet machining system for brittle materials. *Journal of Laser Applications,* 20(2), pp.127-134.

Kalyanasundaram, D., Shrotriya, P. and Molian, P., 2010. Fracture mechanics-based analysis for hybrid laser/waterjet (lwj) machining of yttria-partially stabilized zirconia (y-psz). *International Journal of Machine Tools & Manufacture,* 50(1), pp.97-105.

Karapatis, N., Van Griethuysen, J. and Glardon, R., 1998. Direct rapid tooling: A review of current research. *Rapid Prototyping Journal,* 4(2), pp.77-89.

Karunakaran, K., Pushpa, V., Akula, S. and Suryakumar, S., 2008. Techno-economic analysis of hybrid layered manufacturing. *International Journal of Intelligent Systems Technologies and Applications,* 4(1), pp.161-176.

Karunakaran, K., Suryakumar, S., Pushpa, V. and Akula, S., 2010. Low cost integration of additive and subtractive processes for hybrid layered manufacturing. *Robotics and Computer-Integrated Manufacturing,* 26 (2010), pp.490-499.

Karunakaran, K.P., Sreenathbabu, A. and Pushpa, V., 2004. Hybrid layered manufacturing: Direct rapid metal tool-making process. *Proceedings of the Institution of Mechanical Engineers Part B-Journal of Engineering Manufacture,* 218(12), pp.1657-1665.

Karunakaran, K.P., Suryakumar, S., Pushpa, V. and Akula, S., 2009. Retrofitment of a CNC machine for hybrid layered manufacturing. *International Journal of Advanced Manufacturing Technology,* 45(7-8), pp.690-703.

Kechagias, J., Maropoulos, S. and Karagiannis, S., 2004. Process build-time estimator algorithm for laminated object manufacturing. *Rapid Prototyping Journal,* 10(5), pp.297-304.

Kelkar, A. and Koc, B., 2008. Geometric planning and analysis for hybrid re-configurable molding and machining process. *Rapid Prototyping Journal,* 14(1), pp.23-34.

Kelkar, A., Nagi, R. and Koc, B., 2005. Geometric algorithms for rapidly reconfigurable mold manufacturing of free-form objects. *Computer-Aided Design,* 37(1), pp.1-16.

Kerbrat, O., Mognol, P. and Hascoet, J., 2010. Manufacturing complexity evaluation at the design stage for both machining and layered manufacturing. *CIRP Journal of Manufacturing Science and Technology,* 59(2), pp.208-215.

Kerbrat, O., Mognol, P. and Hascoet, J.Y., 2011. A new dfm approach to combine machining and additive manufacturing. *Computers in Industry,* 62(7), pp.684-692.

Kim, S., Kim, B.H., Chung, D.K., Shin, H.S. and Chu, C.N., 2010. Hybrid micromachining using a nanosecond pulsed laser and micro edm. *Journal of Micromechanics and Microengineering,* 20(1), pp.015037(8pp).

Kiritsis, D., 1995. A review of knowledge-based expert systems for process planning. Methods and problems. *The International Journal of Advanced Manufacturing Technology,* 10(4), pp.240-262.

Klingbeil, N.W., Beuth, J.L., Chin, R.K. and Amon, C.H., 1998. Measurement and modeling of residual stress-induced warping in direct metal deposition processes, Solid freeform fabrication proceedings, august, 1998. Austin: Univ Texas Austin.

Klocke, F., Dambon, O., Bulla, B. and Heselhaus, M., 2009. Direct diamond turning of steel molds for optical replication. Proceedings of SPIE (Vol. 7283), Chengdu, China. 22 - 24 May, 2009

Klocke, F., Roderburg, A. and Zeppenfeld, C., 2011. Design methodology for hybrid production processes. *Procedia Engineering,* 9, pp.417-430.

Klocke, F., Wegner, H., Roderburg, A. and Nau, B., 2010. Ramp-up of hybrid manufacturing technologies. Proceedings of 43rd CIRP Conference on Manufacturing Systems, Vienna, Austria. pp.407-415.

Kolleck, R., Vollmer, R. and Veit, R., 2011. Investigation of a combined micro-forming and punching process for the realization of tight geometrical tolerances of conically formed hole patterns. *CIRP Annals-Manufacturing Technology,* 60(2), pp.331-334.

Komanduri, R., Lucca, D.A., Tani, Y. and Int Inst Prod Engn Res, I.I.P.E.R., 1997. Technological advances in fine abrasive processes. *CIRP Annals 1997 - Manufacturing Technology, Volume 46/2/1997 - Annals of the International Institution for Production Engineering Research*, pp.545-596.

Kozak, J. and Oczos, K.E., 2001. Selected problems of abrasive hybrid machining. *Journal of Materials Processing Technology,* 109(3), pp.360-366.

Kozak, J., Rajurkar, K. and Santhanam, P., 2003. Study of self-dressing and sequence of operations in abrasive electro discharge grinding (aedg). *Computer Aided Production Engineering: CAPE 2003*, pp.401.

Kozak, J. and Rajurkar, K.P., 2000. Hybrid machining process evaluation and development. Proceedings of 2nd International Conference on Machining and Measurements of Sculptured Surfaces, Keynote Paper, Krakow, Poland. pp.501-536. 20 - 22 September, 2000

Krain, H.R., Sharman, A.R.C. and Ridgway, K., 2007. Optimisation of tool life and productivity when end milling inconel 718tm. *Journal of Materials Processing Technology,* 189(1-3), pp.153-161.

Kramar, D., Krajnik, P. and Kopac, J., 2010. Capability of high pressure cooling in the turning of surface hardened piston rods. *Journal of Materials Processing Technology,* 210(2), pp.212-218.

Kratky, A., Liedl, G. and Bielak, R., 2004. Ladd-laser assisted deep drawing. *Geiger, M und A Otto (Herausgeber): Laser Assisted Net Shape Engineering,* 4, pp.1125–1134.

Kray, D., Hopman, S., Spiegel, A., Richerzhagen, B. and Willeke, G.P., 2007. Study on the edge isolation of industrial silicon solar cells with waterjet-guided laser. *Solar Energy Materials and Solar Cells,* 91(17), pp.1638-1644.

Kulkarni, P., Marsan, A. and Dutta, D., 2000. A review of process planning techniques in layered manufacturing. *Rapid Prototyping Journal,* 6(1), pp.18-35.

Kumar, G.P. and Regalla, S.P., 2012. Optimization of support material and build time in fused deposition modeling (fdm), Mechanical and aerospace engineering, pts 1-7. Stafa-Zurich: Trans Tech Publications Ltd.

Kumar, K. and Choudhury, S.K., 2008. Investigation of tool wear and cutting force in cryogenic machining using design of experiments. *Journal of Materials Processing Technology,* 203(1-3), pp.95-101.

Kumar, M., Melkote, S. and Lahoti, G., 2011. Laser-assisted microgrinding of ceramics. *CIRP Annals-Manufacturing Technology,* 60(2), pp.367-370.

Kumar, S., 2008. *Step-nc compliant process control for CNC manufacture*. Thesis (Ph.D). University of Bath, Bath, UK.

Kuo, C.L., Huang, J.D. and Liang, H.Y., 2002. Precise micro-assembly through an integration of micro-edm and nd-yag. *International Journal of Advanced Manufacturing Technology,* 20(6), pp.454-458.

Kuo, C.L., Huang, J.D. and Liang, H.Y., 2003. Fabrication of 3d metal microstructures using a hybrid process of micro-edm and laser assembly. *International Journal of Advanced Manufacturing Technology,* 21(10-11), pp.796-800.

Kwon, Y.J., Ertekin, Y.M. and Tseng, B., 2005. In-process and post-process quantification of machining accuracy in circular CNC milling. *Machining Science and Technology,* 9(1), pp.27-38.

Lam, S. and Wong, T., 2000. Recognition of machining features-a hybrid approach. *International Journal of Production Research,* 38(17), pp.4301-4316.

Lanzetta, M. and Cutkosky, M.R., 2008. Shape deposition manufacturing of biologically inspired hierarchical microstructures. *CIRP Annals-Manufacturing Technology,* 57(1), pp.231-234.

Lauwers, B., Klocke, F. and Klink, A., 2010. Advanced manufacturing through the implementation of hybrid and media assisted processes. International Chemnitz Manufacturing Colloquium, ICMC2010, Chemnitz. pp.205 - 220. 29 - 30 September, 2010

Lauwers, B., Plakhotnik, D., Vanparys, M. and Liu, W., 2008. Tool path generation functionality and ultrasonic assisted machining of ceramic components using multi-axis machine tools. Proceedings of the MTTRF 2008 Annual Meeting, San Francisco, USA. pp.133-152. 1 - 2 July, 2008

Lee, C., Kim, S., Kim, H. and Ahn, S., 2007. Measurement of anisotropic compressive strength of rapid prototyping parts. *Journal of Materials Processing Technology,* 187, pp.627-630.

Lee, D.H., Kiritsis, D. and Xirouchakis, P., 2004. Iterative approach to operation selection and sequencing in process planning. *International Journal of Production Research,* 42(22), pp.4745-4766.

Lee, H.S. and Jeong, H.D., 2009. Chemical and mechanical balance in polishing of electronic materials for defect-free surfaces. *CIRP Annals-Manufacturing Technology,* 58(1), pp.485-490.

Lei, S., Shin, Y.C. and Incropera, F.P., 2001. Experimental investigation of thermo-mechanical characteristics in laser-assisted machining of silicon nitride ceramics. *Journal of Manufacturing Science and Engineering-Transactions of the Asme,* 123(4), pp.639-646.

Leshock, C.E., Kim, J.N. and Shin, Y.C., 2001. Plasma enhanced machining of inconel 718: Modeling of workpiece temperature with plasma heating and experimental results. *International Journal of Machine Tools & Manufacture,* 41(6), pp.877-897.

Levy, G.N., Schindel, R. and Kruth, J.P., 2003. Rapid manufacturing and rapid tooling with layer manufacturing (lm) technologies, state of the art and future perspectives. *CIRP Annals-Manufacturing Technology,* 52(2), pp.589-609.

Li, C.F., Johnson, D.B. and Kovacevic, R., 2003. Modeling of waterjet guided laser grooving of silicon. *International Journal of Machine Tools & Manufacture,* 43(9), pp.925-936.

Li, L. and Achara, C., 2004. Chemical assisted laser machining for the minimisation of recast and heat affected zone. *CIRP Annals-Manufacturing Technology,* 53(1), pp.175-178.

Li, L., Diver, C., Atkinson, J., Giedl-Wagner, R. and Helml, H.J., 2006. Sequential laser and edm micro-drilling for next generation fuel injection nozzle manufacture. *CIRP Annals-Manufacturing Technology,* 55(1), pp.179-182.

Li, L., Kim, J.H. and Shukor, M.H.A., 2005a. Grit blast assisted laser milling/grooving of metallic alloys. *CIRP Annals-Manufacturing Technology,* 54(1), pp.183-186.

Li, W.D., Ong, S.K. and Nee, A.Y.C., 2004. Optimization of process plans using a constraint-based tabu search approach. *International Journal of Production Research,* 42(10), pp.1955-1985.

References

Li, Y.D. and Gu, P.H., 2004. Free-form surface inspection techniques state of the art review. *Computer-Aided Design,* 36(13), pp.1395-1417.

Li, Z.C., Jiao, Y., Deines, T.W., Pei, Z.J. and Treadwell, C., 2005b. Rotary ultrasonic machining of ceramic matrix composites: Feasibility study and designed experiments. *International Journal of Machine Tools & Manufacture,* 45(12-13), pp.1402-1411.

Liao, Y.S., Chen, Y.C. and Lin, H.M., 2007. Feasibility study of the ultrasonic vibration assisted drilling of inconel superalloy. *International Journal of Machine Tools & Manufacture,* 47(12-13), pp.1988-1996.

Lim, H.S., Fathima, K., Kumar, A.S. and Rahman, M., 2002a. A fundamental study on the mechanism of electrolytic in-process dressing (elid) grinding. *International Journal of Machine Tools & Manufacture,* 42(8), pp.935-943.

Lim, H.S., Kumar, A.S. and Rahman, M., 2002b. Improvement of form accuracy in hybrid machining of microstructures. *Journal of Electronic Materials,* 31(10), pp.1032-1038.

Liou, F., Choi, J., Landers, R., Janardhan, V., Balakrishnan, S. and Agarwal, S., 2001. Research and development of a hybrid rapid manufacturing process. Proceedings of the Twelfth Annual Solid Freeform Fabrication Symposium 2001, Austin, USA. pp.138-145. 19 - 21 August, 2001

Liou, F., Slattery, K., Kinsella, M., Newkirk, J., Chou, H.N. and Landers, R., 2007. Applications of a hybrid manufacturing process for fabrication of metallic structures. *Rapid Prototyping Journal,* 13(4), pp.236-244.

Liu, L.M., Wang, J.F. and Song, G., 2004. Hybrid laser-tig welding, laser beam welding and gas tungsten arc welding of az31b magnesium alloy. *Materials Science and Engineering a-Structural Materials Properties Microstructure and Processing,* 381(1-2), pp.129-133.

Lucchetta, G. and Baesso, R., 2007. Polymer injection forming (pif) of thin walled sheet metal parts—preliminary experimental results. Proceedings of the 10th ESAFORM International Conference on Material Forming, Zaragoza, Spain. pp.1046. 18 - 20 April

MAG,2010. Mag the global machine tool manufacturer [Online]. Available from [http://www.mag-ias.com/en.html], accessed on 7 June 2010.

Malone, E. and Lipson, H., 2006. Freeform fabrication of ionomeric polymer-metal composite actuators. *Rapid Prototyping Journal,* 12(5), pp.244-253.

Malone, E., Rasa, K., Cohen, D., Isaacson, T., Lashley, H. and Lipson, H., 2004. Freeform fabrication of zinc-air batteries and electromechanical assemblies. *Rapid Prototyping Journal,* 10(1), pp.58-69.

Markov, A.I. and Neppiras, E., 1966. *Ultrasonic machining of intractable materials,* Iliffe, London.1966.

References

Maropoulos, P., 1995. A novel process planning architecture for product-based manufacture. *Proceedings of the Institution of Mechanical Engineers, Part B: Journal of Engineering Manufacture,* 209(4), pp.267-276.

Maropoulos, P.G., Baker, R.P. and Paramor, K.Y.G., 2000. Integration of tool selection with design - part 2: Aggregate machining time estimation. *Journal of Materials Processing Technology,* 107(1-3), pp.135-142.

Marri, H., Gunasekaran, A. and Grieve, R., 1998. Computer-aided process planning: A state of art. *The International Journal of Advanced Manufacturing Technology,* 14(4), pp.261-268.

Mazak,2011. Mazak products [Online]. Available from [http://www.mazak.eu/jkcm/Default.aspx?pg=26&lang=1], accessed on 25 June 2011.

Melkote, S., Kumar, M., Hashimoto, F. and Lahoti, G., 2009. Laser assisted micro-milling of hard-to-machine materials. *CIRP Annals-Manufacturing Technology,* 58(1), pp.45-48.

Menzies, I. and Koshy, P., 2008. Assessment of abrasion-assisted material removal in wire edm. *CIRP Annals-Manufacturing Technology,* 57(1), pp.195-198.

Merchant, M.E., 2003. Twentieth century evolution of machining in the united states - an interpretative review. *Sadhana-Academy Proceedings in Engineering Sciences,* 28, pp.867-874.

Merz, R., 1994. *Shape deposition manufacturing*. Thesis (Ph.D). Stanford University, Stanford, USA.

Miao, H.K., Sridharan, N. and Shah, J.J., 2002. Cad-cam integration using machining features. *International Journal of Computer Integrated Manufacturing,* 15(4), pp.296-318.

Micari, F., Ambrogio, G. and Filice, L., 2007. Shape and dimensional accuracy in single point incremental forming: State of the art and future trends. *Journal of Materials Processing Technology,* 191(1-3), pp.390-395.

Mognol, P., Jegou, L., Mickael, R. and Furet, B., 2006. High speed milling, electro discharge machining and direct metal laser sintering: A method to optimize these processes in hybrid rapid tooling. *International Journal of Advanced Manufacturing Technology,* 29(1-2), pp.35-40.

Molian, R., Neumann, C., Shrotriya, P. and Molian, P., 2008. Novel laser/water-jet hybrid manufacturing process for cutting ceramics. *Journal of Manufacturing Science and Engineering-Transactions of the Asme,* 130(3), pp.031008.1-031008.10.

Nandy, A.K., Gowrishankar, M.C. and Paul, S., 2009. Some studies on high-pressure cooling in turning of ti-6al-4v. *International Journal of Machine Tools & Manufacture,* 49(2), pp.182-198.

Nassehi, A., Newman, S., Dhokia, V., Zhu, Z. and Asrai, R.I., 2011. Using formal methods to model hybrid manufacturing processes. 4th International Conference on Changeable,

Agile, Reconfigurable and Virtual Production (CARV2011), Montreal, Canada. pp.52-56. 2-5 October, 2011

National Aerospace Standard 979, 1969. Uniform cutting tests - nas (national aerospace standard) series: Metal cutting equipment specifications.

NatureWorks,2012. Natureworks® pla polymer 6302d fiber melt spinning [Online]. Available from [http://www.natureworksllc.com/Japan/~/media/Technical_Resources/Technical_Data_Sheets/TechnicalDataSheet_6302D_pdf.pdf], accessed on 10 September 2012.

Nau, B., Roderburg, A. and Klocke, F., 2011. Ramp-up of hybrid manufacturing technologies. *CIRP Journal of Manufacturing Science and Technology,* 4 (3), pp.313 - 316.

Newman, S.T., Nassehi, A., Imani-Asrai, R. and Dhokia, V., 2012. Energy efficient process planning for CNC machining. *CIRP Journal of Manufacturing Science and Technology,* 5(2), pp.127-136.

Nguyen, T., Zarudi, I. and Zhang, L.C., 2007. Grinding-hardening with liquid nitrogen: Mechanisms and technology. *International Journal of Machine Tools & Manufacture,* 47(1), pp.97-106.

Nickel, A.H., Barnett, D.M. and Prinz, F.B., 2001. Thermal stresses and deposition patterns in layered manufacturing. *Materials Science and Engineering a-Structural Materials Properties Microstructure and Processing,* 317(1-2), pp.59-64.

Niebel, B.W., 1965. Mechanized process selection for planning new designs. *ASME paper,* no. 737.

Novak, J.W., Shin, Y.C. and Incropera, F.P., 1997. Assessment of plasma enhanced machining for improved machinability of inconel 718. *Journal of Manufacturing Science and Engineering-Transactions of the Asme,* 119(1), pp.125-129.

Nowotny, S., Muenster, R., Scharek, S. and Beyer, E., 2010. Integrated laser cell for combined laser cladding and milling. *Assembly Automation,* 30(1), pp.36-38.

Okasha, M.M., Mativenga, P.T., Driver, N. and Li, L., 2010. Sequential laser and mechanical micro-drilling of ni superalloy for aerospace application. *CIRP Annals-Manufacturing Technology,* 59(1), pp.199-202.

Ono, M., Shinbo, Y., Yoshitake, A. and Ohmura, M., 2002. *Development of laser-arc hybrid welding*. NKK, pp.70-74

Onsrud,2011. Lmt onsrud lp cutting tool data catalogue [Online]. Available from [http://www.onsrud.com/xdoc/FeedSpeeds], accessed on 10 July 2011.

Onwubolu, G.C., Davim, J.P., Oliveira, C. and Cardoso, A., 2007. Prediction of clad angle in laser cladding by powder using response surface methodology and scatter search. *Optics and Laser Technology,* 39(6), pp.1130-1134.

Pajak, P.T., Desilva, A.K.M., Harrison, D.K. and McGeough, J.A., 2006. Precision and efficiency of laser assisted jet electrochemical machining. *Precision Engineering-Journal of the International Societies for Precision Engineering and Nanotechnology,* 30(3), pp.288-298.

Pfefferkorn, F.E., Incropera, F.P. and Shin, Y.C., 2005. Heat transfer model of semi-transparent ceramics undergoing laser-assisted machining. *International Journal of Heat and Mass Transfer,* 48(10), pp.1999-2012.

Pfefferkorn, F.E., Shin, Y.C., Tian, Y.G. and Incropera, F.P., 2004. Laser-assisted machining of magnesia-partially-stabilized zirconia. *Journal of Manufacturing Science and Engineering-Transactions of the Asme,* 126(1), pp.42-51.

Pham, D.T. and Wang, X., 2000. Prediction and reduction of build times for the selective laser sintering process. *Proceedings of the Institution of Mechanical Engineers Part B-Journal of Engineering Manufacture,* 214(6), pp.425-430.

Pinilla, J.M. and Prinz, F.B., 2003. Lead-time reduction through flexible routing: Application to shape deposition manufacturing. *International Journal of Production Research,* 41(13), pp.2957-2973.

Potthast, C., Eisseler, R., Klotz, D., Wallaschek, J. and Heisel, U., 2008. Piezoelectric actuator design for ultrasonically assisted deep hole drilling. *Journal of Electroceramics,* 20(3-4), pp.187-192.

Pujana, J., Rivero, A., Celaya, A. and de Lacalle, L.N.L., 2009. Analysis of ultrasonic-assisted drilling of ti6al4v. *International Journal of Machine Tools & Manufacture,* 49(6), pp.500-508.

Qian, Y.P., Huang, J.H. and Zhang, H.O., 2010. Study on the factors influencing the layer precision in hybrid plasma-laser deposition manufacturing. *Advanced Materials Research,* 97-101, pp.3828-3831.

Qian, Y.P., Zhang, H.O. and Wang, G.L., 2006. Research of rapid and direct thick coatings deposition by hybrid plasma-laser. *Applied Surface Science,* 252(18), pp.6173-6178.

Quintana, I., Dobrev, T., Aranzabe, A., Lalev, G. and Dimov, S., 2009. Investigation of amorphous and crystalline ni alloys response to machining with micro-second and pico-second lasers. *Applied Surface Science,* 255(13-14), pp.6641-6646.

Rahman, M., Kumar, A.S., Manzoor Ul, S. and Ling, M.S., 2003. Effect of chilled air on machining performance in end milling. *International Journal of Advanced Manufacturing Technology,* 21(10-11), pp.787-795.

Rajurkar, K.P., Zhu, D., McGeough, J.A., Kozak, J. and De Silva, A., 1999. *New developments in electro-chemical machining, CIRP annals 1999: Manufacturing technology, vol 48 no 2 1999.* 3001 Bern: Hallwag Publishers.

References

Rebro, P.A., Shin, Y.C. and Incropera, F.P., 2002. Laser-assisted machining of reaction sintered mullite ceramics. *Journal of Manufacturing Science and Engineering-Transactions of the Asme,* 124(4), pp.875-885.

Ren, L., Sparks, T., Ruan, J.Z. and Liou, F., 2010. Integrated process planning for a multiaxis hybrid manufacturing system. *Journal of Manufacturing Science and Engineering-Transactions of the Asme,* 132(2),

RepRap,2012a. Fused filament fabrication [Online]. Available from [http://reprap.org/wiki/Fused_filament_fabrication], accessed on 10 September 2012.

RepRap,2012b. Reprap [Online]. Available from [http://reprap.org/wiki/RepRap], accessed on 10 September 2012.

Riveros, R.E., Yamaguchi, H., Mitsuishi, I., Takagi, U., Ezoe, Y., Kato, F., Sugiyama, S., Yamasaki, N. and Mitsuda, K., 2009. Magnetic field assisted finishing of ultra-lightweight and high-resolution mems x-ray micro-pore optics. Proceedings of SPIE Optics + Optoelectronics, EUV and X-ray Optics, Prague, Czech Republic. pp.736013. 20 - 23 April, 2009

Rivette, M., Hacoet, J.Y. and Mognot, P., 2007. A graph-based methodology for hybrid rapid design. *Proceedings of the Institution of Mechanical Engineers Part B-Journal of Engineering Manufacture,* 221(4), pp.685-697.

Roderburg, A., Gerhardt, K., Hinke, C., Park, H.S., Buchholz, S. and Klocke, F., 2011. Design methodology for innovative hybrid manufacturing technologies. Proceedings of the 2011 17th International Conference on Concurrent Enterprising (ICE 2011), Aachen, Germany. pp.1-9. 20-22 June, 2011

Rodriguez, J.F., Thomas, J.P. and Renaud, J.E., 2000. Characterization of the mesostructure of fused-deposition acrylonitrile-butadiene-styrene materials. *Rapid Prototyping Journal,* 6(3), pp.175-185.

Ross, P.J., 1996. *Taguchi techniques for quality engineering: Loss function, orthogonal experiments, parameter and tolerance design,* McGraw-Hill Professional.

Rozvany, G.I.N., 2009. A critical review of established methods of structural topology optimization. *Structural and Multidisciplinary Optimization,* 37(3), pp.217-237.

Rozzi, J.C., Pfefferkorn, F.E., Shin, Y.C. and Incropera, F.P., 2000. Experimental evaluation of the laser assisted machining of silicon nitride ceramics. *Journal of Manufacturing Science and Engineering-Transactions of the Asme,* 122(4), pp.666-670.

Ruan, J., Eiamsa-ard, K. and Liou, F., 2005. Automatic process planning and toolpath generation of a multiaxis hybrid manufacturing system. *Journal of manufacturing processes,* 7(1), pp.57-68.

Sadek, A., Attia, M., Meshreki, M. and Shi, B., 2013. Characterization and optimization of vibration-assisted drilling of fibre reinforced epoxy laminates. *CIRP Annals-Manufacturing Technology (in press)*,

Safari, A., Danforth, S.C., Jafari, M., Allahverdi, M., Jadidian, B. and Mohammadi, F., 2000. *Processing and properties of piezoelectric actuators developed by fused deposition technique, Proceedings of the 2001 12th ieee international symposium on applications of ferroelectrics, vols i and ii*. New York: Ieee.

Salonitis, K., Chondros, T. and Chryssolouris, G., 2008. Grinding wheel effect in the grind-hardening process. *International Journal of Advanced Manufacturing Technology,* 38(1-2), pp.48-58.

Salonitis, K. and Chryssolouris, G., 2007. Cooling in grind-hardening operations. *International Journal of Advanced Manufacturing Technology,* 33(3-4), pp.285-297.

Sankar, R.S., Asokan, P., Prabhaharan, G. and Phani, A.V., 2008. A capp framework with optimized process parameters for rotational components. *International Journal of Production Research,* 46(20), pp.5561-5587.

Sanz, C., Fuentes, E. and Gonzalo, O., 2007. Turning performance optimisation of aeronautical materials by using high pressure cooling technology. *International Journal of Machining and Machinability of Materials,* 2(2), pp.270-281.

Scallan, P., 2003. *Process planning: The design/manufacture interface,* Butterworth-Heinemann.

Schopf, M., Beltrami, I., Boccadoro, M. and Kramer, D., 2001. Ecdm (electro chemical discharge machining), a new method for trueing and dressing of metal-bonded diamond grinding tools. *CIRP Annals-Manufacturing Technology,* 50(1), pp.125-128.

Schuocker, D., 2001. Mathematical modeling of laser-assisted deep drawing. *Journal of Materials Processing Technology,* 115(1), pp.104-107.

Schuocker, D., Schroder, K. and Zeinar, C., 1999. Laser assisted deep drawing (ladd) - a new process for elevated beam power. *Lasers in Engineering,* 8(2), pp.89-103.

Sells, E.A., 2009. *Towards a self-manufacturing rapid prototyping machine*. Thesis (Ph.D). University of Bath, Bath, UK.

Shah, J.J. and Mäntylä, M., 1995. *Parametric and feature-based cad/cam: Concepts, techniques, and applications,* Wiley-interscience.

She, C.H. and Hung, C.W., 2008. Development of multi-axis numerical control program for mill-turn machine. *Proceedings of the Institution of Mechanical Engineers Part B-Journal of Engineering Manufacture,* 222(6), pp.741-745.

Shen, H., Shi, Y.J., Yao, Z.Q. and Hu, J., 2006. An analytical model for estimating deformation in laser forming. *Computational Materials Science,* 37(4), pp.593-598.

Shenghua, Y., Zhong, W. and Xinghua, Q., 2000. Review and prospect of precision inspection. *China Mechanical Engineering,* 11(3), pp.262-263.

Shih, A.J., Lewis, M.A. and Strenkowski, J.S., 2004. End milling of elastomers - fixture design and tool effectiveness for material removal. *Journal of Manufacturing Science and Engineering-Transactions of the Asme,* 126(1), pp.115-123.

Shokrani, A., Dhokia, V., Munoz-Escalona, P. and Newman, S., 2013. State-of-the-art cryogenic machining and processing. *International Journal of Computer Integrated Manufacturing,* 26(7), pp.616-648.

Shokrani, A., Dhokia, V. and Newman, S.T., 2012. Environmentally conscious machining of difficult-to-machine materials with regard to cutting fluids. *International Journal of Machine Tools and Manufacture,* 57, pp.83-101.

Singh, R. and Melkote, S.N., 2007. Characterization of a hybrid laser-assisted mechanical micromachining (lamm) process for a difficult-to-machine material. *International Journal of Machine Tools & Manufacture,* 47(7-8), pp.1139-1150.

Slic3r,2013. Slic3r g-code generator for 3d printers [Online]. Available from [http://slic3r.org], accessed on 11 January 2013.

Smith, S., Woody, B., Ziegert, J. and Huang, Y., 2007. Deformation machining - a new hybrid process. *CIRP Annals-Manufacturing Technology,* 56(1), pp.281-284.

So, B.S., Jung, Y.H., Park, J.W. and Lee, D.W., 2007. Five-axis machining time estimation algorithm based on machine characteristics. *Journal of Materials Processing Technology,* 187, pp.37-40.

Song, G., Liu, L.M. and Wang, P.C., 2006. Overlap welding of magnesium az31b sheets using laser-arc hybrid process. *Materials Science and Engineering a-Structural Materials Properties Microstructure and Processing,* 429(1-2), pp.312-319.

Song, Y.A. and Park, S., 2006. Experimental investigations into rapid prototyping of composites by novel hybrid deposition process. *Journal of Materials Processing Technology,* 171(1), pp.35-40.

Sonmez, F.O. and Hahn, H.T., 1998. Thermomechanical analysis of the laminated object manufacturing (lom) process. *Rapid Prototyping Journal,* 4(1), pp.26-36.

Sood, A.K., Ohdar, R.K. and Mahapatra, S.S., 2009. Improving dimensional accuracy of fused deposition modelling processed part using grey taguchi method. *Materials & Design,* 30(10), pp.4243-4252.

Sood, A.K., Ohdar, R.K. and Mahapatra, S.S., 2010. Parametric appraisal of mechanical property of fused deposition modelling processed parts. *Materials & Design,* 31(1), pp.287-295.

Sorby, K. and Tonnessen, K., 2006. High-pressure cooling of face-grooving operations in ti6al4v. *Proceedings of the Institution of Mechanical Engineers Part B-Journal of Engineering Manufacture,* 220(10), pp.1621-1627.

Stopp, S., Wolff, T., Irlinger, F. and Lueth, T., 2008. A new method for printer calibration and contour accuracy manufacturing with 3d-print technology. *Rapid Prototyping Journal,* 14(3), pp.167-172.

Stratasys,2012. Stratasys inc. [Online]. Available from [http://www.stratasys.com/], accessed on 10 September 2012.

Sun, Q., Rizvi, G., Giuliani, V., Bellehumeur, C. and Gu, P., 2004. Experimental study and modeling of bond formation between abs filaments in the fdm process. ANTEC... conference proceedings, pp.1158-1162.

Sun, S., Brandt, M. and Dargusch, M.S., 2010. Thermally enhanced machining of hard-to-machine materials-a review. *International Journal of Machine Tools & Manufacture,* 50(8), pp.663-680.

Sundaram, M.M., Pavalarajan, G.B. and Rajurkar, K.P., 2008. A study on process parameters of ultrasonic assisted micro edm based on taguchi method. *Journal of Materials Engineering and Performance,* 17(2), pp.210-215.

Suryakumar, S., Karunakaran, K.P., Bernard, A., Chandrasekhar, U., Raghavender, N. and Sharma, D., 2011. Weld bead modeling and process optimization in hybrid layered manufacturing. *Computer-Aided Design,* 43(4), pp.331-344.

Swift, K. and Booker, J., 2003. *Process selection: From design to manufacture,* Oxford: Butterworth-Heinemann.

Taylor, J.B., Cormier, D.R., Joshi, S. and Venkataraman, V., 2001. Contoured edge slice generation in rapid prototyping via 5-axis machining. *Robotics and Computer-Integrated Manufacturing,* 17(1-2), pp.13-18.

Terry, W., 2010. Wohlers report 2010: Additive manufacturing state of the industry. Annual Worldwide Progress Report, Fort Collins, Colorado.

Tian, Y.G. and Shin, Y.C., 2006. Thermal modeling for laser-assisted machining of silicon nitride ceramics with complex features. *Journal of Manufacturing Science and Engineering-Transactions of the Asme,* 128(2), pp.425-434.

Tian, Y.G., Wu, B.X., Anderson, M. and Shin, Y.C., 2008. Laser-assisted milling of silicon nitride ceramics and inconel 718. *Journal of Manufacturing Science and Engineering-Transactions of the Asme,* 130(3), pp.031013.1-031013.9.

TolchoeiRad, M. and Bidhendi, I.M., 1997. On the optimization of machining parameters for milling operations. *International Journal of Machine Tools & Manufacture,* 37(1), pp.1-16.

Tsuchiya, H., Inoue, T. and Miyazaki, M., 1985. Wire electro-chemical discharge machining of glasses and ceramics. *Bull. Jpn. Soc. Precis. Eng.,* 19(1), pp.73-74.

Uhlmann, E. and Hübert, C., 2007. Ultrasonic assisted grinding of advanced ceramics. Proceedings of the ASPE Spring Topical Meeting, Raleigh, N.C., USA. 16-17 April, 2007

Umbrello, D., 2013. Analysis of the white layers formed during machining of hardened aisi 52100 steel under dry and cryogenic cooling conditions. *International Journal of Advanced Manufacturing Technology,* 64(5-8), pp.633-642.

Vatani, M., Barazandeh, F., Rahimi, A. and Nezhad, A.S., 2012. Distortion modeling of sl parts by classical lamination theory. *Rapid Prototyping Journal,* 18(3), pp.188-193.

Venugopal, K.A., Tawade, R., Prashanth, P.G., Paul, S. and Chattopadhyay, A.B., 2003. Turning of titanium alloy with tib2-coated carbides under cryogenic cooling. *Proceedings of the Institution of Mechanical Engineers Part B-Journal of Engineering Manufacture,* 217(12), pp.1697-1707.

Verma, A.K. and Rajotia, S., 2010. A review of machining feature recognition methodologies. *International Journal of Computer Integrated Manufacturing,* 23(4), pp.353-368.

Wang, T.M., Xi, J.T. and Jin, Y., 2007. A model research for prototype warp deformation in the fdm process. *International Journal of Advanced Manufacturing Technology,* 33(11-12), pp.1087-1096.

Wang, W., Liu, Z., Zhang, W., Huang, Y. and Allen, D., 2011. Abrasive electrochemical multi-wire slicing of solar silicon ingots into wafers. *CIRP Annals-Manufacturing Technology,* 60(2), pp.255-258.

Wang, W., Liu, Z.D., Tian, Z.J., Huang, Y.H. and Liu, Z.X., 2009. High efficiency slicing of low resistance silicon ingot by wire electrolytic-spark hybrid machining. *Journal of Materials Processing Technology,* 209(7), pp.3149-3155.

Wang, W., Liu, Z.D., Tian, Z.J., Huang, Y.H., Liu, Z.X., Ekere, N.N. and Ieee, 2008. Study of wire electrolytic-spark hybrid machining of silicon solar wafer and surface characteristics. Proceedings of ESTC 2008: 2nd Electronics System-Integration Technology Conference, Vols 1 and 2, London, UK. pp.593-596. 1-4 September, 2008

Wang, Z.Y. and Rajurkar, K.P., 2000. Cryogenic machining of hard-to-cut materials. *Wear,* 239(2), pp.168-175.

Wang, Z.Y., Rajurkar, K.P., Fan, J., Lei, S., Shin, Y.C. and Petreseu, G., 2003. Hybrid machining of inconel 718. *International Journal of Machine Tools & Manufacture,* 43(13), pp.1391-1396.

Wang, Z.Y., Rajurkar, K.P. and Munugappan, M., 1996. Cryogenic pcbn turning of ceramic (si3n4). *Wear,* 195(1-2), pp.1-6.

Weill, R., Spur, G. and Eversheim, W., 1982. Survey of computer-aided process planning systems. *CIRP Annals-Manufacturing Technology,* 31(2), pp.539-551.

Wiedemann, B., Dusel, K.H. and Eschl, J., 1995. Investigation into the influence of material and process on part distortion. *Rapid Prototyping Journal,* 1(3), pp.17-22.

Wysk, R.A., 1977. *An automated process planning and selection program: Appas*. Thesis (Ph.D). Purdue University, West Lafayette, Indiana, USA.

Xiong, X., Haiou, Z., Guilan, W. and Guoxian, W., 2009. Hybrid plasma deposition and milling for an aeroengine double helix integral impeller made of superalloy. *Robotics and Computer-Integrated Manufacturing,* 26(2010), pp.291-295.

Xu, H., Zhang, Y., Lu, B. and Chen, D., 2004. Numerical simulation of solidified deformation of resin parts in stereolithography rapid prototyping. *Jixie Gongcheng Xuebao(Chinese Journal of Mechanical Engineering)(China),* 40(6), pp.107-112.

Xu, X., Wang, L.H. and Newman, S.T., 2011. Computer-aided process planning - a critical review of recent developments and future trends. *International Journal of Computer Integrated Manufacturing,* 24(1), pp.1-31.

Ya, G., Qin, H.W., Yang, S.C. and Xu, Y.W., 2002. Analysis of the rotary ultrasonic machining mechanism. *Journal of Materials Processing Technology,* 129(1-3), pp.182-185.

Yamaguchi, H., Kang, J. and Hashimoto, F., 2011. Metastable austenitic stainless steel tool for magnetic abrasive finishing. *CIRP Annals-Manufacturing Technology,* 60(2), pp.339-342.

Yamaguchi, H., Riveros, R.E., Mitsuishi, I., Takagi, U., Ezoe, Y., Yamasaki, N., Mitsuda, K. and Hashimoto, F., 2010. Magnetic field-assisted finishing for micropore x-ray focusing mirrors fabricated by deep reactive ion etching. *CIRP Annals-Manufacturing Technology,* 59(1), pp.351-354.

Yan, X. and Gu, P., 1996. A review of rapid prototyping technologies and systems. *Computer-Aided Design,* 28(4), pp.307-318.

Yang, H.J., Hwang, P.J. and Lee, S.H., 2002a. A study on shrinkage compensation of the sls process by using the taguchi method. *International Journal of Machine Tools & Manufacture,* 42(11), pp.1203-1212.

Yang, Z.Y., Chen, Y.H. and Sze, W.S., 2002b. Layer-based machining: Recent development and support structure design. *Proceedings of the Institution of Mechanical Engineers Part B-Journal of Engineering Manufacture,* 216(7), pp.979-991.

Yanyan, Y., Bo, Z. and Junli, L., 2009. Ultraprecision surface finishing of nano-zro2 ceramics using two-dimensional ultrasonic assisted grinding. *The International Journal of Advanced Manufacturing Technology,* 43(5), pp.462-467.

Yasa, E. and Kruth, J.P., 2008. Experimental study of the combined process of selective laser melting and selective laser erosion. Proceedings of RAPID, Florida, USA. 20-22 May, 2008

Yasa, E., Kruth, J.P. and Deckers, J., 2011. Manufacturing by combining selective laser melting and selective laser erosion/laser re-melting. *CIRP Annals-Manufacturing Technology,* 60(2), pp.263-266.

Yeo, S.H. and Tan, L.K., 1999. Effects of ultrasonic vibrations in micro electro-discharge machining of microholes. *Journal of Micromechanics and Microengineering,* 9(4), pp.345-352.

Yildiz, Y. and Nalbant, M., 2008. A review of cryogenic cooling in machining processes. *International Journal of Machine Tools & Manufacture,* 48(9), pp.947-964.

You, C.F., Sheen, B.T. and Lin, T.K., 2007. Selecting optimal tools for arbitrarily shaped pockets. *International Journal of Advanced Manufacturing Technology,* 32(1-2), pp.132-138.

Yu, J., Lin, X., Ma, L.A., Wang, J.J., Fu, X.L., Chen, J. and Huang, W.D., 2011. Influence of laser deposition patterns on part distortion, interior quality and mechanical properties by laser solid forming (lsf). *Materials Science and Engineering a-Structural Materials Properties Microstructure and Processing,* 528(3), pp.1094-1104.

Yu, Z.Y., Zhang, Y., Li, J., Luan, J., Zhao, F. and Guo, D., 2009. High aspect ratio micro-hole drilling aided with ultrasonic vibration and planetary movement of electrode by micro-edm. *CIRP Annals-Manufacturing Technology,* 58(1), pp.213-216.

Zhang, H., Xu, J.W. and Wang, J.M., 2009a. Investigation of a novel hybrid process of laser drilling assisted with jet electrochemical machining. *Optics and Lasers in Engineering,* 47(11), pp.1242-1249.

Zhang, H.O., Qian, Y.P. and Wang, G.L., 2006. Study of rapid and direct thick coating deposition by hybrid plasma-laser manufacturing. *Surface & Coatings Technology,* 201(3-4), pp.1739-1744.

Zhang, J. and Liou, F., 2004. Adaptive slicing for a multi-axis laser aided manufacturing process. *Journal of Mechanical Design,* 126(2), pp.254-261.

Zhang, S., Li, J.F., Sun, J. and Jiang, F., 2010. Tool wear and cutting forces variation in high-speed end-milling ti-6al-4v alloy. *International Journal of Advanced Manufacturing Technology,* 46(1-4), pp.69-78.

Zhang, S.H., Cho, T.Y., Yoon, J.H., Li, M.X., Shum, P.W. and Kwon, S.C., 2009b. Investigation on microstructure, surface properties and anti-wear performance of hvof sprayed wc-crc-ni coatings modified by laser heat treatment. *Materials Science and Engineering B-Advanced Functional Solid-State Materials,* 162(2), pp.127-134.

Zhang, X., Nassehi, A., Safaieh, M. and Newman, S.T., 2013. Process comprehension for shopfloor manufacturing knowledge reuse. *International Journal of Production Research,* (ahead-of-print), pp.1-15.

Zhang, Y. and Chou, K., 2008. A parametric study of part distortions in fused deposition modelling using three-dimensional finite element analysis. *Proceedings of the Institution of Mechanical Engineers Part B-Journal of Engineering Manufacture,* 222(8), pp.959-967.

Zhang, Y.W. and Faghri, A., 1999. Melting of a subcooled mixed powder bed with constant heat flux heating. *International Journal of Heat and Mass Transfer,* 42(5), pp.775-788.

Zhao, W.S., Wang, Z.L., Di, S.C., Chi, G.X. and Wei, H.Y., 2002. Ultrasonic and electric discharge machining to deep and small hole on titanium alloy. *Journal of Materials Processing Technology,* 120(1-3), pp.101-106.

Zhong, Z.W. and Lin, G., 2006. Ultrasonic assisted turning of an aluminium-based metal matrix composite reinforced with sic particles. *International Journal of Advanced Manufacturing Technology,* 27(11-12), pp.1077-1081.

Zhou, J.G., Herscovici, D. and Chen, C.C., 2000. Parametric process optimization to improve the accuracy of rapid prototyped stereolithography parts. *International Journal of Machine Tools and Manufacture,* 40(3), pp.363-379.

Zhu, D., Zeng, Y., Xu, Z. and Zhang, X., 2011. Precision machining of small holes by the hybrid process of electrochemical removal and grinding. *CIRP Annals-Manufacturing Technology,* 60(2), pp.247-250.

Zhu, D., Zhu, Z.W. and Qu, N.S., 2006. Abrasive polishing assisted nickel electroforming process. *CIRP Annals-Manufacturing Technology,* 55(1), pp.193-196.

Zhu, Z., Dhokia, V., Nassehi, A. and Newman, S.T., 2013. A review of hybrid manufacturing processes - state of the art and future perspectives. *International Journal of Computer Integrated Manufacturing,* 26(7), pp.596-615.

Zhu, Z., Dhokia, V.G., Nassehi, A., Jones, R.O. and Newman, S.T., 2012. CNC machining of plastic layered parts. Proceedings of the 22nd International Conference on Flexible Automation and Intelligent Manufacturing (FAIM), Helsinki, Finland. pp.1159-1165. 10-13 June, 2012

Appendix A: Publications

Journal papers:

1. **Zhu, Z.**, Dhokia, V., Nassehi, A. and Newman, S.T., 2013. A review of hybrid manufacturing processes - state of the art and future perspectives. *International Journal of Computer Integrated Manufacturing,* 26(7), pp.596-615.

2. **Zhu, Z.**, Dhokia, V. and Newman, S.T., 2013. The development of a novel process planning algorithm for an unconstrained hybrid manufacturing process. *Journal of Manufacturing Processes (in press), http://dx.doi.org/10.1016/j.jmapro.2013.06.006*

3. **Zhu, Z.**, Dhokia, V., Newman, S.T. and Nassehi, A., 2013. Application of a hybrid process for high precision manufacture of difficult to machine prismatic parts. (*In review – submitted to Journal of Materials Processing Technology*)

4. **Zhu, Z.**, Dhokia, V., Nassehi, A. and Newman, S.T., 2013. Investigation of Part Distortions as a Result of Hybrid Manufacturing. (*to be submitted to Proceedings of the Institution of Mechanical Engineers Part B – Journal of Engineering Manufacture*)

Conference papers:

1. **Zhu, Z.**, Dhokia, V.G. and Newman, S.T., 2013. A methodology for the estimation of build time for operation sequencing in process planning for a hybrid process. *Proceedings of the 23rd International Conference on Flexible Automation and Intelligent Manufacturing (FAIM2013), Porto, Portugal. pp.159-172. 26-28 June 2013*

2. **Zhu, Z.**, Dhokia, V.G. & Newman, S.T. 2013. A reactionary process planning algorithm for an unconstrained hybrid process integrating additive, subtractive and inspection processes. *Proceedings of the 41st North American Manufacturing Research Conference (NAMRC 41), Madison, Wisconsin, United States. pp.541-550. 10-14 June 2013*

3. **Zhu, Z.**, Dhokia, V.G. and Newman, S.T., 2012. A novel process planning approach for hybrid manufacturing consisting of additive, subtractive and inspection processes. *Proceedings of 2012 IEEE International Conference on Industrial Engineering and*

Engineering Management (IEEM2012), Hong Kong, China. pp.1617-1621. 10-13 December 2012

4. **Zhu, Z.**, Dhokia, V.G., Newman, S.T. and Nassehi, A., 2012. Unconstrained manufacture of plastic parts - a novel concept of hybrid manufacturing process. *In Proceedings of the 12th European Society for Precision Engineering and Nanotechnology (EUSPEN) International Conference, Stockholm, Sweden. pp.254-257. 4-8 June 2012*

5. **Zhu, Z.**, Dhokia, V.G., Nassehi, A., Jones, R.O. and Newman, S.T., 2012. CNC machining of plastic layered parts. *Proceedings of the 22nd International Conference on Flexible Automation and Intelligent Manufacturing (FAIM), Helsinki, Finland. pp.1159-1165. 10-13 June, 2012*

6. Dhokia, V., Newman, S.T., **Zhu, Z.** and Shokrani, A., 2011. A novel method for rapid part inspection and verification. *Proceedings of the 11th International Conference of the european society for precision engineering and nanotechnology (EUSPEN), Como, Italy. pp.340-343. 23-27 May 2011*

7. Nassehi, A., Newman, S., Dhokia, V., **Zhu, Z.** and Asrai, R.I., 2011. Using formal methods to model hybrid manufacturing processes. *In Proceedings of the 4th International Conference on Changeable, Agile, Reconfigurable and Virtual Production (CARV2011), Montreal, Canada. pp.52-56. 2-5 October, 2011*
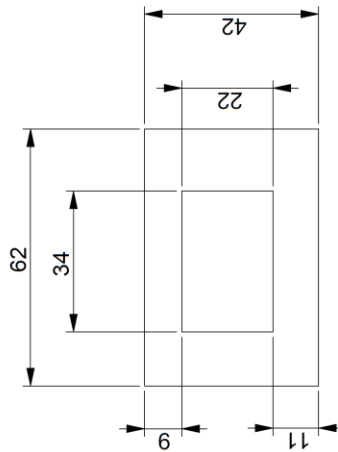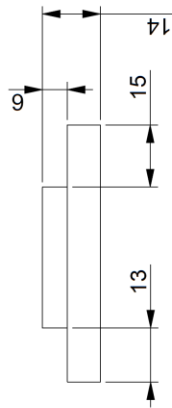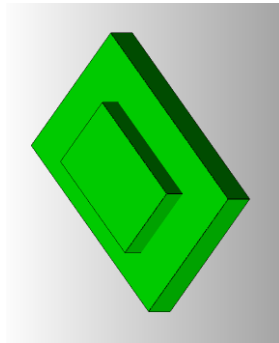
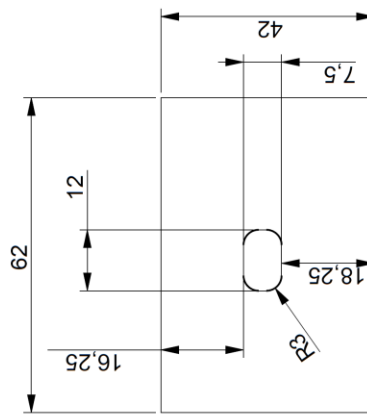## Appendix B: Drawings of Test Part III and the Existing Parts

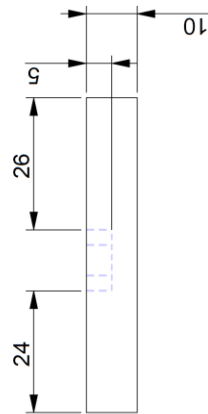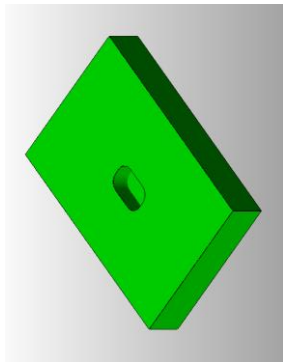### Test Part III
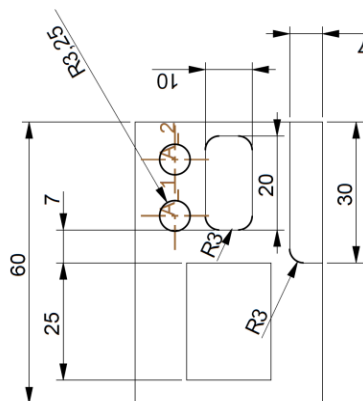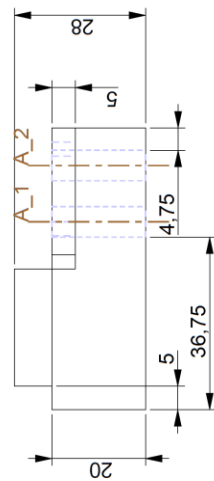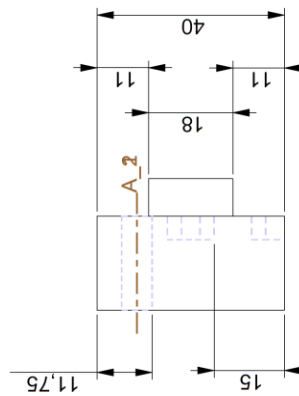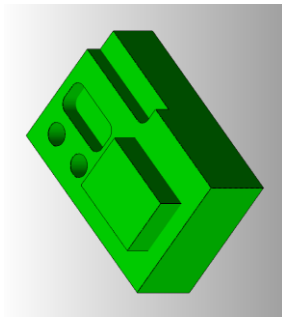
The Existing Part with a Boss

The Existing Part with a Pocket

The Final Part with an Unqualified Boss